REPORT DOCUMENTATION PAGE

Form Approved
OMB No. 0704-0188

PLEASE DO NOT RETURN YOUR FORM TO THE ABOVE ORGANIZATION.

1. REPORT DATE *(DD-MM-YYYY)*	2. REPORT TYPE	3. DATES COVERED *(From - To)*
08-11-2018	Research Project Final Report	1 JANUARY 2016 – 31 AUGUST 2018

4. TITLE AND SUBTITLE
Study of Biomarkers and Acute Radiation Sickness (ARS) Prognosis/Outcome Factors after Mixed-Field (Neutron and Gamma) Radiation in a Mouse Total-body Irradiation Model for Use in an FDA-Approved Point-of-Care Biodosimetry System

5a. CONTRACT NUMBER

5b. GRANT NUMBER
DWAM52221

5c. PROGRAM ELEMENT NUMBER

6. AUTHOR(S)
Ossetrova, Natalia, I., Ph.D.

5d. PROJECT NUMBER
G1B23704

5e. TASK NUMBER

5f. WORK UNIT NUMBER

7. PERFORMING ORGANIZATION NAME(S) AND ADDRESS(ES)
Armed Forces Radiobiology Research Institute (AFRRI), Uniformed Services University of the Health Sciences (USUHS),
4555 South Palmer Road, Bldg 42
Bethesda, MD 20889-5648, USA

8. PERFORMING ORGANIZATION REPORT NUMBER

9. SPONSORING/MONITORING AGENCY NAME(S) AND ADDRESS(ES)
97-DEFENSE RESEARCH AND ENGINEERING-DODHQ0287
ATTN: PETRO, JAMES B., Ph.D.
WASHINGTON HEADQUARTERS SERVICES (97008003)
THE PENTAGON
WASHINGTON, DC-20301-1155

10. SPONSOR/MONITOR'S ACRONYM(S)
ASD(R&E)

11. SPONSOR/MONITOR'S REPORT NUMBER(S)
N/A

12. DISTRIBUTION/AVAILABILITY STATEMENT
DISTRIBUTION A. Approved for public release: distribution is unlimited.

13. SUPPLEMENTARY NOTES

14. ABSTRACT
The detonation of a nuclear weapon or a nuclear accident represent possible mass-casualty events with significant exposure to mixed neutron and gamma radiation fields in the first few minutes after the event with the ensuing fallout extending for miles from the epicenter that would primarily consist of photon exposure. Circulating biomarkers represent a crucial source of information in a mass casualty radiation exposure triage scenario. Evaluated multiple blood biodosimetry and organ-specific biomarkers for early-response assessment of radiation exposure using a mouse total-body irradiation model, exposed to pure photons over a broad dose range (3 – 12 Gy) and dose rates of either 0.6 or 1.9 Gy/min and compared the results with those obtained after exposure of mice with a mixed-field (neutrons and photons) using Armed Forces Radiobiology Research Institute Co-60 gamma source and Training, Research, Isotope, General Atomic Mark-F nuclear research reactor. The mixed-field studies were performed over a broad dose range (1.5 – 6 Gy), dose rates of either 0.6 or 1.9 Gy/min, and using different proportions of neutrons and gammas. Efforts supplement the goal to deliver an FDA approved biodosimetry device by expanding the use of its capability for a broader spectrum radiation exposure.

15. SUBJECT TERMS
Biological Dosimetry, Mixed Neutrons and Gammas, Total-Body Irradiation, Biomarkers, Radiation Dose Response, Acute Radiation Sickness Severity Score System and Prediction Outcome.

16. SECURITY CLASSIFICATION OF:			17. LIMITATION OF ABSTRACT	18. NUMBER OF PAGES	19a. NAME OF RESPONSIBLE PERSON
a. REPORT	b. ABSTRACT	c. THIS PAGE			Ossetrova, Natalia, Ph.D.
U	U	U	U	125	19b. TELEPHONE NUMBER *(Include area code)* (301) 295-1619

Study of Biomarkers and Acute Radiation Sickness (ARS) Prognosis/Outcome Factors after Mixed-Field (Neutron and Gamma) Radiation in a Mouse Total-body Irradiation Model for Use in an FDA Approved Point-of-Care Biodosimetry System

RESEARCH PROJECT FINAL REPORT
1 JANUARY 2016 – 31 AUGUST 2018

PREPARED BY NATALIA I. OSSETROVA, PH.D.
Senior Scientist, Research Biologist, Principal Investigator (PI)

Biological Dosimetry Group, Scientific Research Department,
Armed Forces Radiobiology Research Institute (AFRRI),
Uniformed Services University of the Health Sciences (USUHS)

8 November 2018

Table of Contents

1. INTRODUCTION

The use of ionizing radiation sources for military, industrial, medical, and research purposes has increased the risk of accidental occupational exposures. Large numbers of individuals have been exposed to various levels of radiation caused by nuclear accidents such as Chernobyl (Guskova et al. 1990; Baranov et al. 1995) and Fukushima Daiichi (Katata et al. 2012), atmospheric nuclear testing (Fehner and Gosling 2006), the atomic bombing at Hiroshima and Nagasaki (Awa et al. 1971; Egbert et al. 2007), various medical radiological procedures, and occupational exposures (Chida et al. 2013). In addition to these, a radiological terrorist attack to disperse of radioactive substances through the use of conventional explosives or detonation of a nuclear weapon represent possible radiation scenarios with significant exposure to mixed neutron and gamma radiation fields in the first few minutes after the event, and the ensuing fallout for miles from the epicenter would also primarily consist of photon (gamma- and/or x-ray) exposure, resulting in mass casualties.

The mechanisms of injury of these low linear energy transfer (LET) radiations (pure gamma) are different from those of high-LET radiation such as neutrons or mixed-field, and these differences may affect the radiation dose assessment and countermeasure efficacy. Acute mortality from radiation exposure is well known to be influenced by physics-based parameters such as radiation quality (neutrons or gamma-rays) and dose rate. An enhanced radiation weapon, if detonated, would emit a large portion of neutron radiation with increased radius of exposure and penetration capability, leading to increased damage requiring radiation quality-specific biodosimetry. Currently, a dose of 2 Gy of acute whole-body exposure is thought of as the threshold for medical intervention (Fliedner et al. 2001; Koenig et al. 2005; AFRRI 2010; Moyer et al. 2015). However, absolute reliance on this threshold ignores the impact of radiation quality and is of concern because neutrons are a significant component of the initial radiation released by a fission nuclear device. Hence, there is a current need to accurately determine exposure levels where mixed field combinations of neutrons and gamma are a threat. We have successfully completed three standard gamma only biodosimetry projects funded by DTRA, DARPA, DOE, and have one ongoing funded by BARDA, the final goal of which is to deliver an FDA-approved hand-held, field deployable proteomic-based point-of-care biodosimetry device, which determines quickly (in few minutes) the radiation dose absorbed by evaluating blood protein biomarker levels after a large-scale radiological or nuclear event (Ossetrova et al. 2007-2018; Sigal et al. 2013). In those projects, we have established animal (*Mus musculus*, *Macaca mulatta*) total-body irradiation (TBI, γ-exposure) models and evaluated a panel of radiation-responsive proteins that, together with peripheral blood cell counts, create a multi-parametric dose-predictive algorithm with a threshold for detection of ~1 Gy from 1 to 7 days after exposure. We also demonstrated the multi-parametric acute radiation sickness (ARS) severity score system along with the survival response categories (RC), which was created in a similar fashion to the Medical Treatment Protocols (METREPOL) for radiation accident victims developed by Dr. Fliedner and colleagues (Fliedner et al. 2001) and expanded it by including proteomic biomarkers (Ossetrova et al. 2007, 2009, 2010, 2011, 2014a, 2014b, 2016a, 2016b). Since those studies were performed using only a gamma-ray exposure, the needed dose-assessment modifications for mixed neutron and gamma exposures, a very militarily relevant scenario, remain unknown.

The Armed Forces Radiobiology Research Institute (AFRRI) Training, Research, Isotope, General Atomic (TRIGA) Mark-F nuclear research reactor was used to simulate radiation environments produced by nuclear weapon detonations and to produce neutrons for a variety of radiation countermeasure animal studies. Relative biological effectiveness (RBE) values for TRIGA reactor-generated Dn/Dt using ^{60}Co γ-rays and 250-kVp x-rays as reference standards were

earlier investigated by AFRRI scientists in animal radiation countermeasure survival studies. It was demonstrated that as neutron (n) proportions in the total (t) radiation dose (Dn/Dt) increased, lethal dose (LD) values decreased (McChesney et al. 1990; MacVittie et al. 1991; Ledney et al. 1991; Ledney et al. 2000; Landauer et al. 1997; Ledney and Elliott 2010; Cary et al. 2012). For biodosimetry purposes, TRIGA nuclear reactor (along with x- and γ-ray radiation sources) was also used to establish in vitro human lymphocyte-dicentric assay calibration curves (Prasanna et al. 2002).

Acute radiation sickness (ARS) is characterized by time and dose-dependent expression of various subsyndromes of organ specific (i.e. hematopoietic, gastrointestinal, and cerebral-vascular) systems. Changes in tissue- and organ-specific bioindicators in blood or plasma following radiation exposure often proceed or coincide with the severity pattern of clinical signs and symptoms for various ARS-relevant organ systems. Measurement of blood plasma/serum biochemical markers indicative of radiation exposure for use in early triage and injury assessment of radiation casualties has been prioritized, and the combined use of these biomarkers and clinical signs and symptoms provides an effective assessment of ARS risk and outcome (Bertho et al. 2008, 2009, Fliedner et al. 2001; Ossetrova et al. 2007-2018). At the time of emergency, use of complimentary methods of dosimetry is the best appropriate method. At present, protein and gene expression profiling biomarkers have been widely suggested and demonstrated for using in absorbed radiation dose assessment (Bertho et al. 2001, 2008, 2009; Ossetrova et al. 2007 – 2018; Dressman et al. 2007; Paul and Amundson 2008). Protein biomarkers of radiation exposure are the fundamental relevance for the biodosimetry and therapeutic strategies. After exposure, the level of a number of proteins is up- and down- regulated at different time intervals. The oxidative stress response pathway responds to different physiological stresses and expresses many components, such as cytokines, growth factors, cell-cycle and gene regulatory proteins, apoptosis, cell-signaling proteins and DNA repair enzyme proteins.

In this project, biomarkers, multi-parametric biodosimetry algorithm and survival response categories/criteria of ARS outcome were evaluated in a mouse total-body irradiation (TBI) model following either mixed-field (neutrons and gamma-rays) or pure gamma-ray exposure. TBI of B6D2F1/J male and female mice were carried out in the AFRRI TRIGA nuclear research reactor and ^{60}Co pure γ-rays facilities over a broad dose range (1.5 - 12 Gy), dose rates of 0.6 and 1.9 Gy/min, and different proportions of neutrons (n) and gammas (γ) in mixed-field studies from 1 to 7 days after TBI. A list of evaluated biomarkers includes blood cell counts and differentials (CBC/diff), hematopoietic cytokines, organ-specific, and acute phase protein biomarkers. Concept to use of multiple proteomic biomarkers for radiation injury and dose assessment along with a SAS-based multi-parametric algorithm described in AFRRI U.S. Patent “Biomarker Panels for Assessing Radiation Injury and Exposure”, No. 8,871,455 (PCT No: PCT/US2007/013752), issued on October 28, 2014.

Our project studies examine and contribute to further understanding of mechanisms of neutron damage, the RBE for different tissue and organ effects, and how these effects can be correlated to the impact of the whole system would enable us to better estimate the impact of neutron exposure. A murine TBI model with a minimal supportive care was used in order to simulate a catastrophic event involving a large number of casualties. In this scenario, there will be limited medical and physical resources. Early and rapid dose assessment is required in radiation disasters that involve a large number of victims and a finite amount of medical resources available to responders and healthcare providers. The goal of this project is to develop biodosimetric assays to permit early and rapid radiation exposure assessment applicable for a forward field application.

1.1. NON-TECHNICAL SYNOPSIS

The vast majority of studies on the acute radiation syndrome or sickness (ARS) and biodosimetry have been performed using photon irradiation (gamma- and/or x-rays). Risks for acute mortality from radiation exposure are well known to be influenced by physics-based parameters, such as a radiation quality, low or high linear energy transfer (LET), dose rate, total-body vs. partial body exposure, etc. (Hall and Giarcia, 2011). After an enhanced radiation weapon (ERW) or nuclear device detonation, initial radiation at the time of the nuclear reaction consists of gamma-rays and neutrons (mixed-field) produced within the first minute after detonation and its penetration capability, leading to increased damage requiring radiation-quality specific biodosimetry as neutrons, with a higher relative biological effectiveness (RBE), have different mechanisms of injury to cells and tissues compared to photons.

The AFRRI Biological Dosimetry Group has advocated transitioning the proteomics-based approach to deployable platforms to provide a field-deployable point-of-care (POC) and high-throughput (HT) clinical diagnostics. In a 2010-2015 project funded by Biomedical Advanced Research and Development Authority (BARDA), AFRRI supported the Meso Scale Diagnostics (MSD)'s development and evaluation of a minimally invasive (small drop-finger stick), self-administered (ideally), hand-held, field-deployable POC biodosimetry device capable of quickly determining (in few minutes) the radiation dose absorbed by evaluating blood protein biomarker levels after a large-scale radiological or nuclear event. In mouse studies performed, the proteomic biomarkers were evaluated on the MSD multiplex platform in combination with several confounding factors (i.e., stress-effect, infection, 15% of total-body skin surface trauma or burns) alone as well as in combination with total-body gamma-irradiations. Studies were performed in B6D2F1 female mice total-body irradiated (TBI) with a broad range of radiation doses from 1.5 to 14 Gy and blood samples were collected up to 7 days. From a total of twelve protein biomarkers evaluated in those studies, a subset of six injury-insensitive biomarkers was found and used to create the multi-parametric biodosimetry algorithm (dose-response calibration curves) (Sigal et al. 2013). In order to simulate the dose assessment in a real triage situation, blood plasma samples from control and irradiated mice were encoded by AFRRI and given "blinded" to MSD to perform biomarker measurements to assess the irradiation doses using the constructed dose-response calibration curves. The algorithm verification performed independently by AFRRI and MSD demonstrated (93.7 ± 2.1) % accuracy in radiation dose prediction. Proteomic biodosimetry using the multiplex platform and POC device was also evaluated by MSD in nonhuman primate studies performed at AFRRI (Ossetrova et al. 2016a). Those efforts resulted in a preparation of the pre-submission package with data collected in two animal TBI models (mouse and nonhuman primate) required by FDA and also a meeting with FDA in July 2014. Since those animal studies were performed using only gamma-ray exposure, the biomarker levels and the needed dose-assessment modifications for mixed neutron and gamma exposures remained unknown.

The present work evaluated biomarkers for radiation dose assessment (biodosimetry), ARS prognosis/outcome, gender and dose-rate effects following either a mixed-field (gamma-rays and neutrons) using AFRRI TRIGA (Training, Research, Isotope, General Atomic) nuclear research reactor testing different percentage of neutrons and gammas or ^{60}Co pure gamma-rays in a mouse (B6D2F1/J) TBI model. Biomarker measurements were performed using the MSD high-throughput MULTI-ARRAY plate-format platform and some results from ^{60}Co pure gamma-rays studies were compared with ones obtained earlier by MSD and AFRRI in project funded by BARDA. Current efforts supplement an ongoing project to deliver an FDA approved biodosimetry device by potentially expanding the use of its capability for a broader spectrum radiation exposure

(mixed neutrons and gamma-rays). This effort is entirely novel. AFRRI is one of a limited number of facilities with the capability to study mixed-field exposures. The studies on radiation biomarker responses to mixed-field irradiation for use with the Meso Scale Diagnostics biodosimetry system is completely new ground. We expect that this project will contribute to bridge a gap that exists in the current capabilities to identify and then rapidly as well as effectively to assess radiation exposure early after a radiation exposure and especially after a mass-casualty radiological incident. In particular, these efforts contribute to validating an early test to distinguish individuals exposed and injured by radiation in order to assist physicians to choose the appropriate medical treatments and hence reducing the adverse acute effects or long-term risks associated with radiation exposure. The advancement in this type of research might also provide a powerful tool for the accurate assessment of an individual's radiation risk response early after an incident, especially after a mass-casualty radiological incident.

1.2. RELEVANCE TO DOD EMERGENCY PREPAREDNESS MISSION

Radiological terrorist attack or accidental mass-casualty exposures are highly possible. Military personnel responding to such emergencies can be exposed to radiation. Recognizing unpredictable mass casualties, U.S. Department of Defense has given top priority, as stated in the "Defense Technology Objectives (DTO)" to the development of rapid biodosimetry and medical countermeasures to radiation exposure against both early- and late-arising health effects. In the case of mass casualties, it is difficult to screen out the severely exposed patient from the less exposed or not exposed individuals due to lack of immediate and convenient dose measurement technology.

The studies target needs to support radiation diagnostic device (simple, rapid, HT and POC) development efforts based on a multi-parametric biomarker-based biodosimetry diagnostic approach to facilitate treatment triage in a mass-casualty situation, and are also essential to the optimal use of scarce therapeutic resources. This strategy addresses the need for developing a high-throughput multi-parametric "***Field Radiological Biodosimetry***" system and promotes effective command decisions and force structure planning to ensure mission success. This system should be compatible with military field laboratories, homeland security applications, as well as with radiation therapy centers to assess radiation exposure based on blood protein biomarkers capability. In addition, assessment of a population's exposure to other radiation threats, such as nuclear accidents and terrorism mass casualty scenarios addresses the need for a "***Clinical Radiological Biodosimetry***" system to provide physicians with the ability to triage radiation victims, make appropriate treatment decisions, and reduce uncertainties associated with the variability of individual response to radiation exposure.

2. BACKGROUND

The increasing threat from a radiological weapon of mass destruction has underscored the need for early biodosimetric evaluation as part of initial medical triage. Several scenarios of large-scale radiological events include the use of improvised nuclear devices (IND) that may produce gamma rays and a significant neutron component with prompt radiation exposure (National Planning Scenarios [final version 21.3]. Homeland Security Council. 2006). Specifically, the prompt radiation from this type of detonation is expected to be qualitatively similar to that of the 15-kT device exploded over Hiroshima (Egbert et al. 2007). The use of ionizing radiation sources for medical, industrial, military, and research purposes has increased the risk of accidental occupational exposures. Large numbers of individuals have been exposed to various levels of

mixed-field radiation caused by nuclear accidents such as Chernobyl (Guskova et al. 1990; Baranov et al. 1995) and Fukushima Daiichi (Katata et al. 2012), atmospheric nuclear testing (Fehner and Gosling 2006), the atomic bombing at Hiroshima and Nagasaki (Awa et al. 1971; Egbert et al. 2007) and some industrial criticality accidents in Oak Ridge (Goans et al. 2015, 2017) and Tokai-mura JCO facilities (Muramatsu et al. 2001).

Of all ionizing particles, neutrons can cause significant damage regardless of their energy level, are the most difficult to shield from, and the only type of radiation that can contaminate any absorbing material thereby rendering it radioactive. While low-linear-energy-transfer (low-LET) radiation, such as photons (γ- or x-rays) and electrons, causes ionization sparsely distributed along their track and, almost homogeneously within a cell, high-LET radiation, such as neutrons, causes dense/clustered ionizations and localized DNA damage that is more difficult to repair than the diffuse DNA damage caused by low-LET radiations (Mognato et al. 2011). Studies of neutron vs. photon effects in tissues have shown differences in gene expression related to DNA damage, cell cycle delays, oxidative stress degeneration, regeneration, apoptosis and transcription (Cary et al. 2012). Double strand breaks (DSB) and non-DSB-clustered DNA lesions are hallmarks of high-LET radiations. Tsoulou and colleagues used the perturbed angular correlation (PAC) and the thermal transition spectrophotometry (TTS) methods, two different approaches to study of the effects of radiation on DNA, in order to demonstrate that neutron and gamma irradiation of buffered solutions of calf thymus DNA resulted in changes in the dynamics of the macromolecule. Both methods showed that neutrons are more effective than gamma rays in inducing DNA damage and the flexibility of DNA decreased as indicated by slower rotation of the molecules (Tsoulou et al. 2003, 2005). As a result, laboratory studies show that, compared with pure photon irradiation, mixed-field (n + γ) irradiation causes increased mortality, decreased survival time and latency period in ARS, and delays the healing time of injuries (wound and/or burn) suffered in combination with radiation (Ledney et al. 2000; MacVittie et al. 1991; Ledney and Elliott 2010). The mechanisms of injury of low-LET radiation are different from those of high-LET radiation, which may affect dose assessment/prediction and radiation countermeasure efficacy (MacVittie et al. 1991; Ledney et al. 2000; Cary et al. 2012).

In addition to a direct biological damage by neurons described above, there is also a process of neutron radiation-induced radioactivity in materials or tissues. Neutron activation process occurs when atomic nuclei capture free neutrons, becoming heavier and entering excited states. The excited nucleus often decays immediately by emitting gamma rays, or particles such as beta particles, alpha particles, fission products, and neutrons (in nuclear fission). Thus, the process of neutron capture, even after any intermediate decay, often results in the formation of an unstable activation product. Such radioactive nuclei can exhibit half-lives ranging from small fractions of a second to many years. For example, activation of sodium in the human body to sodium-24 (in blood), and phosphorus to phosphorus-32 (in hair), can give a good immediate estimate of acute accidental neutron exposure (ORNL Report 1993). A comprehensive review of accident neutron dosimetry using blood and hair analysis was performed and summarized in this report. Experiments and calculations were conducted at Oak Ridge National Laboratory (ORNL) and the University of Tennessee (UT) to develop measurement techniques for the activity of ^{24}Na in blood and ^{32}P in hair for nuclear accident dosimetry. An operating procedure was established for the measurement of ^{24}Na in blood using an HPGe detector system. This nuclear accident dosimetry system makes it possible to estimate an individual's neutron dose within a few hours after an accident if the accident spectrum can be approximated from one of 98 tabulated neutron spectrum descriptions. If the information on accident and spectrum description is not available, the activity

ratio of ^{32}P in hair and ^{24}Na in blood can provide information related to the neutron spectrum for dose assessment (ORNL Report 1993).

Figure 2.1 shows the concentrations of radionuclides determined in biological materials collected from three patients exposed in the Tokai-mura criticality accident. The activation products, such as ^{24}Na, ^{42}K and ^{82}Br, which were produced by neutrons bombarding the respective target isotopes (^{23}Na, ^{41}K and ^{81}Br) in the body, were detected 26-27 hours after the exposure. Biological materials, such as blood, urine, vomit and hair, were collected from the workers and analyzed for radio-activities, produced/activated by the neutron irradiation. Activation products, such as ^{24}Na, ^{42}K and ^{82}Br, and many other isotopes were found in these materials by gamma-ray spectrometry using HPGe detectors. Isotope activity levels were detected in a strongly radiation dose-dependent manner. Radioactive isotopes ^{24}Na (γ-rays energy of 1.4 MeV, half life time is about 15 hours) and ^{42}K (γ-rays energy of 1.5 MeV, half-life time is about of 12.4 hours) were found in blood as ^{82}Br (beta-decay, energy of 0.7 MeV, half-life time is about of 35 hours) was found in urine and vomit (Muramatsu et al. 2001).

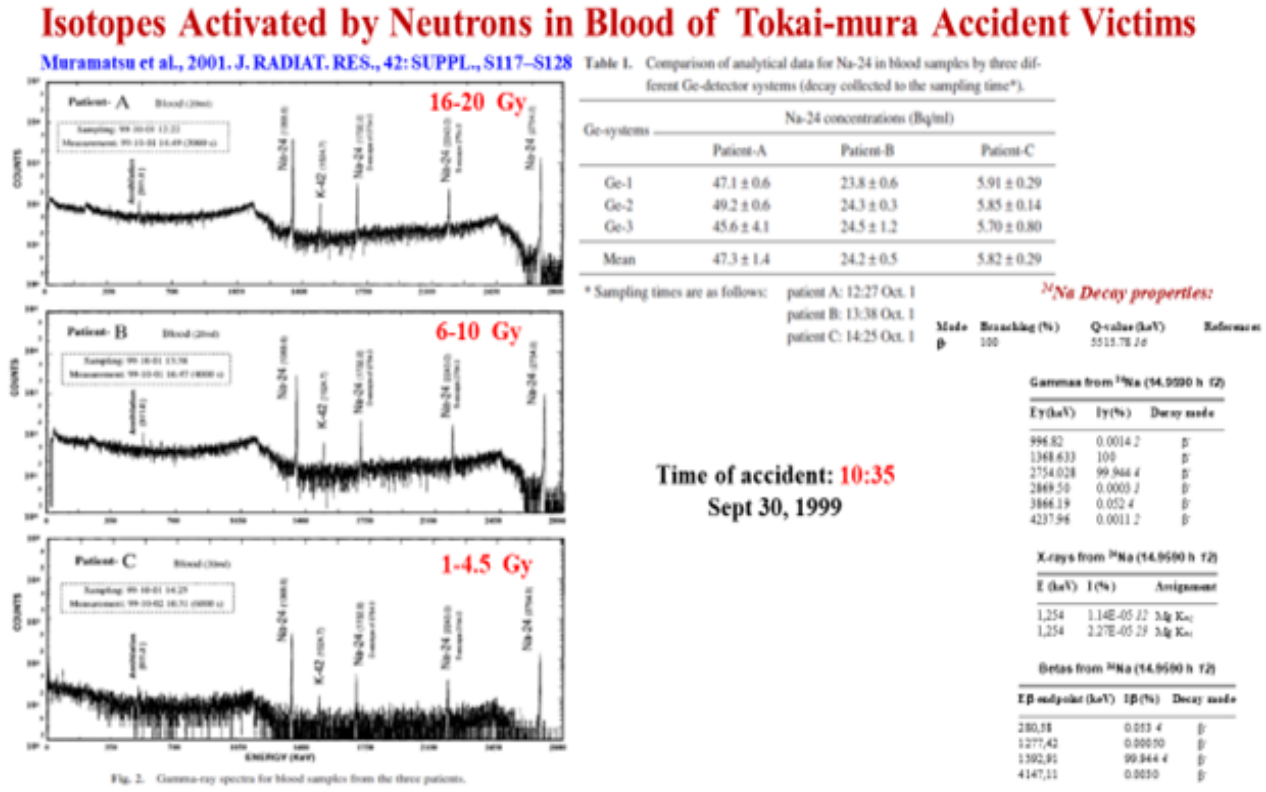

Table 1. Comparison of analytical data for Na-24 in blood samples by three different Ge-detector systems (decay collected to the sampling time*).

Ge-systems	Na-24 concentrations (Bq/ml)		
	Patient-A	Patient-B	Patient-C
Ge-1	47.1 ± 0.6	23.8 ± 0.6	5.91 ± 0.29
Ge-2	49.2 ± 0.6	24.3 ± 0.3	5.85 ± 0.14
Ge-3	45.6 ± 4.1	24.5 ± 1.2	5.70 ± 0.80
Mean	47.3 ± 1.4	24.2 ± 0.5	5.82 ± 0.29

* Sampling times are as follows: patient A: 12:27 Oct. 1; patient B: 13:38 Oct. 1; patient C: 14:25 Oct. 1

Figure 2.1. Neutron activation analysis results for concentrations of radionuclides in biological materials collected from three patients exposed in the Tokai-mura criticality accident (Muramatsu et al. 2001).

It was demonstrated at AFRRI that in mammalian species, the activation products of primary concern include ^{24}Na, ^{38}Cl, and ^{42}K because of their relative abundance in living cells. Those isotopes have a short half-life time (few hours) and were reported to be neutron-activated at the very low residual radioactivity (<0.5 uCi) (Hall DE, 2009. Modeling and Validation of Dosimetry Measurement Assumptions Within The Armed Forces Radiobiology Research Institute

TRIGA Mark-F Reactor and associated Exposure Facilities using Monte Carlo Techniques. In a recent guidance for medical aspects of radiation incidents published by the Radiation Emergency Assistance Center/Training Site (REAC/TS), it is stated that the medical management of patients with acute, moderate to severe radiation exposure (effective whole-body dose > 2 Gy) should emphasize the rapid administration of colony-stimulating factors (CSF) to enhance hematopoietic recovery (REAC/TS 2017). Therefore, in triage categories, a 2 Gy dose of effective whole-body exposure is currently considered the threshold for medical intervention (AFRRI 2013; Moyer et al. 2015). However, absolute reliance on this threshold ignores the impact of radiation quality and is of concern because neutrons are a significant component of the radiation initially released by a fission nuclear device; hence, there is a current need to accurately determine exposure levels where mixed field combinations of neutrons and gamma are a threat.

3. PROJECT STUDY DESIGN

3.1. TASKS AND EXECUTION PLAN

The project included the following overlapping tasks as in original Statement of Work (SOW) listed below and summarized in Table 3.1.1:

- **Task 1**: Prepare the Institutional Animal Care and Use Committee (IACUC) protocol, write standard operating procedure (SOP) protocols, create the Contact with Jackson Lab to deliver the mice (i.e., B6D2F1/J female and male), plan and prepare animal orders and coordinate with Veterinary Sciences Department (VSD), schedule use of radiation sources (TRIGA nuclear reactor and ^{60}Co γ-rays) and VSD resources for radiation studies. Get the RAD-PI Authorization to perform TRIGA nuclear reactor studies, hiring the Henry M. Jackson Foundation (HJF) personnel, complete VSD and Rad trainings for personnel, preparing labs and lab supplies, etc.

- **Task 2**: Perform the dose-response radiation mixed-field (67% n + 33% γ) study (1.5, 3, and 6 Gy at dose-rate of 0.6 Gy/min) using 14-16-wk old female mice.

- **Task 3**: Perform the dose-response radiation mixed-field (30% n + 70% γ) study (1.5, 3, and 6 Gy at 0.6 Gy/min) using 14-16-wk old female mice.

- **Task 4**: Perform low-LET dose-rate effect study with ^{60}Co γ-rays (3, 6 and 12 Gy and dose-rates of 0.6 and 1.9 Gy/min) using 14-16-wk old female mice.

- **Task 5**: Perform high-LET dose-rate effect study with MF (67% n + 33% γ) doses of 1.5 , 3 and 6 Gy and dose-rate of either 0.6 or 1.9 Gy/min) using 14-16-wk female old mice.

- **Task 6**: Perform the 30-d survival study after radiation with MF (67% n + 33% γ) to doses of 4, 5, 6, 7 Gy at dose-rate of 0.6 Gy/min) using 16-wk female old mice to investigate the effect of exposure to different doses of MF in order to find associations between protein expression profile, hematology parameters, body weight, temperature, symptoms and signs related to the radiation dose and hematopoietic and gastrointestinal sub-syndromes of the ARS and create the Acute Radiation Sickness (ARS) severity score system. Compare results with ones collected earlier in ^{60}Co γ-rays studies.

- **Task 7**: Perform gender comparison studies with low-LET (^{60}Co γ-rays; doses of 3, 6 and 12 Gy) and MF (67% n + 33% γ) doses of 1.5, 3 and 6 Gy) at dose-rate of 0.6 Gy/min) using 14-16-wk old female and male mice.

- **Task 8**: Perform proteomic biomarker measurements using a Meso Scale Diagnostics (MSD) high-throughput (HT) MULTI-ARRAY plate-format platform and enzyme-linked immunosorbent assay (ELISA) kits. Perform hematological biomarker measurements and preliminary data analysis on time of experiment.

- **Task 9**: Analyze biomarker data collected in mixed-field (n + γ) studies (i.e., different percentage of neutrons and gammas, dose-rates, gender comparison) and compare results with ones collected in ^{60}Co (100% γ-rays) studies.

- **Task 10**: Perform the advanced statistical data analyses on <u>all data</u> collected and create the mixed-field (n + γ) and pure γ-rays biodosimetry algorithm equations using the multi-parametric statistical analysis software (SAS or STATISTICA 12, multi-ROC, Table Curve 2D and 3D, Sigma Plot, etc.).

- **Task 11**: Prepare a Final Report.

Table 3.1.1. Research Plan and Execution as in Original Statement of Work (SOW).

#	Brief Task Description (24-month project)	Duration
1	IACUC protocol, SOP protocols, RAD-PI Authorization, hiring HJF personnel, Contact with Jackson Lab, VSD and Rad trainings, preparing labs and lab supplies, etc.	4 months
2	Mixed Field (MF) (67% n + 33% γ) radiation study (1.5, 3, and 6 Gy at 0.6 Gy/min)	2 months
3	MF (30% n + 70% γ) radiation study (1.5, 3, and 6 Gy at 0.6 Gy/min)	2 months
4	^{60}Co γ-rays (3, 6 and 12 Gy) dose-rate study (0.6 and 1.9 Gy/min)	3 months
5	MF (67% n + 33% γ) (1.5, 3 and 6 Gy) dose-rate study (0.6 and 1.9 Gy/min)	3 months
6	30-day survival study & ARS severity score system; MF (67% n + 33% γ) irradiation (4, 5, 6, 7 Gy) at 0.6 Gy/min	2 months
7	Gender comparison studies MF (67% n + 33% γ) (1.5, 3, and 6 Gy) and ^{60}Co γ-rays (3, 6, 12 Gy) at 0.6 Gy/min	3 months
8	Proteomic biomarker measurements using a MSD HT MULTI-ARRAY plate-format platform and ELISAs.	4 months
9	Perform advanced statistical data analyses on all data collected and create the mixed-field (n + γ) and pure γ-rays biodosimetry algorithm equations. Compare results with ones earlier obtained in ^{60}Co γ-rays studies. Prepare a Final Report.	4 months

Period of Performance

The period of performance (POP) with multiple tasks overlapping is 24 months starting from the day when funds being loaded to Finance System (DAI) and Henry M. Jackson Foundation (HJF) for the Advancement of Military Medicine (for project personnel).

3.2. DATA ANALYSIS

Number of animals n=8-14 per group (dose, and sampling time-point) is necessary for the dose-response, dose-rate and gender-comparison experiments. It has been determined by AFRRI statistician from similar studies to provide power >90% for two-tailed Student's t-test to get two standard deviations (2 STD) or 95% confidence interval in distinguishing animal groups and less than 10% shifts in biomarker values (reproducibility). Values of $P < 0.05$ were considered statistically significant. An increase in the number of animals per group up to n=10-14 for TBI doses of ≥3 Gy (TRIGA) and ≥ 6 Gy (^{60}Co) at sampling time-points 4 and 7d is necessary in order to provide the sufficient statistical accuracy because at this dose and later time points there is expected to be potential early morbidity (from 30% to 70% in the 30-d monitoring period) by developing hematopoietic syndrome as well as a broadening of the distribution of radiation responsive biomarkers.

In 30-day survival study, 20-32 mice per treatment group were used for measurement of animal survival endpoints. Number of mice were increased from 20 to 32 due to statistical justification provided below. The 20 mice per group could have 80% power to detect a significant difference between two groups, given type I error of 5% and a treatment group survival rate of at least 73%, if the control group is 25%. Similar statements would apply, provided the treatment groups display survival of at least 86%, 83%, or 78%, if the respective control groups would be 40%, 35%, and 30%, respectively. Note: power analysis may suggest smaller groups are adequate. However, radiobiologists at AFRRI and elsewhere observe considerable variability from experiment to experiment in mouse survival studies that is not reflected in the power analysis. In fact, some institutions have gone to a group size of 30 in these types of experiments for this reason.

Statistical software, PC SAS, were used for statistical data analysis (SAS Institute Inc., 2000) as previously described (Ossetrova et al. 2007-2018). Multivariate analysis of variance (MANOVA) Wilks' Lambda statistics were used when comparing more than two groups and two-sided Student's *t* test were used when comparing two groups to determine significant differences among observational time-points in radiation biomarkers studies and ARS severity degree categories.

Multiple linear regression analysis was used to develop dose-response relationships for multiple biomarkers for radiation dose prediction at the 95% confidence level (CL). To study the dependence of each biomarker on dose assessment the analysis was performed according to following model: $Y=a+b1*X1+b2*X2+...+bp*Xp$, where Y variable (dose prediction in Gy) can be expressed in terms of a constant (a) and a slope (b) times the X variables (biomarker data in pg/ml, or ng/ml, or number of cells per μl), p is a number of biomarkers in the model. The standardized raw regression coefficients (b) represent the independent contributions of each independent variable (biomarker) to the prediction of the dependent variable (dose). The magnitude of b coefficients allows one to compare the relative contribution of each independent variable in the prediction of radiation dose absorbed.

The PC SAS stepwise multivariate discriminant function analysis was performed to separate irradiated animal groups from non-irradiated ones and also to demonstrate accurate radiological detection into tertiles of doses 0-1.5 Gy, 1.5-3 Gy, and 3-6 Gy and ARS RCs based on selected biomarker or combination of biomarkers detected from biological samples. The discriminant function can use several quantitative variables (biomarkers); each of them makes an independent contribution to the overall discrimination. Taking into consideration the effect of all quantitative variables, this discriminant function produces the statistical decision for predicting to which subgroup of classification variable each subject (animal) belongs.

The Table Curve 2D and 3D statistical software were used to create the dose- and time-dependent fitting equations for biodosimetry-based biomarkers in order to estimate the radiation dose received based on biomarker level(s) at any time-point other than at collection time in experiment (i.e., d1, d2, d4 and d7).

Receiver Operating Characteristic curve (or ROC curve) was used to demonstrate the sensitivity and specificity of the proposed protein and hematological biomarkers to reflect subgroup (dose and sampling time-point) differences. Results were shown as a ROC plot of the true positive rate against the false positive rate for the different possible cut-points of a diagnostic test. Kaplan-Meier survival curves were constructed to determine the survival time probability and compare with survival results obtained in ^{60}Co γ-rays studies. Biomarker results and ARS severity score system received in high-LET (mixed-field) experiments were compared with ones received in irradiations performed with low-LET (^{60}Co γ-rays) (Ossetrova et al. 2009-2018).

4. MOUSE RADIATION MODEL AND SPECIES JUSTIFICATION

4.1. SPECIES JUSTIFICATION

The mouse model was chosen for this *in vivo* validation study for the following reasons: (1) FDA two-animal rule in radiation biodosimetry and countermeasure studies; (2) it is well-defined immunological animal model for this type of research; (3) qualitative similarities exist between human and mouse proliferative tissue including bone marrow (Thompson 1962); (4) molecular responses of mouse and human peripheral blood to gamma radiation are expected to be similar; (3) the ease of use of a mouse model system ensures reliable data collection; (6) median lethal doses (LD50/30) for radiation-induced death for this strains of mice is known (Hendry 1995; Ledney et al. 1990, 2010; Kiang et al. 2014); (7) model provides experimental and statistical validity; (8) AFRRI staff has an extensive experience with mice, including B6D2F1 mice, in radiation injury and countermeasure research.

B6D2F1/J female and male mice obtained from the Jackson Laboratory (Bar Harbor, ME), 14-18 wk old (weighing approximately 22 – 26 g) were used for these studies. Mice were housed under conventional conditions in microisolator filter-top cages in a facility fully-accredited by the Association for Assessment and Accreditation of Laboratory Animal Care (AAALAC) International and treated in accordance with principles outlined in the *Guide for the Care and Use of Laboratory Animals* of the Institute for Laboratory Animal Research, National Research Council. Animal rooms were provided with 10 – 12 air changes h^{-1} of 100 % fresh conditioned air and maintained at 22 (± 2) °C and a relative humidity of 50 (± 20) %. Animals remained on 12:12-h full-spectrum light: dark cycles and received *ad libitum* food (Rodent Diet #8604, Harlan Teklad, Madison, WI) and water (acidified with HCl to a pH of 2.5 – 2.8). Mice were acclimated a few days before sham treatment or exposure to ionizing radiation either with TRIGA or Cobalt.

Total of 1302 mice (1032 females and 270 males) were used in studies. In both radiation studies, animals were either total-body irradiated (TBI) or treated in the same manner but were not exposed to the radiation source (sham-irradiated). Control mice were not placed into aluminum tubes or Plexiglas® boxes nor transported to the radiation facilities. Comparison of results for sham- and control-group evaluated any effect of stress induced through the handling of the mice as it was performed in earlier ^{60}Co studies (Ossetrova et al. 2011-2016).

B6D2F1/J mice were selected for those studies based on earlier work done in low-LET (^{60}Co γ-rays) studies to evaluate the proteomic biomarkers, in both TBI-only studies as well as in studies including confounding factors (i.e., stress, wound, burn, infection, combined injury) in order to create the biodosimetry algorithm on Meso Scale Diagnostics' (MSD) point-of-care

(POC) and high-throughput (HT) multiplex platforms (Sigal et al. 2013; Ossetrova et al. 2016b). At AFRRI, this strain is well characterized as high- and low-LET radiation combined (TBI and wound/burn) injury murine model by Dr. Ledney and colleagues (Ledney et al. 1991, 2010; Stewart et al. 1982; McChesney et al. 1990; Brook et al. 1993).

4.2. ANIMAL HOUSING AND IDENTIFICATION

Mice were housed in groups of 4-6 per cage. They were identified by cage cards using GLP SOP Rodent Cage Cards. Each card states the investigator's name, protocol number, experiment number, cage number, start date, end date, species, item number (animal lot), birthdate, gender, strain, number of animals in the cage, vendor, arrival date, treatments, and dates of death, including the initials of the staff person who found and removed the dead animals. In addition, mice in mixed-field survival study were identified by tattoo for individual tracking (Fig. 4.2.1).

http://www.somarkinnovations.com/ 30

Fig. 4.2.1. Animal identification by tattoo for individual tracking in TRIGA reactor mixed-field survival study.

In a pure γ-rays survival study, mice were identified by IPTT-200, Bio Medic Data System (BMDS) implantable programmable transponders/microchips (BMDS, Seaford, DE) implanted subcutaneously between the shoulder blades under isoflurane anesthesia, 14 days prior to irradiation (Fig. 4.2.2.). Two weeks were a sufficient amount of time for complete recovery after the microchip implantations. Observations were recorded using the BMDS electronic data recording system.

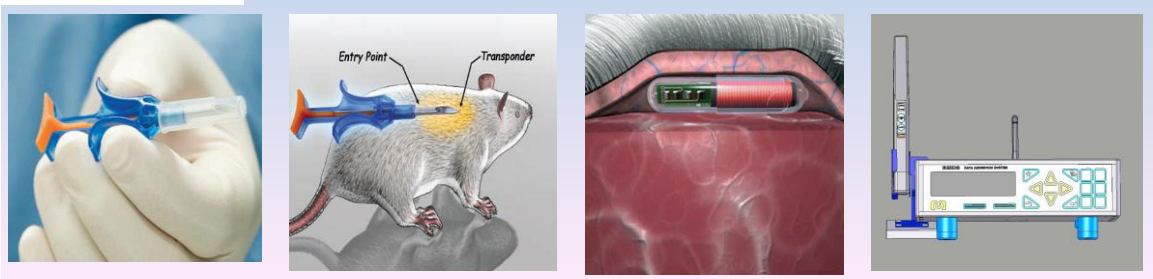

Fig. 4.2.2. Animal identification by BMDS implantable programmable transponders/microchips for individual tracking in ^{60}Co γ-rays survival study.

4.3. STUDY ENDPOINT

The endpoint of the studies was euthanasia at the predetermined terminal blood collections (dose-response, dose-rate and gender-comparison studies) and based on assessment of moribundity (survival study). Clinical observations for pain and distress in mice were conducted by the project personnel at least twice daily and the number of observations were increased in a critical period of ARS (pancytopenia). This monitoring schedule included weekends and holidays.

To minimize animal pain or distress, moribund animals were scored according to observational mouse intervention score system/sheet with criteria for rodent euthanasia (IACUC policy #10 developed at the AFRRI VSD) and euthanized, if criteria were met, as outlined in section Euthanasia. This mouse intervention score system was developed to define the morbidity or moribundity in irradiated mice and includes numerical values (score) for appearance, respiratory rate, general behavior, provoked behavior, and body weight loss (Koch et al. 2016; Ossetrova et. al. 2016). Mice that survived the 30-d monitoring period after irradiation were euthanized. Sham mice from survival study may be transferred to another VSD approved protocol.

4.4. ANESTHESIA / ANALGESIA / TRANQUILIZATION

In these studies, experiments were conducted with a minimal supportive care in order to simulate a catastrophic event involving large number of casualties. In this scenario, there will be limited medical and physical resources. Systemic antibiotics, anesthetics or analgesics will not be used as in previous radiation only (not combined injury) studies. If wounding occurs via in-cage fighting, topical antibiotics will be applied under the guidance of the veterinarian in accordance with standard treatment measures.

Anesthesia using standard isoflurane rodent anesthesia machine under the guidance of the VSD was carried out in mice for blood collection. Animals were placed in the induction chamber and delivered a metered amount of 3-5% isoflurane mixed with 100% oxygen (at the flow rate of 500-1000 cc/min) until all voluntary motor movement ceases and the animal is recumbent for 10 seconds. Animal's respiration rate was closely monitored through the Plexiglas chamber during induction of anesthesia. The toe pinch response was used to determine the depth of anesthesia. The tail was pinched for reflexive movement, indicative of insufficient anesthesia. If there is no response, the animal was moved to the station with individual nose cone for maintenance of anesthesia at 1-3% isoflurane and 100% oxygen at 500-1000 cc/min to perform blood collection.

4.5. EUTHANASIA

In studies with terminal blood sample collections, mice first were deeply anesthetized with isoflurane and then euthanized by cervical dislocation that was performed by protocol personnel. In the survival study, irradiated mice that survived monitoring period (30 days) were transferred to the VSD training protocol. Moribund animals that met IACUC Policy #10 euthanasia criteria were euthanized by VSD staff or protocol personnel. Euthanasia of mice was performed by CO_2 inhalation followed by cervical dislocation and their carcasses were disposed according to VSD SOPs.

4.6. EXCEPTIONS

Mice were socially (group) housed, except for the possibility that during survival study cagemates may be lost through attrition and for a period of time the sole surviving mouse may remain singly housed until the end of the 30-day study. When this occurs, singly housed animals were able to view con-specifics in neighboring cages housed on the same rack in the same room.

4.7. BIOHAZARDS / SAFETY

The primary radiation hazard to project personnel arises from potential exposure to mouse tissues made radioactive as a result of neutron activation of various elements within those tissues. Activation products of primary concern include ^{24}Na, ^{38}Cl, and ^{42}K because of their relative abundance in living cells. Those isotopes have a short half-life time (few hours) and were reported to be neutron-activated at the very low residual radioactivity (<0.5 uCi) (Hall DE, 2009. Modeling and Validation of Dosimetry Measurement Assumptions Within The Armed Forces Radiobiology Research Institute TRIGA Mark-F Reactor and associated Exposure Facilities using Monte Carlo Techniques).

All protocol personnel have had a VSD safety training, general radiation users training and additional ones specialized to irradiations with reactor provided by Health Physics Department (HPD) and Radiation Sciences Department (RSD). Appropriate personal dosimeters (i.e., TLD, self-reading pocket chamber and finger-ring dosimeter) were worn at all time when working in reactor area. Reactor-irradiated mice were monitored for radiation level by HPD staff and were released to the project personnel when declared non-radioactive.

5. IRRADIATIONS WITH TRIGA NUCLEAR REACTOR (MIXED NEUTRONS AND GAMMA RAYS)

Total-body irradiations of mice were performed using AFRRI 1-MW TRIGA (Training, Research, Isotope, General Atomic) Mark-F reactor in an exposure room with thermal neutron flounces drastically diminished by gadolinium paint. The radiation fields providing various contributions to the total dose from neutrons and photons are created by varying thicknesses of water and lead shields, which have different absorption abilities with respect to radiation of these different modalities (Fig. 5.1.).

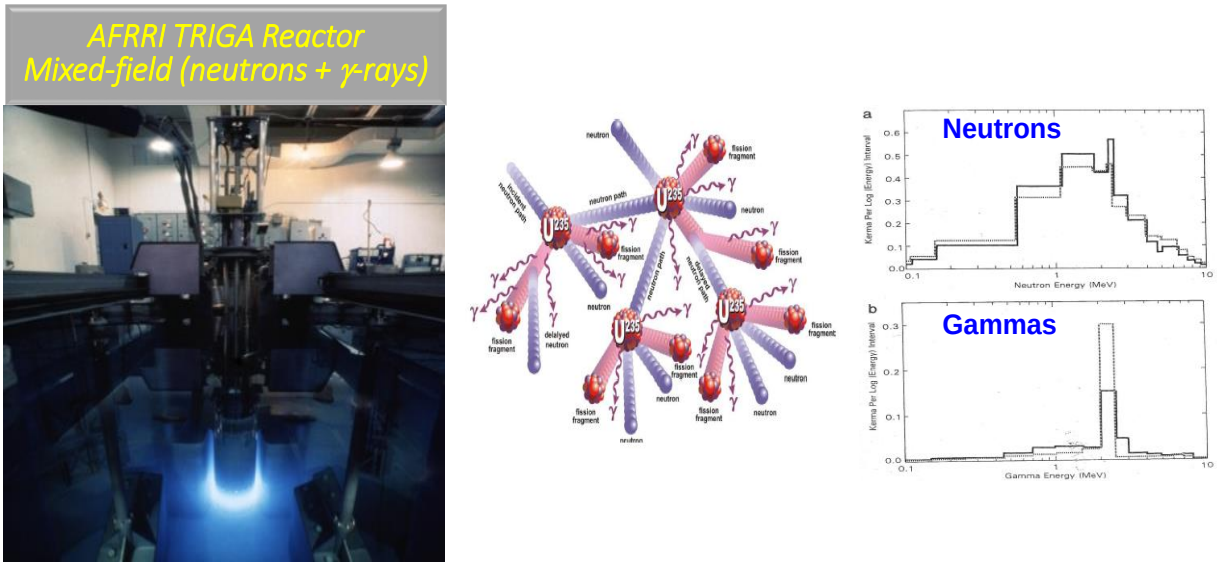

Fig. 5.1. AFRRI TRIGA (Training, Research, Isotope, General Atomic) Mark-F reactor for radiation studies. The reactor-produced energies for gammas and neutrons ranged from 10 keV to 10 MeV and from 0.1 to 10 MeV, respectively. The average gamma and neutron energy for these spectra were ~1.5 and 2 MeV, respectively.

The 1-MW TRIGA (Training, Research, Isotope, General Atomic) Mark-F nuclear research reactor is capable of delivering a mixed linear energy transfer (LET) field of fission neutrons and gamma-rays (infinitely variable neutron/gamma ratio from 97% neutron to 97% gamma) to a number of experimental targets. Large exposure rooms allow the flexibility of variable shielding configurations to customize the neutron-gamma ratio. The ratio ranges from a nearly pure neutron field to a nearly pure gamma-ray field. In addition, the moveable core, combined with neutron filtering material, permits shifting of the neutron spectrum energies within the exposure rooms. Large exposure rooms enable spectral manipulation (full range from slow to fast neutrons to simulate different exposure scenarios.

Steady state operation of the reactor delivers a peak in-core neutron flux of approximately 1013 n/cm^2/s. Pulsing operation of the reactor is capable of simulating nuclear weapon detonations by producing a lethal dose in milliseconds. Steady state exposure produces a wide range of dose rates from low chronic levels to extremely high exposure rates. Fields with neutrons providing 67% and 30% of the total dose were used. The reactor-produced energies for gammas and neutrons ranged from 10 keV to 10 MeV and from 0.1 to 10 MeV, respectively. The average gamma and neutron energy for these spectra were ~1.5 and 2 MeV, respectively as shown in Fig. 5.1.

Mice were irradiated in a specially designed mouse rotator made of aerated aluminum tubes, which contained 40 mice in vertical positions. Mice were restrained vertically in 1.8-mm-thick aluminum tubes that were rotated at 1.5 rpm and received mixed-field of fission neutron and gamma radiation produced by the reactor while it was operated in a steady-state mode. TBI was given as a single exposure. Mouse rotator was placed 255 cm from the core center at the center of a table (Fig. 5.2). The desired ratio of neutron and gamma doses was produced by means of shielding that consisted of a minimal possible thickness of water between the reactor core in the pool (approximately 60 cm in diameter), the reactor tank wall, and a 6-inch lead wall. Irradiations were done at steady-state with mean energy of 0.71 MeV using uranium zirconium-hydride (UZrH) as the fuel element. Animals were either total-body irradiated or treated in the same manner, but not exposed to the radiation source (sham-irradiated). Control mice were not placed into tubes nor transported to the radiation facilities. Comparison of results for sham and control group evaluated effect of stress induced by handling of mice as it was performed in earlier ^{60}Co γ-rays studies (Ossetrova et al. 2011-2018ab).

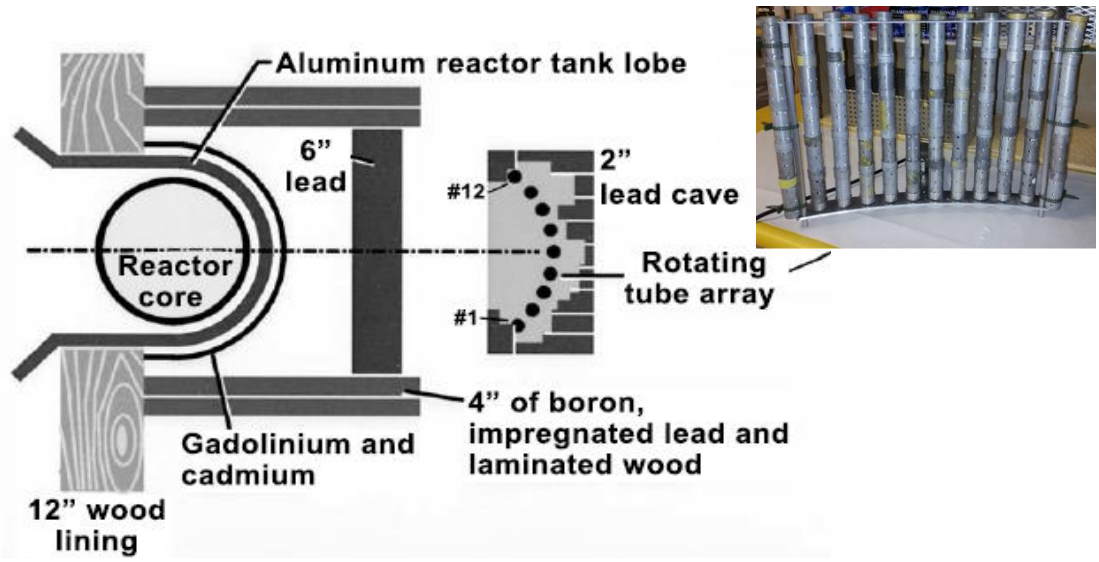

Fig. 5.2. TRIGA-reactor exposure array for mouse irradiation experiments.

Dosimetry was performed with paired ionization chambers that had different sensitivities to neutrons and photons (ICRU Report 26. 1977; Wootton et al. 1980; Goodman 1985). A tissue-equivalent chamber filled with a tissue-equivalent gas exhibited comparable sensitivities to neutrons and photons. The paired magnesium chamber filled with argon had much higher sensitivity to photons than to neutrons. The sensitivity coefficients of each chamber in the specific radiations fields were determined by calculating spectrum-weight-averages of the gas ionization energies, stopping powers and mass energy absorption coefficients using neutron and photon spectra of the fields.

Table 5.1 shows the TRIGA reactor mixed-field radiation biodosimetry study design in mouse irradiation model. Reactor study includes the dose-response at different percentage of neutrons (67% vs. 30%), dose-rate (0.6 vs. 1.9 Gy/min), gender-comparison (females vs. males) and a 30-day survival experiments. Blood was collected 1, 2, 4, and 7 days after TBI in all experiments, except the 30-day survival study.

Table 5.1. TRIGA reactor mixed-field (n + γ) radiation biodosimetry and survival studies design in mouse irradiation model.

Exp # /Code	Date of TBI	Radiation doses	Study Title	# of runs	Mixed-field percentage conditions	Dose rate, Gy/min	# of mice
1 (**T1**)	5/16/16	Sham, 1.5, 3, and 6 Gy	Dose-response study	3	67% n + 33% γ	0.6	106 irradiated, 24 sham, 20 control/ females
2 (**T5**)	6/1/16	Control, 4, 5, 6, 7 Gy	Survival Study	4	67% n + 33% γ	0.6	92 irradiated, 12 control/ females
3 (**T2**)	6/6/16	Sham, 1.5, 3, and 6 Gy	Dose-response study	3	30% n + 70% γ	0.6	106 irradiated, 32 sham, 27 control/ females
4 (**T3**)	6/20/16	Sham, 1.5, 3, and 6 Gy	Dose-rate study	3	67% n + 33% γ	0.6	106 irradiated, 32 sham / females
5 (**T4**)	7/11/16	Sham, 1.5, 3, and 6 Gy	Dose-rate study	3	67% n + 33% γ	1.9	110 irradiated, 32 sham / females
6 (**T6**)	7/25/16	Sham, 1.5, 3, and 6 Gy	Gender comparison study	3	67% n + 33% γ	0.6	108 irradiated, 32 sham /males

6. IRRADIATION WITH ^{60}Co (PURE GAMMA RAYS)

In pure gamma-rays studies, the bilateral total-body irradiations of mice were performed in well-ventilated Plexiglas® boxes at the AFRRI ^{60}Co γ-ray facility. The large, wet source storage panoramic ^{60}Co irradiator provides a 1.17 and 1.33 MeV gamma-ray field covering a wide range of dose rates. The bilateral irradiation configuration is ideal for dose uniformity, and is capable of delivering chronic and acute dosing schemes in excess of 75 Sv/min (7,500 rem/min) (Fig. 6.1).

TBI was given as a single exposure. Mice (females and males) in dose cohorts (n = 8 – 12) were irradiated with total doses of 3, 6 and 12 Gy at the dose rate of either 0.6 or 1.9 Gy/min (Table 6.1). Dosimetry was performed using an alanine/electron paramagnetic resonance system, with calibration factors traceable to the National Institute of Standards and Technology and

confirmed by an additional check against the national standard ^{60}Co source of the UK National Physics Laboratory.

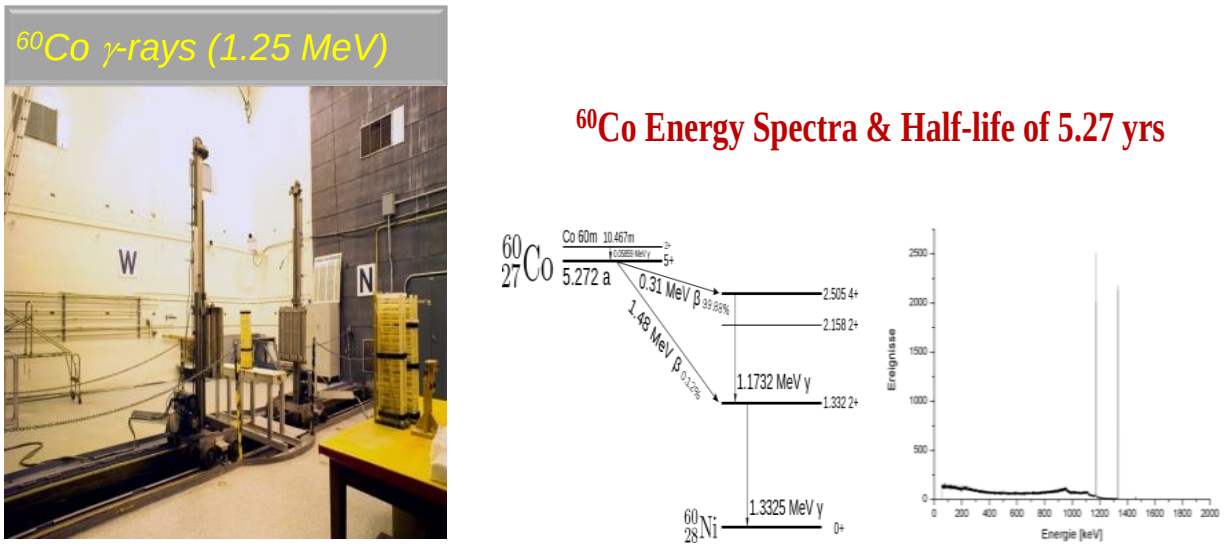

Fig. 6.1. AFRRI high ^{60}Co γ-rays facility (left) and ^{60}Co γ-rays energy spectra (right).

Table 6.1. ^{60}Co γ-rays radiation biodosimetry study design in mouse irradiation model.

Exp # /Code	Date of TBI	Radiation doses	Study Title	# of runs	Dose rate, Gy/min	# of mice/ gender
1 (**C1**)	3/27/17	Sham, 3, 6, 12 Gy	Dose-response study	3	0.6	98 irradiated, 32 sham / females
2 (**C3**)	5/15/17	Sham, 3, 6, 12 Gy	Dose-rate study	3	0.6	98 irradiated, 32 sham /females
3 (**C4**)	6/12/17	Sham, 3, 6, 12 Gy	Dose-rate study	3	1.9	104 irradiated, 32 sham / females
4 (**C6**)	4/17/17	Sham, 3, 6, 12 Gy	Gender comparison study	3	0.6	98 irradiated, 32 sham / males

7. MOUSE BLOOD SAMPLE COLLECTIONS FOR BIODOSIMETRY ASSAYS

Blood sample collections

Peripheral blood was drawn from mice while under anesthesia via cardiac puncture at the designated sampling time points after exposure (1 d, 2 d, 4 d, and 7 d). Drawn blood was collected into potassium EDTA vacutainer tubes (Becton, Dickinson and Company, Franklin Lakes, NJ) for complete blood cell counts with differentials (CBC/diff) and proteomics bioassays.

Peripheral blood biosampling, blood cell counts and protein bioassays

Blood for CBC/diff was analyzed using a clinical hematology analyzer (Bayer Advia 120, Bayer, Tarrytown, NY) at the AFRRI Veterinary Sciences Department (VSD) facility on time of each blood sample collection. The remaining blood was centrifuged at 10,000 g for 10 min, and plasma was collected, and stored at -80 °C for protein bioassays. Radiation-responsive protein biomarkers were measured using the MSD's HT MULTI-ARRAY® electrochemiluminescence (ECL) detection technology plate-format platform (http://www.mesoscale.com). To characterize biomarker performance in mouse radiation models, assays for the radiation biomarkers were developed as multiplexed panels in MULTI-ARRAY 96-well plates and read on a QuickPlex 120 Imager (Fig. 7.1). This detection technology enables array-based multiplexed measurements to be carried out with high sensitivity and dynamic range (Debad et al. 2004; Sigal et al. 2013). Due to a high-sensitivity of multiplex MSD's assay platform ECL technology that allows to measure simultaneously multiple biomarkers using only up to ~25 µL of plasma per plate well, all biomarker measurements were performed on samples from individual mouse. IL-18, DAO, I-FABP and PCT were measured using commercially available enzyme-linked immunosorbent assay (ELISA) kits manufactured by MBL International, Woburn, MA, and Biomatik USA, LLC, Wilmington, DE since those assays were not available/developed on the MSD's MULTIARRAY platform. All assays were performed according to the manufacturers' instructions. Calibration curves for standard proteins demonstrated very good reproducibility of assays performed by different technicians on different days. All standards and samples were run in duplicate. The optical density in ELISAs was measured using a spectrophotometer (BIO-TEK Instruments, Inc., Winooski, VT).

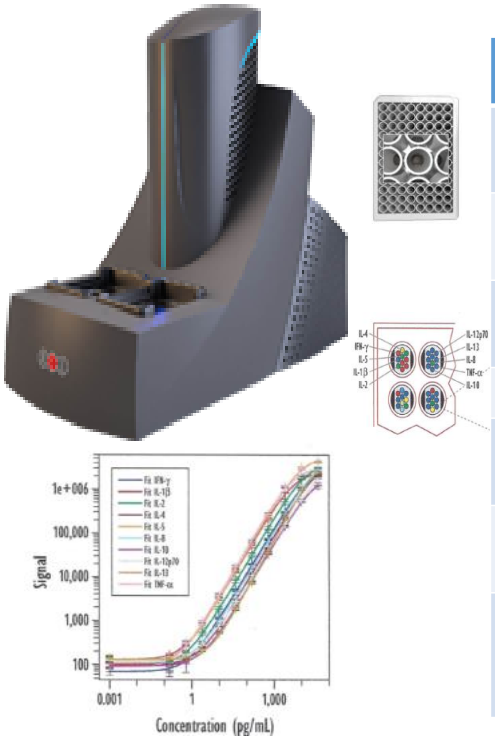

QuickPlex SQ 120 Imager Specifications	
Detection Technology	**Electrochemiluminescence (ECL)**
Multiplexing Capability	**Up to 10 assay spots per well / 25-50 uL of plasma**
High Sensitivity	**0.05 to 1 pg/mL for specific assays**
Dynamic Range	**10^5**
Plate Read Time / Throughput	**22 plates per hour**
Plate Stacker Capability	**5 plates input stack / 5 plates output stack**
Weight Size (W x D x H)	**44.5 lbs (20.2 kg) 13 in x 23 in x 21 in (33 cm x 58 cm x 53 cm)**

Fig. 7.1. Meso Scale Diagnostics's QuickPlex SQ 120 Multiplex-Array Platform.

Citrulline was measured using the liquid chromatography tandem mass spectrometry (LC-MS/MS), performed by University of Maryland, Baltimore as described previously (Jones et al. 2014) and depicted in Fig. 7.2.

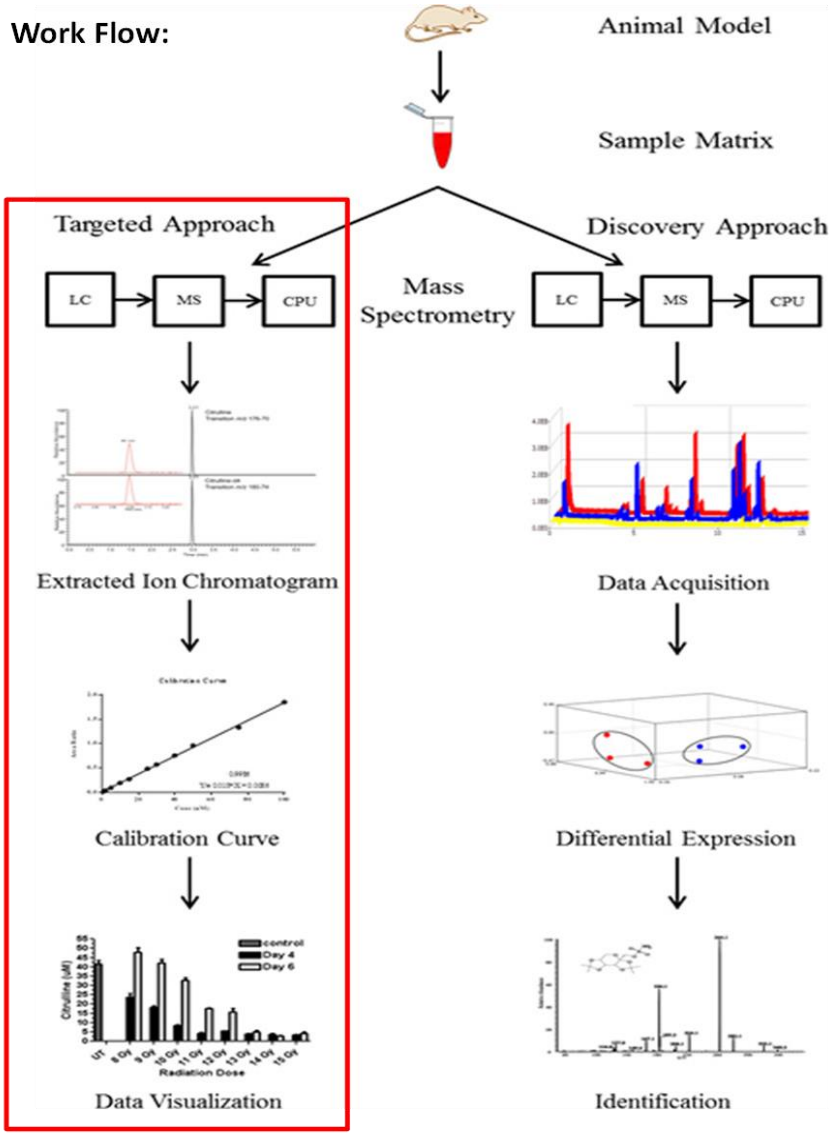

Fig. 7.2. Work-flow scheme for citrulline measurements using liquid chromatography tandem mass spectrometry (LC-MS/MS) performed at the University of Maryland, Baltimore (picture adopted from the paper by Jones et al. 2014).

A list of selected radiation-responsive blood-based hematological and proteomic biomarkers along with their activation pathways and functions for radiation injury and dose assessment is shown in Table 7.1. Concept to use of multiple biomarkers for radiation injury and dose assessment along with a SAS-based multi-parametric algorithm described in AFRRI U.S. Patent "Biomarker Panels for Assessing Radiation Injury and Exposure", No. 8,871,455 (PCT No: PCT/US2007/013752), issued on October 28, 2014. A list of evaluated biomarkers includes blood cell counts and

differentials (CBC/diff), hematopoietic cytokines, organ-specific, and acute phase protein biomarkers.

Table 7.1. List of selected radiation-responsive blood-based hematological and proteomic biomarkers showing their activation pathways and functions for radiation injury and dose assessment.

Biomarker	Pathways	References
Absolute lymphocyte count (ALC), absolute neutrophil count (ANC), Platelets (PLT) and Red Blood Cells (RBC)	Hematopoietic tissue injury	Goans et al. 1997; Baranov et al. 1995; Guskova et al. 1988; Dainiak et al. 2003; Ossetrova et al. 2007 – 2018.
CD27 (serum ALC) , CD45 (serum ANC) proteins	Hematopoietic tissue injury	Sigal et al. 2013; Ossetrova et al. 2016, 2018.
Fms-related tyrosin kinase 3 ligand (Flt-3L)	Hematopoietic tissue injury. Bone marrow aplasia. Regulation of the hematopoietic system recovery.	Bertho et al. 2001, 2008; Ossetrova et al. 2014-2018.
Granulocyte colony simulating factors: G-CSF and GM-CSF	Immunomodulatory effects on bone marrow cells. Hematopoietic tissue injury	Metcalf 1985; Bertho et al. 2008; MacVittie et al. 1990; Ossetrova et al. 2014-2018.
Serum amyloid A SAA) , Lipopolysaccharide binding protein (LBP)	Acute-phase reaction	Pepys et al. 1983; Jensen et al. 1998; Ossetrova et al. 2009-2018.
Thrombopoietin (TPO)	Regulation of megakaryocytopoiesis and platelet production. Liver and kidneys are major sites for TPO production	Lok et al. 1994; Bartley et al. 1994; Ossetrova et al. 2014-2018.
Erythropoietin (EPO)	Aplastic anemia. Erythropoiesis regulation	Elliott et al. 2008; Ossetrova et al. 2014-2018.
Intestinal fatty acid binding protein (I-FABP), Procalcitonin (PCT), citrulline, Diamine oxidase (DAO)	Gastrointestinal injury (GI)	DeBell et al. 1987; Castillo et al. 2017; Lutgens et al. 2007; Jones et al. 2014, 2015; Biju et al. 2012; Ossetrova et al. 2018.
Interleukin (IL) -18	Produced by activated immune cells, dendritic cells, monocytes and macrophages, T and B lymphocytes, natural killer cells, endothelial cells and neutrophils	Shan et al. 2007; Ha et al. 2014, 2016; Xiao et al. 2016; Ossetrova et al. 2018.
IL-12	Primarily produced by antigen-presenting cells	Wolf et al. 1994; Gerber et al. 2015; Ossetrova et al. 2016, 2018.
IL-5	Maturation/differentiation factor for eosinophils and B cells	Han et al. 2006; Kiang et al. 2018; Ossetrova et al. 2018.
IL-10	Produced primarily by monocytes and lymphocytes	Thompson et al. 1991; Cary et al. 2012; Kiang et al. 2018; Ossetrova et al. 2018.
*Concept to use of multiple biomarkers for radiation injury and dose assessment (AFRRI U.S. Patent "Biomarker Panels for Assessing Radiation Injury and Exposure", No. 8,871,455 (PCT No: PCT/US2007 /013752), issued on October 28, 2014.		

8. SURVIVAL STUDY RESULTS

The 30-day survival study after radiation with reactor mixed-field (67% n + 33% γ) to doses of 4, 5, 6, 7 Gy at dose-rate of 0.6 Gy/min) was performed using 16-wks female old mice to investigate the effect of exposure to different doses of mixed-field in order to find associations between protein expression profile, hematology parameters, body weight, symptoms and signs related to the radiation dose and hematopoietic and gastrointestinal subsyndromes of the ARS and create the ARS severity score system. Results were compared with ones collected earlier in ^{60}Co γ-rays studies, in which the ARS severity score system was created in mouse TBI model (1-14 Gy, at 0.6 Gy/min) based on multiple biodosimetric endpoints that include the acute radiation sickness severity Observational Grading System, survival rate, body weight and temperature changes, peripheral blood cell counts and radiation-responsive protein expression profiles (Ossetrova et al. 2013-2016; Koch et al. 2016).

In survival study, 104 mice were used (Table 5.1). Numbers of animals per group were determined by the AFRRI statistician from similar studies to provide power > 90% for two-tailed Student's t-tests of less than 10% shifts in value (Ossetrova et al. 2016). Mice were acclimated for one week before identification procedure (tail tattoo, Fig. 4.2.1), then one week rest was given to allow for stress reduction before total-body irradiation. Mice were weighed on a Sartoruis ED5201 scale (Bio Medic Data System (BMDS or BMDS data acquisition system) and the weight was recorded to electronic data files. Observations were recorded into electronic data recording system files.

The ARS response category assessment tool was created in order to quantify severity responses for ARS sub-syndromes and determine the criteria and bioindicators for early prognosis of lethality and point of euthanasia. The ARS severity degrees or response categories (RC), defined under the radiation-dose controlled conditions and animal recovery prognosis, were as follows: RC0 (Degree 0) control/sham; RC1 (Degree 1) for animal recovery was certain with a low risk of critical phase (mild radiation damage); RC2 (Degree 2) was for animal recovery was likely with a high risk of critical phase (moderate, but reversible damage); RC3 (Degree 3) was for animal recovery was most unlikely (severe, irreversible damage).

In pure gamma-rays study, RCs were associated with the exposure dose as follow: RC1 - for the dose-range of 1-3 Gy; RC2 - for the dose-range of 6-8 Gy; RC3 - for the dose-range of 10-14 Gy (Ossetrova et al. 2016). In reactor mixed-field study, RCs were found associated with the exposure dose as follow: RC1 - for the dose-range of ≤ 2 Gy; RC2 - for the dose-range of > 2 - < 6 Gy; RC3 - for the dose-range of ≥ 6 Gy (Ossetrova et al. 2018).

8.1. OBSERVATION SCHEME AND DATA COLLECTED

Table 8.1.1 shows the observational grading system (OGS) criteria along with data collected in survival studies. The OGS was developed at AFRRI as part of the Institutional Animal Care and Use Committee (IACUC) policy 10 and has been proved highly effective in preventing non-euthanasia based ARS mortality (Koch et al. 2016; Ossetrova et al. 2016).

Table 8.1.1. OGS or Mouse Intervention Score System and data collected in survival studies.

Mouse Intervention Score System		
Appearance:	Normal (smooth coat, clear eyes/nose)	**0**
	Hunched and/or fluffed	**1**
	Ocular discharge, and/or edema	**3**
	Pale, white mucus membranes/skin**	**6**
	Blue mucus membranes/skin (cyanosis)*	**12**
Respiratory rate:	Normal breathing	**0**
	Increased breathing (double normal rate, rapid, shallow)	**6**
	Abdominal breathing (+/-gasping or open mouth breathing)*	**12**
General behavior	Normal (based in baseline observations)	**0**
	Decreased mobility	**2**
	Ataxia, wobbly, weak**	**6**
	Inability to stand*	**12**
Provoked behavior	Normal (moves when cage is disturbed, runs from hand)	**0**
	Subdued; responds to stimulation (moves away briskly)	**1**
	Subdued even to stimulation (moves away slowly)	**3**
	Unresponsive to gentle prodding**	**6**
	Does not right when placed on side within 5 seconds*	**12**
Weight loss	Normal < 20%	**0**
	20-25%	**3**
	26-30%	**6**
	31-35%	**9**
	≥35%*	**12**
Total Score		

Score:	
< 6	Normal
6 – 11	Morbid: Monitor at least 3 times per day; notify appropriate personnel immediately
≥ 12	Moribund: Notify responsible personnel immediately for euthanasia if no single criterion is 12*. Any single criteria of 12* euthanize immediately; consider as 'found dead'.

- Body weight (BW) and % BW loss (once daily)
- Mortality (currently plotted by day, some time of day is available)
- Scoring system (4 times daily during pancytopenia, highest score retained, various score takers) according to criteria per the **IACUC policy #10** guidelines established at AFRRI
- ARS severity scores

Observable symptoms selected to define the radiation-induced morbidity in mice were evaluated using the OGS with euthanasia intervention upon a score of 12 or independent determination of moribund state by veterinary staff, laboratory staff, or principal investigator. The purpose of those established criteria, which by tracking animals individually, could significantly and accurately predict imminent death. With this predictive system, the length of time animals suffer could be significantly reduced through close observation and the better recognition of the signs that lead to morbidity and moribundity. The OGS includes scores for appearance, respiratory rate, general behavior, provoked behavior, and percentage body weight loss. On the day before irradiation (pre-TBI) and for 30 days post-TBI, sham/controls and mice irradiated to doses of 4, 5, 6, or 7 Gy, were weighed daily, and observed 3 times a day, with two additional observations per day during pancytopenia, which occurred from d6 to d17 post-TBI.

8.2. SURVIVAL RATE

Survival rate in mixed-field (67% n + 33% γ) and pure γ-rays studies is represented in Kaplan Meier plots, with each point representing percentage surviving at a given time as shown in Fig. 8.2.1 (a, b).

(**a**) TBI with mixed-field (67%n + 33%γ)

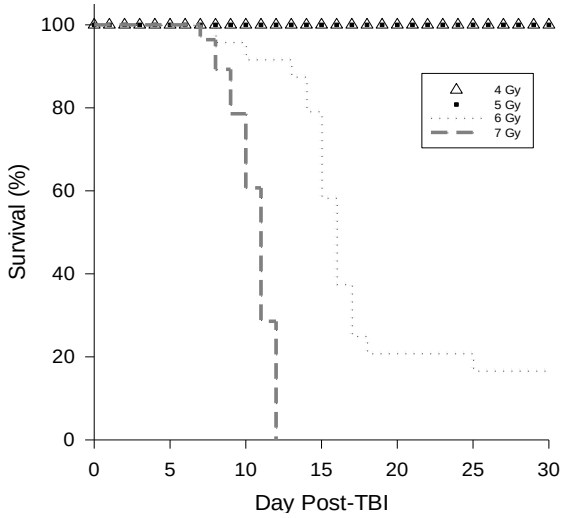

(**b**) TBI with pure γ-rays (^{60}Co)

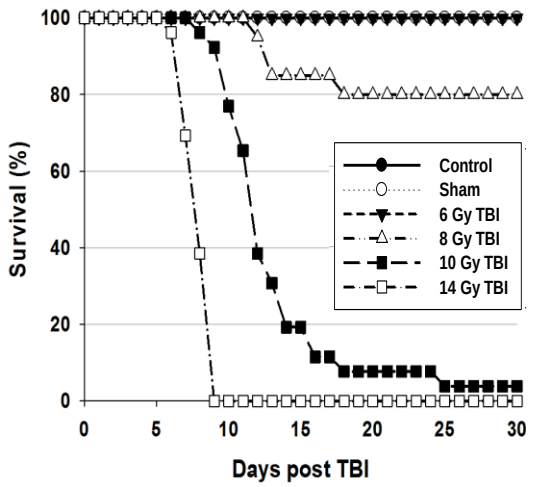

Fig. 8.2.1 (a, b). Kaplan-Meier curves for mice total-body irradiated to mixed-field (67%n + 33%γ) doses of 4, 5, 6, and 7 Gy (n = 20-28 per group) (**a**) and for mice total-body irradiated to pure g-rays doses of 6, 8, 19 and 14 Gy (n = 20-26 per group) (**b**). Survival was monitored for 30 days post-TBI.

In mixed-field survival study, the mortality was seen in mice irradiated to 6 and 7 Gy between d7 and d26 post-TBI (Fig. 8.2.1 a). Of 104 mice in this study (92 irradiated), 48 did not survive the 30-day observational period, 40 of which were euthanized based on the euthanasia criteria established at AFRRI (IACUC Policy 10), and 8 of which were found dead, though the majority of these instances of mortality occurred overnight during the largest gap between observations. All mice irradiated to 7 Gy (n = 28) were euthanized by d12 post-TBI, while mice irradiated to 6 Gy (n = 24) had 83% mortality at the conclusion of the experiment. No mortality was observed in other experimental groups (sham, 4 Gy, and 5 Gy) (Table 8.2.1 and Figs. 8.2.1a and 8.2.2). Broken down by RCs, survival rate was 100% in RC0 - RC2 throughout the observational period, and declined in RC3 from 100% to 88%, 38%, and 16% on d12, d16 and d30 post TBI, respectively (see in section "ARS Severity System").

Table 8.2.1. Cases surviving after the TBI with mixed-field (67% n + 33% γ). Numbers in red color represent difference compared to pre-TBI numbers.

Cases surviving																														
Day Post TBI	0	1	2	3	4	5	6	7	8	9	10	11	12	13	14	15	16	17	18	19	20	21	22	23	24	25	26	27	28	29	30
Sham	12	12	12	12	12	12	12	12	12	12	12	12	12	12	12	12	12	12	12	12	12	12	12	12	12	12	12	12	12	12	12
4 Gy	20	20	20	20	20	20	20	20	20	20	20	20	20	20	20	20	20	20	20	20	20	20	20	20	20	20	20	20	20	20	20
5 Gy	20	20	20	20	20	20	20	20	20	20	20	20	20	20	20	20	20	20	20	20	20	20	20	20	20	20	20	20	20	20	20
6 Gy	24	24	24	24	24	24	24	24	24	24	24	22	22	21	19	14	9	6	5	5	5	5	5	5	5	5	4	4	4	4	4
7 Gy	28	28	28	28	28	28	28	27	26	24	20	12	0	0	0	0	0	0	0	0	0	0	0	0	0	0	0	0	0	0	0

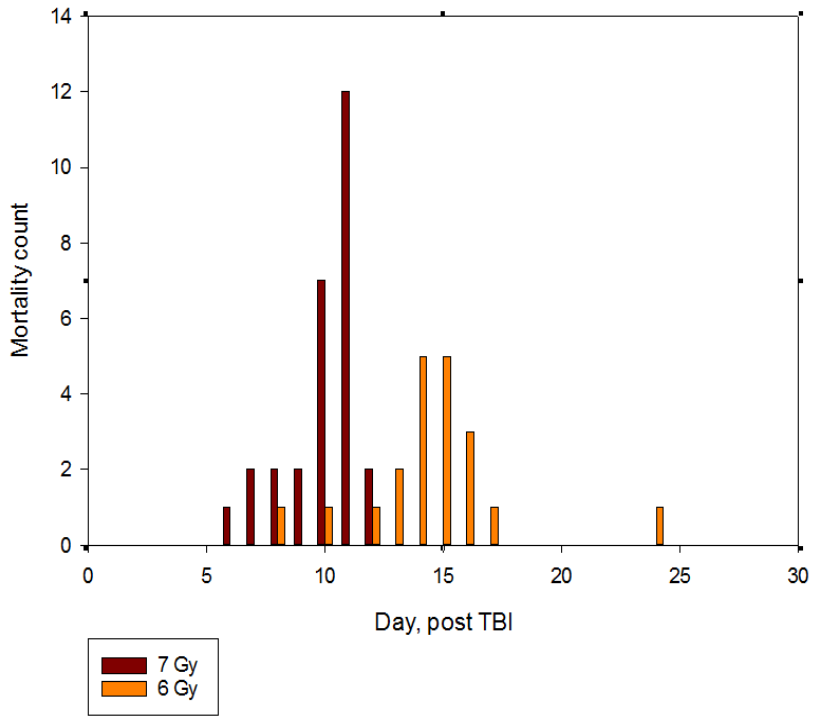

Fig. 8.2.2. Mortality histograms for 6- and 7-Gy groups (data shown in Table 8.2.1).

Our mixed-field survival study results are in a good agreement with ones from radiation countermeasure studies published by AFRRI (Cary et al. 2012; Ledney and Elliott 2010).

In pure γ-rays survival study (Fig. 8.2.1 b), from a total of 132 mice (control, sham, 6, 8, 10, and 14 Gy), (92 irradiated), 77 mice survived, 4 mice (7% of non-survivors) were found dead after overnight periods between observations, and 51 mice were euthanized based on established criteria It was demonstrated that mice irradiated to 6 or 8 Gy showed mild or moderate damage and their recovery was certain without or with low risk of critical phase, respectively. In mice irradiated to lethal doses (≥10 Gy), there is severe or fatal damage with a high risk of critical phase and recovery most unlikely due to the hematopoietic (HP) sub-syndrome in the 10-Gy group and a combination of HP and GI sub-syndromes in the 14-Gy group (Fig. 8.2.1 b) (Koch et al. 2016; Ossetrova et al. 2016).

8.3. BODY WEIGHT

Mice were weighed on a Sartoruis ED5201 scale (BMDS data acquisition system) and the weight was recorded to tenths of a gram. Body weight (BW) and percentage body weight loss (%BW) experienced by different dose groups in mixed-field (right panel) and pure γ-rays (left panel) survival studies are shown in Fig. 8.3.1.

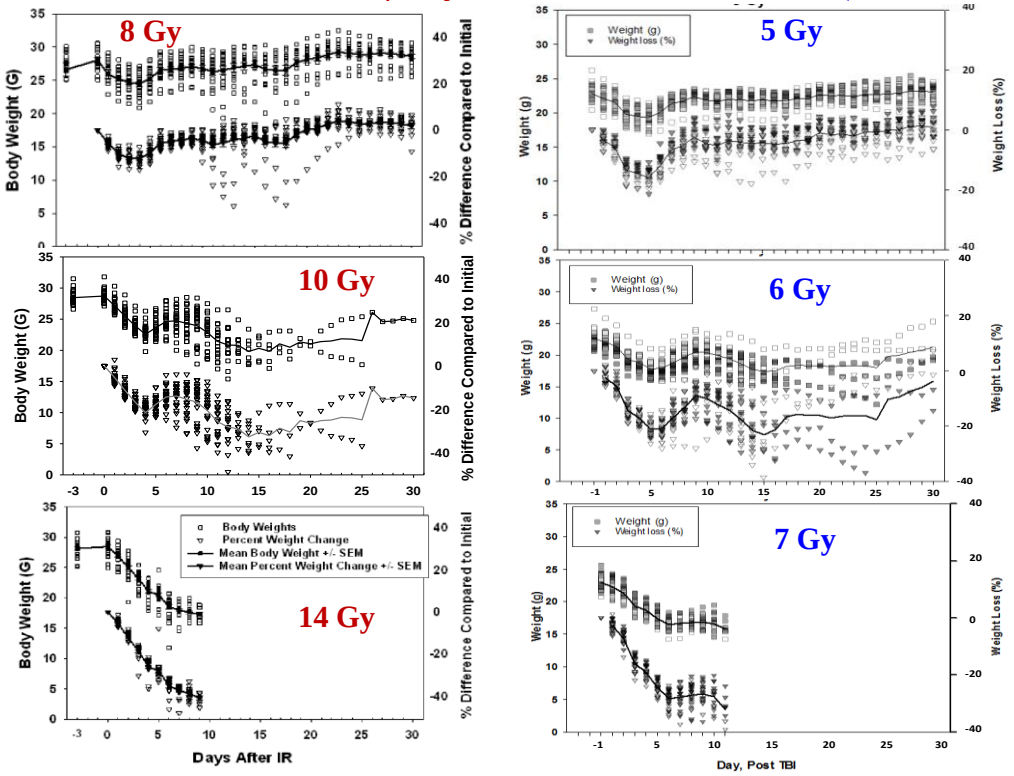

Fig 8.3.1. Time- and dose-dependent changes in body weight and percentage difference in body weight compared to pre-TBI level in sham and irradiated mice over a 30-day monitoring period in pure γ-rays (left panel) and mixed-field (right panel) studies. The symbols represent individual body weight (□) and percentage difference (∇) and lines represent the mean values per group.

In mixed-field study, the body weight in sham-irradiated mice was 23.9 ± 1.2 g pre-TBI and increased steadily to 25.6 ± 2.3 g by d30 post-TBI. Baseline weight of mice irradiated to 4 Gy was 23.0 ± 1.5 g, and decreased, becoming significantly different from sham mice on d1 ($p = 0.018$), falling to a minimum of 20.8 ± 1.2 g by d3, and rebounding to be statistically non-distinct from sham irradiated mice by d7. Mice irradiated to 5 Gy had a pre-TBI weight of 22.9 ± 1.3 g, which fell to a minimum of 19.3 ± 1.2 g by d5, but returned to pre-TBI levels by d7 ($p = 0.005$). Weight of mice in this group differed significantly from that of the sham group on all days post-TBI ($p \leq 0.025$) with the exception of d7 ($p = 0.19$), due to the uninterrupted increase in body weight in the sham irradiated group.

Body weight of mice irradiated to 6 Gy was 22.6 ± 1.4 g pre-TBI, and decreased to a minimum of 17.4 ± 1.5 g on d15. This group became significantly different from sham irradiated mice on a day to day comparison from d1 post-TBI until the conclusion of the experiment ($p \leq 0.043$), but became statistically non-distinct from their own pre-TBI weight on d23, reaching 21.3 ± 2.8 g by d30 post-TBI.

Mice irradiated to 7 Gy had a pre-TBI weight of 23.0 ± 1.1 g, which decreased to a minimum of 15.9 ± 1.1 g by d11 post-TBI after which all subjects in this group had succumbed to mortality. Weight of these cases was significantly different from the sham group on all days after irradiation ($p \leq 0.009$). When partitioned and interpolated into RCs, body weight remained relatively constant in RC0 and RC1, ranging from 24.2 g to 23.9 g and 23.7 g to 22.3 g,

respectively, during the scope of the experiment, while RC2 saw a moderate decline from 23.3 g to 20.7 g, and RC3 decreased from 22.1 g to 17.5 g on d30 post-TBI.

Decrease in body weight in individual mice paired with corresponding mortality is shown in Fig. 8.3.2. Mean percentage of weight lost reached a maximum of 9.5%, 15.9%, 23.1% and 31.9% in mice irradiated to 4, 5, 6, and 7 Gy respectively, corresponding to d3, d5, d15, and d11 post-TBI. Mice irradiated to < 6 Gy did not experience levels of weight loss that scored on the OGS, while nearly every mouse irradiated to ≥ 6 Gy did, with the exception of two that survived the experiment. Five mice in the 6 Gy group and thirteen mice in the 7 Gy group were euthanized as mandated by percentage weight loss (30% cutoff). Of the 40 mice euthanized during this survival study, 21 were selected based on OGS criteria (including some cases with weight loss exceeding 30%), 8 based on extreme weight loss alone, and 11 were categorized as moribund by laboratory or veterinary observers based on subjective assessment outside the scope of the OGS.

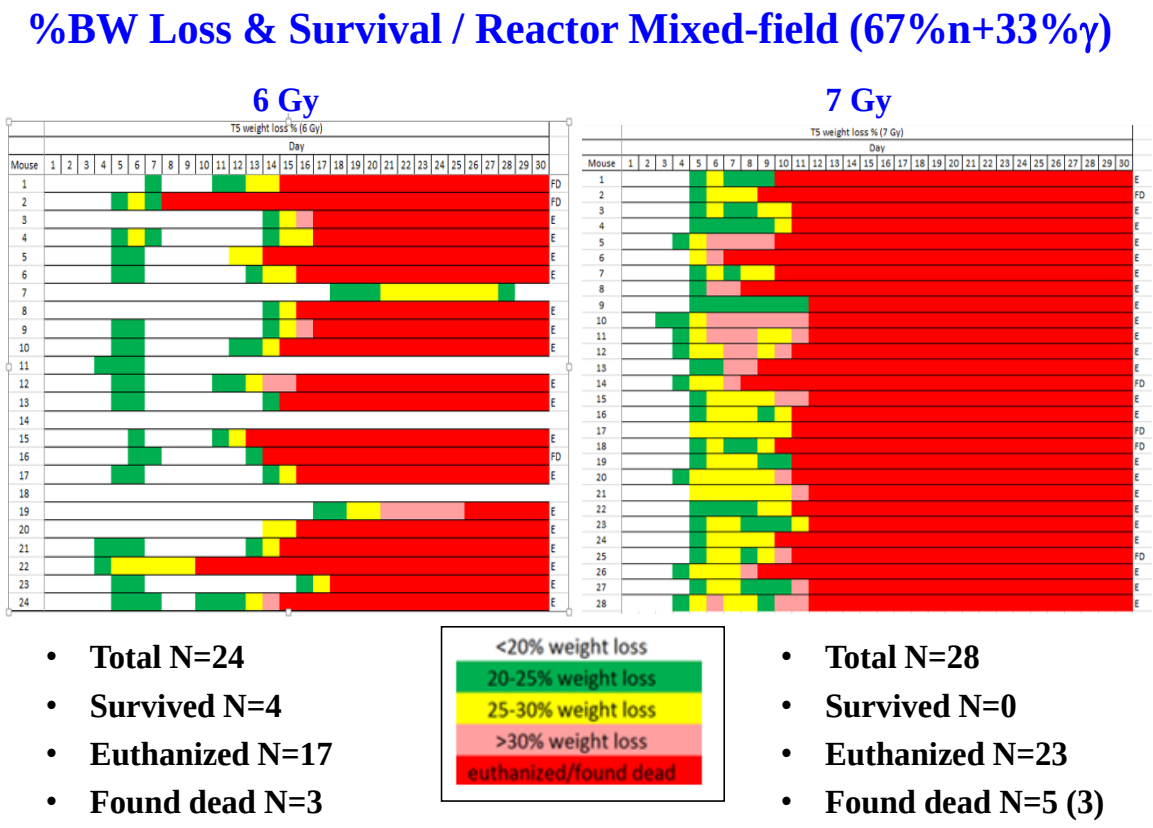

Fig. 8.3.2. Body weight loss in individual mice exposed to mixed-field radiation doses of 6 Gy (n = 24) and 7 Gy (n = 28) over a 30-day monitoring period. Results are color coded: less than 20% weight loss – white, 20-25% weight loss – green, 25-30% weight loss – yellow, more than 30% weight loss – pink, euthanized or found dead – red. Sham mice and mice irradiated to 4 Gy are not shown as no clinically significant weight change occurred in those groups.

Single variable ROC showed percentage body weight loss to be the most predictive indicator of mortality, peaking on d6 post-TBI (AUC=0.995) (Fig. 8.3.3).

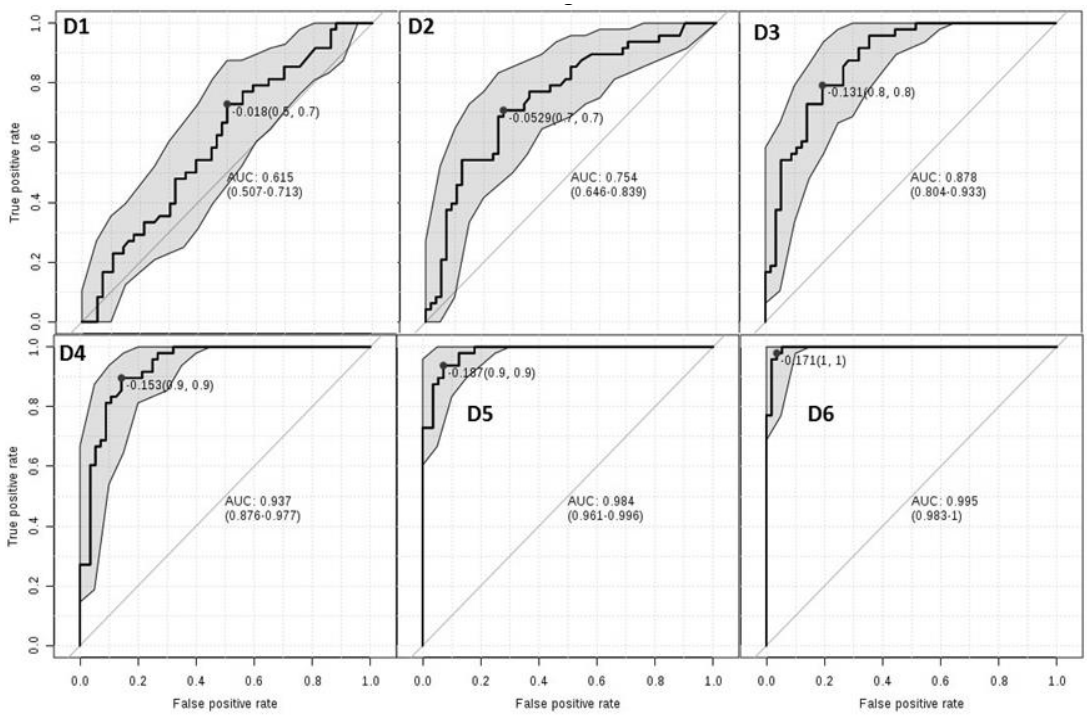

Fig. 8.3.3. The receiver operator characteristic (ROC) curves of body weight loss of mice on 1-6 days post-TBI irradiated to doses of 6 or 7 Gy to predict mortality.

Other markers from the OGS showed inferior predictive ability. Expansion of ROC analysis into multiple variable models found no multivariable models to be superior to that which used solely data of percentage body weight loss observed on d6.

8.4. ARS SEVERITY SCORE SYSTEM

ARS Severity Scoring System in mouse mixed-field TBI model consists of the observational grading scores (OGS), survival rate, body weight (presented as mean value ± standard deviation), and percentage body weight loss partitioned by the RC and radiation dose as shown in Table 8.4.1 and biomarker levels (shown in section "BIOMARKER RESULTS IN MIXED-FIELD STUDIES"). This ARS system was created in earlier investigations, performed on mice irradiated with gamma-rays and it was found that an OGS developed at AFRRI as part of the Institutional Animal Care and Use Committee (IACUC) policy 10 proved highly effective in preventing non-euthanasia based ARS mortality (Koch et al. 2016; Ossetrova et al. 2016). In order to match clinically observable responses to a more realistic radiation exposure incident with biochemical measurements, and expand the RC criterion to include mixed-field exposure, the following survival study in an established murine model was performed at AFRRI and paired with measurements of circulating biomarkers reported earlier in the same model (Ossetrova et al. 2018a). In addition, it expands upon established OGS to include subjects exposed to mixed-field radiation in the hopes of reducing non-euthanasia based, ARS-attributed mortality in this, and future studies.

Table 8.4.1. Observational grading system (OGS), survival rate, body weight, and body-weight loss for ARS response categorization in sham- and total-body irradiated mice.

Group	Sham	0-2 Gy	2-6 Gy	≥6 Gy
Parameter	Normal Degree 0 (RC0)	Mild Degree 1 (RC1)	Moderate Degree 2 (RC2)	Severe Degree 3 (RC3)
Appearance				
percent of group that displayed category symptoms	0	0	0	100
Mean maximum*	0	0	0	1.4
General Behavior				
percent of group that displayed category symptoms	0	0	0	100
Mean maximum*	0	0	0	3.5
Provoked Behavior				
percent of group that displayed category symptoms	0	0	0	100
Mean maximum*	0	0	0	2.4
		*=mean of maximum score for each mouse over 30 days		
Survival Rate (%)				
Day 7	100	100	100	100
Day 12	100	100	100	88
Day 16	100	100	100	38
Day 30	100	100	100	16
Body Weight (g)				
Day 1	24.2±2	23.7±1.8†	23.3±1.7†	22.1±1.3
Day 2	24.1±2.3	23.4±2.1†	22.7±1.8†	21.3±1.3
Day 4	24.5±2.1	23.1±1.9†	21.7±1.7†	18.8±1.2
Day 7	23.5±2	22.3±1.9†	21.1±1.8†	18.8±1.5
Day 12	23.7±1.6	22.6±1.6†	21.5±1.6†	19.4±1.6
Day 16	23.9±1.7	22.3±1.7†	20.7±1.8†	17.5±1.8
Day 30	25.6±2.3	24.5±2.4†	23.4±2.6†	21.3±2.8
Body Weight Loss (%)				
Day 1	-1.3	-0.4†	0.5†	2.4
Day 2	-1	0.6†	2.2†	5.5
Day 4	-2.2	2.6†	7.4†	16.9
Day 7	1.7	5.5†	9.2†	16.7
Day 12	0.7	4.2†	7.5†	14.3
Day 16	0.1	5.4†	10.6†	21.2

Mice irradiated to doses ≥ 6 Gy showed increases in appearance score corresponding to hunched posture, and five of these developed ocular discharge. Of these five cases, only one survived to the conclusion of the observational period. Scores in respiratory rate were seen in only 3 mice, all of which corresponded with immediate euthanasia. General behavior in mice irradiated to ≥ 6 Gy began to shift on d7 post-TBI on the basis of loss of mobility. All but one mouse exposed to 7 Gy demonstrated some loss in mobility, with eight displaying ataxia or inability to stand immediately prior to euthanasia. All mice irradiated to 6 Gy displayed some loss in mobility throughout the course of the study, the first of which was observed on d7 post-TBI. Twelve cases in this group progressed to ataxia or inability to stand during the observational period, which was immediately followed by study-mandated euthanasia.

Changes in provoked behavior were first observed on d8 post-TBI in mice irradiated to ≥ 6 Gy. All but one of these cases displayed some change in provoked behavior, with 21 of them progressing to a state of unresponsiveness or inability to right itself, all of which corresponded with reaching the scoring cut off, prompting immediate euthanasia. Maximum mean score of provoked behavior in mice irradiated to 6 and 7 Gy was 2.9 and 4.6 respectively. In total score on the OGS, mice that reached a score of 12 were immediately euthanized. Mice irradiated to 6 and 7 Gy reached mean maximum scores of 7.6 and 8.8 respectively. Sham mice and those irradiated to less than 6 Gy (RC0 - RC2) did not exhibit scores in any OGS category, while animals in RC3 universally scored in every category, with maximum mean values of 1.4, 3.5, and 2.4 in appearance, general behavior, and provoked behavior respectively.

8.5. SURVIVAL STUDY RESULTS DISCUSSION

Due to a lack of human data in mixed-field radiation accidents, numerous animal studies for a variety of biological endpoints have been performed using research nuclear reactors that have the ability to simulate radiation environments produced by nuclear weapon detonations with results compared to those after pure-photon exposure. The comparative effects of neutrons and photons on the whole body lead to the conclusion that for the same amount of ionization, neutrons are more biologically destructive than photons. After both forms of radiation in biologically equivalent doses, the gross pathological findings were quite similar. Preliminary observations indicated that the mechanism of death after irradiation with mixed neutrons and photons was similar to that observed after photon-radiation. It has previously been demonstrated that total-body irradiation of mice with neutrons in sufficient quantities, leads to a clinical, bacteriological and anatomical picture similar to that following photon-irradiation. The mucosa of the small intestine and the lymphoid and hematopoietic tissues are the most radiosensitive. The mechanism of death after both forms of radiation seems to be a combination of tissue destruction and enterogenous infection, the former predominating in the acute deaths after large doses (Lawrence and Tennant 1937; Alpen 1991; MacVittie et al. 1991; Ledney et al. 2000; Ledney and Elliott 2010; Cary et al. 2012). Lawrence and Tennant reported both bacteriological and pathological evaluations in studies performed in mice irradiated to either large doses of x-rays (10 Gy) or neutrons (2.5 – 3 Gy) and concluded that infection is not a necessary finding, and death within a few days was associated with marked destructive changes in the various viscera, giving rise to a toxemia from tissue breakdown products. However, as the doses are decreased and the animals live longer, bacteremia is a usual finding and infection probably a more important factor in the cause of death. This is supported by the anatomical finding of numerous ulcers in an otherwise normal intestinal mucosa and focal necrosis in the liver in some of the animals surviving 9 to 14 days after irradiation. Furthermore, the animals in this group uniformly had positive postmortem blood cultures.

Presumably the organisms (usually B. coli) gain entrance to the circulation through the damaged mucosa of the intestine (Lawrence and Tennant 1937). For example, for relative biological effectiveness (RBE) determinations for hematopoietic and gastrointestinal cell system failure, Ledney and colleagues performed series of studies examining survival-mortality responses in B6D2F1 female mice irradiated with mixed-field irradiations of Dn/Dt (neutrons to total irradiation) 0.43, 0.67, 0.94 or pure ^{60}Co γ-rays. Reported LD50/30s were 6.01, 4.94, and 3.93 Gy for the three mixed-field experimental conditions, respectively, and 9.63 Gy for ^{60}Co γ-rays. When compared to ^{60}Co γ-rays, as the Dn/Dt increased, the RBE increased from 1.6 to 2.5. For Dn/Dt=0.67, the estimated RBEs for hematopoietic and gastrointestinal cell system failure were 1.8 and 2.2, respectively. It was also shown that proliferative cell systems of the bone marrow (BM) and GI tract are susceptible to radiation damage and sustain greater injury after fission-neutron irradiation than after photon irradiation resulting in higher RBEs, at their respective LD50 time points (Ledney and Elliott 2010). The primary purpose of the studies presented here was to demonstrate that mixed-field radiations were more damaging than photon radiations of comparable physical doses for a number of life-threatening situations. Hence, it was of interest to determine, in terms of response of different organ-specific biomarkers that might be predictive for death from gastrointestinal or BM proliferative cell system failure, which system was most affected by changes in the proportion of Dn to Dt and different dose rates. It was demonstrated that (1) equivalent doses of pure gamma-rays and mixed-field do not produce equivalent biological effects and hematopoietic syndrome occurs at lower doses of mixed-field radiation, (2) in general, survival rate and biomarker results are in agreement with the RBE=1.95 (Dn/Dt=0.67) reported earlier by AFRRI scientists in mouse survival countermeasure studies, (3) results for hematological biomarkers, hematopoietic cytokines, organ-specific, and acute phase proteins demonstrated dose- and time-dependent changes reflecting the time course and severity of ARS (Ossetrova et al. 2018a, 2018b and in section "BIOMARKER RESULTS IN MIXED-FIELD STUDIES").

The survival study described here demonstrated a steeper mortality curve and onset of symptoms than that seen in similar ^{60}Co γ-rays studies. This may have been due to the above described shift in ARS sub-syndromes previously seen in mixed-field exposure, though further study is required for confirmation. In this study, the murine ARS severity score system was used to observe and categorize mice irradiated with a mixed-field exposure. Factors defined in RC classification system included survival, weight loss, percentage of body weight loss, OGS scores, blood cell counts, and circulating cytokine concentrations. Furthermore, the updated OGS employed here for the first time in mixed-field studies successfully maintained a low rate of non-euthanasia mortality, thereby minimizing ARS induced pain and distress in our animal model. Rationale for doses selected in this study (4, 5, 6, and 7 Gy) was based on an extrapolation of contemporary findings in ^{60}Co (pure gamma-rays) survival studies performed in a similar setting according to a mixed-field RBE of approximately 2.0 (Ledney and Elliott. 2010; Ossetrova et al. 2018). In the ^{60}Co study, doses corresponding to double those administered here yielded increasing proportions of factors contributing to the ARS severity score system (Ossetrova et al. 2016). While the study performed here showed a clear increase in all ARS contributing factors, the transition from non-symptomatic to highly lethal was observed between just two dose groups examined. This steep increase in response may be due to differences in energy deposition inherent in neutron radiation resulting in a higher probability of gastrointestinal sub-syndrome in mice irradiated with mixed-field exposure. While the majority of survival studies performed on B6D2F1 mice have employed pure gamma irradiation, some reports examined survival after exposure to mixed-field irradiation. Experiments by Landauer, Ledney and colleagues performed at AFRRI utilized similar

proportions of neutrons to those in this experiment (67% n + 33% γ), though dose rate and dose applied were not consistent (0.4 Gy/min, 5.6 Gy, and 0.38 Gy/min, 3.5 Gy respectively). The survival results presented here are in rough agreement with the report of 35% survival performed by Landauer and colleagues, though exact comparison cannot be made because of differences in dose administered and alternative euthanasia criteria utilized in this study. Direct comparison with work by Ledney et al. was not practical due to absence of data reported for mice not treated with a countermeasure agent (Landauer et al. 1997; Ledney et al. 2000).

While the vast majority of mortality in this study was, as planned, through euthanasia, several factors point to a potential evolution of the OGS. First, rationale for euthanasia varied between individuals, but, in most cases, coincided with protocol-mandated euthanasia due to body weight loss. This highlights the importance of daily weight measurements to supplement observations and that an increased emphasis should be placed on extreme weight loss. Second, some mice were euthanized based on the judgement of the laboratory staff independent of scoring criteria. While this does not invalidate the OGS, it may indicate that an expansion of scorable observations is needed. Third, only one subject reached an OGS score of 6 and survived the full 30 days indicating that a reduction in score-based euthanasia could be imposed. In a related result, only one subject of those found dead reached an OGS score of 6 before being found so, suggesting that, while the current system has merit, non-euthanasia based mortality is virtually unavoidable in this type of experiment.

This study examined the effect of mixed-field radiation on 30-day survival of mice. Previous work has been performed to reduce the distress suffered by animal subjects utilized in radiation dosimetry research (Plett et al. 2012; Nunamaker et al. 2013). While these reports focused on cases exposed to different radiation qualities, a comparison of the efficacy of their efforts to reduce animal distress can still be made. A system with a similar aim was employed in research done by Nunamaker and colleagues in 2013, in which subjects were graded daily without handling on a nine point scale consisting of three categories including posture, eye appearance and general behavior, used in conjunction with body weight measurements done once a week. Comparison between this and the grading system employed in the present study shows overlap in the areas of general behavior and posture (roughly equivalent to the 'appearance' category), with key divergences in eye appearance, provoked behavior, and frequencies of observations (once per day in Nunamaker et al. 2013) and weighing (once per week). This method produced a mitigation of non-euthanasia animal mortality (25 mice found dead in a study of 109) inferior to the levels achieved by work done using AFRRI IACUC policy 10 OGS. It should be noted however, that the authors correlated non-euthanasia-mandating scores in their system with imminent mortality, and recommended that future utilization of their grading system use a lower score to mandate euthanasia. Additionally, such a scoring system might produce improved results when combined with more frequent observations and weight measurements. Any of these modifications might help bring unscheduled mortality to lower levels, though it is most likely not possible to compare handling-induced mortality between the two systems at this time considering the number of other study criteria which are not matched (mouse strain, dose, radiation source).

More closely related to the present work is the investigation which originally tested the OGS, performed by Ossetrova and colleagues (Ossetrova et al. 2016; Koch et al. 2016). Performed on 92 murine subjects, 51 of which were euthanized and only four were found dead, this study achieved a superior rate of mitigation of non-euthanasia mortality among its subjects to that reached here, despite being the original test of the OGS. There are several factors which may account for this, the first of which being the change in quality of radiation, which produced a more

rapid observable decline in the health of exposed mice. To add to this, the current study employed an updated version of the OGS, though this is unlikely to have caused a decrease in observation of moribund behavior. Additional changes in study design include the strain of mouse used, gender of mice, and staff tasked with OGS in study, any of which may have affected the proportion of non-euthanasia mortalities.

Observations of humans exposed to radiation have attempted to establish measurable early markers and symptoms by which to predict the severity of ARS. These originally included clinical symptoms corresponding to radiation sensitive organ systems, and later developed to include quantitative measurements of blood cell counts and circulating biomarkers. While the mouse model has been well utilized for identification and validation of radiation biomarkers due to its economy, well defined and conserved hematopoietic system, and extensively described genetic variants, organismal differences greatly limit the expansion of our understanding of the human response to radiation. Not all molecular pathways are consistent between the two species and the human system is complicated by an extensive amount of coexisting conditions which can affect circulating biomarker concentrations, as well as potential medical interventions for mitigation of radiation damage which are not practical in mouse models (such as bone marrow transplant, blood transfusions and cytokine therapies). Despite these limitations, it can be inferred from the results of the experiments described here that circulating biomarkers could be highly successful in the effort to triage patients exposed to mixed-field radiation. Patterns of response in circulating biomarkers studied here may be conserved in the context of human mixed-field exposure, though it will be difficult to be certain of this without empirical evidence.

This study will serve as a valuable resource in defining the effect of mixed-field radiation upon radiation-reactive circulating blood biomarkers using the murine ARS response categories system. The ability to stratify dose response might benefit from expanding the scope of this investigation to include response categorization and study of survival of exposure of different strains and genders of mice, the effect of partial body irradiation, alternative proportions of neutrons and gamma rays, alternative dose rates, combined injury, effect of countermeasures upon circulating biomarkers and survival, and alternative animal models, such as non-human primates. Additionally, while mortality dose-based trends in this survival study roughly validated previous observations that mixed-field radiation has a RBE of approximately 2.0, the total decline in mortality between groups receiving 5 and 6 Gy rendered probit analysis impossible in this study. Although, it was not a primary purpose for our survival study. If needed, the further study with a higher resolution of doses between 5 and 6 Gy may help to bring the dose-mortality curve into sharper focus. Results presented here help to bridge the gap between existing knowledge and that required to simulate plausible radiation dispersal events, as well as supplement ongoing efforts to attend to the anticipated need for rapid point-of-care biodosimetry device for use in a mixed-field mass casualty exposure incident.

9. BIOMARKER RESULTS

9.1. BIOMARKER RESULTS IN TRIGA MIXED-FIELD STUDY

We evaluated the utility of multiple blood biomarkers for early-response assessment of radiation exposure using a mouse (B6D2F1, males and females) TBI model, exposed to a mixed-field (neutrons and γ-rays) using AFRRI TRIGA Mark-F nuclear research reactor. TBI was given as a single exposure over a dose range from 1.5 to 6 Gy, dose rates of either 0.6 or 1.9 Gy/min, and

different proportions of neutrons and gammas: either 67% n + 33% γ or 30% n + 70% γ as shown in Table 5.1. Blood was collected 1, 2, 4, and 7 days after TBI. Blood for complete blood cell counts with differentials (CBC/diff) with specific interest in absolute lymphocyte counts (ALC), absolute neutrophil counts (ANC), ratio of ANC to ALC, platelets (PLT), and red blood cell counts (RBC) was analyzed using a clinical hematology analyzer at the AFRRI VSD facility on time of each experiment. Radiation-responsive protein biomarkers (Table 7.1) were measured using the Meso Scale Diagnostics' (MSD) high-throughput (HT) MULTI-ARRAY plate-format platform (QuickPlex 120 Imager) and enzyme-linked immunosorbent assay (ELISA) kits.

9.1.1. HEMATOLOGY RESULTS

Results for ALC, ANC, ratio of ANC to ALC, PLT, and RBC in blood of mice after a mixed-field TBI under different experimental conditions are shown in Figs. 9.1.1.1 – 9.1.1.3 and Tables 9.1.1.1 – 9.1.1.4. Among all evaluated hematological biomarkers, stress-effect associated with sham-irradiation was observed in mice only on d1 post-procedure resulting in ~20-35% increase in ANC in sham-group compared to counts in control group. In irradiated animal groups, on d1 and d2 after TBI, significant decline was found in ALC whereas ANC increased due to the demargination process. Beginning from d4, all blood cell counts decreased in a dose-dependent manner. RBC and PLT were not immediately affected after irradiation but began to decrease in 3- and 6-Gy groups on d4. It was also reported in nonhuman primate studies that RBC continued to fall for several more weeks due to the fact that radiation does not affect mature, circulating RBCs. Radiation exposure affects the progenitor cells forming within the bone marrow and the ability of bone marrow to produce new RBCs; therefore, there was a delayed response that corresponds to the rate at which the bone marrow is creating new cells (Ossetrova et al. 2016a).

Fig. 9.1.1.1 and data in Tables 9.1.1.1 and 9.1.1.2 show dose- and time-dependent changes in hematological profile in blood of female mice after a mixed-field TBI with either (67% n + 33% γ) or (30% n + 70% γ) at a dose rate of 0.6 Gy/min. Since peripheral ALC are highly radiation-sensitive, a significant decline began on d1 with a progressive decline up to 4-, 10- and 100-fold observed in 1.5-, 3- and 6-Gy groups, respectively, on d7 after exposure in animal groups irradiated with either (67% n + 33% γ) or (30% n + 70% γ) with no significant differences between them ($p > 0.094$). No significant differences were observed between irradiated animal groups for ANC, ANC to ALC ratio, and RBC for any dose and at any time after exposure ($p > 0.114$). PLT levels were significantly different only in 3- and 6-Gy groups on d7 ($p < 0.039$).

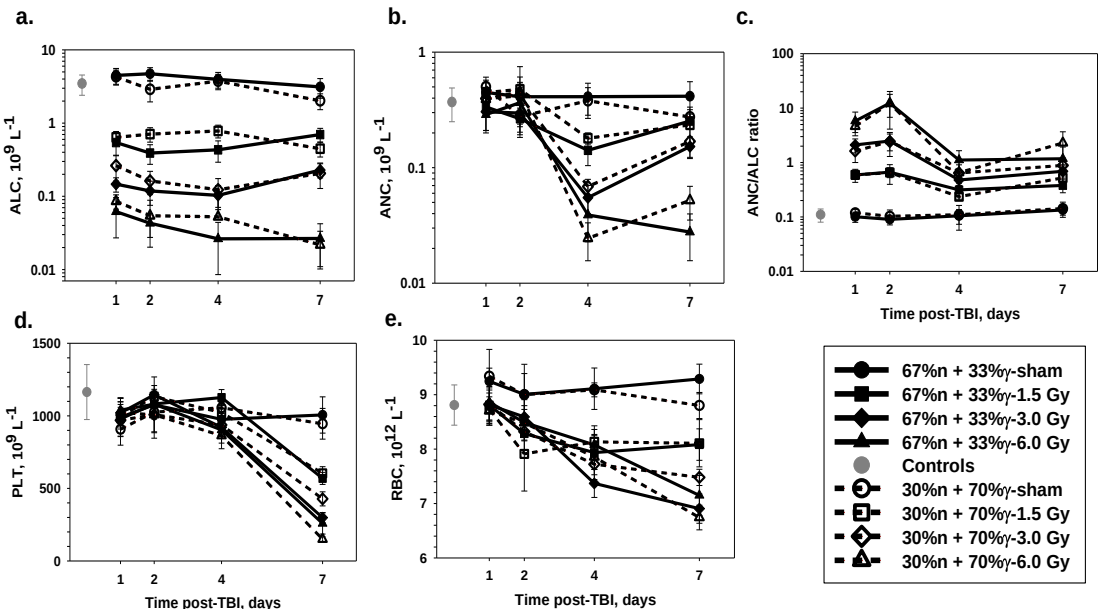

Fig. 9.1.1.1. Dose- and time-dependent changes for ALC (a), ANC (b), ANC to ALC ratio (c), PLT (d) and RBC (e) in blood of female mice after a mixed-field TBI with either (67% n + 33% γ) (solid lines) or (30% n + 70% γ) (dashed lines) at the dose rate of 0.6 Gy/min. The symbols represent the mean values for n = 8 animals per group and error bars represent the standard deviation (STD). The data are also shown in Tables 9.1.1.1 and 9.1.1. 2.

Table 9.1.1.1. Hematological biomarker levels in B6D2F1 female mice irradiated with mixed-field (67% n and 33% γ) at 0.6 Gy/min. Shaded data represent a significant difference between control (non-irradiated) and irradiated groups at 95% CL.

Biomarker	**Day**	**Biomarker Level (Mean ± STD)**			
(control values)	**post-TBI**	**Sham (0 Gy)**	**1.5 Gy**	**3.0 Gy**	**6.0 Gy**
ALC (x10^9 L^{-1}) (3.47 ± 1.07)	**1**	4.72 ± 1.17	0.54 ± 0.18	0.15 ± 0.03	0.06 ± 0.03
	2	4.43 ± 1.21	0.39 ± 0.12	0.12 ± 0.04	0.04 ± 0.02
	4	4.28 ± 1.18	0.43 ± 0.14	0.10 ± 0.04	0.03 ± 0.02
	7	3.62 ± 0.55	0.70 ± 0.15	0.23 ± 0.05	0.03 ± 0.02
ANC (x10^9 L^{-1}) (0.37 ± 0.12)	**1**	0.44 ± 0.11	0.34 ± 0.13	0.31 ± 0.09	0.29 ± 0.09
	2	0.39 ± 0.11	0.27 ± 0.08	0.30 ± 0.10	0.37 ± 0.13
	4	0.39 ± 0.12	0.14 ± 0.04	0.06 ± 0.02	0.04 ± 0.02
	7	0.48 ± 0.12	0.25 ± 0.04	0.15 ± 0.03	0.03 ± 0.01
ANC/ALC ratio (0.11 ± 0.03)	**1**	0.09 ± 0.02	0.59 ± 0.16	2.11 ± 0.61	5.79 ± 2.68
	2	0.09 ± 0.01	0.67 ± 0.14	2.49 ± 0.85	12.36 ± 5.57
	4	0.09 ± 0.03	0.31 ± 0.10	0.48 ± 0.17	1.11 ± 0.54
	7	0.13 ± 0.03	0.38 ± 0.10	0.69 ± 0.18	1.18 ± 0.75
PLT (x10^9 L^{-1}) (1,164 ± 190)	**1**	981 ± 108	979 ± 119	1,021 ± 75	1,040 ± 80
	2	1,068 ± 75	1,082 ± 61	1,146 ± 64	1,080 ± 103
	4	1,000 ± 101	1,126 ± 55	921 ± 34	903 ± 91
	7	1,007 ± 110	569 ± 42	298 ± 35	258 ± 73
RBC (x10^{12} L^{-1}) (8.81 ± 0.37)	**1**	9.23 ± 0.47	8.81 ± 0.28	8.81 ± 0.34	8.87 ± 0.36
	2	9.13 ± 0.36	8.29 ± 0.31	8.59 ± 0.32	8.49 ± 0.24
	4	9.20 ± 0.42	7.94 ± 0.31	7.37 ± 0.26	8.08 ± 0.28
	7	9.37 ± 0.27	8.08 ± 0.29	6.91 ± 0.27	7.15 ± 0.37

Table 9.1.1.2. Hematological biomarker levels in B6D2F1 female mice irradiated with mixed-field (30% n and 70% γ) at 0.6 Gy/min. Shaded data represent a significant difference between control (non-irradiated) and irradiated groups at 95% CL.

Biomarker (control values)	Day post-TBI	Biomarker Level (Mean ± STD)			
		Sham (0 Gy)	1.5 Gy	3.0 Gy	6.0 Gy
ALC (x10^9 L^{-1}) (3.47 ± 1.07)	1	4.30 ± 0.99	0.64 ± 0.13	0.26 ± 0.10	0.09 ± 0.02
	2	2.89 ± 0.94	0.71 ± 0.16	0.16 ± 0.06	0.05 ± 0.03
	4	3.75 ± 0.89	0.78 ± 0.16	0.12 ± 0.05	0.05 ± 0.06
	7	2.02 ± 0.49	0.45 ± 0.10	0.21 ± 0.08	0.02 ± 0.01
ANC (x10^9 L^{-1}) (0.37 ± 0.12)	1	0.50 ± 0.11	0.45 ± 0.12	0.40 ± 0.10	0.39 ± 0.10
	2	0.28 ± 0.05	0.48 ± 0.27	0.42 ± 0.13	0.45 ± 0.15
	4	0.38 ± 0.11	0.18 ± 0.02	0.07 ± 0.01	0.02 ± 0.01
	7	0.28 ± 0.06	0.24 ± 0.08	0.17 ± 0.05	0.05 ± 0.02
ANC/ALC ratio (0.11 ± 0.03)	1	0.12 ± 0.02	0.59 ± 0.10	1.63 ± 0.63	4.63 ± 1.06
	2	0.10 ± 0.03	0.66 ± 0.26	2.43 ± 1.14	12.17 ± 8.05
	4	0.11 ± 0.05	0.24 ± 0.03	0.64 ± 0.26	0.65 ± 0.37
	7	0.14 ± 0.04	0.52 ± 0.12	0.89 ± 0.32	2.29 ± 1.38
PLT (x10^9 L^{-1}) (1,164 ± 190)	1	908 ± 110	994 ± 84	970 ± 90	1,024 ± 100
	2	1,026 ± 136	1,133 ± 135	1,009 ± 162	1,008 ± 124
	4	1,056 ± 37	1,023 ± 68	937 ± 80	864 ± 90
	7	946 ± 106	604 ± 46	428 ± 48	150 ± 17
RBC (x10^{12} L^{-1}) (8.81 ± 0.37)	1	9.34 ± 0.15	8.74 ± 0.30	8.82 ± 0.30	8.70 ± 0.26
	2	9.00 ± 0.56	7.91 ± 0.68	8.32 ± 0.17	8.48 ± 0.32
	4	9.09 ± 0.13	8.13 ± 0.29	7.72 ± 0.19	7.86 ± 0.41
	7	8.80 ± 0.24	8.11 ± 0.43	7.48 ± 0.15	6.74 ± 0.23

Fig. 9.1.1.2 and data in Tables 9.1.1.1 and 9.1.1.3 show the dose and time-dependent changes in hematological profile in blood of female mice after mixed-field TBI with (67% n + 33% γ) at a dose rate of either 0.6 or 1.9 Gy/min (dose-rate comparison study).

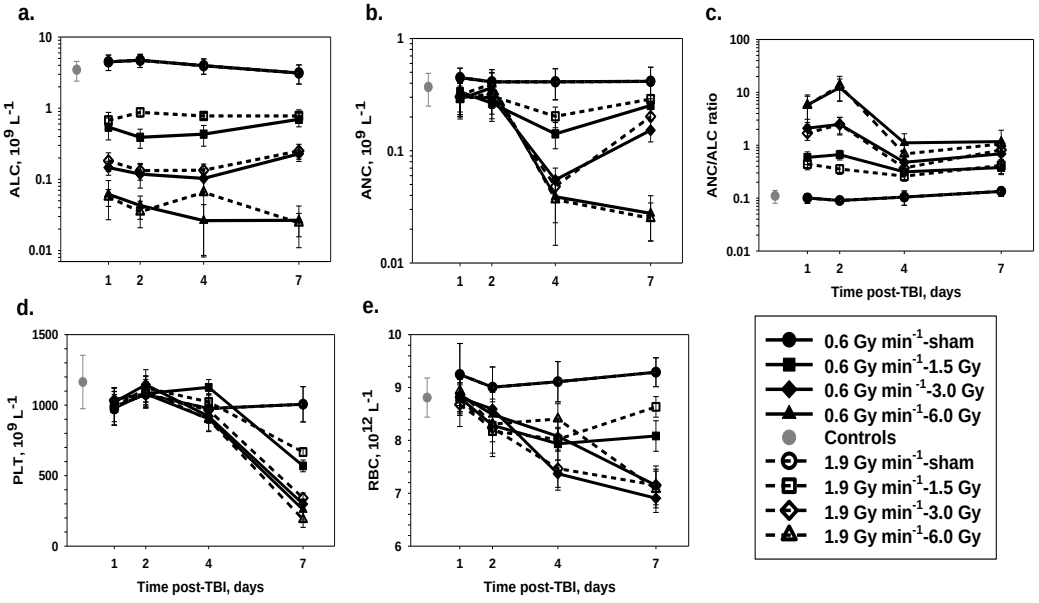

Fig. 9.1.1.2. Dose- and time-dependent changes for ALC (a), ANC (b), ANC to ALC ratio (c), PLT (d) and RBC (e) in blood of female mice after a mixed-field TBI with (67% n + 33% γ) at the

dose rate of either 0.6 Gy/min (solid lines) or 1.9 Gy/min (dashed lines). The symbols represent the mean values for n = 8 animals per group and error bars represent the standard deviation (STD). The data are also shown in Tables 9.1.1.1 and 9.1.1.3.

No significant differences were observed between irradiated animal groups for ANC, ANC to ALC ratio, PLT, and RBC for any dose and at any time after exposure ($p > 0.154$) except PLT levels in 6-Gy groups on d7 ($p < 0.031$).

Table 9.1.1.3. Hematological biomarker levels in B6D2F1 female mice irradiated with mixed-field (67% n and 33% γ) at 1.9 Gy/min. Shaded data represent a significant difference between control (non-irradiated) and irradiated groups at 95% CL.

Biomarker	**Day**	**Biomarker Level (Mean ± STD)**			
(control values)	**post-TBI**	**Sham (0 Gy)**	**1.5 Gy**	**3.0 Gy**	**6.0 Gy**
ALC ($x10^9$ L^{-1}) (3.47 ± 1.07)	**1**	4.48 ± 1.09	0.68 ± 0.20	0.18 ± 0.05	0.06 ± 0.02
	2	4.72 ± 0.99	0.88 ± 0.12	0.13 ± 0.04	0.04 ± 0.01
	4	3.96 ± 0.96	0.78 ± 0.06	0.13 ± 0.03	0.07 ± 0.06
	7	3.12 ± 0.94	0.78 ± 0.17	0.25 ± 0.06	0.02 ± 0.01
ANC ($x10^9$ L^{-1}) (0.37 ± 0.12)	**1**	0.45 ± 0.10	0.30 ± 0.10	0.30 ± 0.10	0.31 ± 0.09
	2	0.41 ± 0.12	0.31 ± 0.06	0.32 ± 0.11	0.40 ± 0.10
	4	0.41 ± 0.13	0.20 ± 0.04	0.05 ± 0.01	0.04 ± 0.02
	7	0.42 ± 0.14	0.29 ± 0.10	0.20 ± 0.05	0.03 ± 0.01
ANC/ALC ratio (0.11 ± 0.03)	**1**	0.10 ± 0.02	0.44 ± 0.10	1.69 ± 0.45	5.70 ± 3.26
	2	0.09 ± 0.01	0.36 ± 0.07	2.48 ± 0.91	13.54 ± 6.63
	4	0.10 ± 0.03	0.26 ± 0.05	0.37 ± 0.09	0.69 ± 0.36
	7	0.13 ± 0.03	0.42 ± 0.12	0.82 ± 0.18	1.06 ± 0.18
PLT ($x10^9$ L^{-1}) (1,164 ± 190)	**1**	991 ± 134	980 ± 97	1,036 ± 86	987 ± 47
	2	1,076 ± 90	1,123 ± 129	1,076 ± 53	1,103 ± 100
	4	976 ± 103	1,023 ± 76	966 ± 71	898 ± 81
	7	1,006 ± 125	667 ± 30	341 ± 36	189 ± 56
RBC ($x10^{12}$ L^{-1}) (8.81 ± 0.37)	**1**	9.25 ± 0.59	8.80 ± 0.25	8.68 ± 0.41	8.94 ± 0.23
	2	9.01 ± 0.38	8.18 ± 0.42	8.24 ± 0.54	8.31 ± 0.19
	4	9.11 ± 0.38	8.02 ± 0.20	7.47 ± 0.41	8.41 ± 0.29
	7	9.29 ± 0.27	8.63 ± 0.20	7.15 ± 0.30	7.07 ± 0.35

Fig. 9.1.1.3 and data in Tables 9.1.1.1 and 9.1.1.4 show the dose and time-dependent changes in hematological profile in blood of female and male mice after mixed-field TBI with (67% n + 33% γ) at a dose rate of 0.6 Gy/min (gender-comparison study). No significant differences were observed between irradiated female and male groups for ANC, ANC to ALC ratio, PLT, and RBC for any dose and at any time after exposure ($p > 0.096$). By d7, the partial recovery of circulating ANC and ALC was found in groups irradiated with non-lethal doses (1.5 and 3 Gy). However, even at 1.5 Gy, the lowest dose of exposure, there was still about a 40% reduction in blood cell population (Tables 9.1.1.1 – 9.1.1.4).

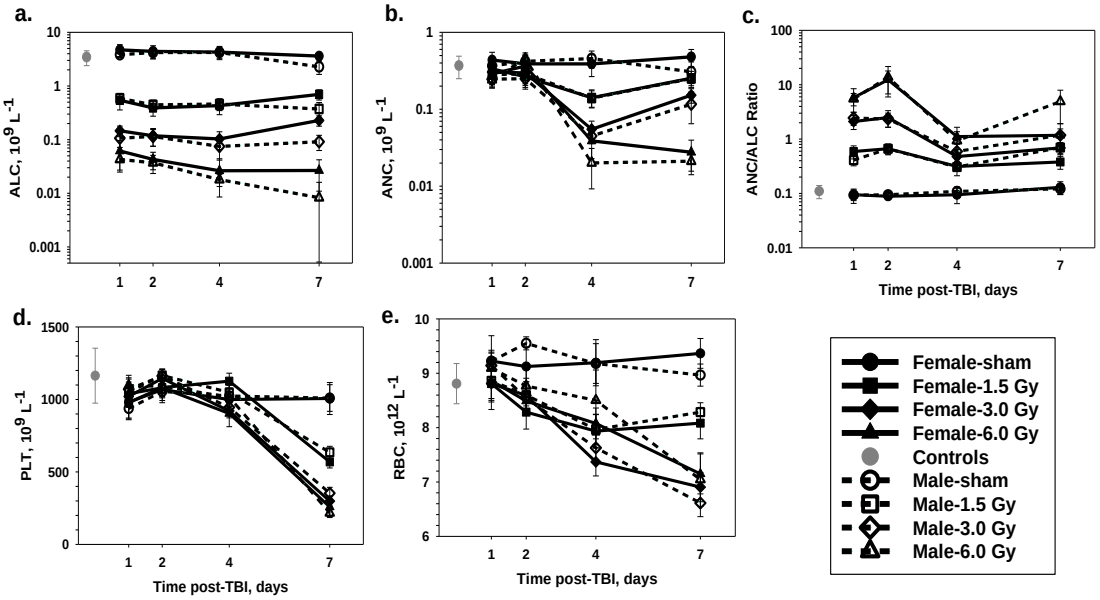

Fig. 9.1.1.3. Dose- and time-dependent changes for ALC (a), ANC (b), ANC to ALC ratio (c), PLT (d) and RBC (e) in blood of female (solid lines) and male (dashed lines) mice after a mixed-field TBI with (67% n + 33% γ) at the dose rate of 0.6 Gy/min. The symbols represent the mean values for n = 8 animals per group and error bars represent the standard deviation (STD). The data are also shown in Tables 9.1.1.1 and 9.1.1.4.

Table 9.1.1.4. Hematological biomarker levels in B6D2F1 male mice irradiated with mixed-field (67% n and 33% γ) at 0.6 Gy/min. Shaded data represent a significant difference between control (non-irradiated) and irradiated groups at 95% CL.

Biomarker (control values)	Day post-TBI	Biomarker Level (Mean ± STD)			
		Sham (0 Gy)	1.5 Gy	3.0 Gy	6.0 Gy
ALC (x10^9 L^{-1}) (3.47 ± 1.07)	1	3.84 ± 0.44	0.59 ± 0.11	0.11 ± 0.04	0.04 ± 0.02
	2	4.21 ± 0.99	0.45 ± 0.10	0.12 ± 0.04	0.04 ± 0.01
	4	4.24 ± 0.96	0.46 ± 0.11	0.08 ± 0.03	0.02 ± 0.00
	7	2.28 ± 0.63	0.37 ± 0.12	0.09 ± 0.03	0.01 ± 0.01
ANC (x10^9 L^{-1}) (0.37 ± 0.12)	1	0.37 ± 0.08	0.28 ± 0.07	0.25 ± 0.06	0.24 ± 0.05
	2	0.42 ± 0.09	0.29 ± 0.07	0.25 ± 0.05	0.45 ± 0.09
	4	0.46 ± 0.11	0.14 ± 0.03	0.05 ± 0.01	0.02 ± 0.01
	7	0.31 ± 0.11	0.25 ± 0.06	0.12 ± 0.05	0.02 ± 0.01
ANC/ALC ratio (0.11 ± 0.03)	1	0.09 ± 0.03	0.41 ± 0.09	2.46 ± 0.67	5.50 ± 1.41
	2	0.09 ± 0.01	0.66 ± 0.15	2.33 ± 0.67	13.80 ± 7.84
	4	0.11 ± 0.02	0.31 ± 0.04	0.59 ± 0.21	0.93 ± 0.44
	7	0.12 ± 0.03	0.70 ± 0.16	1.18 ± 0.36	4.93 ± 3.01
PLT (x10^9 L^{-1}) (1,164 ± 190)	1	937 ± 72	1,051 ± 90	1,071 ± 96	1,096 ± 53
	2	1,055 ± 44	1,166 ± 41	1,163 ± 48	1,092 ± 73
	4	1,025 ± 52	1,049 ± 51	946 ± 72	1,016 ± 62
	7	1,010 ± 92	635 ± 42	353 ± 40	217 ± 23
RBC (x10^{12} L^{-1}) (8.81 ± 0.37)	1	9.23 ± 0.15	8.86 ± 0.53	9.14 ± 0.28	9.09 ± 0.16
	2	9.55 ± 0.12	8.60 ± 0.24	8.55 ± 0.30	8.77 ± 0.37
	4	9.18 ± 0.37	7.97 ± 0.27	7.63 ± 0.27	8.50 ± 0.56
	7	8.97 ± 0.20	8.29 ± 0.17	6.61 ± 0.25	7.04 ± 0.49

9.1.2. PROTEOMICS RESULTS

Very good reproducibility in standard calibration curves and control samples was reported in proteomic assays performed by different people on different days; see reproducibility plots in Figs. 9.1.2.1 – 9.1.2.3.

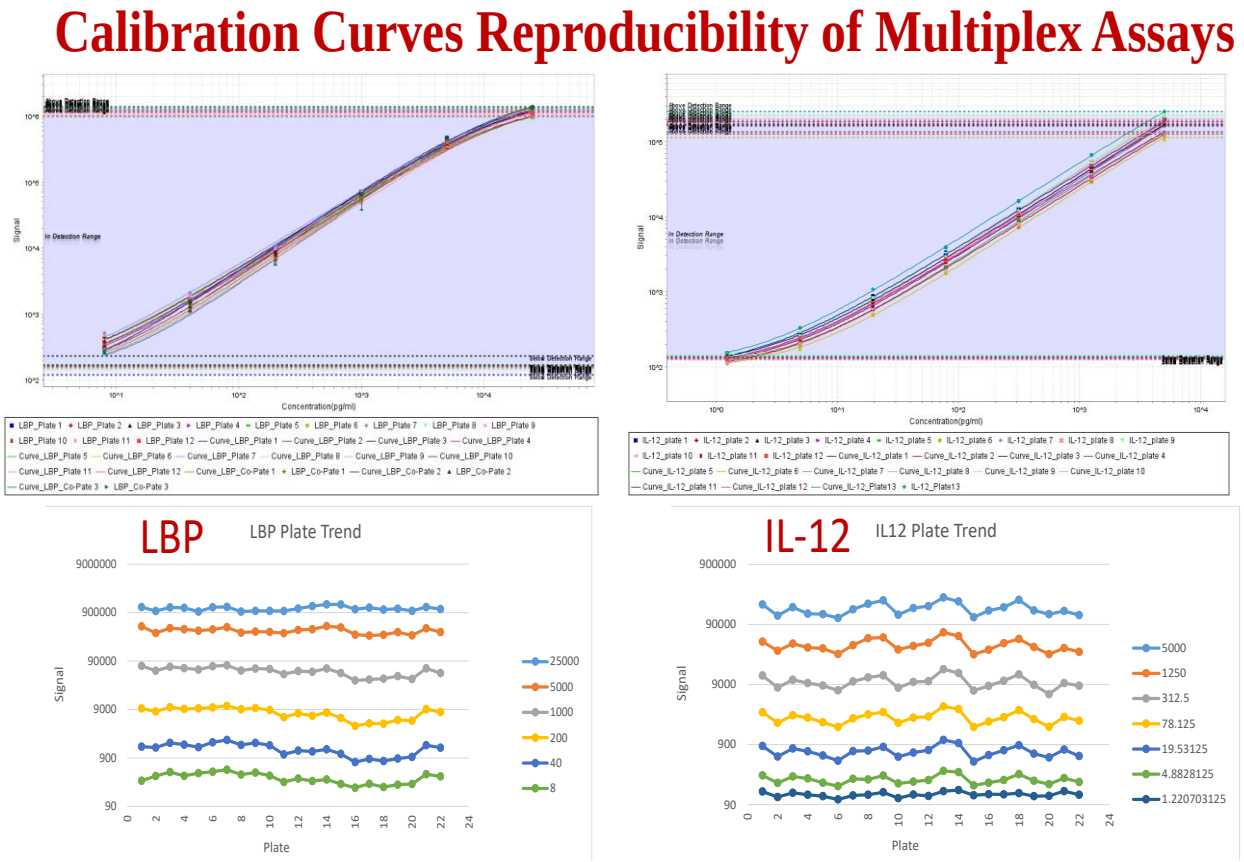

Fig. 9.1.2.1. Calibration curves reproducibility of multiplex assays on MSD multiplex platform. Upper pictures were taken from QuickPlex SQ 120 statistical software. Lower plots were made using excel software for each standard curve point as in pictures above.

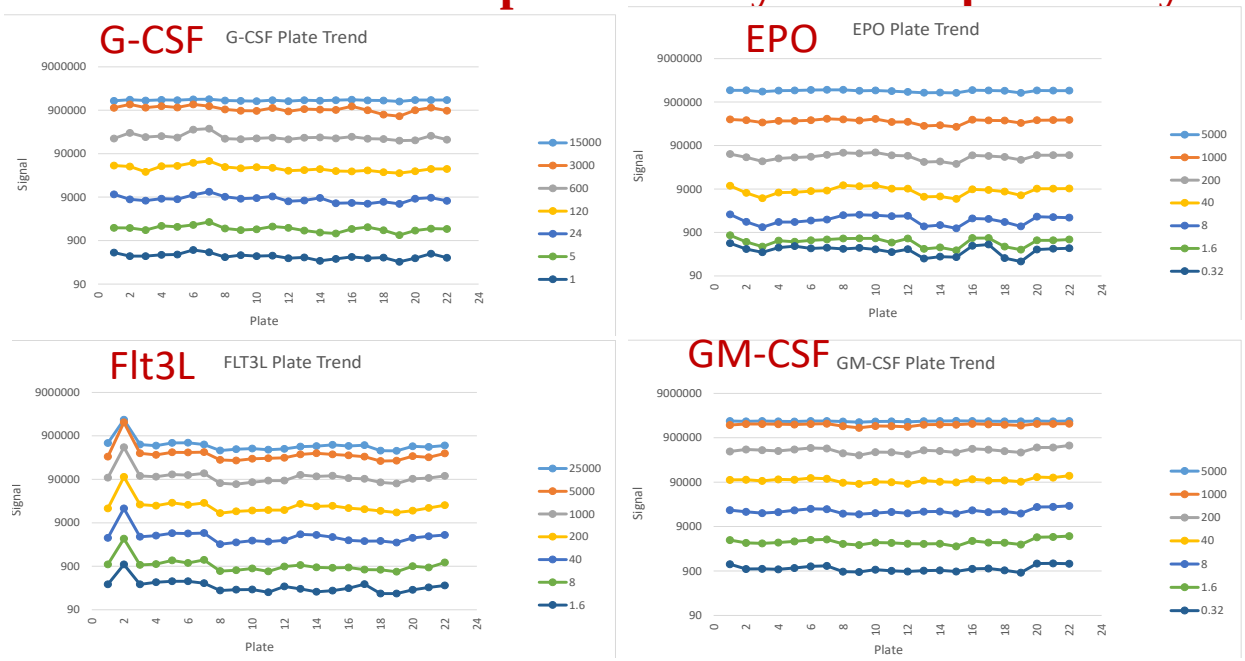

Fig. 9.1.2.2. Calibration curves reproducibility of multiplex assays on MSD multiplex platform. Plots were made using excel software for each standard curve point in MSD multiplex assays.

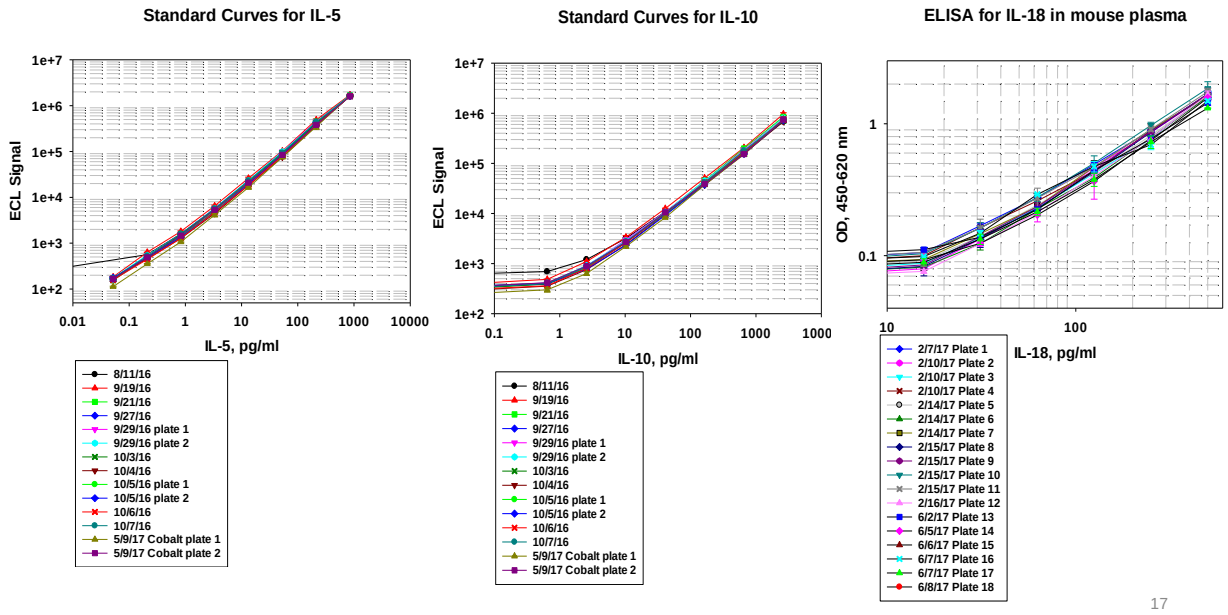

Fig. 9.1.2.3. Calibration curves reproducibility of multiplex assays on MSD multiplex platform. Plots were made using Sigma Plot software for each standard point in MSD assays and ELISAs (for IL-18).

The protein biomarkers were selected from distinctly different pathways: Flt-3 Ligand (Flt3L), IL-5, IL-10, IL-12, IL-18, G-CSF, GM-CSF, TPO, EPO, acute phase proteins (SAA and LBP), surface plasma hematology markers (CD45, CD27, ratio of CD45 to CD27), and PCT (Table 7.1) and were measured in plasma of mice after mixed-field TBI under different experimental conditions and results are shown in Figs. 9.1.2.4 – 9.1.2.7 and Tables 9.1.2.5 – 9.1.2.8. In response to mixed-field ionizing radiation, an increase in concentration of Flt3L, IL-5, IL-18, G-CSF, GM-CSF, TPO, EPO, SAA, and ratio of CD45 to CD27 and decrease in concentration of IL-12, CD27 and CD45 were observed in a dose- and time-dependent manner. IL-10 and LBP levels showed no significant changes in any irradiated animal groups compared to control/sham.

Fig. 9.1.2.4 and data in Tables 9.1.2.5 and 9.1.2.6 show the dose- and time-dependent changes in profile of protein biomarkers in blood plasma of female mice after mixed-field TBI with either (67% n + 33% γ) or (30% n + 70% γ) at a dose rate of 0.6 Gy/min. In general, no significant differences for Flt3L were observed between compared animal groups. However, mice irradiated with 1.5 and 3 Gy with 67% n + 33% γ had Flt3L levels of 276 ± 24 pg mL^{-1} and 947 ± 92 pg mL^{-1} on d7, respectively, while mice irradiated with the same doses with 30% n + 70% γ had Flt3L levels of 199 ± 17 pg mL^{-1} and 369 ± 36 pg mL^{-1}, respectively on the same day (Fig. 9.1.2.4a). These findings suggest that in mice irradiated with non-lethal doses the faster bone marrow recovery was found in those animal groups irradiated with a lower percentage of neutrons. No significant differences between irradiated groups were observed ($p > 0.068$) for IL-5 and TPO at any time after TBI (Figs. 9.1.2.4d and 9.1.2.4e). IL-12 results revealed no significant differences between animal groups with one exception on d7 in 3-Gy groups: IL-12 in mice irradiated with 67% n + 33% γ was 67 ± 12 pg mL^{-1} compared to mice irradiated with 30% n + 70% γ (109 ± 28 pg mL^{-1}) reflecting the faster recovery of mice irradiated with smaller percentage of neutrons (Fig. 9.1.2.4j). Beginning from d2, IL-18 and GM-CSF levels were significantly higher in animals irradiated with 67% n + 33% γ compared to those irradiated with 30% n + 70% γ ($p < 0.011$) (Figs. 9.1.2.4m and 9.1.2.4f). No significant differences in EPO levels were observed between any groups except 6-Gy groups on d7. EPO level in the group irradiated with 67% n + 33% γ was about 2-fold less compared to its level in mice irradiated with 30% n + 70% γ (Fig. 9.1.2.4b, Tables 9.1.2.5 and 9.1.2.6). Radiation-induced G-CSF levels changed in a dose- and time-dependent manner with two phases observed (Fig. 9.1.2.4c). The strong dose-dependent first phase of G-CSF expression occurred early (beginning from a few hours to d1 after exposure) as reported earlier (Ossetrova et al. 2014a, 2016b). In the end of a first-phase (on d1), G-CSF level was not significantly different ($p > 0.132$) between compared groups. On d2, a highly elevated G-CSF level was observed only in mice irradiated with 6 Gy with 67% n + 33% γ. Beginning from d4 (second phase), G-CSF levels were significantly higher in animals irradiated with 67% n + 33% γ compared to those irradiated with 30% n + 70% γ ($p < 0.008$) (Fig. 9.1.2.4c). SAA level expression pattern after irradiation is also bi-phasic (Ossetrova et al. 2014a, 2016a). As demonstrated in our earlier studies, the strongly dose-dependent first phase of SAA expression occurred early (within a few hours after exposure) and peaked on d1 (Ossetrova et al. 2016a). In this study, the first-phase SAA level was found up to ~20-fold elevated compared to sham with no significant difference ($p > 0.212$) between compared radiation quality groups on d1. While SAA level was returning to a baseline (sham) level in mice irradiated with 30% n + 70% γ beginning from d4, it remained significantly elevated in groups irradiated with 67% n + 33% γ ($p < 0.007$) (Fig. 9.1.2.4i). Among hematological plasma surface biomarkers, stress-effect associated with the handling of mice was observed only on d1 in CD45 and CD45/CD27, but not in CD27 levels. In irradiated groups, no significant differences were observed ($p > 0.208$) for either CD45 or CD45/CD27 (Fig. 9.1.2.4h

and 9.1.2.4n) at any time-point after TBI. No significant differences were observed between irradiated animal groups for CD27 with one exception on d1: CD27 levels were 678 ± 133 pg mL^{-1} and 368 ± 32 pg mL^{-1} in 6-Gy groups irradiated with 67% n + 33% γ or 30% n + 70% γ, respectively (Fig. 9.1.2.4k). However, this difference could be explained by the large inter-individual variability in group irradiated with 67% n + 33% γ.

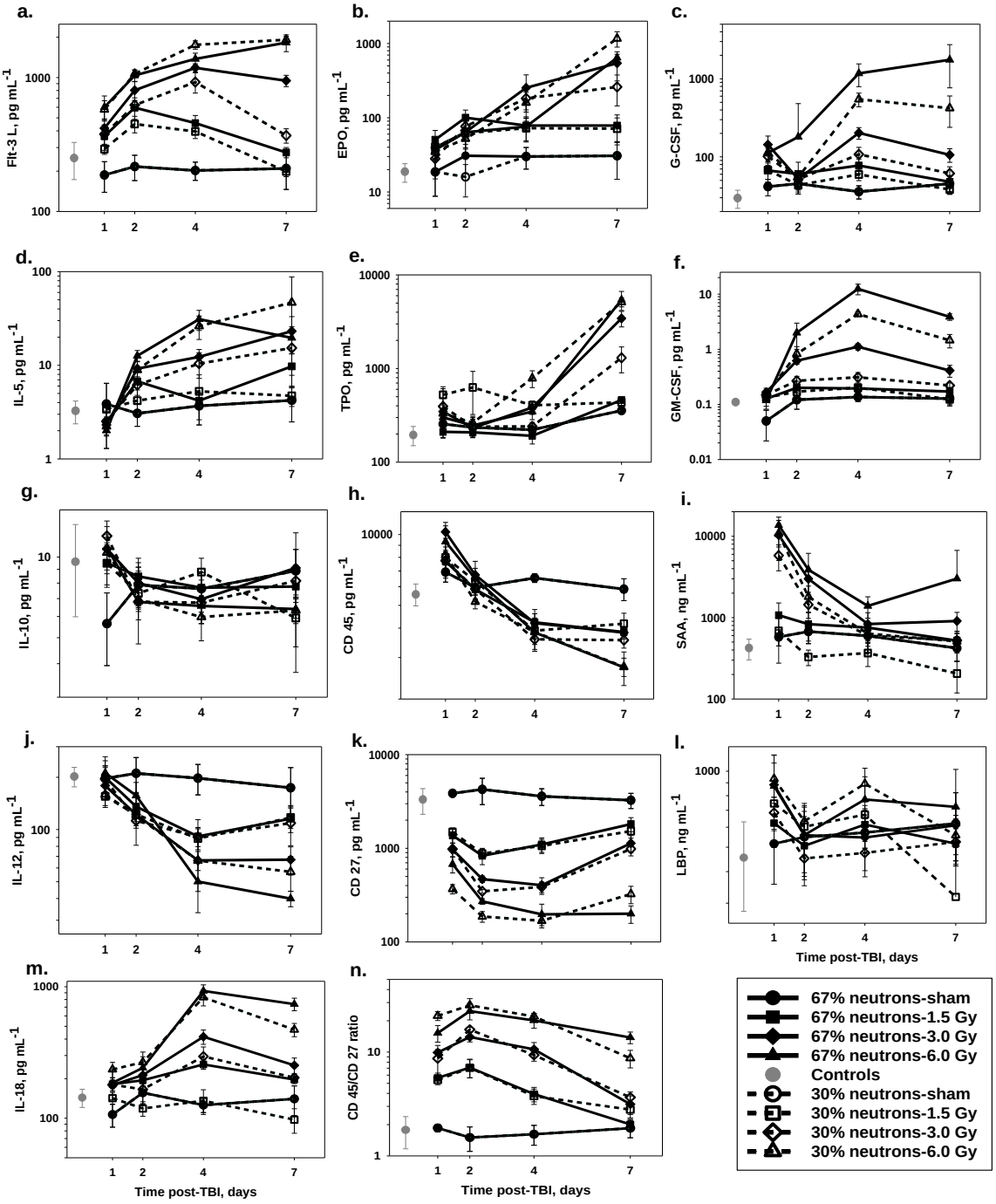

Fig. 9.1.2.4. Dose- and time-dependent changes in profile of protein biomarkers: FLT3L (a), EPO (b), G-CSF (c), IL-5 (d), TPO (e), GM-CSF (f), IL-10 (g), CD45 (h), SAA (i), IL-12 (j), CD27

(k), LBP (l), IL-18 (m), CD45/CD27 (n) in blood plasma of female mice after a mixed-field TBI with either (67% n + 33% γ) (solid lines) or (30% n + 70% γ) (dashed lines) at the dose rate of 0.6 Gy/min. The symbols represent the mean values for n = 8 animals per group and error bars represent the standard deviation (STD). The data are also shown in Tables 9.1.2.5 and 9.1.2.6.

Table 9.1.2.5. Proteomic biomarker levels in B6D2F1 female mice irradiated with mixed-field (67% n and 33% γ) at 0.6 Gy/min. Shaded data represent a significant difference between control (non-irradiated) and irradiated groups at 95% CL.

Biomarker (control values)	Day post-TBI	Biomarker Level (Mean ± STD)				Biomarker (control values)	Day post-TBI	Biomarker Level (Mean ± STD)			
		Sham (0 Gy)	1.5 Gy	3.0 Gy	6.0 Gy			Sham (0 Gy)	1.5 Gy	3.0 Gy	6.0 Gy
Flt3 L (pg mL^{-1}) (250 ± 77)	1	187 ± 48	365 ± 79	419 ± 74	601 ± 128	G-CSF (pg mL^{-1}) (29.7 ± 7.7)	1	41.6 ± 9.9	66.9 ± 19.2	143.6 ± 41.4	112.5 ± 34.3
	2	216 ± 46	596 ± 108	803 ± 128	1038 ± 102		2	45.5 ± 12.0	60.5 ± 25.0	51.9 ± 10.0	180.1 ± 301.5
	4	202 ± 32	457 ± 64	1182 ± 85	1377 ± 144		4	35.8 ± 6.9	77.5 ± 16.3	202.7 ± 34.7	1,173 ± 379.7
	7	209 ± 63	276 ± 24	947 ± 92	1823 ± 262		7	45.4 ± 12.2	48.0 ± 8.6	106.1 ± 21.0	1,753 ± 987.3
IL-5 (pg mL^{-1}) (3.2 ± 0.8)	1	3.8 ± 2.5	2.4 ± 0.3	2.3 ± 0.3	2.0 ± 0.2	GM-CSF (pg mL^{-1}) (0.11 ± 0.01)	1	0.05 ± 0.03	0.13 ± 0.03	0.17 ± 0.03	0.12 ± 0.04
	2	3.0 ± 0.8	6.7 ± 2.8	9.2 ± 2.7	12.6 ± 1.7		2	0.12 ± 0.04	0.20 ± 0.06	0.62 ± 0.05	2.00 ± 0.99
	4	3.6 ± 1.3	4.1 ± 0.7	12.3 ± 2.4	31.0 ± 7.5		4	0.14 ± 0.02	0.19 ± 0.03	1.12 ± 0.14	12.49 ± 2.74
	7	4.2 ± 1.7	9.7 ± 4.5	23.1 ± 9.9	19.6 ± 6.2		7	0.13 ± 0.03	0.17 ± 0.03	0.41 ± 0.10	3.88 ± 0.52
IL-10 (pg mL^{-1}) (9.6 ± 3.6)	1	5.6 ± 1.7	9.5 ± 1.8	10.7 ± 1.3	10.8 ± 2.1	SAA (ng mL^{-1}) (423 ± 121)	1	577 ± 129	1,071 ± 445	10,349 ± 5,312	13,683 ± 3,485
	2	7.8 ± 1.3	8.4 ± 1.4	8.0 ± 1.5	6.8 ± 2.0		2	674 ± 196	830 ± 316	3,000 ± 954	3,877 ± 2,290
	4	7.6 ± 1.1	7.6 ± 0.5	6.9 ± 0.7	6.5 ± 0.9		4	596 ± 225	753 ± 129	833 ± 317	1,393 ± 409
	7	8.8 ± 1.7	7.7 ± 0.9	9.1 ± 3.2	6.4 ± 2.6		7	421 ± 132	521 ± 60	907 ± 253	3,018 ± 3,686
IL-12 (pg mL^{-1}) (202 ± 26)	1	197 ± 35	199 ± 49	179 ± 14	211 ± 51	LBP (ng mL^{-1}) (454 ± 176)	1	516 ± 160	623 ± 125	884 ± 277	873 ± 283
	2	210 ± 49	135 ± 19	121 ± 10	157 ± 29		2	549 ± 84	506 ± 155	558 ± 162	559 ± 187
	4	197 ± 39	91 ± 11	66 ± 8	50 ± 17		4	571 ± 76	615 ± 88	546 ± 165	773 ± 178
	7	173 ± 53	115 ± 19	67 ± 12	40 ± 4		7	621 ± 200	517 ± 75	611 ± 113	722 ± 294
IL-18 (pg mL^{-1}) (143.3 ± 22.7)	1	106.6 ± 21.1	181.4 ± 21.1	178.4 ± 17.2	185.7 ± 47.9	CD27 (pg mL^{-1}) (3,324 ± 1,015)	1	3,861 ± 174	1,374 ± 231	970 ± 160	678 ± 133
	2	156.0 ± 27.4	194.3 ± 17.8	212.9 ± 23.3	241.8 ± 77.0		2	4,259 ± 1,332	834 ± 165	468 ± 36	271 ± 18
	4	125.8 ± 15.5	256.4 ± 20.6	416.4 ± 52.0	929.3 ± 104.7		4	3,597 ± 728	1,098 ± 193	403 ± 82	197 ± 56
	7	140.2 ± 35.7	196.9 ± 13.9	252.4 ± 34.6	737.7 ± 80.8		7	3,261 ± 606	1,813 ± 312	1,133 ± 232	200 ± 42
EPO (pg mL^{-1}) (18.7 ± 5.2)	1	18.6 ± 9.8	50.5 ± 16.9	39.6 ± 12.8	36.8 ± 9.3	CD45 (pg mL^{-1}) (5,568 ± 593)	1	6,923 ± 645	7,692 ± 1,164	10,197 ± 593	9,336 ± 1,924
	2	30.7 ± 13.1	100.2 ± 26.6	63.8 ± 14.7	63.5 ± 25.9		2	5,950 ± 122	5,853 ± 317	6,737 ± 446	6,500 ± 1,197
	4	30.0 ± 9.7	78.6 ± 11.0	253.0 ± 125.3	75.9 ± 27.1		4	6,537 ± 280	4,233 ± 374	4,200 ± 601	3,836 ± 587
	7	30.7 ± 15.9	78.5 ± 30.7	543.2 ± 229.9	642.9 ± 73.7		7	5,861 ± 625	3,851 ± 149	3,830 ± 234	2,725 ± 443
TPO (pg mL^{-1}) (195.2 ± 45.4)	1	255.8 ± 38.0	210.8 ± 27.2	346.4 ± 76.9	300.9 ± 59.1	CD45/CD27 ratio (1.78 ± 0.61)	1	1.86 ± 0.15	5.64 ± 0.63	9.91 ± 0.69	15.25 ± 2.79
	2	234.9 ± 52.1	208.1 ± 22.5	231.9 ± 40.5	246.6 ± 53.2		2	1.50 ± 0.40	7.09 ± 1.45	13.97 ± 1.44	24.81 ± 4.41
	4	221.9 ± 35.0	191.1 ± 34.8	383.4 ± 60.2	347.1 ± 62.7		4	1.62 ± 0.35	3.94 ± 0.63	10.63 ± 1.74	20.16 ± 3.20
	7	355.6 ± 26.9	460.2 ± 35.7	3,433 ± 647.9	5,418 ± 1,244		7	1.85 ± 0.35	2.01 ± 0.25	3.14 ± 0.64	13.82 ± 1.78

Table 9.1.2.6. Proteomic biomarker levels in B6D2F1 female mice irradiated with mixed-field (30% n and 70% γ) at 0.6 Gy/min. Shaded data represent a significant difference between control (non-irradiated) and irradiated groups at 95% CL.

Biomarker (control values)	Day post-TBI	Biomarker Level (Mean ± STD)				Biomarker (control values)	Day post-TBI	Biomarker Level (Mean ± STD)			
		Sham (0 Gy)	1.5 Gy	3.0 Gy	6.0 Gy			Sham (0 Gy)	1.5 Gy	3.0 Gy	6.0 Gy
Flt3 L (pg mL^{-1}) (250 ± 77)	1	187 ± 48	292 ± 25	378 ± 64	578 ± 94	G-CSF (pg mL^{-1}) (29.7 ± 7.7)	1	41.6 ± 9.9	67.8 ± 21.2	101.6 ± 26.6	113.3 ± 30.0
	2	216 ± 46	450 ± 64	622 ± 46	1067 ± 71		2	45.5 ± 12.0	43.5 ± 6.0	51.5 ± 12.9	55.1 ± 9.0
	4	202 ± 32	396 ± 46	926 ± 160	1755 ± 125		4	35.8 ± 6.9	59.5 ± 9.9	107.8 ± 24.7	547.5 ± 108.5
	7	209 ± 63	199 ± 17	369 ± 46	1915 ± 116		7	45.4 ± 12.2	38.2 ± 2.1	61.4 ± 13.3	421.4 ± 181.8
IL-5 (pg mL^{-1}) (3.2 ± 0.8)	1	3.8 ± 2.5	3.3 ± 0.8	2.5 ± 0.7	2.2 ± 0.3	GM-CSF (pg mL^{-1}) (0.11 ± 0.01)	1	0.05 ± 0.03	0.13 ± 0.01	0.15 ± 0.02	0.15 ± 0.02
	2	3.0 ± 0.8	4.1 ± 1.2	6.1 ± 1.3	8.9 ± 2.1		2	0.12 ± 0.04	0.17 ± 0.03	0.27 ± 0.06	0.83 ± 0.29
	4	3.6 ± 1.3	5.2 ± 2.6	10.4 ± 3.1	26.2 ± 7.3		4	0.14 ± 0.02	0.20 ± 0.06	0.31 ± 0.07	4.37 ± 0.45
	7	4.2 ± 1.7	4.7 ± 1.0	15.3 ± 7.5	46.7 ± 41.0		7	0.13 ± 0.03	0.12 ± 0.02	0.22 ± 0.03	1.46 ± 0.40
IL-10 (pg mL^{-1}) (9.6 ± 3.6)	1	5.6 ± 1.7	9.4 ± 1.6	11.9 ± 1.6	10.4 ± 1.4	SAA (ng mL^{-1}) (423 ± 121)	1	577 ± 129	686 ± 411	5,792 ± 2,031	10759 ± 3,375
	2	7.8 ± 1.3	7.3 ± 0.9	6.8 ± 0.5	6.9 ± 1.1		2	674 ± 196	328 ± 71	1,444 ± 464	1,805 ± 635
	4	7.6 ± 1.1	8.7 ± 1.1	6.7 ± 1.1	5.9 ± 1.1		4	596 ± 225	367 ± 116	598 ± 154	635 ± 139
	7	8.8 ± 1.7	5.9 ± 1.3	8.1 ± 1.1	6.3 ± 0.6		7	421 ± 132	205 ± 87	524 ± 157	510 ± 122
IL-12 (pg mL^{-1}) (202 ± 26)	1	197 ± 35	155 ± 21	195 ± 32	159 ± 21	LBP (ng mL^{-1}) (454 ± 176)	1	516 ± 160	745 ± 126	684 ± 103	934 ± 144
	2	210 ± 49	122 ± 41	112 ± 10	120 ± 15		2	549 ± 84	603 ± 91	451 ± 68	634 ± 97
	4	197 ± 39	88 ± 12	90 ± 23	66 ± 22		4	571 ± 76	673 ± 58	474 ± 71	892 ± 136
	7	173 ± 53	117 ± 15	109 ± 28	57 ± 12		7	621 ± 200	318 ± 351	525 ± 84	557 ± 91
IL-18 (pg mL^{-1}) (143.3 ± 22.7)	1	106.6 ± 21.1	142.0 ± 14.6	179.5 ± 12.0	234.8 ± 31.2	CD27 (pg mL^{-1}) (3,324 ± 1,015)	1	3,861 ± 174	1,495 ± 156	984 ± 347	368 ± 42
	2	156.0 ± 27.4	118.4 ± 15.0	165.5 ± 7.7	266.7 ± 26.9		2	4,259 ± 1332	878 ± 102	347 ± 17	187 ± 24
	4	125.8 ± 15.5	135.6 ± 29.0	295.1 ± 53.2	830.6 ± 115.6		4	3,597 ± 728	1,063 ± 182	387 ± 50	168 ± 19
	7	140.2 ± 35.7	97.3 ± 20.6	203.4 ± 12.7	471.4 ± 54.4		7	3,261 ± 606	1,526 ± 239	987 ± 156	324 ± 68
EPO (pg mL^{-1}) (18.7 ± 5.2)	1	18.6 ± 9.8	40.3 ± 13.2	28.1 ± 13.1	34.7 ± 15.8	CD45 (pg mL^{-1}) (5,568 ± 593)	1	6,923 ± 645	7,993 ± 449	7,749 ± 816	8,187 ± 1,021
	2	16.0 ± 7.4	61.8 ± 31.7	76.6 ± 24.3	52.1 ± 12.8		2	5,950 ± 122	6,345 ± 338	5,869 ± 549	5,183 ± 348
	4	30.0 ± 9.7	72.4 ± 25.4	182.4 ± 63.1	159.8 ± 60.6		4	6,537 ± 280	3,903 ± 205	3,585 ± 394	3,849 ± 441
	7	30.7 ± 15.9	71.2 ± 28.2	260.4 ± 116.0	1,167 ± 272.0		7	5,861 ± 625	4,177 ± 453	3,556 ± 266	2,737 ± 244
TPO (pg mL^{-1}) (195.2 ± 45.4)	1	255.8 ± 38.0	523.9 ± 115.4	394.5 ± 213.9	331.3 ± 36.5	CD45/CD27 ratio (1.78 ± 0.61)	1	1.86 ± 0.15	5.39 ± 0.54	8.68 ± 2.90	22.33 ± 2.22
	2	234.9 ± 52.1	627.9 ± 305.2	238.8 ± 25.0	262.9 ± 46.3		2	1.50 ± 0.40	7.05 ± 1.38	16.48 ± 0.82	28.23 ± 4.45
	4	221.9 ± 35.0	404.4 ± 44.4	241.0 ± 24.7	786.3 ± 160.5		4	1.62 ± 0.35	3.76 ± 0.64	9.36 ± 1.18	22.02 ± 1.65
	7	355.6 ± 26.9	434.9 ± 42.1	1,301 ± 401.0	5,127 ± 567.7		7	1.85 ± 0.35	2.79 ± 0.46	3.66 ± 0.46	8.72 ± 1.67

Fig. 9.1.2.5 and data in Tables 9.1.2.5 and 9.1.2.7 show the dose- and time-dependent changes in profile of protein biomarkers in blood plasma of female mice after mixed-field TBI with (67% n + 33% γ) at a dose rate of either 0.6 or 1.9 Gy/min. No significant differences were observed between animal groups for Flt3L, IL-5, TPO, IL-12, IL-18, EPO, G-CSF, GM-CSF, SAA, CD27, and CD45/CD27 levels ($p > 0.161$). No differences were observed in CD45 levels except slightly significant differences in 3- and 6-Gy groups on d7 (in 3-Gy groups: 3830 ± 234 vs. 3108 ± 155 pg mL^{-1} and in 6-Gy groups: 2725 ± 443 vs. 2005 ± 189 pg mL^{-1} at dose rates of 0.6 and 1.9 Gy/min, respectively). This difference correlates to the very low ANC level (0.01 ± 0.01× 10^9 L^{-1}) (ANC nadir) in those mouse groups.

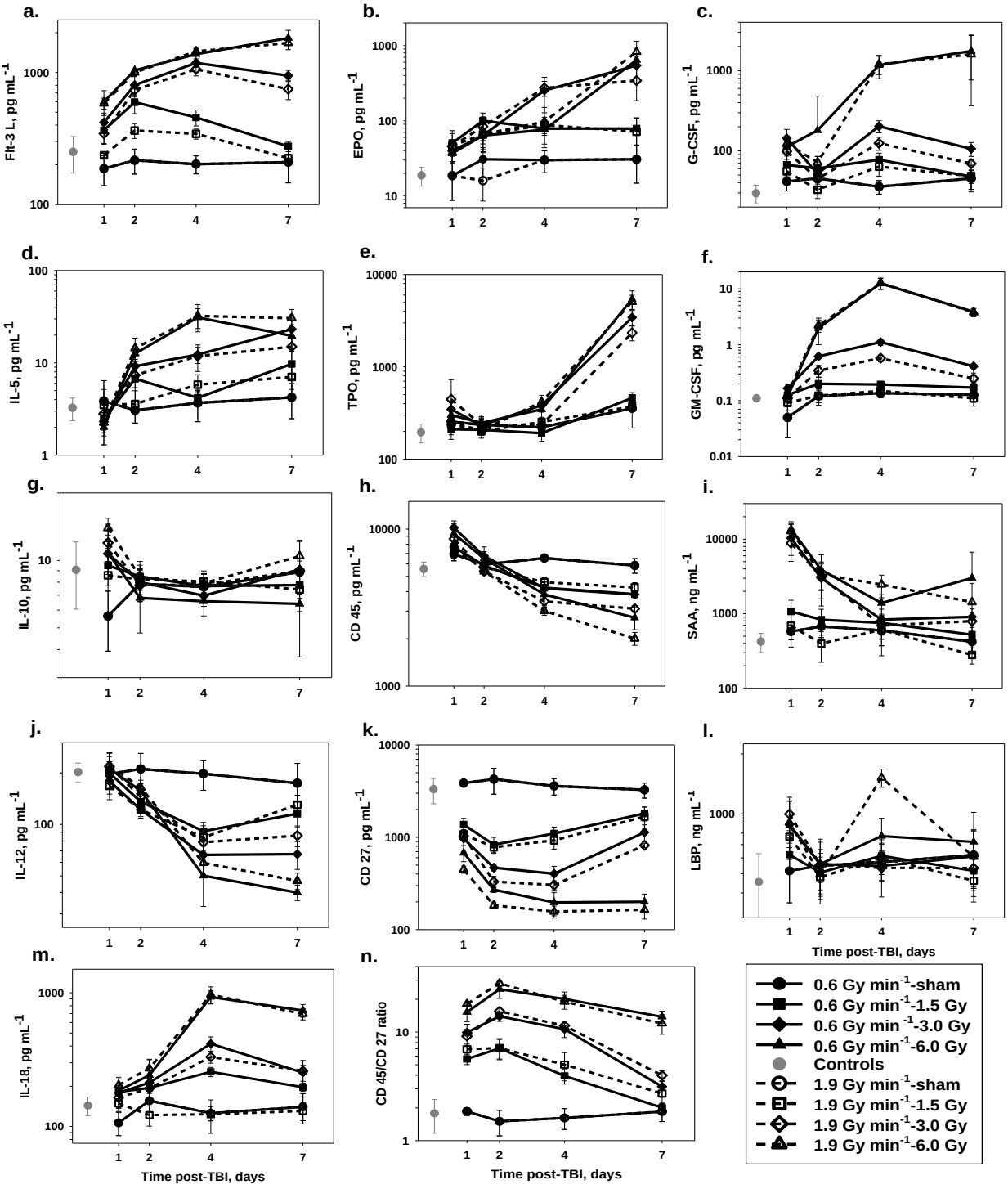

Fig. 9.1.2.5. Dose- and time-dependent changes in profile of protein biomarkers: FLT3L (a), EPO (b), G-CSF (c), IL-5 (d), TPO (e), GM-CSF (f), IL-10 (g), CD45 (h), SAA (i), IL-12 (j), CD27 (k), LBP (l), IL-18 (m), CD45/CD27 (n) in blood plasma of female mice after a mixed-field TBI with (67% n + 33% γ) at the dose rate of either 0.6 Gy/min (solid lines) or 1.9 Gy/min (dashed lines). The symbols represent the mean values for n = 8 animals per group and error bars represent the standard deviation (STD). The data are also shown in Tables 9.1.2.5 and 9.1.2.7.

Table 9.1.2.7. Proteomic biomarker levels in B6D2F1 female mice irradiated with mixed-field (67% n and 33% γ) at 1.9 Gy/min. Shaded data represent a significant difference between control (non-irradiated) and irradiated groups at 95% CL.

Biomarker (control values)	Day post-TBI	Biomarker Level (Mean ± STD)				Biomarker (control values)	Day post-TBI	Biomarker Level (Mean ± STD)			
		Sham (0 Gy)	1.5 Gy	3.0 Gy	6.0 Gy			Sham (0 Gy)	1.5 Gy	3.0 Gy	6.0 Gy
Flt3 L (pg mL^{-1}) (250 ± 77)	1	187 ± 48	236 ± 8	344 ± 55	584 ± 56	G-CSF (pg mL^{-1}) (29.7 ± 7.7)	1	41.6 ± 9.9	55.6 ± 14.2	98.4 ± 33.9	122.4 ± 25.5
	2	216 ± 46	363 ± 47	737 ± 82	1001 ± 55		2	45.5 ± 12.0	32.8 ± 7.3	45.0 ± 6.5	72.1 ± 12.8
	4	202 ± 32	343 ± 30	1060 ± 117	1446 ± 77		4	35.8 ± 6.9	63.6 ± 15.1	124.5 ± 23.1	1,202 ± 309.6
	7	209 ± 63	224 ± 15	748 ± 125	1673 ± 183		7	45.4 ± 12.2	48.5 ± 17.7	69.4 ± 8.3	1,598 ± 1,233
IL-5 (pg mL^{-1}) (3.2 ± 0.8)	1	3.8 ± 2.5	3.5 ± 1.6	2.8 ± 0.7	2.2 ± 0.6	GM-CSF (pg mL^{-1}) (0.11 ± 0.01)	1	0.05 ± 0.03	0.09 ± 0.03	0.11 ± 0.03	0.13 ± 0.02
	2	3.0 ± 0.8	3.5 ± 1.4	7.3 ± 1.9	14.4 ± 4.1		2	0.12 ± 0.04	0.12 ± 0.03	0.35 ± 0.08	2.22 ± 0.55
	4	3.6 ± 1.3	5.8 ± 1.6	11.8 ± 3.7	32.2 ± 10.5		4	0.14 ± 0.02	0.15 ± 0.03	0.57 ± 0.08	12.64 ± 2.90
	7	4.2 ± 1.7	7.0 ± 2.4	14.9 ± 8.2	30.5 ± 7.3		7	0.13 ± 0.03	0.11 ± 0.03	0.25 ± 0.04	3.81 ± 0.64
IL-10 (pg mL^{-1}) (9.6 ± 3.6)	1	5.6 ± 1.7	8.5 ± 1.3	11.9 ± 2.5	13.9 ± 1.4	SAA (ng mL^{-1}) (423 ± 121)	1	577 ± 129	688 ± 332	8,876 ± 2,825	12842 ± 3,180
	2	7.8 ± 1.3	8.2 ± 0.8	7.7 ± 0.8	8.4 ± 0.5		2	674 ± 196	397 ± 175	3112 ± 1841	3,372 ± 1,271
	4	7.6 ± 1.1	8.0 ± 0.6	7.8 ± 0.8	7.9 ± 1.0		4	596 ± 225	609 ± 336	693 ± 241	2,469 ± 829
	7	8.8 ± 1.7	7.4 ± 1.1	8.9 ± 0.9	10.4 ± 1.7		7	421 ± 132	280 ± 69	793 ± 245	1,433 ± 1,126
IL-12 (pg mL^{-1}) (202 ± 26)	1	197 ± 35	167 ± 28	218 ± 42	221 ± 39	LBP (ng mL^{-1}) (454 ± 176)	1	516 ± 160	767 ± 56	997 ± 215	903 ± 143
	2	210 ± 49	122 ± 13	144 ± 27	164 ± 17		2	549 ± 84	480 ± 66	554 ± 104	495 ± 111
	4	197 ± 39	83 ± 14	78 ± 11	59 ± 8		4	571 ± 76	601 ± 139	534 ± 75	1,518 ± 159
	7	173 ± 53	130 ± 17	86 ± 11	46 ± 5		7	621 ± 200	460 ± 100	534 ± 123	608 ± 224
IL-18 (pg mL^{-1}) (143.3 ± 22.7)	1	106.6 ± 21.1	148.8 ± 19.3	164.5 ± 27.8	204.3 ± 22.7	CD27 (pg mL^{-1}) (3,324 ± 1,015)	1	3861 ± 174	1077 ± 139	1025 ± 324	448 ± 40
	2	156.0 ± 27.4	121.7 ± 21.1	192.7 ± 37.0	272.1 ± 43.4		2	4259 ± 1332	783 ± 94	331 ± 47	183 ± 16
	4	125.8 ± 15.5	123.4 ± 34.7	331.6 ± 33.8	970.0 ± 137.4		4	3597 ± 728	927 ± 182	304 ± 34	157 ± 23
	7	140.2 ± 35.7	130.6 ± 20.1	260.4 ± 51.8	694.5 ± 67.3		7	3261 ± 606	1678 ± 453	818 ± 44	164 ± 34
EPO (pg mL^{-1}) (18.7 ± 5.2)	1	18.6 ± 9.8	46.3 ± 27.4	45.7 ± 9.2	37.5 ± 8.8	CD45 (pg mL^{-1}) (5,568 ± 593)	1	6,923 ± 645	7,402 ± 444	8,651 ± 388	7,941 ± 542
	2	15.9 ± 7.4	65.6 ± 26.7	83.8 ± 29.2	66.0 ± 24.5		2	5,950 ± 122	5,717 ± 350	5,388 ± 297	5,375 ± 164
	4	30.0 ± 9.71	87.7 ± 23.8	273.1 ± 61.4	97.2 ± 53.4		4	6,537 ± 280	4,589 ± 313	3,463 ± 279	3,004 ± 180
	7	30.7 ± 15.9	71.4 ± 37.8	342.6 ± 157.8	827.0 ± 315.1		7	5,861 ± 625	4,250 ± 308	3,108 ± 155	2,005 ± 189
TPO (pg mL^{-1}) (195.2 ± 45.4)	1	255.8 ± 38.0	237.2 ± 34.3	445.8 ± 282.1	248.0 ± 35.9	CD45/CD27 ratio (1.78 ± 0.61)	1	1.86 ± 0.15	6.95 ± 0.79	9.15 ± 2.66	18.15 ± 0.68
	2	234.9 ± 52.1	200.6 ± 31.7	234.4 ± 41.7	205.1 ± 17.7		2	1.50 ± 0.40	7.13 ± 1.57	15.55 ± 1.44	28.09 ± 1.97
	4	221.9 ± 35.0	253.2 ± 18.1	235.5 ± 39.9	417.1 ± 74.9		4	1.62 ± 0.35	5.01 ± 1.46	11.45 ± 0.66	19.02 ± 2.80
	7	355.6 ± 26.9	371.7 ± 154.5	2,340 ± 426.1	5,076 ± 886.8		7	1.85 ± 0.35	2.71 ± 0.79	3.99 ± 0.41	12.00 ± 2.46

Fig. 9.1.2.6 and data in Tables 9.1.2.5 and 9.1.2.8 show the dose- and time-dependent changes in profile of protein biomarkers in blood plasma of female and male mice after a mixed-field TBI with (67% n + 33% γ) at a dose rate of 0.6 Gy/min (gender-comparison study). No significant differences were observed between animal groups for Flt3L, IL-12, IL-18, EPO, G-CSF, GM-CSF, and SAA ($p > 0.088$). IL-5 level in sham male mice was about 2-fold less than in female mice. While a strong dose- and time-dependency was observed in female and males, the IL-5 level in irradiated mice remained at about 2-fold less in all animal groups (Fig. 9.1.2.6d). No significant differences in TPO concentration were observed except in 6-Gy groups on d4. TPO in males was 1670 ± 216 pg mL^{-1} while in females it was 347 ± 63 pg mL^{-1} (Tables 9.1.2.5 and 9.1.2.8). While CD27 in sham female groups remained level on d1-d7 (3578 ± 441 pg mL^{-1}), CD27 level in sham male mice ranged from 3013 ± 1190 pg mL^{-1} (d1) to 1742 ± 342 pg mL^{-1} (d7) (Fig. 9.1.2.6h). In irradiated mice, the only significant difference found was in 1.5-Gy groups on days 2, 4 and 7 ($p < 0.008$). With a similar pattern observed for CD45 levels, CD45/CD27 ratios showed no significant difference between male and female mice ($p > 0.096$).

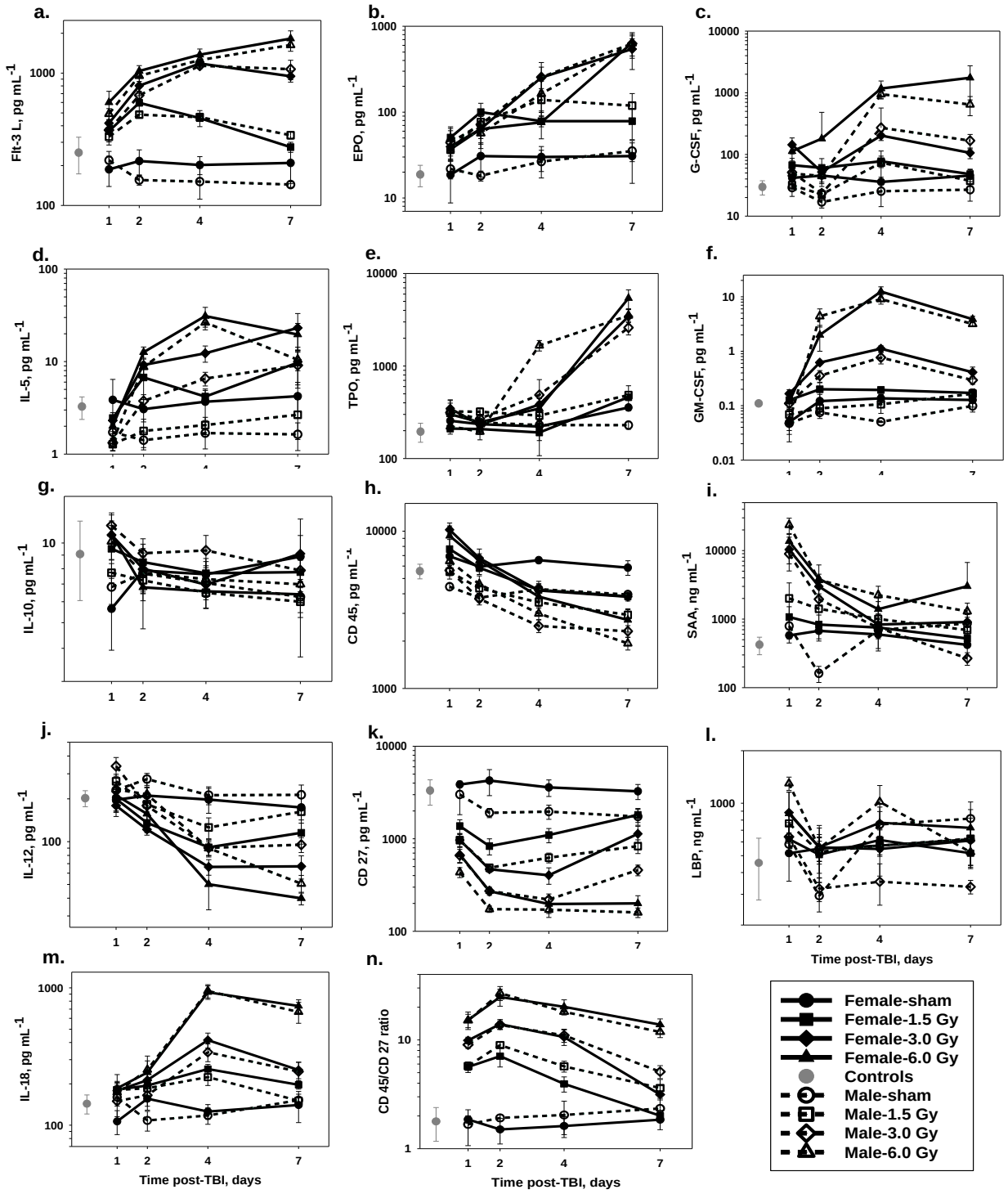

Fig. 9.1.2.6. Dose- and time-dependent changes in profile of protein biomarkers: FLT3L (a), EPO (b), G-CSF (c), IL-5 (d), TPO (e), GM-CSF (f), IL-10 (g), CD45 (h), SAA (i), IL-12 (j), CD27 (k), LBP (l), IL-18 (m), CD45/CD27 (n) in blood plasma of female (solid lines) and male (dashed lines) mice after a mixed-field TBI with (67% n + 33% γ) at the dose rate of 0.6 Gy/min. The symbols represent the mean values for n = 8 animals per group and error bars represent the standard deviation (STD). The data are also shown in Tables 9.1.2.5 and 9.1.2.8.

Table 9.1.2.8. Proteomic biomarker levels in B6D2F1 male mice irradiated with mixed-field (67% n and 33% γ) at 0.6 Gy/min. Shaded data represent a significant difference between control (non-irradiated) and irradiated groups at 95% CL.

Biomarker (control values)	Day post-TBI	Biomarker Level (Mean ± STD)				Biomarker (control values)	Day post-TBI	Biomarker Level (Mean ± STD)			
		Sham (0 Gy)	1.5 Gy	3.0 Gy	6.0 Gy			Sham (0 Gy)	1.5 Gy	3.0 Gy	6.0 Gy
Flt3 L (pg mL^{-1}) (250 ± 77)	1	219 ± 37	330 ± 29	371 ± 19	493 ± 47	G-CSF (pg mL^{-1}) (29.7 ± 7.7)	1	28.9 ± 8.0	31.8 ± 2.2	51.1 ± 15.5	48.9 ± 9.0
	2	155 ± 13	486 ± 22	680 ± 50	954 ± 89		2	16.9 ± 3.4	22.4 ± 4.4	23.4 ± 2.0	44.7 ± 14.5
	4	151 ± 40	465 ± 33	1138 ± 57	1255 ± 79		4	25.3 ± 11.0	73.4 ± 40.3	271.6 ± 295.5	950.3 ± 136.3
	7	144 ± 7	339 ± 21	1071 ± 179	1631 ± 169		7	26.8 ± 9.3	37.4 ± 7.3	167.1 ± 44.2	646.6 ± 222.1
IL-5 (pg mL^{-1}) (3.2 ± 0.8)	1	1.7 ± 0.2	1.2 ± 0.2	1.3 ± 0.1	1.3 ± 0.2	GM-CSF (pg mL^{-1}) (0.11 ± 0.01)	1	0.05 ± 0.02	0.07 ± 0.02	0.11 ± 0.02	0.05 ± 0.02
	2	1.4 ± 0.3	1.7 ± 0.6	3.7 ± 0.6	8.7 ± 1.8		2	0.08 ± 0.02	0.09 ± 0.02	0.36 ± 0.09	4.39 ± 1.60
	4	1.6 ± 0.5	2.0 ± 0.4	6.5 ± 1.1	26.5 ± 4.4		4	0.05 ± 0.00	0.11 ± 0.03	0.77 ± 0.18	9.06 ± 1.73
	7	1.6 ± 0.5	2.6 ± 1.2	9.1 ± 3.5	10.4 ± 2.5		7	0.10 ± 0.02	0.17 ± 0.02	0.30 ± 0.05	3.17 ± 0.27
IL-10 (pg mL^{-1}) (9.6 ± 3.6)	1	6.8 ± 0.9	7.7 ± 0.6	11.6 ± 1.1	10.1 ± 1.5	SAA (ng mL^{-1}) (423 ± 121)	1	792 ± 275	2,007 ± 1,367	8,956 ± 2,563	23668 ± 5,969
	2	7.6 ± 1.2	7.2 ± 1.1	9.1 ± 1.2	7.7 ± 0.3		2	162 ± 43	1,414 ± 752	1,952 ± 383	3,735 ± 788
	4	7.0 ± 0.3	6.5 ± 0.8	9.3 ± 1.3	7.3 ± 1.2		4	692 ± 349	1,002 ± 188	747 ± 1285	2,243 ± 773
	7	6.2 ± 1.0	6.0 ± 0.5	7.8 ± 0.7	6.9 ± 1.0		7	862 ± 199	691 ± 99	267 ± 56	1,296 ± 417
IL-12 (pg mL^{-1}) (202 ± 26)	1	230 ± 31	265 ± 32	339 ± 51	233 ± 25	LBP (ng mL^{-1}) (454 ± 176)	1	581 ± 54	766 ± 122	642 ± 133	1,298 ± 113
	2	275 ± 26	183 ± 25	179 ± 59	215 ± 27		2	294 ± 56	526 ± 79	323 ± 51	552 ± 89
	4	212 ± 30	125 ± 21	90 ± 12	89 ± 10		4	755 ± 141	571 ± 65	354 ± 94	1,019 ± 244
	7	213 ± 36	162 ± 20	95 ± 11	50 ± 7		7	817 ± 102	627 ± 89	331 ± 30	524 ± 86
IL-18 (pg mL^{-1}) (143.3 ± 22.7)	1	159.8 ± 16.6	180.3 ± 28.1	149.6 ± 34.2	173.4 ± 31.1	CD27 (pg mL^{-1}) (3,324 ± 1,015)	1	3,013 ± 1,190	967 ± 142	661 ± 107	434 ± 54
	2	108.3 ± 17.7	185.6 ± 22.9	165.1 ± 27.7	253.5 ± 40.6		2	1,910 ± 220	485 ± 45	272 ± 28	174 ± 14
	4	117.6 ± 16.0	223.8 ± 29.2	340.4 ± 50.2	949.3 ± 105.7		4	1,967 ± 343	624 ± 76	220 ± 13	171 ± 15
	7	152.3 ± 15.8	150.7 ± 9.1	245.8 ± 42.1	668.3 ± 116.0		7	1,742 ± 342	833 ± 142	458 ± 60	160 ± 19
EPO (pg mL^{-1}) (18.7 ± 5.2)	1	21.7 ± 5.1	36.5 ± 5.7	44.1 ± 16.6	48.7 ± 15.9	CD45 (pg mL^{-1}) (5,568 ± 593)	1	4,433 ± 212	5,526 ± 565	5,631 ± 404	6,462 ± 595
	2	18.1 ± 2.4	76.6 ± 12.5	71.7 ± 12.5	56.7 ± 14.4		2	3,776 ± 214	4,341 ± 324	3,715 ± 317	4,605 ± 594
	4	26.5 ± 9.4	139.1 ± 48.9	255.4 ± 79.1	164.2 ± 64.9		4	4,283 ± 354	3,531 ± 210	2,495 ± 231	2,991 ± 256
	7	35.1 ± 8.6	119.1 ± 45.5	628.6 ± 178.4	634.1 ± 209.4		7	3,952 ± 215	2,936 ± 278	2,310 ± 199	1,935 ± 181
TPO (pg mL^{-1}) (195.2 ± 45.4)	1	309.1 ± 87.7	322.3 ± 108.9	313.0 ± 40.8	222.3 ± 27.2	CD45/CD27 ratio (1.78 ± 0.61)	1	1.67 ± 0.61	5.76 ± 0.52	9.04 ± 0.68	15.08 ± 2.12
	2	245.0 ± 20.4	320.2 ± 31.3	269.6 ± 26.8	194.9 ± 35.6		2	1.92 ± 0.13	8.97 ± 0.56	13.72 ± 1.27	26.96 ± 3.97
	4	229.9 ± 122.6	290.9 ± 33.5	486.8 ± 226.0	1,670 ± 215.9		4	2.04 ± 0.70	5.72 ± 0.66	11.03 ± 1.52	18.13 ± 0.68
	7	229.4 ± 22.3	484.5 ± 127.2	2,601 ± 432.3	3,513 ± 560.6		7	2.34 ± 0.46	3.61 ± 0.71	5.10 ± 0.70	11.85 ± 1.34

The dose- and time-dependent changes in PCT levels in individual mice are shown in Fig. 9.1.2.7. Our results demonstrate that PCT level increased in a dose- and time-dependent manner beginning from d4 post-TBI. PCT level was significantly higher in mice irradiated with a higher percentage of neutrons. The symbols represent the PCT concentration for individual animals (n = 8 - 12 animals per group) measured on day 4 and day 7 post TBI. PCT level was higher in mice irradiated with a higher percentage of neutrons (i.e., 67% vs. 30%).

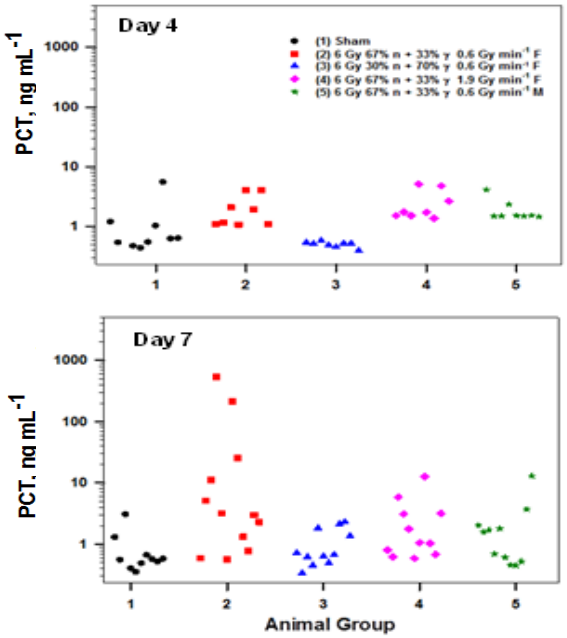

Fig. 9.1.2.7. Dose- and time-dependent changes in PCT level in blood plasma of female (F) and male (M) mice after a mixed-field TBI to 6.0 Gy with either (67% n + 33% γ) or (30% n + 70% γ) at the dose rate of either 0.6 Gy/min or 1.9 Gy/min.

Figs. 9.1.2.8 and 9.1.2.9 show correlations between CBC/diff and selected proteomic biomarkers in TRIGA mixed-field studies.

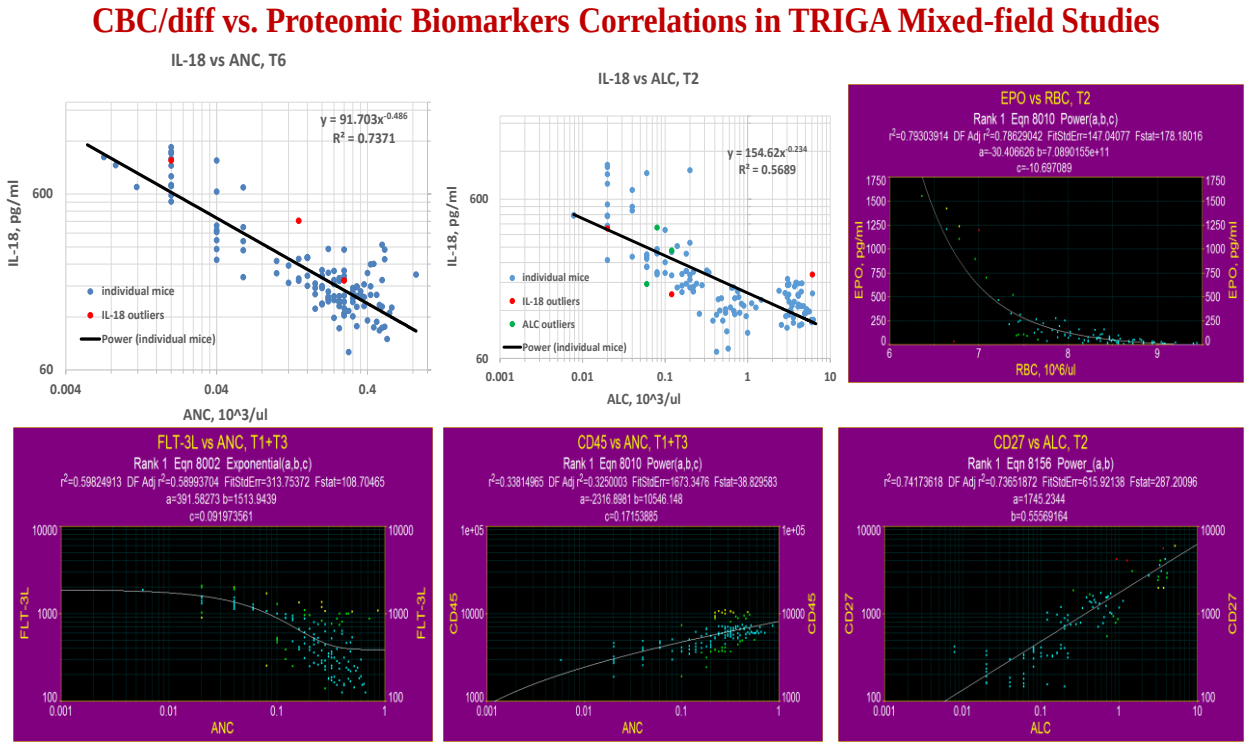

Fig. 9.1.2.8 Correlations between CBC/diff and selected proteomic biomarkers in TRIGA mixed-field studies performed by using SAS and Table Curve 2D software.

Selected Proteomic Biomarkers Correlations in TRIGA Mixed-field Studies

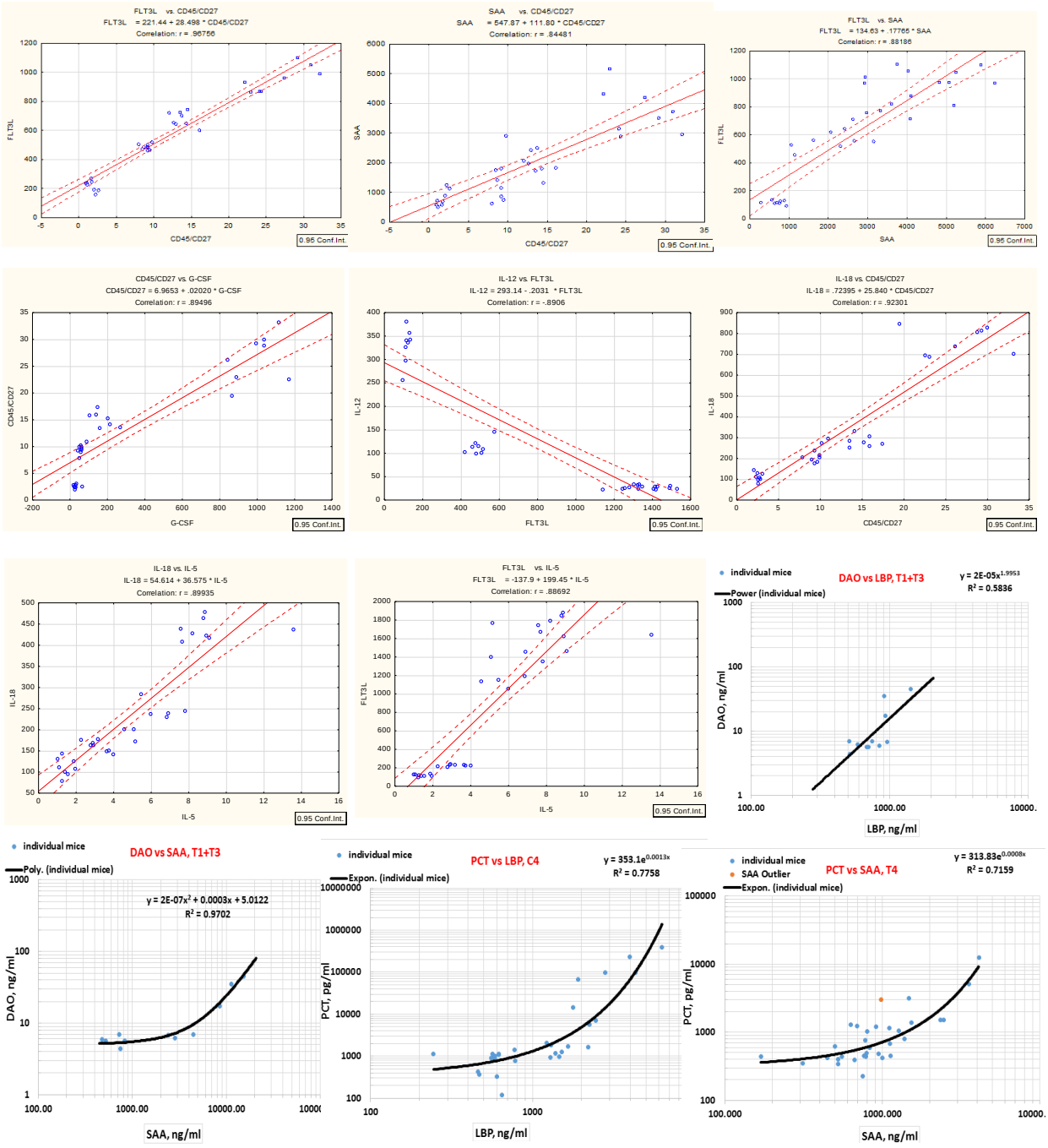

Fig. 9.1.2.9. Correlations between selected proteomic biomarkers in TRIGA mixed-field studies performed by using SAS and Table Curve 2D software.

9.1.3. DISCUSSION

In our mixed-field studies, we evaluated the utility of multiple blood biomarkers for early-response radiation injury assessment in a mouse TBI model after exposure to a mixed-field (neutrons and γ-rays) using the AFRRI's TRIGA nuclear research reactor. Studies included: (1) exposing animals

to radiation doses 1.5, 3 and 6 Gy, (2) testing different proportions of neutrons and γ-rays (67% n + 33% γ or 30% n + 70% γ), (3) different dose rates (0.6 or 1.9 Gy/min) and (4) evaluating biomarker differences between male and female mice. A list of evaluated biomarkers includes blood cell counts, hematopoietic cytokines, organ-specific, and acute phase protein biomarkers (Table 7.1). Results demonstrate: 1) dose- and time-dependent changes in fms-related tyrosin kinase 3 ligand (Flt-3 Ligand or Flt3L), interleukins IL-5, IL-10, IL-12, and IL-18, granulocyte stimulating factors (G-CSF and GM-CSF), thrombopoietin (TPO), erythropoietin (EPO), acute phase proteins (serum amyloid A or SAA and lipopolysaccharide binding protein or LBP), surface plasma neutrophil (CD45) and lymphocyte (CD27) markers, ratio of CD45 to CD27, and procalcitonin (PCT); 2) dose- and time-dependent changes in blood cell counts: lymphocytes, neutrophils, platelets, red blood cells and ratio of neutrophils to lymphocytes; 3) levels of IL-18, G-CSF, GM-CSF, SAA and PCT were significantly higher in animals irradiated with 67% n + 33% γ compared to those irradiated with 30% n + 70% γ ($p < 0.015$), while no significant differences ($p > 0.114$) were observed in hematological biomarker counts; 4) exposure with 3-fold difference in dose rate (0.6 or 1.9 Gy min^{-1}) revealed no significant differences in hematological and protein biomarker levels ($p > 0.154$); 5) no significant differences in hematological and protein biomarker levels were observed in gender-comparison study for any radiation dose at any time after exposure ($p > 0.088$). Results show that the dynamic changes in the levels of selected hematopoietic cytokines, organ-specific, and acute phase protein biomarkers reflect the time course and severity of acute radiation syndrome (ARS) and may function as prognostic indicators of ARS outcome.

Hematological biomarkers of exposure to ionizing radiation are well characterized and used in medical management of radiological casualties (Dainiak et al. 2003). Measurements of lymphocyte depletion kinetics (Goans et al. 1997) and time- and exposure- severity changes in neutrophil cell counts observed after irradiation provide clinical information soon after exposure. However, the accurate estimation of radiation exposure dose absorbed using the lymphocyte depletion kinetics becomes problematic after doses close to the LD_{50}, and certainly for higher doses due to significant declines (< 200 cells μL^{-1}) in peripheral lymphocyte counts by 24 h (Baranov et al. 1995; Goans et al. 1997). Our results demonstrate that no significant differences ($p > 0.114$) were observed in blood cell counts in mice irradiated at different experimental conditions (i.e., 67% n + 33% γ vs. 30% n + 70% γ; 0.6 vs. 1.9 Gy/min; or males vs. females). These findings indicate that ALC depletion kinetics might be used in biodosimetry to estimate the radiation dose received regardless of mixed-field exposure conditions. However, at doses 3 Gy and higher, accurate radiation dose assessment is questionable, but still valuable to separate irradiated from non-irradiated individuals at any post-exposure time. Our results demonstrate that, while absolute lymphocyte counts decrease and plateau at doses ≥3 Gy beginning from d2 after exposure, proteins show progressive dose-dependent changes, which indicates that these radiation responsive proteins have considerable potential as biodosimeters.

While the traditional radiation exposure biomarkers based on cytogenetic assays and lymphocyte depletion kinetics are well characterized and used in medical management of radiological casualties (Baranov et al. 1995; Goans et al. 1997; Fliedner et al. 2001; Dainiak et al. 2003), the development of rapid and non- or minimally-invasive methods to assess the radiation exposure level and radiation injury are needed for biodosimetry triage in mass casualty radiation exposure scenarios. Numerous studies have demonstrated the advantages of proteomics to reach those goals (Bertho et al. 2001, 2008; Sigal et al. 2013; Schaff et al. 2013; Bazan et al. 2014; Ossetrova et al. 2007- 2016a, 2016b). It was previously reported that the production of cytokines is

increased after exposure to radiation (Dainiak et al. 2003). Radiation-induced increases in circulating cytokines and chemokines that are involved in the protection of animals by regulating proliferation, differentiation, and migration of residual hematopoietic stem and progenitor cells have been reported in numerous studies (Cary et al. 2012; Kiang et al. 2010, 2018; Ossetrova et al. 2007-2018; Ha et al. 2014). Hematopoietic cytokines and growth factors selected for this study have been shown to be essential contributors to natural resistance to lethal irradiation and their expression showed a significant effect on hematopoietic recovery after radiation by stimulating the proliferation and differentiation of various blood cell progenitors (MacVittie et al. 1991; Bertho et al. 2001; Dainiak et al. 2003).

Our results demonstrate that levels of IL-18, G-CSF, GM-CSF, and SAA were significantly higher in animals irradiated with 67% n + 33% γ compared to those irradiated with 30% n + 70% γ ($p < 0.015$) while no significant differences ($p > 0.114$) observed in blood cell counts. TBI exposure of mice with a 3-fold difference in dose rate (0.6 or 1.9 Gy min^{-1}) revealed no significant differences in protein biomarker levels ($p > 0.154$). No significant differences were observed in gender-comparison study for any radiation dose and at any time after exposure ($p > 0.088$).

Since some inflammatory cytokines and acute phase proteins might be elevated due to non-radiation pathologies, such as heart disease, inflammation, stress or trauma, their utility for biodosimetry might be limited especially because a radiological or nuclear event would be expected to involve victims with mixed injuries as well as individuals with unrelated pre-existing pathologic processes. However, results from this study might provide a better understanding of the biology of the tissue- and organ-specific radiation injury and contribute to development of pharmacological, medical countermeasures to radiation injury that can be used by military personnel and emergency responders. In addition, we expect that these results will contribute to the advancement of medical radiation countermeasures.

In our past research in the B6D2F1 female mouse TBI model, Flt3L was not elevated in the blood of mice challenged with stress, infection, or trauma (15% non-lethal total-body surface skin burns or wounds) performed within 1 hour after radiation injury. Those findings suggest that Flt3L is a highly radiation-specific biomarker. In nonhuman primate radiation model, Flt3L was found persistently elevated up to three weeks, peaking two days before ANC nadir with a very good correlation between its level and ANC (Bertho et al. 2001; Ossetrova et al. 2014b, 2016a, 2016b, 2018). Flt3L also strongly correlated with ANC in both animal models and humans (radiation therapy patients and radiation accident victims) reported in numerous publications. Those findings make Flt3L very useful in estimating the radiation dose received and the severity of radiation-induced bone-marrow aplasia, which was already applied in radiation accidents (Bertho et al. 2008). The advantage of monitoring plasma Flt3L levels to predict bone marrow injury severity was demonstrated in a partially-irradiated murine model (Prat et al. 2006) and during the course of local fractionated radiotherapy (Huchet et al. 2003) as its level strongly correlated with both the radiation dose and the percentage of bone marrow irradiated.

Radiation-induced aplastic anemia occurs due to the inability of damaged stem cells in the bone marrow to manufacture new red blood cells. EPO has been shown as a principal factor in regulating erythropoiesis in mammals and promotes survival, proliferation, and differentiation of erythroid progenitor/precursor cells (Elliott et al. 2008; Paschos et al. 2008). The kidney, especially the peritubular interstitial cells, is the main production site of EPO. Among other organs, kidneys are probably less sensitive to ionizing radiation, but at gamma-radiation doses of 6 – 8 Gy they show serious damage (Safwat et al. 2000), which is further responsible for a decrease in EPO production. In the present study, a significant decrease in plasma EPO level was observed in

animals irradiated with 6 Gy and was more pronounced in animal groups irradiated with a higher percentage of neutrons. In animal radiation models, G-CSF and SAA expression both show a bi-phasic post-radiation pattern (Ossetrova et al. 2011, 2014a, 2016a, 2016b). While no significant difference in compared groups was observed in either protein during the first strong dose-dependent phase, their levels were significantly higher in animals irradiated with 67% n + 33% γ compared to those irradiated with 30% n + 70% γ ($p < 0.003$). LBP, known as an acute phase protein, in our mouse studies, in contrast with nonhuman primate radiation model (Ossetrova et al. 2016a) did not show good dose- and time-dependent changes.

It's well known that materials with high atomic mass numbers, such as lead, best attenuate γ-radiation, while neutron radiation is best attenuated by hydrogen-rich compounds (e.g., paraffin, water and, in human tissue, fat). Tissues with high lipid concentrations, such as brain, fat, muscles, and tissues with high water concentration, such as the gastrointestinal (GI) epithelium, will therefore be more sensitive to the effects of neutron irradiation. The relative biological effectiveness (RBE) for neutrons is higher in the gastrointestinal tract than in skin, cartilage and hematopoietic tissue (in that order). For example, at the Nevada Test Site, mice shielded from γ-irradiation by lead hemispheres, died in around 4 to 10 days from prominent gastrointestinal signs and symptoms (i.e., bloody diarrhea and loss of appetite) with relative sparing of the bone marrow. This observation was verified in laboratory experiments in pigs and the conclusion drawn was that neutron irradiation aggravated GI tract injury with relative sparing of the blood elements (Fehner and Gosling 2006).

Acute radiation syndrome (ARS) is characterized by damage to the gastrointestinal and hematopoietic systems. Gastrointestinal damage may lead to the translocation of intestinal microflora, which, combined with hematological damage and a compromised immune system, may lead to septicemia and death. We have examined the utility of PCT, which is known as a clinical sepsis biomarker (Guven et al. 2002). Our results demonstrate that in mice irradiated with TRIGA reactor mixed-field, PCT concentration shows a dose- and time-dependent increase beginning from d4 post-TBI and is significantly higher in mice irradiated with a higher percentage of neutrons (67% vs. 30%) reflecting the fact that the GI epithelium is more sensitive to neutron irradiation. As expected, good correlations were observed between PCT and acute phase proteins SAA and G-CSF ($R > 0.834$). However, no strong correlations were found between PCT and LBP. Biju and colleagues recently reported PCT and LBP results in mice total-body irradiated with ^{137}Cs to lethal doses (9 or 10 Gy) with a dose rate of 1.35 Gy/min and demonstrated that PCT level increased significantly beginning from d4, and its level correlated with radiation-induced intestinal mucosal permeability and bacterial translocation. Authors also reported that LBP, contradictory to expectation, did not exhibit consistent early changes post irradiation (Biju et al. 2012). Our data are in agreement with results reported by Biju and colleagues if an RBE = 1.9 is taken into account when comparing pure photon doses with Dn/Dt = 0.67 (Ledney and Elliott 2010). While the microbiological evaluation of tissues from mice irradiated with mixed-field was not part of this study, these PCT results demonstrate its value as an early biomarker in radiation-induced bacteremia for mouse studies and suggest that clinical results from other septic conditions may apply to post-radiation septicemia in humans.

Survival study in B6D2F1 female mice irradiated with TRIGA reactor to doses ranging from 4 to 7 Gy at dose rate of 0.6 Gy/min and 67% n + 33% γ was performed to find associations between survival rate, biomarker profiles, body-weight, and clinical observations related to radiation dose and hematopoietic and GI sub-syndromes of the ARS (see in section "SURVIVAL STUDY RESULTS"). Using results from this study, the multi-parametric ARS Severity Response Category scoring system for radiation inquiry assessment and ARS prognosis created earlier in pure γ-rays

studies (Ossetrova et al. 2016b; Koch et al. 2016) was expanded to mixed-field exposure conditions. The data collected for 6-Gy group irradiated with mixed-field show the similar trend as data reported earlier in mice irradiated with 10 Gy ^{60}Co γ-rays at 0.6 Gy/min (Ossetrova et al. 2016b).

In our studies, TBI of mice were performed in a steady-state reactor mode at a dose rate of either 0.6 or 1.9 Gy/min. AFRRI's TRIGA reactor has been designed to provide radiation exposure in both a steady-state and a pulsed mode allowing one to make comparisons of the effectiveness of a fission-spectrum neutron source with both high and low dose rates without significant changes in the neutron spectrum. While dosimetry for a reactor steady-state mode allows for controlled dose rates, in pulsed mode, the reactor instantaneously increases in power to maximum (about 10^4 Gy min^{-1}) and returns to zero The average power for pulsed mode was such that the average dose rate was between 0.4 and 1.0×10^4 Gy/min. Post-irradiation survival study results in mice and large animals irradiated with TRIGA reactor (RBE = 2.6) have yielded the conclusion that neutron irradiation significantly shortened the $LD_{50/30}$ survival time in comparison to cobalt studies, but the dose rate (pulsed mode and 1 Gy min^{-1} in a steady-state mode) at which the exposure was made in these reports has no effect over the range studied (Ainsworth et al. 1964a, 1964b; Alpen 1991). Dose-response relationships for the induction of neoplastic transformation in CH3 10T1/2 cells irradiated at AFRRI with fission neutrons at dose rates of either 0.44 cGy/min or 10.6 cGy/min did not reveal any significant differences ($p < 0.001$) (Balcer-Kubiczek et al. 1991).

9.2. BIOMARKER RESULTS IN ^{60}Co PURE GAMMA-RAY STUDY

We evaluated multiple blood biodosimetry and organ-specific biomarkers (Table 7.1) for early-response assessment of radiation exposure using a mouse (B6D2F1, males and females) TBI model, exposed to ^{60}Co γ-rays over a broad dose range (3 – 12 Gy) and dose rates of either 0.6 or 1.9 Gy/min (see list of experiments in Table 6.1, in section "IRRADIATION WITH ^{60}Co PURE GAMMA RAYS").

9.2.1. HEMATOLOGY RESULTS

Very good reproducibility was observed in CBC/diff results collected in current project ^{60}Co γ-rays studies (n=8 animal per group) compared with ones collected earlier in ^{60}Co γ-rays radiation studies (n=42 animals per group) (i.e., project funded by BARDA in support of development and evaluation of MSD's hand-held field-deployable POC biodosimetry device in 2010 - 2014) as shown in Figs. 9.2.1.1 - 9.2.1.3. Data shown in the same strain of mice (B6D2F1 females), from the same vendor (Jackson Labs), in sham group and in animal groups irradiated to the same radiation doses, dose-rate (0.6 Gy/min) and collection time points.

ANC Reproducibility in Mouse Blood in Current Project Cobalt Studies vs. BARDA Project

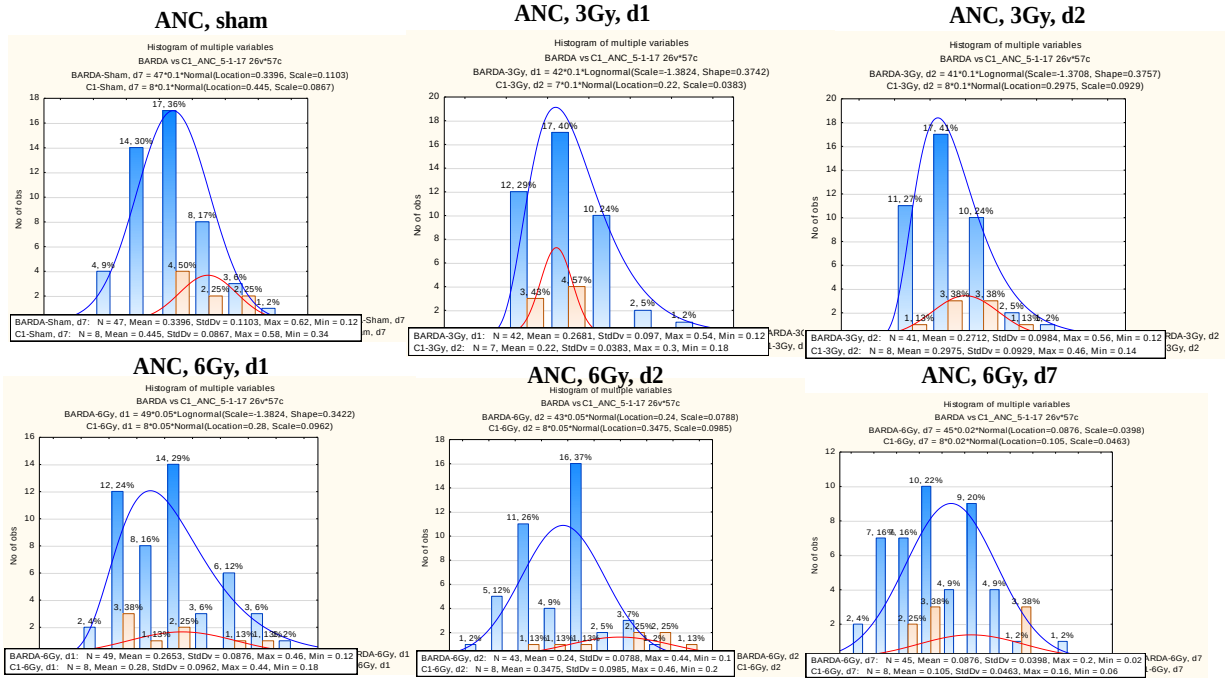

Fig. 9.2.1.1. ANC reproducibility in mouse blood collected in current project Cobalt studies (orange plots; n=8 animal per group) vs. BARDA project (blue plots; n=42 animals per group) (2010 - 2014).

ALC Reproducibility in Mouse Blood in Current Project Cobalt Studies vs. BARDA Project

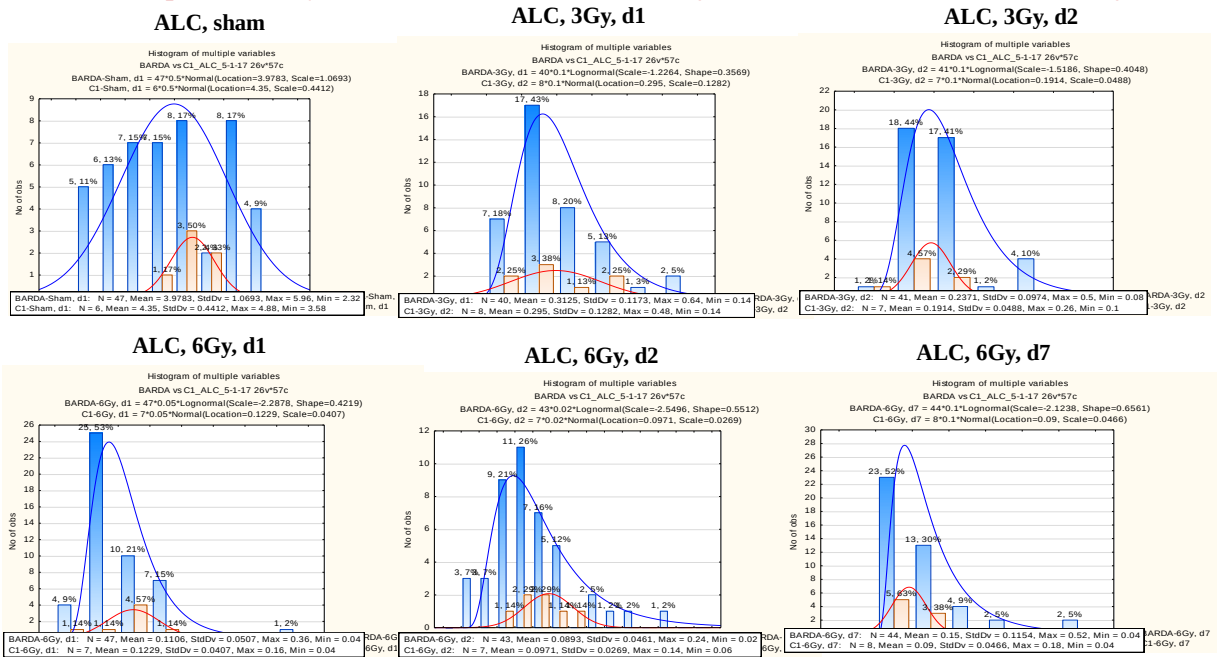

Fig. 9.2.1.2. ALC reproducibility in mouse blood collected in current project Cobalt studies (orange plots; n=8 animal per group) vs. BARDA project (blue plots; n=42 animals per group) (2010 - 2014).

PLT Reproducibility in Mouse Blood in Current Project Cobalt Studies vs. BARDA Project

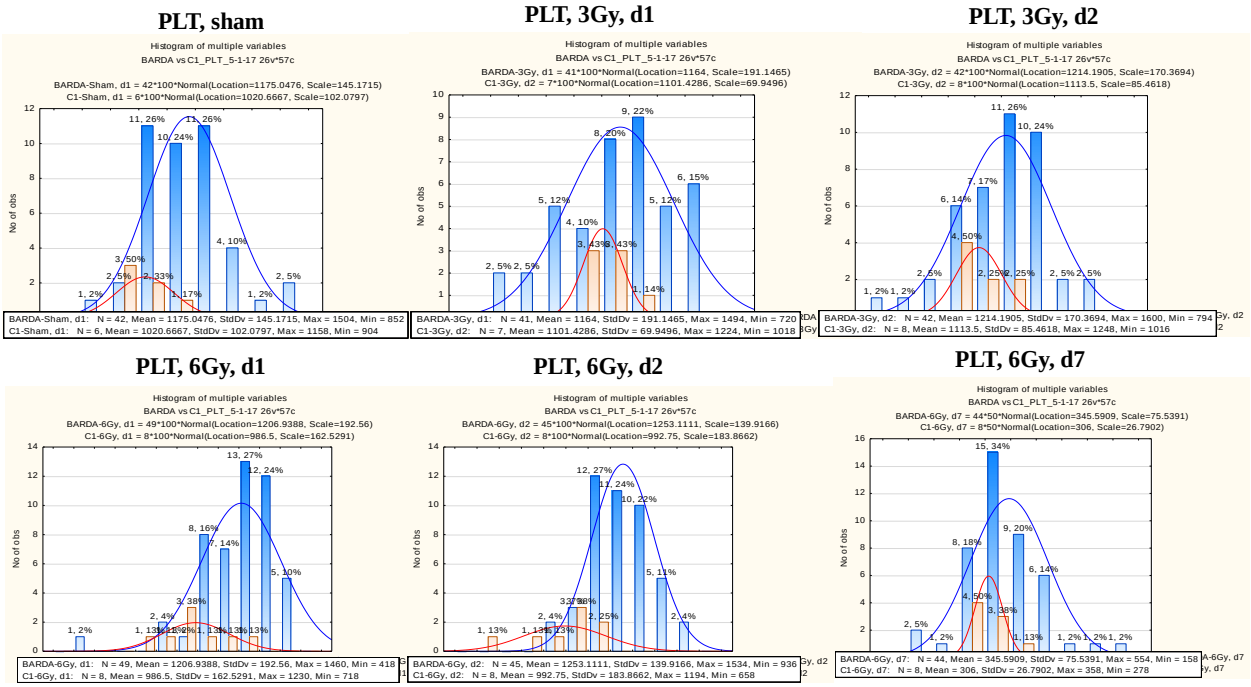

Fig. 9.2.1.3. PLT reproducibility in mouse blood collected in current project Cobalt studies (orange plots; n=8 animals per group) vs. BARDA project (blue plots; n=42 animals per group) (2010 - 2014).

Current project results for ALC, ANC, ratio of ANC to ALC, PLT, and RBC in blood of sham/control mice and mice after a TBI with ^{60}Co γ-rays under different experimental conditions are shown in Figs. 9.2.1.4 and 9.2.1.5. Data are also shown in Tables 9.2.1.1 – 9.2.1.3.

Fig. 9.2.1.4 and data in Tables 9.2.1.2 and 9.2.1.3 show dose- and time-dependent changes in hematological profile in blood of female mice after TBI with ^{60}Co γ-rays at a dose rate of either 0.6 or 1.9 Gy/min (dose-rate comparison study). No significant differences were observed between animal groups for ANC, ANC to ALC ratio, PLT, and RBC for any radiation dose and at any time after exposure ($p > 0.148$) except PLT levels in 12-Gy groups on d4 ($p < 0.021$). In Tables with the raw data, shaded data represent a significant difference between control (non-irradiated) and irradiated groups at 95% CL. In plots, data shown as mean values for n=8 animals per group and error bars represent the standard deviation (STD).

In gender-comparison study (Fig. 9.2.1.5 and data in Tables 9.2.1.1 and 9.2.1.3), with one exception for PLT count in 12-Gy groups on d4 ([1002 ± 98] × 109 L-1 in female mice vs. [839 ± 66] × 109 L-1 in male mice), no significant differences were observed between female and male groups for ANC, ANC to ALC ratio, PLT, and RBC for any radiation dose at any time after exposure ($p > 0.114$).

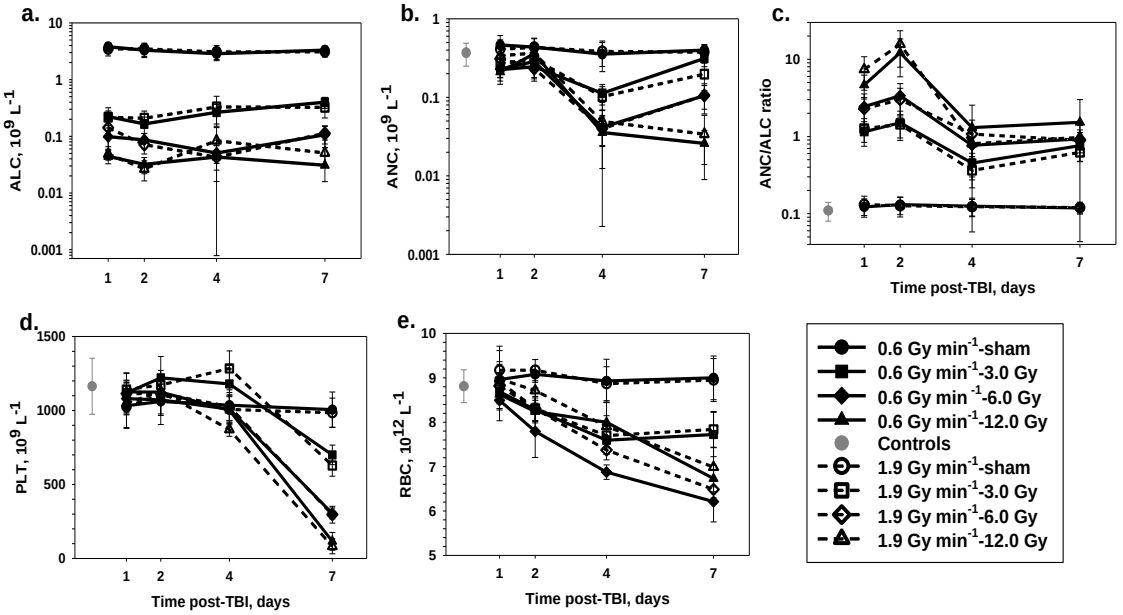

Fig. 9.2.1.4. Dose- and time-dependent changes for ALC (a), ANC (b), ANC to ALC ratio (c), PLT (d) and RBC (e) in blood of female mice after ^{60}Co γ-rays TBI at the dose rate of either 0.6 Gy/min (solid lines) or 1.9 Gy/min (dashed lines). The symbols represent the mean values for n=8 animals per group and error bars represent the standard deviation (STD). Data are shown in Tables 9.2.1.1 and 9.2.1.3.

Table 9.2.1.1. Hematological biomarker levels in B6D2F1 female mice irradiated with ^{60}Co γ-rays at 0.6 Gy/min. Shaded data represent a significant difference between control (non-irradiated) and irradiated groups at 95% CL.

Biomarker (control values)	Day post-TBI	Biomarker Level (Mean ± STD)			
		Sham (0 Gy)	3.0 Gy	6.0 Gy	12.0 Gy
ALC (x10^9 L^{-1}) (3.47 ± 1.07)	1	3.80 ± 0.71	0.22 ± 0.10	0.10 ± 0.04	0.04 ± 0.01
	2	3.31 ± 0.86	0.17 ± 0.05	0.09 ± 0.03	0.03 ± 0.01
	4	2.87 ± 0.61	0.27 ± 0.10	0.05 ± 0.02	0.04 ± 0.04
	7	3.31 ± 0.60	0.40 ± 0.09	0.11 ± 0.04	0.03 ± 0.03
ANC (x10^9 L^{-1}) (0.37 ± 0.12)	1	0.46 ± 0.15	0.23 ± 0.05	0.23 ± 0.08	0.21 ± 0.05
	2	0.44 ± 0.13	0.25 ± 0.07	0.29 ± 0.11	0.36 ± 0.13
	4	0.36 ± 0.14	0.11 ± 0.03	0.04 ± 0.02	0.04 ± 0.03
	7	0.40 ± 0.07	0.31 ± 0.07	0.11 ± 0.04	0.03 ± 0.01
ANC/ALC ratio (0.11 ± 0.03)	1	0.12 ± 0.03	1.15 ± 0.40	2.44 ± 1.12	4.65 ± 1.59
	2	0.13 ± 0.03	1.51 ± 0.62	3.38 ± 1.47	12.16 ± 6.22
	4	0.13 ± 0.03	0.45 ± 0.15	0.77 ± 0.22	1.30 ± 1.25
	7	0.12 ± 0.02	0.76 ± 0.15	0.93 ± 0.46	1.53 ± 1.48
PLT (x10^9 L^{-1}) (1164 ± 190)	1	1,032 ± 153	1,119 ± 81	1,080 ± 110	1,126 ± 129
	2	1,061 ± 156	1,221 ± 145	1,072 ± 105	1,124 ± 77
	4	1,036 ± 103	1,179 ± 125	1,009 ± 98	1,002 ± 98
	7	1,006 ± 119	700 ± 66	304 ± 37	116 ± 60
RBC (x10^{12} L^{-1}) (8.81 ± 0.37)	1	8.96 ± 0.65	8.69 ± 0.41	8.49 ± 0.46	8.63 ± 0.21
	2	9.08 ± 0.18	8.28 ± 0.27	7.79 ± 0.59	8.24 ± 0.26
	4	8.93 ± 0.49	7.59 ± 0.32	6.88 ± 0.16	8.00 ± 0.46
	7	9.00 ± 0.49	7.72 ± 0.50	6.21 ± 0.46	6.73 ± 0.30

Fig. 9.2.1.5 and data in Tables 9.2.1.1 and 9.2.1.3 show the dose- and time-dependent changes in hematological profile in blood of female and male mice after a TBI with ^{60}Co γ-rays at a dose rate of 0.6 Gy/min (gender-comparison study).

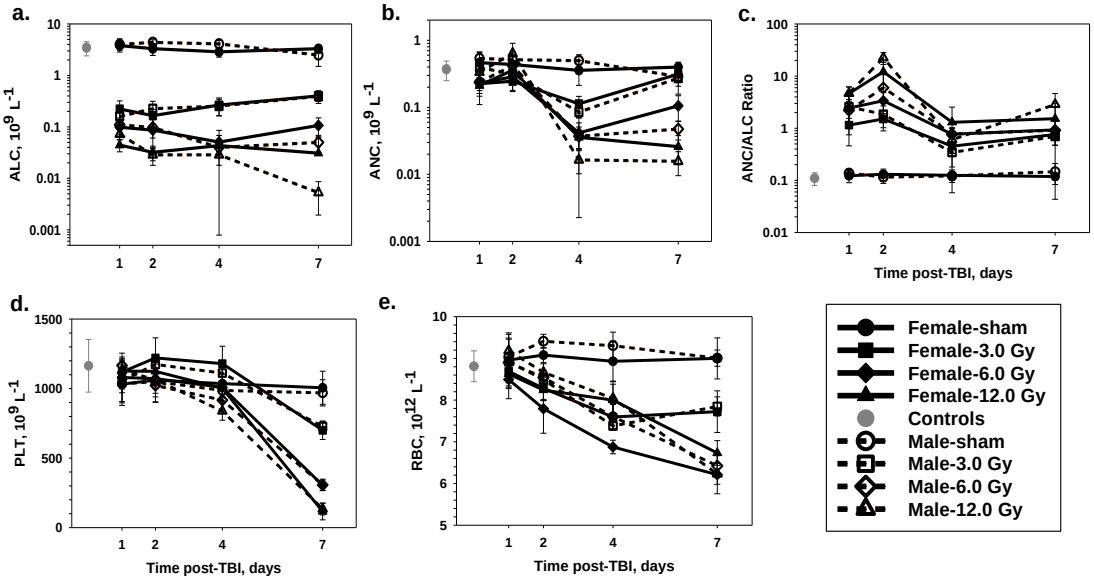

Fig. 9.2.1.5. Dose- and time-dependent changes for ALC (a), ANC (b), ANC to ALC ratio (c), PLT (d) and RBC (e) in blood of female (solid lines) and male (dashed lines) mice after a ^{60}Co γ-rays TBI at the dose rate of 0.6 Gy/min. The symbols represent the mean values for n=8 animals per group and error bars represent the standard deviation (STD). Data are shown in Tables 9.2.1.1 and 9.2.1.2.

Table 9.2.1.2. Hematological biomarker levels in B6D2F1 male mice irradiated with ^{60}Co γ-rays at 0.6 Gy/min. Shaded data represent a significant difference between control (non-irradiated) and irradiated groups at 95% CL.

Biomarker (control values)	Day post-TBI	Biomarker Level (Mean ± STD)			
		Sham (0 Gy)	3.0 Gy	6.0 Gy	12.0 Gy
ALC (x10^9 L^{-1}) (3.47 ± 1.07)	1	4.00 ± 1.15	0.17 ± 0.04	0.11 ± 0.04	0.07 ± 0.03
	2	4.40 ± 0.53	0.23 ± 0.09	0.10 ± 0.06	0.03 ± 0.01
	4	4.11 ± 0.67	0.25 ± 0.09	0.04 ± 0.01	0.03 ± 0.01
	7	2.50 ± 0.99	0.40 ± 0.11	0.05 ± 0.02	0.01 ± 0.00
ANC (x10^9 L^{-1}) (0.37 ± 0.12)	1	0.54 ± 0.13	0.70 ± 0.79	0.24 ± 0.04	0.33 ± 0.09
	2	0.51 ± 0.17	0.32 ± 0.07	0.42 ± 0.20	0.64 ± 0.27
	4	0.50 ± 0.11	0.09 ± 0.01	0.04 ± 0.01	0.02 ± 0.01
	7	0.29 ± 0.13	0.27 ± 0.07	0.05 ± 0.01	0.02 ± 0.01
ANC/ALC ratio (0.11 ± 0.03)	1	0.14 ± 0.03	4.02 ± 4.00	2.22 ± 1.08	4.67 ± 1.50
	2	0.12 ± 0.03	1.86 ± 0.83	5.98 ± 4.65	22.50 ± 5.77
	4	0.12 ± 0.02	0.34 ± 0.16	0.78 ± 0.25	0.60 ± 0.28
	7	0.15 ± 0.06	0.70 ± 0.07	0.92 ± 0.44	2.87 ± 1.79
PLT (x10^9 L^{-1}) (1164 ± 190)	1	1,034 ± 137	1,015 ± 169	1,166 ± 61	1,131 ± 84
	2	1,051 ± 47	1,174 ± 67	1,023 ± 122	1,064 ± 124
	4	987 ± 41	1,112 ± 60	917 ± 93	839 ± 66
	7	970 ± 94	727 ± 37	307 ± 41	134 ± 42
RBC (x10^{12} L^{-1}) (8.81 ± 0.37)	1	9.04 ± 0.45	8.92 ± 0.17	8.90 ± 0.56	9.19 ± 0.39
	2	9.41 ± 0.17	8.49 ± 0.50	8.54 ± 0.17	8.67 ± 0.20
	4	9.31 ± 0.32	7.38 ± 0.10	7.61 ± 0.29	8.04 ± 0.34
	7	9.01 ± 0.20	7.85 ± 0.23	6.42 ± 0.26	6.23 ± 0.25

Table 9.2.1.3. Hematological biomarker levels in B6D2F1 female mice irradiated with ^{60}Co γ-rays at 1.9 Gy/min. Shaded data represent a significant difference between control (non-irradiated) and irradiated groups at 95% CL.

Biomarker (control values)	Day post-TBI	Biomarker Level (Mean ± STD)			
		Sham (0 Gy)	3.0 Gy	6.0 Gy	12.0 Gy
ALC (x10^9 L^{-1}) (3.47 ± 1.07)	1	3.49 ± 0.87	0.22 ± 0.06	0.14 ± 0.08	0.05 ± 0.01
	2	3.49 ± 0.91	0.21 ± 0.07	0.07 ± 0.02	0.03 ± 0.01
	4	3.09 ± 0.93	0.33 ± 0.18	0.04 ± 0.03	0.08 ± 0.06
	7	3.11 ± 0.61	0.33 ± 0.11	0.11 ± 0.04	0.05 ± 0.04
ANC (x10^9 L^{-1}) (0.37 ± 0.12)	1	0.41 ± 0.13	0.27 ± 0.09	0.31 ± 0.05	0.34 ± 0.13
	2	0.43 ± 0.12	0.31 ± 0.08	0.23 ± 0.07	0.37 ± 0.11
	4	0.38 ± 0.14	0.10 ± 0.03	0.04 ± 0.02	0.05 ± 0.04
	7	0.38 ± 0.09	0.20 ± 0.08	0.11 ± 0.04	0.03 ± 0.03
ANC/ALC ratio (0.11 ± 0.03)	1	0.13 ± 0.04	1.27 ± 0.43	2.29 ± 0.91	7.38 ± 3.40
	2	0.13 ± 0.04	1.43 ± 0.47	3.00 ± 1.22	15.67 ± 7.77
	4	0.12 ± 0.03	0.36 ± 0.15	1.08 ± 0.55	0.81 ± 0.53
	7	0.12 ± 0.02	0.62 ± 0.14	0.90 ± 0.23	0.98 ± 0.24
PLT (x10^9 L^{-1}) (1,164 ± 190)	1	1,025 ± 140	1,142 ± 64	1,114 ± 137	1,049 ± 63
	2	1,106 ± 129	1,173 ± 98	1,116 ± 64	1,130 ± 70
	4	1,008 ± 86	1,285 ± 118	1,027 ± 95	871 ± 46
	7	985 ± 99	628 ± 72	296 ± 57	82 ± 51
RBC (x10^{12} L^{-1}) (8.81 ± 0.37)	1	9.17 ± 0.54	8.92 ± 0.45	8.82 ± 0.30	8.98 ± 0.33
	2	9.17 ± 0.24	8.31 ± 0.27	8.31 ± 0.47	8.71 ± 0.28
	4	8.87 ± 0.38	7.70 ± 0.27	7.38 ± 0.22	7.91 ± 0.24
	7	8.95 ± 0.48	7.84 ± 0.40	6.48 ± 0.19	6.99 ± 0.44

Among all evaluated blood cell counts, stress-effect associated with sham-irradiation was observed in mice only on d1 post-procedure resulting in ~25-40% increase in ANC in sham-group compared to counts in control group. ALC and ANC partial recovery was found only in 3-Gy groups on d7. In irradiated animal groups, a significant decline in all blood cells was observed in dose- and time-dependent manner after TBI. Significant decline in RBC was observed beginning from d2 ($p < 0.031$) in all irradiated mice while a significant decline in PLT was observed in 3-Gy group on d7 ($p < 0.037$) and in 6- and 12-Gy groups beginning from d4 ($p < 0.011$).

9.2.2. PROTEOMICS RESULTS

Very good reproducibility in standard calibration curves and control samples was reported in proteomic assays performed by different people on different days; see reproducibility plots in Figs. 9.1.2.1 – 9.1.2.3. The protein biomarkers were selected from distinctly different pathways: Flt-3 Ligand, IL-5, IL-10, IL-12, IL-18, G-CSF, GM-CSF, TPO, EPO, acute phase proteins (SAA and LBP), surface plasma hematology protein markers (CD45, CD27, ratio of CD45 to CD27), and PCT (Table 7.1) were measured in plasma of mice after ^{60}Co γ-rays TBI of 3, 6, and 12 Gy in dose-rate and gender-comparison studies. Results are shown in Figs. 9.2.2.1 and 9.2.2.2 and data are also presented in Tables 9.2.2.1 – 9.2.2.3.

In response to pure gamma radiation, an increase in concentration of Flt3L, IL-5, IL-18, G-CSF, GM-CSF, TPO, EPO, SAA, and ratio of CD45 to CD27 and decrease in concentration of IL-12, CD27 and CD45 were observed in a dose- and time-dependent manner. IL-10, LBP and I-

FABP levels showed no significant changes in any irradiated animal groups compared to control/sham.

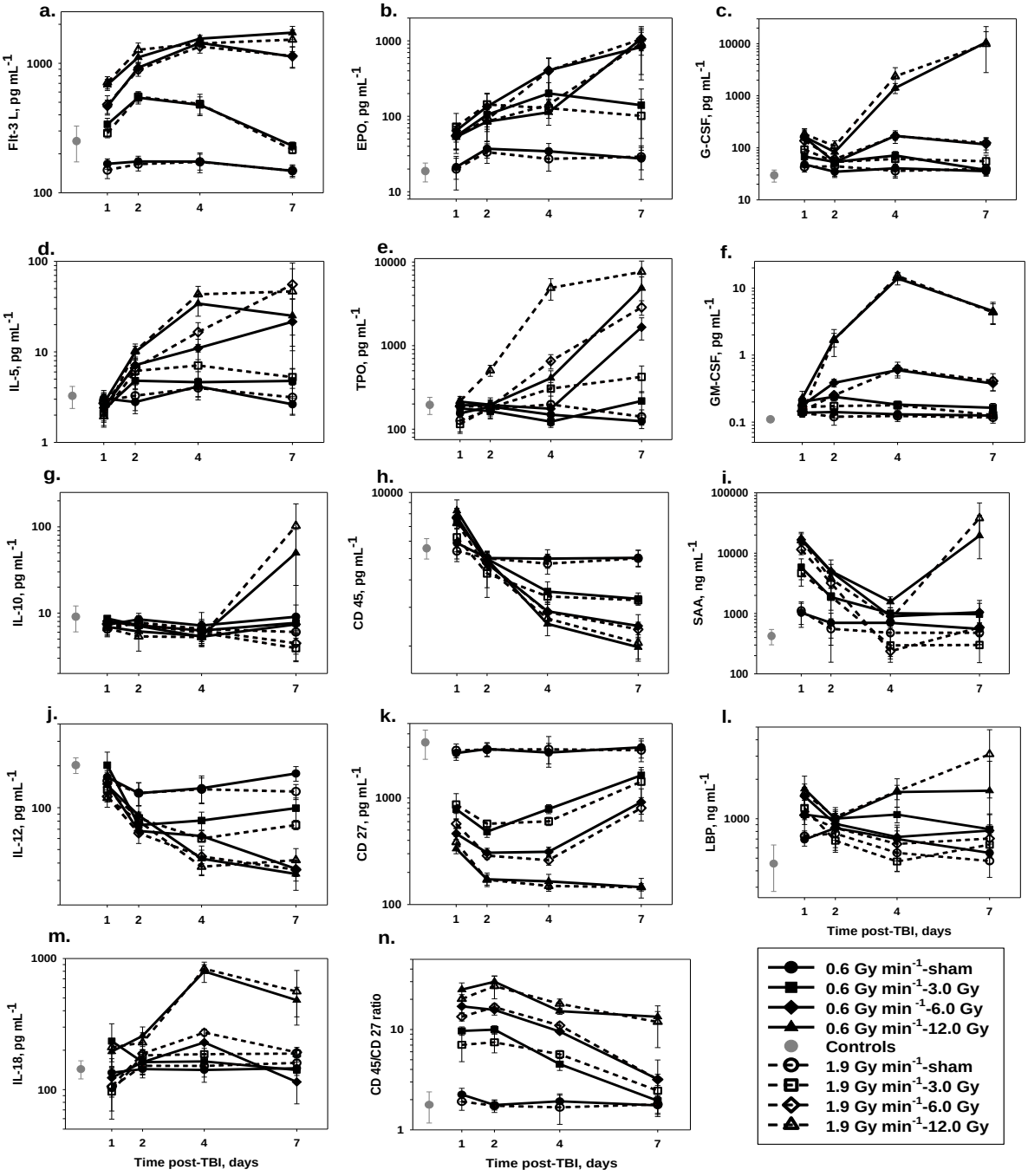

Fig. 9.2.2.1. Dose- and time-dependent changes in profile of protein biomarkers: FLT3L (a), EPO (b), G-CSF (c), IL-5 (d), TPO (e), GM-CSF (f), IL-10 (g), CD45 (h), SAA (i), IL-12 (j), CD27 (k), LBP (l), IL-18 (m), CD45/CD27 (n) in blood plasma of female mice after a ^{60}Co γ-rays TBI at the dose rate of either 0.6 Gy/min (solid lines) or 1.9 Gy/min (dashed lines). The symbols represent the mean values for n=8 animals per group and error bars represent the standard deviation (STD).

Table 9.2.2.1. Proteomic biomarker levels in B6D2F1 female mice irradiated with ^{60}Co γ-rays at 0.6 Gy/min. Shaded data represent a significant difference between control (non-irradiated) and irradiated groups at 95% CL.

Biomarker (control values)	Day post-TBI	Biomarker Level (Mean ± STD)				Biomarker (control values)	Day post-TBI	Biomarker Level (Mean ± STD)			
		Sham (0 Gy)	3.0 Gy	6.0 Gy	12.0 Gy			Sham (0 Gy)	3.0 Gy	6.0 Gy	12.0 Gy
Flt3 L (pg mL^{-1}) (250 ± 77)	1	167 ± 15	338 ± 38	464 ± 56	683 ± 66	G-CSF (pg mL^{-1}) (29.7 ± 7.7)	1	48.0 ± 10.6	67.9 ± 17.0	159.3 ± 52.8	163.0 ± 69.6
	2	174 ± 17	543 ± 58	925 ± 90	1112 ± 97		2	34.7 ± 7.8	53.5 ± 13.0	52.9 ± 8.5	82.8 ± 17.7
	4	174 ± 24	477 ± 73	1438 ± 88	1551 ± 92		4	40.4 ± 12.5	71.2 ± 13.8	169.7 ± 29.5	1412 ± 310
	7	148 ± 17	230 ± 16	1126 ± 210	1725 ± 203		7	35.5 ± 5.9	37.4 ± 8.9	115.9 ± 36.0	10,622 ± 10,688
IL-5 (pg mL^{-1}) (3.2 ± 0.8)	1	3.1 ± 0.4	2.3 ± 0.3	2.4 ± 0.9	2.7 ± 0.7	GM-CSF (pg mL^{-1}) (0.11 ± 0.01)	1	0.14 ± 0.02	0.20 ± 0.04	0.18 ± 0.02	0.23 ± 0.06
	2	2.8 ± 0.7	4.8 ± 1.0	7.1 ± 1.6	10.0 ± 1.5		2	0.14 ± 0.03	0.24 ± 0.03	0.38 ± 0.05	1.72 ± 0.39
	4	4.1 ± 1.0	4.6 ± 1.4	11.0 ± 2.8	34.2 ± 9.4		4	0.13 ± 0.02	0.18 ± 0.02	0.60 ± 0.11	13.94 ± 2.80
	7	2.6 ± 0.6	4.8 ± 1.7	21.5 ± 16.6	25.1 ± 13.5		7	0.13 ± 0.02	0.16 ± 0.03	0.38 ± 0.08	4.53 ± 1.60
IL-10 (pg mL^{-1}) (9.6 ± 3.6)	1	7.3 ± 1.9	8.6 ± 0.7	8.1 ± 0.9	6.9 ± 1.3	SAA (ng mL^{-1}) (423 ± 121)	1	1030 ± 441	5839 ± 2,209	16,701 ± 5,468	17,637 ± 3,331
	2	8.5 ± 1.5	7.2 ± 0.6	7.1 ± 1.1	6.1 ± 1.1		2	700 ± 309	1,868 ± 736	4,952 ± 2,779	5,064 ± 1,449
	4	7.2 ± 3.0	6.3 ± 1.8	5.3 ± 1.3	5.4 ± 1.3		4	700 ± 64	1,009 ± 228	899 ± 148	1,567 ± 321
	7	9.1 ± 3.4	7.7 ± 1.6	7.4 ± 1.5	49.8 ± 43.5		7	555 ± 143	974 ± 669	1,049 ± 423	19,526 ± 22,834
IL-12 (pg mL^{-1}) (202 ± 26)	1	166 ± 27	202 ± 49	148 ± 24	145 ± 35	LBP (ng mL^{-1}) (454 ± 176)	1	692 ± 75	1,078 ± 174	1,484 ± 355	1,689 ± 424
	2	127 ± 24	75 ± 12	68 ± 13	88 ± 15		2	850 ± 248	1,002 ± 133	914 ± 183	996 ± 171
	4	138 ± 31	81 ± 12	63 ± 6	43 ± 10		4	700 ± 159	1,076 ± 145	726 ± 167	1,598 ± 200
	7	176 ± 21	99 ± 18	36 ± 4	33 ± 8		7	548 ± 92	832 ± 257	811 ± 262	1,635 ± 1,110
IL-18 (pg mL^{-1}) (143.3 ± 22.7)	1	134.8 ± 37.1	234.5 ± 83.8	123.1 ± 23.3	195.2 ± 32.0	CD27 (pg mL^{-1}) (3,324 ± 1,015)	1	2,639 ± 383	785 ± 69	463 ± 55	334 ± 35
	2	143.4 ± 12.9	162.1 ± 30.3	162.0 ± 39.1	257.0 ± 43.9		2	2,880 ± 429	483 ± 55	306 ± 31	172 ± 25
	4	141.2 ± 27.4	164.1 ± 12.8	229.1 ± 58.7	798 ± 141		4	2,672 ± 580	789 ± 76	313 ± 32	165 ± 27
	7	145.6 ± 17.3	141.0 ± 26.8	114.4 ± 36.6	481 ± 121		7	2,988 ± 619	1,633 ± 305	915 ± 305	146 ± 30
EPO (pg mL^{-1}) (18.7 ± 5.2)	1	21.2 ± 6.6	54.4 ± 18.5	64.3 ± 14.0	53.1 ± 20.9	CD45 (pg mL^{-1}) (5,568 ± 593)	1	5,890 ± 910	7,378 ± 282	7,764 ± 560	8,262 ± 986
	2	37.1 ± 9.2	104.9 ± 37.6	134.5 ± 62.2	84.9 ± 38.5		2	5,029 ± 363	4,988 ± 312	4,753 ± 211	4,966 ± 358
	4	34.3 ± 9.3	200.9 ± 78.2	407.0 ± 187.2	113.1 ± 37.2		4	4,999 ± 486	3,539 ± 381	2,877 ± 290	2,520 ± 294
	7	27.5 ± 13.0	140.5 ± 89.6	827.2 ± 469.5	1,062 ± 325		7	5,038 ± 422	3,277 ± 211	2,468 ± 310	1,976 ± 271
TPO (pg mL^{-1}) (195.2 ± 45.4)	1	154.5 ± 15.9	177.6 ± 16.7	193.2 ± 28.6	213.2 ± 33.6	CD45/CD27 ratio (1.78 ± 0.61)	1	2.25 ± 0.34	9.68 ± 0.93	17.01 ± 2.62	24.99 ± 4.14
	2	186.7 ± 50.1	163.7 ± 19.9	194.4 ± 25.5	196.1 ± 28.0		2	1.77 ± 0.19	9.97 ± 0.94	15.68 ± 1.76	29.90 ± 4.36
	4	148.9 ± 44.1	123.1 ± 13.8	175.5 ± 36.3	408.6 ± 90.9		4	1.93 ± 0.36	4.51 ± 0.60	9.55 ± 0.46	15.23 ± 1.10
	7	124.4 ± 22.9	217.4 ± 64.0	1,660 ± 492	4,876 ± 1,773		7	1.75 ± 0.40	1.95 ± 0.25	3.19 ± 1.77	13.39 ± 1.73

Fig. 9.2.2.1 and data in Tables 9.2.2.1 – 9.2.2.3 show dose- and time-dependent changes in protein profile in blood plasma of female mice after TBI with ^{60}Co γ-rays at the dose rate of either 0.6 or 1.9 Gy/min (dose-rate comparison study). No significant differences were observed between animal groups for Flt3L, IL-5, IL-12, IL-18, EPO, G-CSF, GM-CSF, CD27, CD45 and CD45/CD27 levels ($p > 0.158$). TPO levels in mouse groups irradiated with 1.9 Gy/min were significantly higher ($p < 0.011$) in 3- and 6-Gy groups on d4 and d7 and in 12-Gy groups beginning from d2 than in respective groups irradiated with 0.6 Gy/min. SAA levels in mouse groups irradiated with 1.9 Gy/min was significantly lower ($p < 0.009$) in 3- and 6-Gy groups on d4 and d7 as well as in 12-Gy groups on d4 than in mice irradiated with 0.6 Gy/min.

Table 9.2.2.2. Proteomic biomarker levels in B6D2F1 male mice irradiated with ^{60}Co γ-rays at 0.6 Gy/min. Shaded data represent a significant difference between control (non-irradiated) and irradiated groups at 95% CL.

Biomarker (control values)	Day post-TBI	Biomarker Level (Mean ± STD)				Biomarker (control values)	Day post-TBI	Biomarker Level (Mean ± STD)			
		Sham (0 Gy)	3.0 Gy	6.0 Gy	12.0 Gy			Sham (0 Gy)	3.0 Gy	6.0 Gy	12.0 Gy
Flt3 L (pg mL^{-1}) (250 ± 77)	1	156 ± 14	358 ± 71	444 ± 97	614 ± 73	G-CSF (pg mL^{-1}) (29.7 ± 7.7)	1	28.5 ± 9.6	38.2 ± 10.5	59.1 ± 14.0	59.2 ± 11.6
	2	117 ± 14	554 ± 59	805 ± 86	1031 ± 54		2	31.9 ± 16.2	63.5 ± 44.7	51.1 ± 23.5	79.4 ± 33.2
	4	150 ± 12	490 ± 46	1324 ± 71	1391 ± 127		4	28.7 ± 6.1	54.9 ± 7.7	165.5 ± 60.2	1,063 ± 231
	7	140 ± 15	227 ± 9	1315 ± 232	1707 ± 137		7	35.1 ± 8.7	32.8 ± 14.3	251.4 ± 115	5,237 ± 3,767
IL-5 (pg mL^{-1}) (3.3 ± 0.9)	1	1.9 ± 0.5	1.5 ± 0.2	1.4 ± 0.1	1.4 ± 0.4	GM-CSF (pg mL^{-1}) (0.11 ± 0.01)	1	0.11 ± 0.04	0.15 ± 0.01	0.15 ± 0.03	0.18 ± 0.06
	2	1.4 ± 0.4	1.9 ± 0.3	3.5 ± 0.7	6.0 ± 1.2		2	0.08 ± 0.02	0.22 ± 0.03	0.31 ± 0.03	2.78 ± 0.84
	4	1.4 ± 0.3	2.5 ± 0.4	6.1 ± 1.2	31.6 ± 3.2		4	0.10 ± 0.02	0.19 ± 0.02	0.74 ± 0.10	14.84 ± 2.03
	7	1.9 ± 0.5	3.2 ± 0.6	6.0 ± 1.2	9.1 ± 2.1		7	0.11 ± 0.02	0.15 ± 0.02	0.46 ± 0.04	5.19 ± 1.00
IL-10 (pg mL^{-1}) (9.1 ± 3.0)	1	8.0 ± 1.3	6.9 ± 3.3	5.5 ± 1.4	5.2 ± 0.5	SAA (ng mL^{-1}) (423 ± 121)	1	697 ± 113	4789 ± 2,578	19,060 ± 1,522	17,556 ± 4,615
	2	7.4 ± 0.8	7.1 ± 1.4	5.3 ± 0.9	6.0 ± 0.9		2	686 ± 221	2049 ± 793	3,598 ± 902	4,743 ± 1,110
	4	6.1 ± 1.0	6.2 ± 0.9	8.1 ± 1.4	5.8 ± 0.6		4	525 ± 118	558 ± 100	1,213 ± 441	915 ± 325
	7	7.1 ± 0.7	8.0 ± 1.2	8.4 ± 2.3	20.7 ± 15.7		7	562 ± 346	1,508 ± 833	655 ± 166	17,821 ± 16,444
IL-12 (pg mL^{-1}) (202 ± 26)	1	332 ± 57	319 ± 44	282 ± 67	303 ± 20	LBP (ng mL^{-1}) (454 ± 176)	1	351 ± 56	771 ± 250	922 ± 189	1,216 ± 300
	2	330 ± 38	139 ± 30	109 ± 23	140 ± 31		2	673 ± 113	857 ± 171	644 ± 134	773 ± 190
	4	186 ± 17	114 ± 16	27 ± 4	27 ± 4		4	748 ± 132	620 ± 44	607 ± 157	1,118 ± 149
	7	70 ± 7	48 ± 5	27 ± 9	36 ± 9		7	555 ± 182	1,177 ± 369	559 ± 111	2,304 ± 1,068
IL-18 (pg mL^{-1}) (143.3 ± 22.7)	1	185.3 ± 20.9	174.2 ± 36.7	154.1 ± 27.8	184.6 ± 39.2	CD27 (pg mL^{-1}) (3,324 ± 1,015)	1	1,581 ± 161	384 ± 41	254 ± 29	188 ± 19
	2	111.9 ± 20.7	189.5 ± 31.0	190.0 ± 24.5	233.4 ± 25.3		2	1,602 ± 204	250 ± 43	135 ± 19	85 ± 7
	4	160.8 ± 7.0	211.0 ± 31.6	285.0 ± 26.2	765.5 ± 65.9		4	1,394 ± 225	328 ± 33	207 ± 42	117 ± 23
	7	153.8 ± 17.1	161.6 ± 13.2	226.3 ± 34.1	437.0 ± 25.6		7	1,908 ± 345	957 ± 61	483 ± 50	113 ± 17
EPO (pg mL^{-1}) (18.7 ± 5.3)	1	26.2 ± 5.4	75.5 ± 92.4	48.6 ± 14.7	38.6 ± 10.1	CD45 (pg mL^{-1}) (5,568 ± 593)	1	4,234 ± 222	5,695 ± 277	5,541 ± 931	6,831 ± 610
	2	24.8 ± 7.2	118.2 ± 41.2	93.2 ± 11.2	117.7 ± 57.7		2	4,069 ± 422	4,316 ± 390	4,103 ± 398	4,567 ± 332
	4	46.1 ± 12.2	204.0 ± 45.0	268.0 ± 100.2	205.2 ± 96.3		4	4,179 ± 339	3,062 ± 109	3,126 ± 259	3,013 ± 156
	7	45.6 ± 6.0	127.0 ± 16.8	1049 ± 362	794.3 ± 255.7		7	5,048 ± 574	2,885 ± 627	2,587 ± 177	1,913 ± 160
TPO (pg mL^{-1}) (195.2 ± 45.4)	1	142.6 ± 14.0	145.6 ± 20.2	181.0 ± 30.9	150.0 ± 8.5	CD45/CD27 ratio (1.78 ± 0.61)	1	2.70 ± 0.28	14.60 ± 1.61	21.81 ± 2.64	35.02 ± 3.79
	2	135.0 ± 12.4	334.3 ± 132.8	284.4 ± 62.3	355.7 ± 114.5		2	2.63 ± 0.24	17.61 ± 2.89	30.49 ± 2.24	52.11 ± 9.81
	4	205.0 ± 17.8	237.6 ± 20.1	619.3 ± 205.5	2,610 ± 339		4	3.08 ± 0.30	9.61 ± 0.45	14.70 ± 2.09	25.46 ± 3.72
	7	212.3 ± 44.2	277.2 ± 44.1	2,601 ± 464	5,684 ± 423		7	2.67 ± 0.30	3.03 ± 0.69	5.39 ± 0.54	17.43 ± 3.47

Fig. 9.2.2.2 and data in Tables 9.2.2.1 – 9.2.2.3 show the dose- and time-dependent changes in protein profile in blood plasma of female and male mice after TBI with ^{60}Co γ-rays at the dose rate of 0.6 Gy/min (gender-comparison study). No significant differences were observed between animal groups for Flt3L, IL-18, EPO, G-CSF, GM-CSF, SAA, and CD45 ($p > 0.144$). IL-5 level in sham, male mice is about 2-fold less than in female mice. While IL-5 expression was in a strong dose- and time-dependent manner in both males and females, it remained about 2-fold less in male mice at all radiation doses and time points after TBI. IL-12 level in sham male mice is also about 2-fold higher than in female mice. While IL-12 declined in a strong dose- and time-dependent manner in both males and females, it remained about 2-fold higher in male mice at any given radiation dose and time point after TBI. TPO level was significantly higher ($p < 0.021$) in male mice irradiated with doses of 6 and 12 Gy at time points ≥ d4 and ≥ d2, respectively. SAA showed no significant differences ($p > 0.171$) except in 3-Gy groups on d4: SAA in males was 558 ± 100 ng mL^{-1} while in females it was 1009 ± 228 ng mL^{-1} (Tables 9.2.2.1 and 9.2.2.3). CD27 level in sham, male mice is about 1.7-fold less than in female mice. While CD27 expression was in a strong dose- and time-dependent manner in both males and females, it remained about 1.7-fold

less in male mice at any given radiation dose and time point after TBI. CD45 to CD27 ratio was slightly higher in males than females reflecting the differences in CD27 level.

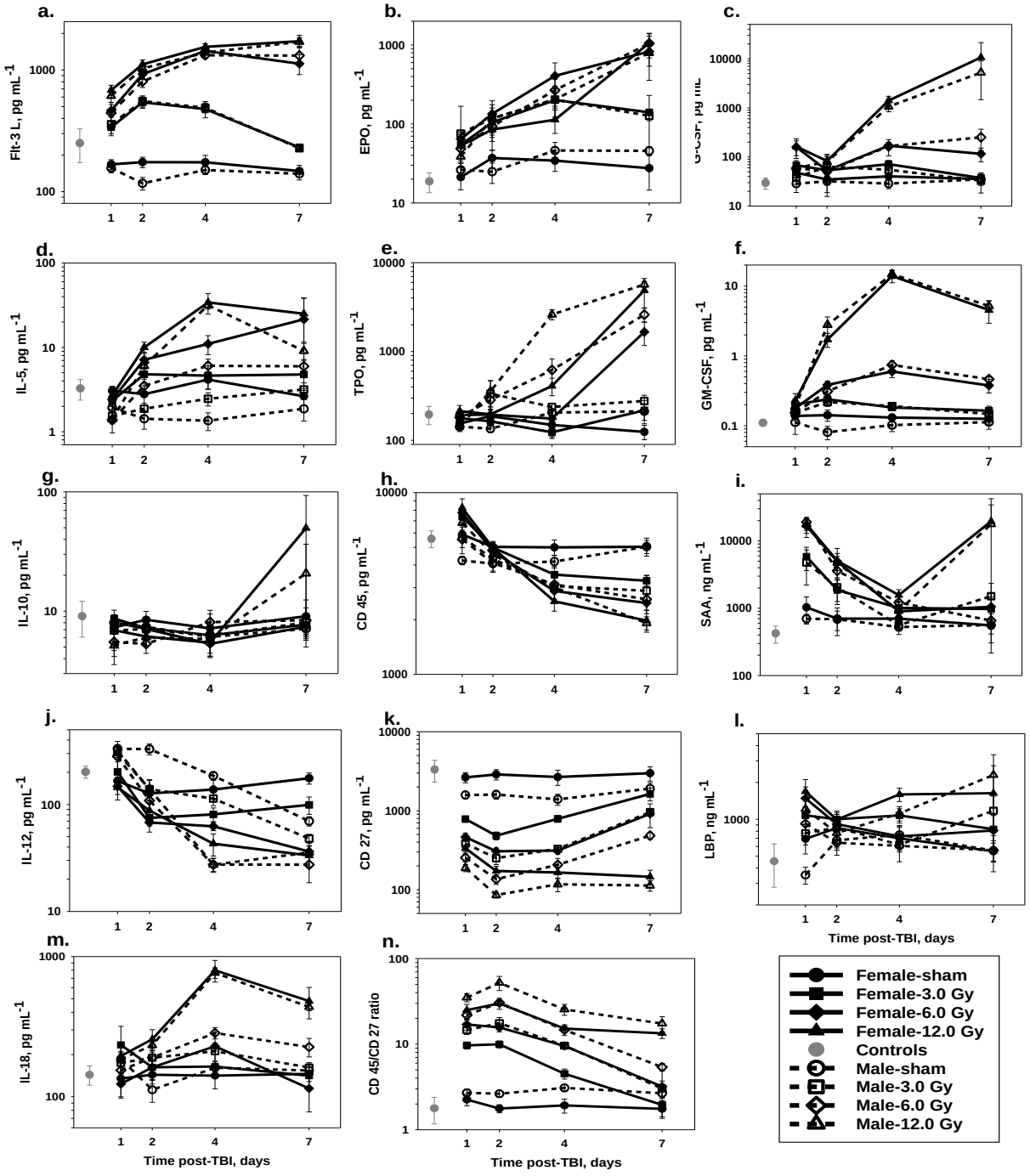

Fig. 9.2.2.2. Dose- and time-dependent changes in profile of protein biomarkers: FLT3L (a), EPO (b), G-CSF (c), IL-5 (d), TPO (e), GM-CSF (f), IL-10 (g), CD45 (h), SAA (i), IL-12 (j), CD27 (k), LBP (l), IL-18 (m), CD45/CD27 (n) in blood plasma of female (solid lines) and male (dashed lines) mice after a after a ^{60}Co γ-rays TBI at the dose rate of 0.6 Gy/min. The symbols represent the mean values for n=8 animals per group and error bars represent the standard deviation (STD). Data are shown in Tables 9.2.2.1 – 9.2.2.3.

Table 9.2.2.3. Proteomic biomarker levels in B6D2F1 female mice irradiated with ^{60}Co γ-rays at 1.9 Gy/min. Shaded data represent a significant difference between control (non-irradiated) and irradiated groups at 95% CL.

Biomarker (control values)	Day post-TBI	Biomarker Level (Mean ± STD)				Biomarker (control values)	Day post-TBI	Biomarker Level (Mean ± STD)			
		Sham (0 Gy)	3.0 Gy	6.0 Gy	12.0 Gy			Sham (0 Gy)	3.0 Gy	6.0 Gy	12.0 Gy
Flt3 L (pg mL^{-1}) (250 ± 77)	1	149 ± 21	288 ± 23	480 ± 82	711 ± 77	G-CSF (pg mL^{-1}) (29.7 ± 7.7)	1	42.6 ± 8.5	92.4 ± 44.9	136.4 ± 42.2	183.9 ± 44.6
	2	166 ± 19	552 ± 52	892 ± 98	1271 ± 163		2	44.3 ± 15.9	53.6 ± 9.2	60.4 ± 11.9	107.5 ± 28.6
	4	173 ± 30	485 ± 91	1347 ± 148	1423 ± 100		4	35.9 ± 9.9	61.2 ± 12.7	167.0 ± 45.5	2,367 ± 1,098
	7	148 ± 14	215 ± 15	1137 ± 207	1523 ± 290		7	39.2 ± 8.2	55.0 ± 17.1	123.8 ± 32.9	9,895 ± 7,108
IL-5 (pg mL^{-1}) (3.2 ± 0.8)	1	2.9 ± 0.7	2.1 ± 0.6	2.7 ± 1.0	1.9 ± 0.2	GM-CSF (pg mL^{-1}) (0.11 ± 0.01)	1	0.14 ± 0.02	0.17 ± 0.02	0.15 ± 0.02	0.14 ± 0.02
	2	3.3 ± 1.0	6.1 ± 2.2	6.6 ± 1.5	10.2 ± 2.0		2	0.12 ± 0.03	0.17 ± 0.02	0.25 ± 0.03	1.68 ± 0.73
	4	4.0 ± 1.0	7.1 ± 2.9	16.6 ± 4.5	43.3 ± 9.7		4	0.12 ± 0.02	0.18 ± 0.03	0.62 ± 0.16	15.20 ± 1.90
	7	3.1 ± 1.1	5.2 ± 1.3	55.6 ± 40.3	46.6 ± 36.3		7	0.12 ± 0.02	0.13 ± 0.01	0.41 ± 0.12	4.34 ± 1.48
IL-10 (pg mL^{-1}) (9.6 ± 3.6)	1	6.5 ± 1.2	7.4 ± 1.0	7.5 ± 0.9	6.7 ± 0.8	SAA (ng mL^{-1}) (423 ± 121)	1	1,106 ± 449	4,679 ± 1,834	11,517 ± 2,093	16,308 ± 2,379
	2	7.8 ± 1.6	7.3 ± 1.3	7.3 ± 1.0	5.4 ± 1.7		2	558 ± 260	1,915 ± 1,759	3,207 ± 1,072	3,769 ± 1,103
	4	6.6 ± 1.9	5.9 ± 1.5	6.3 ± 1.5	5.3 ± 1.0		4	478 ± 285	296 ± 140	237 ± 60	797 ± 216
	7	6.0 ± 3.2	3.9 ± 1.2	4.5 ± 1.1	102.5 ± 81.6		7	479 ± 214	301 ± 147	585 ± 281	38,046 ± 29,958
IL-12 (pg mL^{-1}) (202 ± 26)	1	156 ± 29	135 ± 15	120 ± 10	117 ± 17	LBP (ng mL^{-1}) (454 ± 176)	1	738 ± 68	1,208 ± 226	1065 ± 316	1,560 ± 171
	2	127 ± 24	84 ± 9	66 ± 3	80 ± 11		2	771 ± 218	679 ± 106	850 ± 166	1033 ± 183
	4	136 ± 28	60 ± 3	45 ± 5	38 ± 5		4	549 ± 152	472 ± 78	642 ± 165	1,622 ± 395
	7	131 ± 16	75 ± 6	36 ± 6	42 ± 9		7	476 ± 119	633 ± 125	706 ± 192	3,106 ± 1,666
IL-18 (pg mL^{-1}) (143.3 ± 22.7)	1	103.6 ± 44.0	96.5 ± 27.8	105.7 ± 18.1	210.1 ± 21.8	CD27 (pg mL^{-1}) (3,324 ± 1,015)	1	2,798 ± 415	869 ± 230	573 ± 56	385 ± 52
	2	151.9 ± 22.5	182.7 ± 18.2	188.4 ± 14.0	228.7 ± 42.8		2	2,851 ± 403	574 ± 44	288 ± 23	171 ± 19
	4	151.6 ± 26.9	186.6 ± 20.0	272.6 ± 16.1	836.2 ± 61.0		4	2,862 ± 915	604 ± 54	261 ± 27	149 ± 16
	7	160.0 ± 27.3	188.7 ± 14.6	192.8 ± 17.3	560.9 ± 250.3		7	2,811 ± 620	1,425 ± 415	805 ± 100	145 ± 11
EPO (pg mL^{-1}) (18.7 ± 5.2)	1	20.0 ± 9.4	72.6 ± 36.5	55.2 ± 18.3	57.2 ± 11.8	CD45 (pg mL^{-1}) (5,568 ± 593)	1	5,407 ± 563	6,249 ± 880	7,664 ± 781	7,249 ± 1,214
	2	33.4 ± 9.7	143.6 ± 59.0	90.1 ± 27.5	85.1 ± 39.0		2	5,019 ± 349	4,279 ± 953	4,790 ± 341	4,545 ± 859
	4	27.2 ± 8.5	128.2 ± 34.3	402.4 ± 179.3	142.6 ± 26.5		4	4,742 ± 498	3,361 ± 266	2,851 ± 242	2,666 ± 130
	7	29.0 ± 9.5	101.5 ± 66.0	1,053 ± 409	922.5 ± 619.2		7	5,014 ± 435	3,233 ± 130	2,380 ± 187	2,067 ± 322
TPO (pg mL^{-1}) (195.2 ± 45.4)	1	126.6 ± 33.6	115.3 ± 26.3	187.3 ± 39.9	216.8 ± 18.2	CD45/CD27 ratio (1.78 ± 0.61)	1	1.91 ± 0.35	7.05 ± 2.27	13.43 ± 1.26	20.13 ± 2.11
	2	173.0 ± 40.2	180.0 ± 19.6	186.9 ± 18.6	505.0 ± 75.9		2	1.74 ± 0.25	7.46 ± 1.60	16.72 ± 1.35	27.08 ± 6.87
	4	197.4 ± 83.3	305.3 ± 56.7	652.6 ± 127.9	4,910 ± 1,410		4	1.68 ± 0.54	5.67 ± 0.52	10.99 ± 0.86	18.03 ± 2.07
	7	140.9 ± 29.1	422.0 ± 148.7	2,876 ± 571	7,637 ± 2,641		7	1.79 ± 0.33	2.46 ± 0.59	3.17 ± 0.41	11.90 ± 5.30

Procalcitonin (PCT), known as a biomarker indicative of gastrointestinal (GI) injury as well as a clinical sepsis biomarker, was tested in sham, 6- and 12-Gy groups. While no changes in PCT level were observed in 6-Gy groups (data not shown), the time-dependent changes in PCT level in individual mice irradiated with 12 Gy are shown in Figure 9.2.2.3.

Our results demonstrate that PCT level significantly increased ($p < 0.008$) only in mice irradiated with 12 Gy on d7 post-TBI with no significant differences between groups irradiated at either 0.6 or 1.9 Gy/ min ($p > 0.287$). In our mixed-field and pure gamma studies, I-FABP level was in a range from 1 to 4 ng mL^{-1} regardless of radiation dose and time after TBI and these results are in general agreement with the results published by Castillo and colleagues (Castillo et al. 2017).

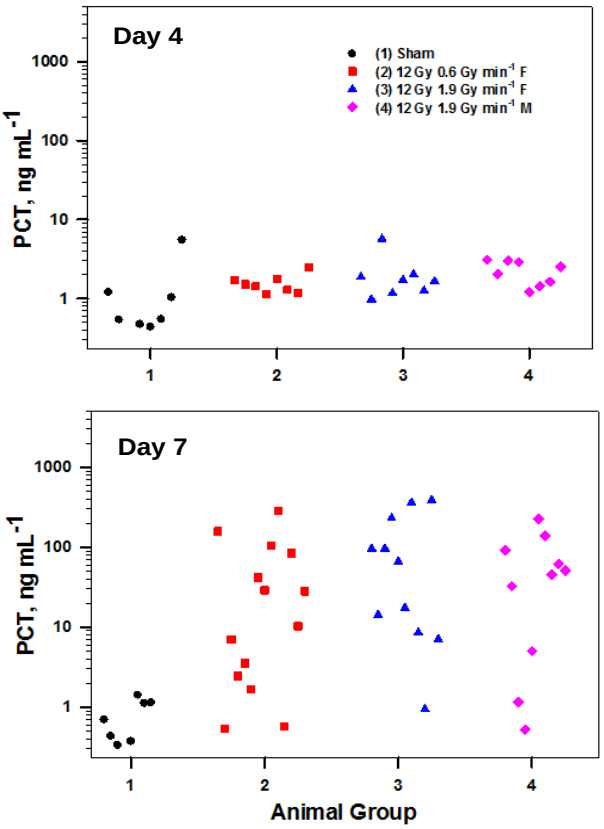

Fig. 9.2.2.3. Dose- and time-dependent changes in PCT level in blood plasma of female (F) and male (M) mice after a ^{60}Co γ-rays TBI to 12 Gy at the dose rate of either 0.6 Gy/min or 1.9 Gy/min. The symbols represent the PCT concentration for individual animals (n=8-14 mice per group) on day 4 and day 7 after TBI.

Good correlations were observed between CBC/diff and proteomic biomarkers (Fig. 9.2.2.4).

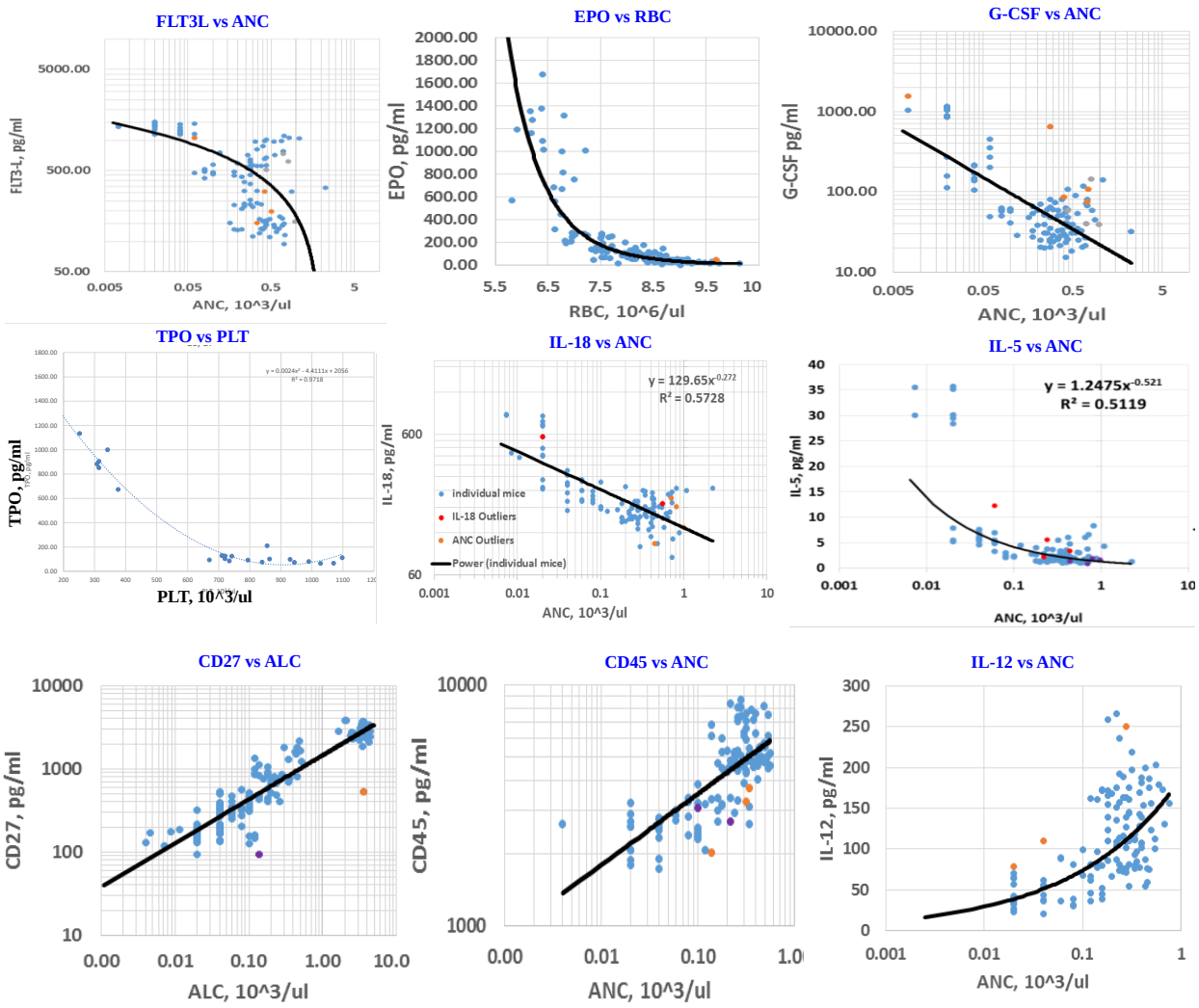

Fig. 9.2.2.4. Correlations between CBC/diff and proteomic biomarkers in ^{60}Co γ-rays studies.

9.2.3. DISCUSSION

In our pure γ-rays studies, we evaluated blood cell counts (CBC/diff), hematopoietic cytokines, organ-specific, and acute phase protein biomarkers (Table 7.1) for early-response assessment of radiation exposure using a mouse (B6D2F1, males and females) TBI model, exposed to ^{60}Co γ-rays over a broad dose range (3 – 12 Gy) and dose rates of either 0.6 or 1.9 Gy/min in order to compare results with those obtained after exposure of mice to a dose range (1.5 – 6 Gy) with a mixed-field (neutrons and γ-rays) using the AFRRI TRIGA Mark-F nuclear research reactor at the same dose rates and testing different proportions of Dn/Dt.

In the ^{60}Co γ-rays gender-comparison study, no significant differences were observed between animal groups in hematological and protein profiles (Flt3L, IL-18, EPO, G-CSF, GM-CSF, SAA, CD45) for any radiation dose at any time after exposure ($p > 0.114$). However, in sham male mice, IL-5 and CD27 were about 2-fold less and IL-12 was about 2-fold higher than in sham/control

female mice. While these proteins showed strong dose- and time-dependent responses, the differences remained the same at any given radiation dose and time after TBI. Similar findings ($p > 0.088$) were reported in our mouse mixed-field exposure (67% n + 33% γ) studies (Ossetrova et al. 2018).

In the ^{60}Co γ-rays dose-rate comparison study (either 0.6 or 1.9 Gy/min), no significant differences were observed between animal groups in hematological and protein profiles (Flt3L, IL-5, IL-12, IL-18, EPO, G-CSF, GM-CSF, CD27, CD45 and ratio of CD45 to CD27) for any radiation dose at any time after exposure ($p > 0.148$). Kiang and colleagues have investigated the response of circulating cytokine/chemokine concentrations in a mouse TBI model after ^{60}Co γ-rays exposure to a broad radiation dose range (3, 6, 8, and 12 Gy) and multiple dose rates ranging from 0.04 to 1.94 Gy/min and provided evidence that radiation dose rates do not influence the cytokine/chemokine responses to ionizing radiation, which is advantageous for radiation dose assessment and triage-based treatment after nuclear weapon detonation or radiological accidents (Kiang et al. 2018).

Our PCT results described herein demonstrated that PCT level significantly increased ($p < 0.008$) only in mice irradiated with 12 Gy on d7 without significant differences between groups irradiated at a dose rate of either 0.6 or 1.9 Gy/min ($p > 0.287$) and our results are in agreement with those reported by Biju and colleagues in mice total-body irradiated with lethal doses (9 or 10 Gy) using a photon radiation source (^{137}Cs) and a dose rate of 1.35 Gy/min (Biju et al. 2012). I-FABP has also been reported as a biomarker of radiation-induced GI injury in animal models (Niewold et al. 2004; Cronk et al. 2006; Li et al. 2010, Castillo et al. 2017). Li and colleagues demonstrated that, in a single abdominal radiotherapy session in BALB/c mice performed using an x-rays source (8-MeV clinical linear accelerator), the I-FABP level increased significantly with increasing radiation dose, radiation dose, roughly 2.5 to 10 times in 6 and 12 Gy groups, respectively, when compared to non-irradiated control mice (Li et al. 2010). Castillo and colleagues investigated the graft copolymer-formulated fibroblast growth factors in order to mitigate the lethality of partial body irradiation injury in C57BL/6J male mice after a partial body irradiation exposure to 15.7 Gy with 6-MeV linear accelerator photon source which targeted the GI system. They reported that the normal blood levels of I-FABP were 11 ± 3 ng mL-1 and these were not statistically different from those in irradiated groups; although, a 3- to 4-fold difference was seen between the non-irradiated and irradiated groups reflecting a large inter-individual variability in mice (Castillo et al. 2017). The use of plasma I-FABP as an early radiation injury biomarker in contrast to citrulline (Lutgens et al. 2007; Jones et al. 2015) is likely limited due to its association with intestinal necrosis (Lieberman et al. 1997). In addition to that, it was reported that the release of I-FABP possesses a fairly short half-life time (~20 min) (Pelsers et al. 2003). In addition to individual variability among mouse strains and a lack of consistency between survival data and changes in plasma I-FABP levels, another cause of differences in data reported could be due to different ELISA kits used (Li et al. 2010; Castillo et al. 2017).

Results from ^{60}Co γ-ray studies demonstrate: 1) significant dose- and time-dependent reductions in circulating mature hematopoietic cells; 2) dose- and time-dependent changes in Flt3L), interleukins IL-5, IL-10, IL-12, and IL-18, G-CSF, GM-CSF), TPO, EPO, SAA, LBP, surface plasma neutrophil (CD45) and lymphocyte (CD27) markers, ratio of CD45 to CD27, PCT but not in I-FABP; 3) no significant differences were observed between dose-rate groups in hematological and protein profiles (Flt3L, IL-5, IL-12, IL-18, EPO, G-CSF, GM-CSF, CD27, CD45 and ratio of CD45 to CD27) for any radiation dose at any time after exposure ($p > 0.148$); 4) no significant differences were observed between gender groups in hematological and protein

profiles (Flt3L, IL-18, EPO, G-CSF, GM-CSF, SAA, CD45) for any radiation dose at any time after exposure ($p > 0.114$); 5) PCT level significantly increased ($p < 0.008$) in mice irradiated with 12 Gy on d7 post-TBI without significant differences between groups irradiated with dose rate of either 0.6 or 1.9 Gy/min ($p > 0.287$).

10. BIOMARKER COMPARISON RESULTS IN TRIGA vs. COBALT STUDIES

As shown in Fig. 10.1, a good reproducibility was observed in CBC/diff results collected in blood of control female mice in current TRIGA mixed-field studies (n=29 animal per group) compared with ones collected earlier in ^{60}Co γ-rays radiation studies (n=99 animals per group) (i.e., project funded by BARDA in support of development and evaluation of MSD's hand-held field-deployable POC biodosimetry device in 2010 - 2014). Results are shown in the same strain of mice (B6D2F1 females) and from the same vendor (Jackson Labs).

CBC/diff in control female mice in ^{60}Co γ-rays and TRIGA mixed-field studies

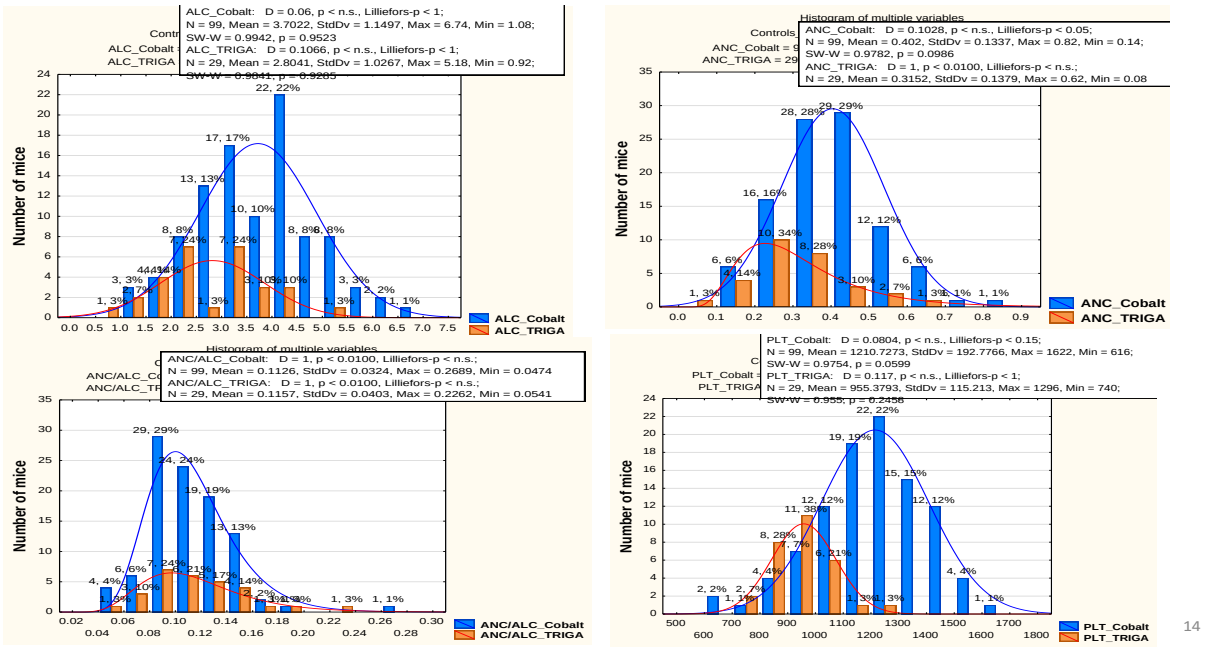

Fig. 10.1. CBC/diff (ALC, ANC, ratio of ANC to ALC and PLT) reproducibility results in blood of control female mice collected in current in current TRIGA mixed-field studies (orange plots; n=29 animal per group) vs. BARDA project ^{60}Co γ-rays (blue plots; n=99 animals per group).

Very good reproducibility in CBC/diff results was also observed in irradiated mice in T1 (dose assessment study) and T3 (dose-rate study) experiments performed at different days at the same conditions: (67% n + 33% γ) and 0.6 Gy/min. Due to this very good reproducibility, T1 and T3 data were combined for further advanced statistical data analyses (i.e., multivariate regression and discriminant analyses to create the dose-response calibration curves, multi-ROC analysis, etc.).
Analysis of outliers was performed using the SAS software for each data set and outliers (out of 95% confidence level or CL) were highlighted in the Data Master List, but not excluded from the data set for further evaluations and correlations with proteomic results. An outlier was defined as

an observation point that is distant from other observations. As an example, analysis of outliers in control mice are shown in Fig. 10.2. An outlier may be due to variability in the response to irradiation or measurement or it may indicate experimental error; the latter are usually excluded from the data set. Outliers may cause a negative effect on data analyses, such as MANOVA and regression, based on distribution assumptions, or may provide useful information about data when we look into an unusual response to a given study. Thus, outlier detection is an important part of data analysis.

CBC/diff analysis of outliers in control mice in ^{60}Co γ-rays and TRIGA mixed-field studies

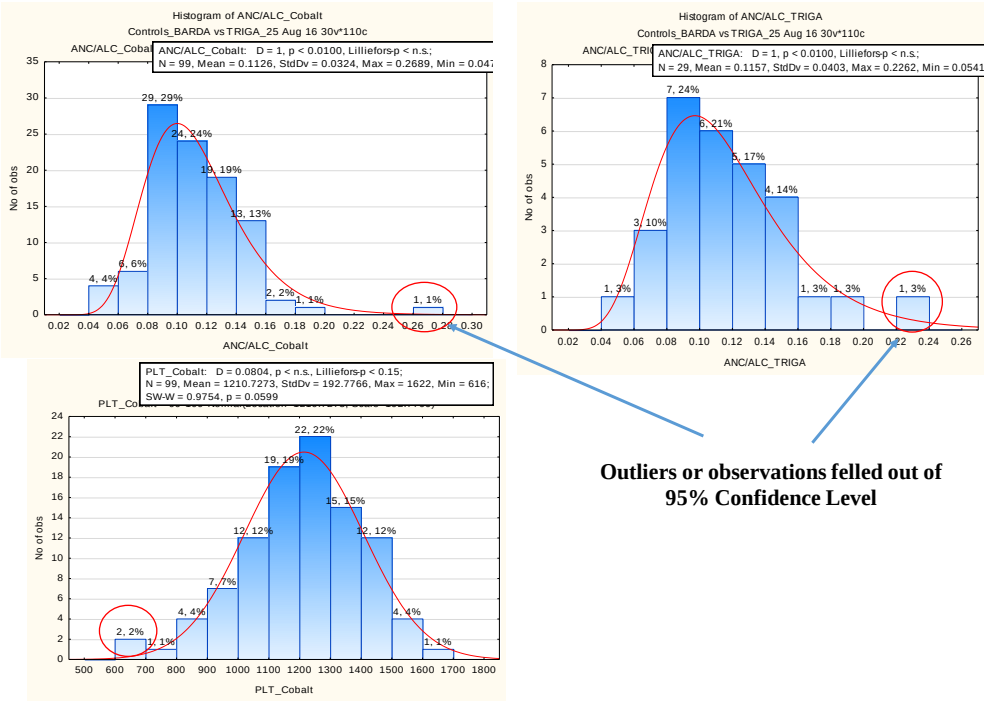

Fig. 10.2. SAS-based analysis of outliers at 95% CL for CBC/diff in control mice in ^{60}Co γ-rays and TRIGA mixed-field studies.

Heat Maps were created using Microsoft Excel software for ratios comparing proteomic and hematological biomarkers obtained in the Cobalt (pure γ-rays) study to those obtained in TRIGA reactor mixed-field (neutrons + γ-rays) studies. Data were generated using a Cobalt dose that is twice as high as the compared TRIGA dose (i.e., 3.0 Gy Cobalt vs. 1.5 Gy TRIGA). These Heat Maps are graphical representations of data where the individual values contained in a matrix are represented as colors. A Heat Map in Excel is a visual representation that quickly shows a comparative view of a dataset. For each biomarker in Tables 10.1.1, 10.2.1 – 10.2.2, a range was established across both (TRIGA and Cobalt) experiments. The lowest value was assigned the darkest shade of green while the highest value was assigned the darkest shade of red. All remaining values were shaded based on their percentage within that range with yellow delineating 50%.

10.1. HEMATOLOGICAL BIOMARKERS COMPARISON AFTER THE MIXED-FIELD (NEUTRONS AND GAMMAS) AND PURE GAMMA RADIATION

In both irradiation studies (mixed-field and pure γ-rays), among all evaluated blood cell counts, stress-effect associated with sham-irradiation was observed in mice only on d1 post-procedure resulting in ~20 - 40% increase in ANC in sham-groups compared to counts in control groups. ANC increase due to the demargination process was observed only in mice irradiated with mixed-field on d1 and d2 after exposure, but not in mice irradiated with ^{60}Co γ-rays. In our earlier animal ^{60}Co γ-ray studies, ANC dose-dependent increases were reported at 4 and 8 h after TBI and returned to pre-TBI levels on d1 in mice irradiated with ≤ 3 Gy, but were still elevated in mice irradiated with ≥ 6 Gy. ANC results in this study are in agreement with those reported earlier (Ossetrova et al. 2014). In irradiated animal groups, a significant decline in all blood cells was observed in dose- and time-dependent manner after TBI. ALC and ANC partial recovery was found only in 3-Gy groups on d7. No significant differences were observed between animal groups for ANC, ANC to ALC ratio, PLT, and RBC for any radiation dose and at any time after exposure ($p > 0.114$) in dose-rate and gender-comparison studies.

Table 10.1.1. Ratio of 2x ^{60}Co dose (100% γ-irradiation) to 1x TRIGA reactor mixed-field dose (67% n + 33% γ) in hematological parameters in: (a) B6D2F1/J female mice after irradiation at dose rate of 1.9 Gy/min, and (b**)** B6D2F1/J male mice after irradiation at dose rate of 0.6 Gy/min.

a.	3 vs 1.5	6 vs 3	12 vs 6	Day post-TBI	3 vs 1.5	6 vs 3	12 vs 6	b.
ANC	0.92	1.02	1.08	1	2.48	0.97	1.38	ANC
	1.00	0.73	0.93	2	1.09	1.67	1.40	
	0.51	0.83	1.35	4	0.61	0.83	0.81	
	0.68	0.53	1.36	7	1.08	0.41	0.74	
ALC	0.32	0.78	0.86	1	0.29	1.03	1.69	ALC
	0.24	0.54	0.76	2	0.51	0.84	0.77	
	0.42	0.32	1.28	4	0.55	0.53	1.59	
	0.42	0.45	2.08	7	1.06	0.55	0.64	
ANC/ALC	2.89	1.35	1.29	1	6.80	1.05	0.81	ANC/ALC
	4.03	1.21	1.16	2	2.68	2.22	1.82	
	1.39	2.90	1.17	4	1.09	1.63	0.54	
	1.49	1.10	0.92	7	1.84	1.33	2.44	
PLT	1.17	1.08	1.06	1	0.97	1.09	1.03	PLT
	1.04	1.04	1.02	2	1.01	0.88	0.98	
	1.26	1.06	0.97	4	1.06	0.97	0.83	
	0.94	0.87	0.44	7	1.14	0.87	0.62	
RBC	1.01	1.02	1.00	1	1.01	0.97	1.01	RBC
	1.02	1.01	1.05	2	0.99	1.00	0.99	
	0.96	0.99	0.94	4	0.93	1.00	0.95	
	0.91	0.91	0.99	7	0.95	0.97	0.88	

Two-thirds of all hematological ratios returned values within the 0.7 and 1.3 range indicating a very strong 2 to 1 dose comparison between Cobalt and TRIGA in both female and

male mice. This reflects the RBE = 1.95 seen in mouse radiation countermeasure survival studies (Ledney and Elliott 2010). Of the values falling outside the 0.7 to 1.3 range, the vast majority (over 70%) can be directly linked to lymphocyte counts. At lower doses (3 Gy Cobalt vs. 1.5 Gy TRIGA and 6 Gy Cobalt vs. 3 Gy TRIGA) calculated ratios returned values less than 0.7. These lower values, when applied further to the ANC/ALC ratio gave lower denominators and higher values were seen as a result (Table 10.1.1).

10.2. PROTEIN BIOMARKERS COMPARISON AFTER THE MIXED-FIELD (NEUTRONS AND GAMMAS) AND PURE GAMMA RADIATION

Acute radiation subsyndromes in humans have been identified and described after exposure to TBI doses greater than 1 Gy that create a risk of developing radiation-induced multi-organ involvement (MOI) and multi-organ failure (MOF) (Fliedner et al. 2005; Friesecke et al. 2001). Radiation-induced GI injury combined with immune system compromise may lead to septicemia and death (Dainiak et al. 2003, Goans and Flynn 2013; Anno et al. 1989). ARS occurs at the molecular, cellular, tissue, and systemic levels and, therefore, the immune system response varies depending on the severity of radiation-induced injury. In response to either mixed-field or pure-gamma radiation, an increase in concentration of Flt3L, IL-5, IL-18, G-CSF, GM-CSF, TPO, EPO, SAA, PCT and ratio of CD45 to CD27 and decrease in concentration of IL-12, CD27 and CD45 were observed in a dose- and time-dependent manner. Only IL-10, LBP, and I-FABP levels showed no significant changes in any irradiated animal groups when compared to control/sham. Similar conclusions were reported earlier in mouse mixed-field studies (Ossetrova et al. 2018). The bi-phasic pattern was observed in SAA and G-CSF expression and results are in agreement with those reported earlier (Ossetrova et al. 2014, 2016b, 2018). Among hematological plasma surface biomarkers, stress-effect associated with the handling of mice was observed only on d1 in CD45 and CD45/CD27, but not in CD27 levels, furthermore, the effect was less pronounced in pure-gamma studies when compared to mixed-field studies likely due to difference in irradiation restraint devices (i.e., Plexiglas® boxes vs. aluminum tubes).

Similar to hematological ratios, proteomics ratios also fell within a 0.7 - 1.3 range over 50% of the time in both female and male mice, 58% and 52%, respectively. Again, this corresponds with the RBE = 1.95 seen in previous mouse radiation countermeasure survival studies (Ledney and Elliott 2010). Of the results leading to values outside of this range, the most notable belong to CD27 and the two colony stimulating factors. CD27 values are directly related to the results seen in lymphocyte counts in hematological biomarkers. The two colony stimulating factors (G-CSF and GM-CSF) are very important in highlighting the increased effect of pure gamma rays on these biomarkers and hematological damage when compared to the majority of all the others. While most hold to the 2:1 dose comparison, both stimulating factors show no such inclination as the raw values (Tables 10.2.1 and 10.2.2) show a dose relationship closer to 1:1.

Table 10.2.1. Ratio of 2x ^{60}Co dose (100% γ-irradiation) to 1x TRIGA reactor mixed-field dose (67% n + 33% γ) in proteomic parameters in B6D2F1/J female mice after irradiation at dose rate of 1.9 Gy/min.

	3 vs 1.5	6 vs 3	12 vs 6	Day post-TBI	3 vs 1.5	6 vs 3	12 vs 6	
IL-5	0.60	0.96	0.86	1	1.22	1.39	1.22	**Flt3 L**
	1.71	0.90	0.71	2	1.52	1.21	1.27	
	1.22	1.40	1.34	4	1.41	1.27	0.98	
	0.75	3.71	1.53	7	0.96	1.52	0.91	
IL-10	0.86	0.62	0.48	1	1.57	1.21	1.52	**EPO**
	0.89	0.94	0.63	2	2.19	1.08	1.29	
	0.73	0.81	0.67	4	1.46	1.47	1.47	
	0.53	0.50	9.81	7	1.42	3.07	1.12	
IL-12	0.80	0.55	0.53	1	0.49	0.42	0.87	**TPO**
	0.69	0.45	0.49	2	0.90	0.80	2.46	
	0.71	0.57	0.63	4	1.21	2.77	11.77	
	0.58	0.42	0.90	7	1.14	1.23	1.50	
IL-18	0.65	0.64	1.03	1	1.66	1.39	1.50	**G-CSF**
	1.50	0.98	0.84	2	1.63	1.34	1.49	
	1.51	0.82	0.86	4	0.96	1.34	1.97	
	1.45	0.74	0.81	7	1.13	1.78	6.19	
CD-45	0.84	0.89	0.91	1	1.83	1.32	1.06	**GM-CSF**
	0.75	0.89	0.85	2	1.42	0.73	0.76	
	0.73	0.82	0.89	4	1.20	1.08	1.20	
	0.76	0.77	1.03	7	1.16	1.66	1.14	
CD-27	0.81	0.56	0.86	1	6.80	1.30	1.27	**SAA**
	0.73	0.87	0.93	2	4.82	1.03	1.12	
	0.65	0.86	0.95	4	0.49	0.34	0.32	
	0.85	0.98	0.89	7	1.07	0.74	26.55	
CD45/CD27	1.01	1.47	1.11	1	1.57	1.07	1.73	**LBP**
	1.05	1.08	0.96	2	1.42	1.53	2.09	
	1.13	0.96	0.95	4	0.78	1.20	1.07	
	0.90	0.80	0.99	7	1.38	1.32	5.11	

Table 10.2.2. Ratio of 2x ^{60}Co dose (100% γ-irradiation) to 1x TRIGA reactor mixed-field dose (67% n + 33% γ) in proteomic parameters in B6D2F1/J male mice after irradiation at dose rate of 0.6 Gy/min.

	3 vs 1.5	6 vs 3	12 vs 6	Day post-TBI	3 vs 1.5	6 vs 3	12 vs 6	
IL-5	1.20	1.04	1.02	1	1.09	1.20	1.25	Flt3 L
	1.05	0.93	0.69	2	1.14	1.18	1.08	
	1.19	0.93	1.19	4	1.05	1.16	1.11	
	1.19	0.66	0.87	7	0.67	1.23	1.05	
IL-10	0.89	0.47	0.51	1	2.07	1.10	0.79	EPO
	0.98	0.58	0.78	2	1.54	1.30	2.08	
	0.95	0.86	0.80	4	1.47	1.05	1.25	
	1.34	1.06	2.97	7	1.07	1.67	1.25	
IL-12	0.73	0.51	0.79	1	1.37	1.77	2.06	TPO
	0.51	0.42	0.45	2	0.37	0.38	0.65	
	0.59	0.41	0.42	4	0.29	0.48	0.56	
	0.42	0.37	0.70	7	0.22	0.35	2.53	
IL-18	0.97	1.03	1.06	1	4.42	1.16	1.21	G-CSF
	1.02	1.15	0.92	2	2.35	2.18	1.78	
	0.94	0.84	0.81	4	0.75	0.61	1.05	
	1.07	0.92	0.65	7	0.88	1.50	8.10	
CD-45	1.03	0.98	1.06	1	2.20	1.40	3.53	GM-CSF
	0.99	1.10	0.99	2	2.44	0.87	0.63	
	0.87	1.25	1.01	4	1.80	0.97	1.64	
	0.98	1.12	0.99	7	0.89	1.57	1.63	
CD-27	0.40	0.38	0.43	1	2.39	2.13	0.74	SAA
	0.52	0.50	0.49	2	1.45	1.84	1.27	
	0.53	0.94	0.68	4	0.56	1.62	0.41	
	1.15	1.05	0.71	7	2.18	2.45	13.75	
CD45/CD27	2.53	2.41	2.32	1	1.01	1.44	0.94	LBP
	1.96	2.22	1.93	2	1.63	1.99	1.40	
	1.68	1.33	1.40	4	1.09	1.71	1.10	
	0.84	1.06	1.47	7	1.88	1.69	4.40	

Our results from the mixed-field exposure (67% n + 33% γ) dose-rate study are in agreement with other dose-response in-vitro studies (Balcer-Kubiczek et al. 1991) and animal survival studies performed using the AFRRI TRIGA reactor (Ainsworth et al. 1964a, 1964b; Alpen 1991). However, there were some debates that fission-neutron dose rates may result in changes in radio-sensitive tissues such as the crypt cells of the gut and influence LD50s and RBEs. For example, a small effect on survival of mice given fission neutrons at 0.012 Gy/min vs. mice given 0.131 Gy/min (Ainsworth et al. 1976; Strike 1970) and a small effect on jejunal crypt cell survival after irradiation with a dose rate of 0.02 Gy/min compared to 22.5 Gy/min have been observed (Griffin and Hornsey 1986).

In our studies, GI injury biomarkers Procalcitonin or PCT and intestinal fatty acid binding protein or I-FABP were evaluated in mice irradiated with either mixed-field or pure-gamma exposure to evaluate the GI injury due to the presence of neutrons as reported in animal studies performed at the Nevada Test Site (Fehner and Gosling 2006).

In addition to already evaluated GI injury biomarkers, a literature search up-to date was performed for additional potential biomarkers of radiation-induced gastrointestinal injury and three potential candidates have been found: Diamine oxidase (DAO), R-Spondin 1 (RSPO1), and citrulline. To our knowledge, RSPO1 and citrulline have been evaluated only in γ- or x-ray studies and their responses after mixed-field irradiation remain unknown. DAO was not evaluated at different percentage of neutrons, dose-rates and gender-comparison. DAO, and RSPO1 were measured using the enzyme-linked immunosorbent assay kits. Citrulline was measured using liquid chromatography tandem mass spectrometry (LC-MS/MS) at the University of Maryland, Baltimore as described previously (Jones et al. 2014).

Diamine oxidase (DAO)

Diamine oxidase (DAO or histaminase) is an enzyme involved in the metabolism, oxidation, and inactivation of histamine in mammals. In the polyamine pathway, it follows ornithine decarboxylase (Brook et al. 1992). DAO can be found in most organs but it's concentration is particularly high in the epithelial cells of the small intestine (Shaff and Beaven 1976, Wollin et al. 1981, Biegański et al. 1983).When intestinal epithelial cells are injured, DAO is released into the intestinal lumen and intercellular space and then is taken up by lymphatic and blood vessels (Wollin et al. 1981). Blood DAO activity has been shown to correlate well with DAO activity in the villi of the small intestinal mucosa (Luk et al. 1980, Luk et al. 1981, Gupta 2014). The plasma DAO activity has been suggested as a candidate marker for measuring ischemic small bowel injury (Bragg et al. 1991, Bounous et al. 1984, Rose et al. 1991, DeBell et al. 1987, Ely et al. 1985). DAO, a cytoplasmic enzyme found in almost all organs is present in a particularly high concentration in the epithelial cells of the small intestine. Following injury to intestinal epithelial cells DAO is released into the intestinal lumen and intercellular space where it is taken up by lymphatics and blood vessels. Circulating DAO is rapidly cleared by the liver.

DeBell and colleagues measured plasma DAO activity in B6D2F1/J mice irradiated to different doses of ^{60}Co γ-rays and fission neutrons on days 2, 4, and 6 after irradiation. They found that plasma DAO activity increased after irradiation, peaking on day 2, and decreased around day 4. DAO activity was dose-dependent: on day 2, the higher the radiation dose was, the higher the DAO activity was; on day 4 DAO activity was diminishing with increasing radiation doses. There is a disagreement in results published by DeBell et al. and by Ely et al. Ely and colleagues measured plasma DAO activity in Sprague-Dawley rats irradiated to different doses with 14.5-MeV electrons on days 1-15 after irradiation. They showed radiation dose-dependent decline in rat plasma DAO activity with nadir on day 3 after irradiation.

In our project, DAO was tested in both TRIGA mixed field and pure γ-ray ^{60}Co studies. DAO results demonstrate the strong dose- and time-dependency peaking on day 1 post TBI with highly significant differences ($p < 0.005$) between all mouse dose-groups in both studies (Figs. 10.2.1 - 10.2.5). In ^{60}Co γ-rays study, on d2 and d4, DAO level in mice irradiated to sub-lethal doses (3 and 6 Gy) was found returning to a level in sham group at later time-points, but remained progressively elevated in mice irradiated to a lethal dose (12 Gy). In 6-Gy mouse groups irradiated with TRIGA mixed-field (67% n + 33% γ), DAO level was still elevated on days 2-7, in contrast with mouse groups irradiated with (30% n +70% γ) (Fig. 10.2.2). However, while all other Cobalt

experiments (dose rate and gender comparison) showed a similar increase on day 7 at 12 Gy, a similar increase was not seen in any other mixed-field experiment (dose rate, gender study, and neutron percentage). Our results, in general, are in agreement with ones demonstrated at AFRRI by Dr. Ledney and colleagues ((DeBell et al. 1987). However, in their studies, the DAO level was found peaking on day 2. As expected, good correlations were found between DAO and SAA and LBP in TRIGA and ^{60}Co studies (Figs. 10.2.6 and 10.2.7).

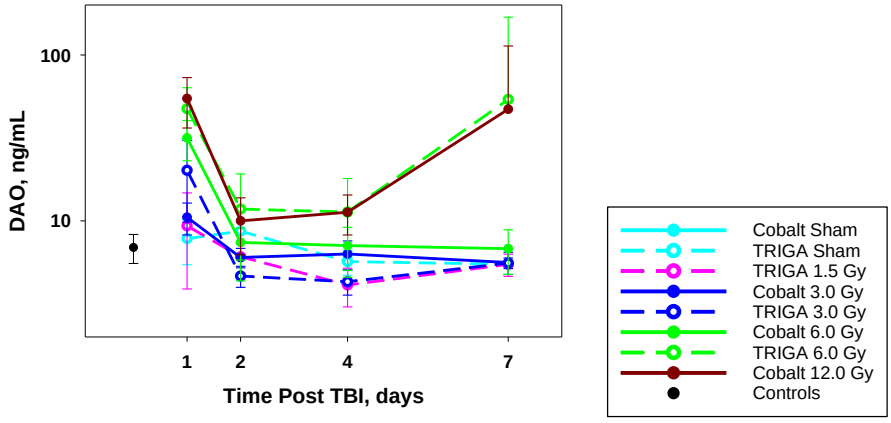

Fig. 10.2.1. Comparison of DAO dose- and time-dependency results in TRIGA mixed-field (67% n + 33% γ) and ^{60}Co γ-ray studies.

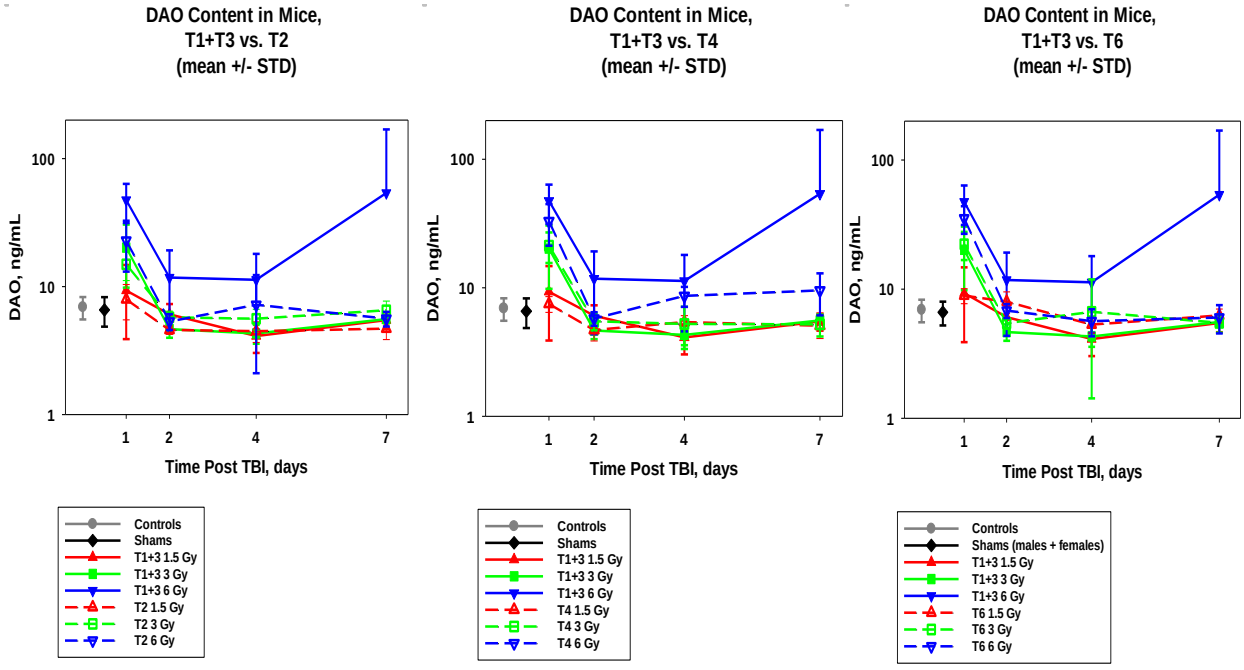

Fig. 10.2.2. Comparison of DAO dose- and time-dependency results in TRIGA mixed-field experiments.

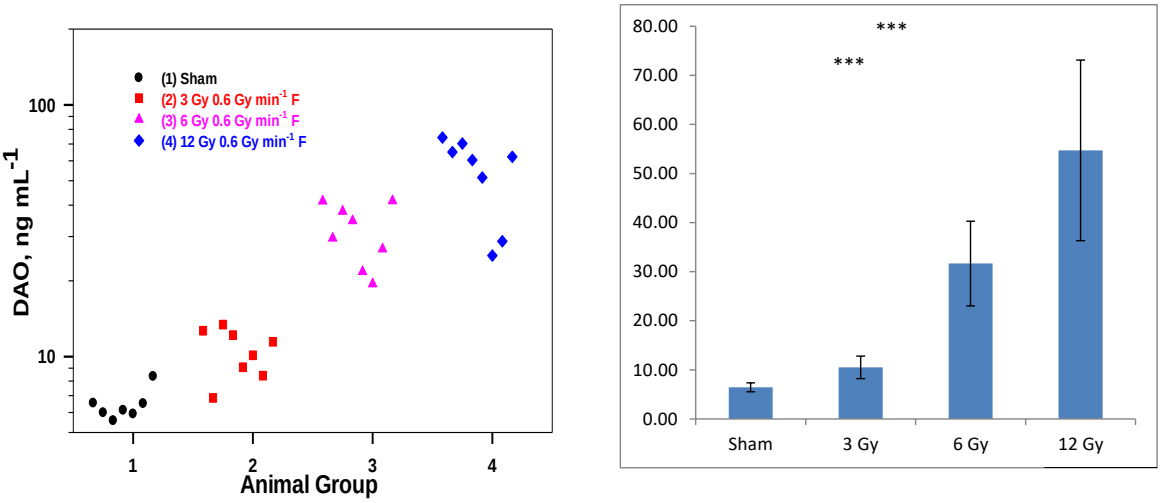

Fig. 10.2.3. DAO dose-dependency results on day 1 in ^{60}Co γ-ray studies.

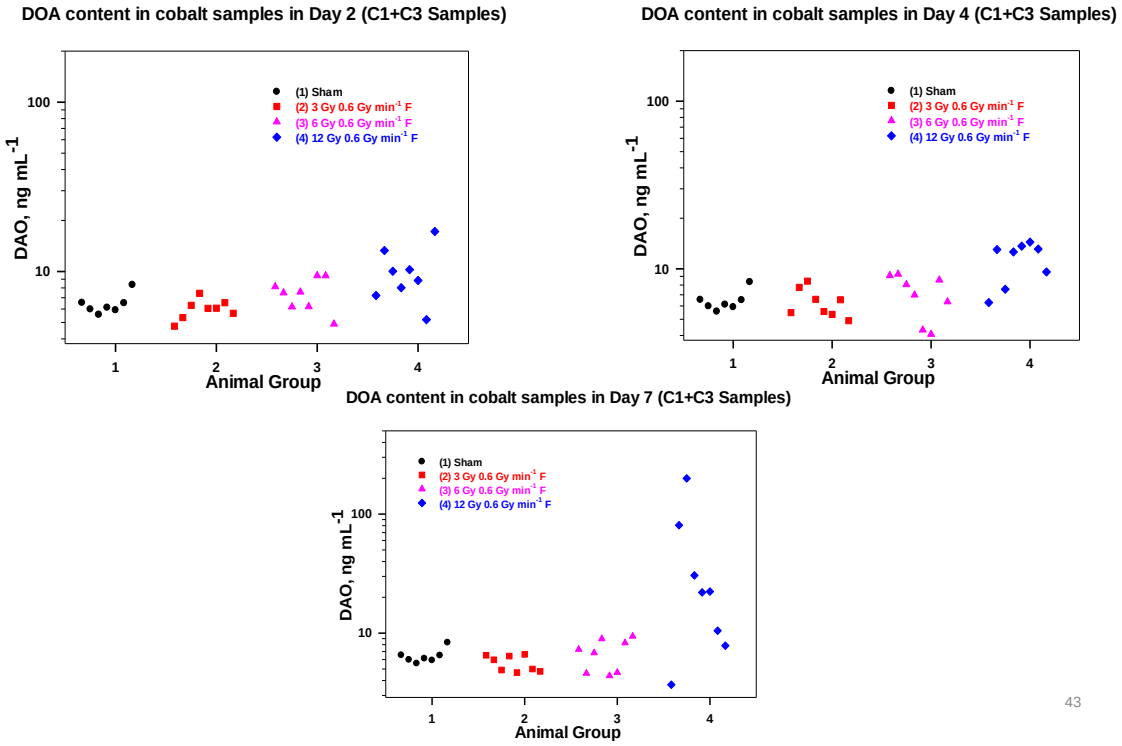

Fig. 10.2.4. DAO dose-dependency results on days 2, 4 and 7 in ^{60}Co γ-ray studies.

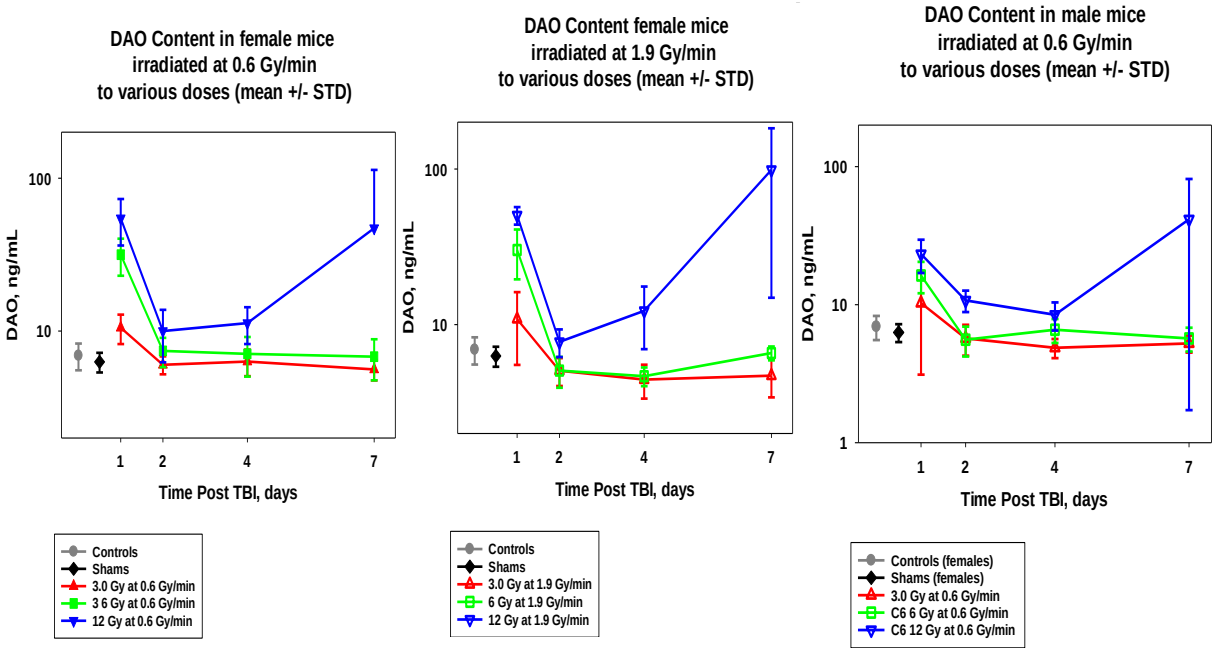

Fig. 10.2.5. Comparison of DAO dose- and time-dependency results in ^{60}Co γ-ray experiments.

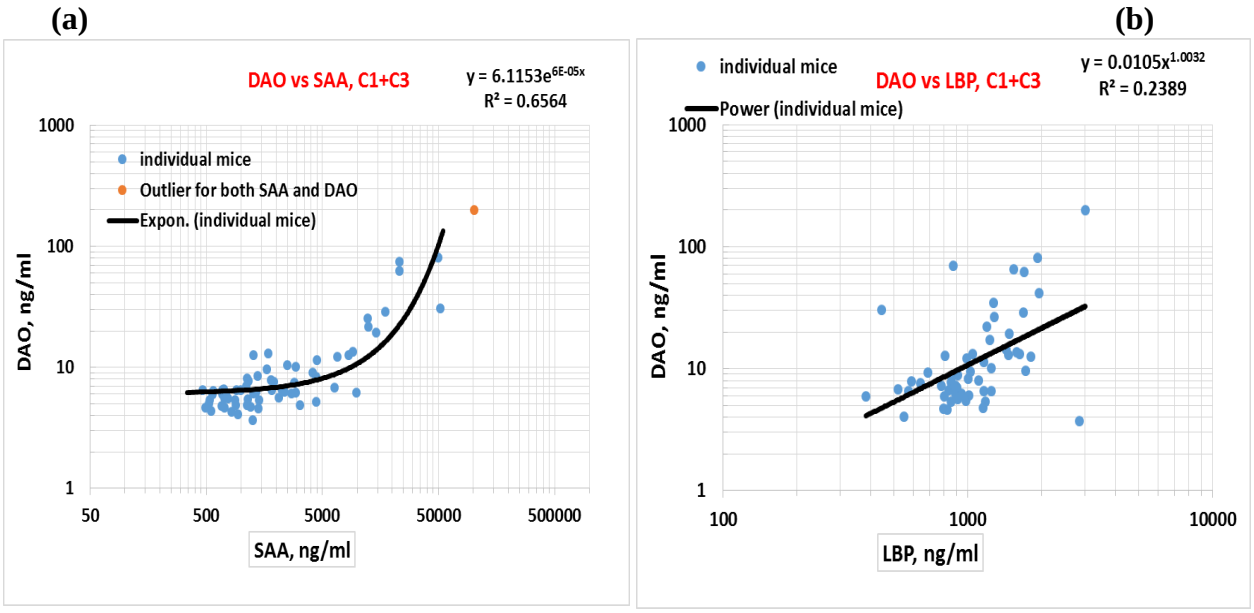

Fig. 10.2.6. Correlations between DAO and SAA (a) and between DAO and LBP (b) in ^{60}Co γ-ray studies.

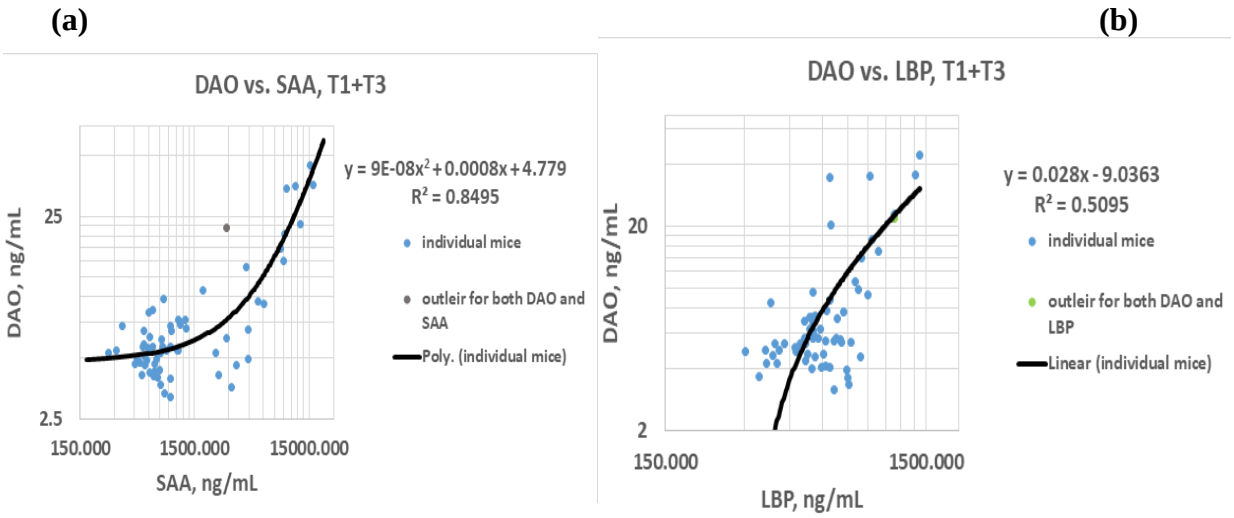

Fig. 10.2.7. Correlations between DAO and SAA (a) and between DAO and LBP (b) in TRIGA mixed-field studies.

R-Spondin 1 (RSPO1)

R-spondins are a family of secreted proteins that are expressed in the small intestine, kidney, prostate, adrenal gland and pancreas. RSPO1 is an agonist of the Wnt signaling pathway which is important in crypt cell proliferation in the intestine and increases the length of the colon of hRSpo1-KI chimeras (Kim et al. 2005). Previous experiments have shown RSPO1 to increase in peripheral blood of C57BL6 in immunoblotting on several days during the week after whole body irradiation mice to 10.4 Gy (^{137}Cs source). This increase was estimated to be two-fold in magnitude 3.5 days after treatment, with pre-irradiation concentration in plasma being almost undetectable. In the same study, systemic administration of adenoviral RSPO1 was associated with reduction in many signs of radiation induced intestinal damage and mortality in subjects subjected to abdominal radiation (not experiencing hematopoietic syndrome) (Bhanja et al. 2009). Immunoblot analysis of the serum of C57BL6 mice that received abdominal radiation (AIR) plus bone marrow transplant (BMASC) showed a 2–8 fold increase in serum concentrations of R-spondin1 at 24 h post-BMASC compared to animals that received AIR alone (Saha et al. 2011). Results from that study showed negligible increase in serum RSPO1 on immunoblot 24 hours after treatment. RSPO1 was detected in peripheral blood of humans using ELISA in a study which found RSPO1 in conjunction with DKK1 to be a predictor of rheumatoid arthritis progression. (Choi 2014). RSPO1 has been reported to play a role in development of several systems in mice, and during osteoporosis (Caruso et al. 2015; Maatouk et al. 2013; Wang et al. 2013). Additionally, it may also play a role in B cell growth and insulin stimulation in the pancreas (Wong et al. 2010).

In our project, RSPO1 results showed no significant differences in time, dose, dose rate, or gender experiments in either the mixed-field or pure γ-ray studies (Fig. 10.2.8).

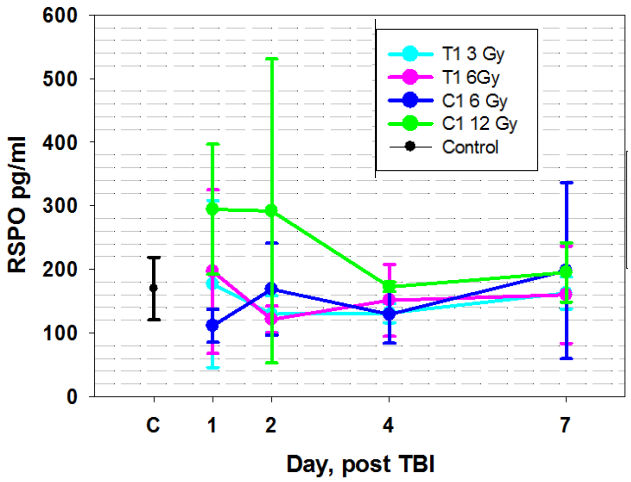

Fig. 10.2.8. RSPO1 dose- and time-dependency results in TRIGA mixed-field and ^{60}Co γ-ray studies.

Citrulline

Citrulline, a non-structural, a non-DNA encoded amino acid, is primarily synthesized in the intestinal mucosa and reflects mucosal mass and acts as a metabolite biomarker of intestinal functions. Plasma citrulline levels are positively correlated with intestinal length and lower levels of plasma citrulline are evident in intestinal failure shown in animal studies and radiation therapy patients (Lutgens et al., 2003; 2004). Analysis of plasma citrulline is challenging using ELISA because of less sensitivity. However, utilization of mass spectrometry makes citrulline as a promising GI biomarker. Jones et al, used mass spectrometry based analytical methods to detect circulating citrulline. Circulating citrulline concentration was correlated with gross histological GI damage following high dose irradiation (Jones et al., 2014, 2015). The decrease of intestinal absorptive function following irradiation has been due to the loss of functionally active enterocytes this constitute the absorptive mucosal surface. The correlation between radiation-induced epithelial cell loss and plasma citrulline level has been well validated in mice (Burnett et al., 2013, Pawar et al., 2014). The use of mass spectrometry-based metabolomics approach to detect plasma citrulline provides a unique opportunity to assess GI damage (Jones et al., 2014, 2015). Jones and colleagues used an LC-MS/MS platform to separate, detect, and quantitate the analyte of interest from control and irradiated samples generating raw data (e.g., extracted ion chromatogram), calibration parameters, and data visualization. The end point being quantitation of the targeted analyte ideally produces differential expression between irradiated vs. non-irradiated samples.

Lutgens and colleagues have evaluated a citrulline as a metabolic end product of small bowel enterocytes and demonstrated that it can be used for quantifying radiation-induced epithelial cell loss in mice. Because small bowel irradiation results in epithelial cell loss and consequently impairs function and metabolism. After radiation, intestinal release of citrulline into the circulation decreases due to the reduction of epithelial cell mass. Thus, citrullinemia is tested as a quantitative marker for small bowel epithelial radiation injury (Lutgens et al., 2003). The time course for citrullinemia has been assessed on 1, 2, 4, 8, and 11 days after single TBI doses of 8–12 Gy. Significant dose–response relationship can be seen for citrullinemia on 2 and 4 days after single-dose TBI. The maximum decrease in epithelial surface lining in this experiment was noticed on

day 4 after TBI. Plasma citrulline levels remained significantly decreased on day 11ater TBI. Based on data published, citrullinemia is a simple and sensitive marker for monitoring small bowel epithelial radiation damage in mice after single TBI doses between 8–12 Gy. Furthermore, citrulline level enables quantification of epithelial cell loss after doses per fraction between 3 and 12 Gy in patients treated with fractionated radiation therapy for abdominal or pelvic cancer sites (Lutgens et al., 2004).

Figures 10.2.9 and 10.2.10 show the results for plasma citrulline concentrations in individual mice over the course of the 7-day collection period and summary results, respectively, analyzed in pure γ-ray study and mixed-field studies involving 30% neutrons and 67% neutrons at a dose rate of 0.6 Gy/min. In general, the results are in agreement with both previous studies involving mice and the RBE=1.95 seen between high dose neutron radiation and pure γ-radiation (6 Gy mixed-field with 67% neutrons and 12 Gy Cobalt studies show similar results). Also of note, the 6 Gy mixed-field study with 30% neutrons falls between the 6 and 12 Gy Cobalt studies, as expected, indicating the increased GI impact of increasing neutron percentage.

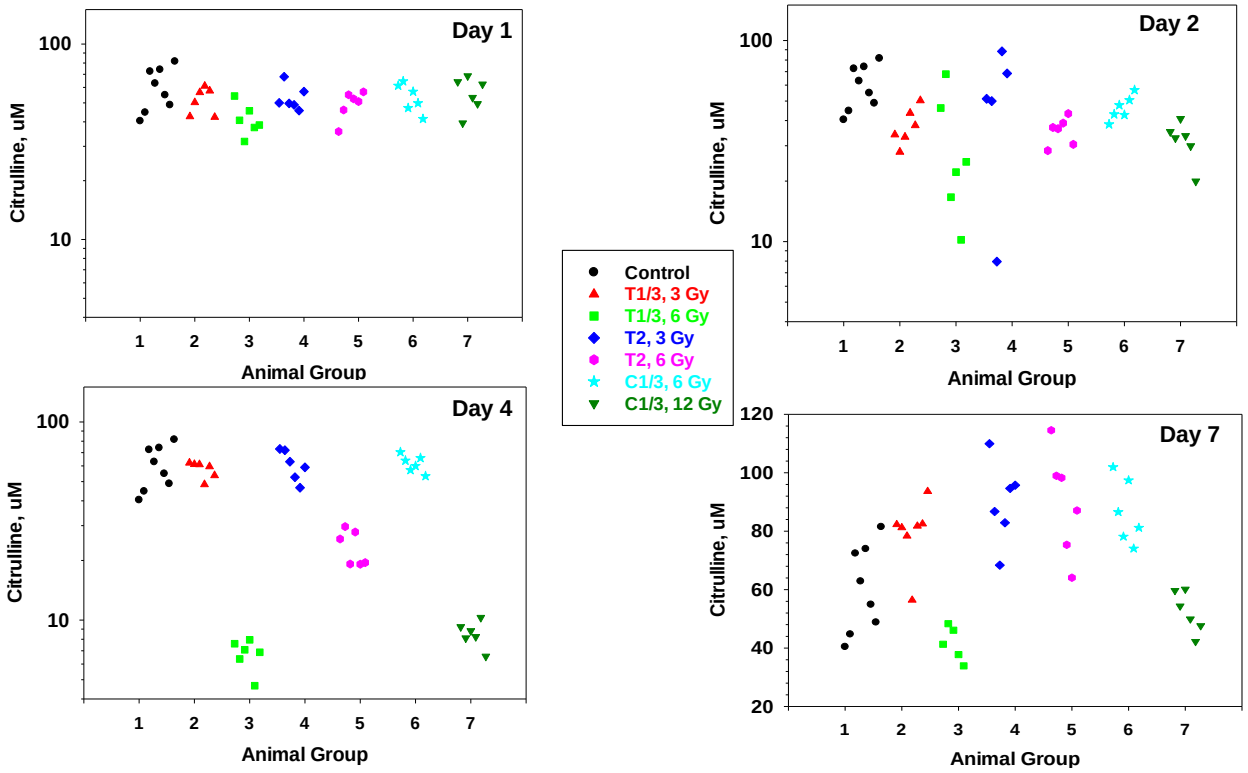

Fig. 10.2.9. Plasma citrulline concentrations in individual mice over the course of the 7-day collection period in TRIGA mixed-field and ^{60}Co γ-rays studies.

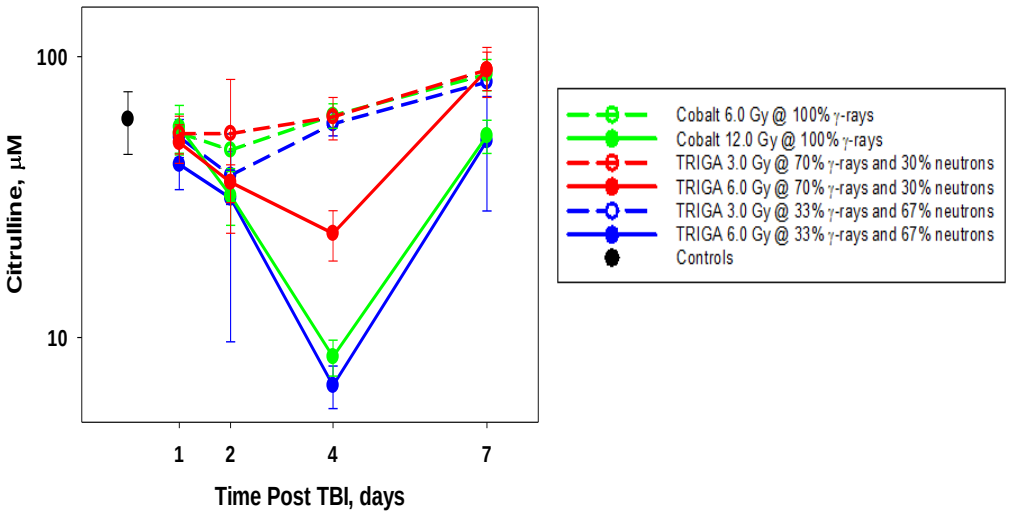

Fig. 10.2.10. Plasma citrulline concentrations summary results in TRIGA mixed-field and ^{60}Co γ-ray studies.

Numerous studies demonstrated the greater RBE of neutrons relative to photons for a number of cell, organ and whole-animal survival endpoints. Normal organ systems in the body, including the gut, kidney, and bone marrow sustain greater injury after mixed fission neutron and γ-rays irradiation than after pure γ-rays irradiation resulting in a higher RBE. For example, an RBE value ranging from 3 to 4 was observed for intestinal cell damage in mice after neutron irradiation (Broerse 1975; DeBell et al. 1987; Hendry et al. 1995). It was concluded that, in general, there is a slower rate of repair of cellular damage after high-LET than after low-LET irradiation, which was observed at the level of DNA double-strand breaks (DSB), chromosome breaks, cell death, and tissue reactions. The slower rate can be interpreted in terms of the greater difficulty in repairing the more severe lesions induced by high-LET irradiation. DNA DSB can induce apoptosis, and the RBE for neutrons varies from 1 to around 4 for different cell types. In general, RBE values are higher for epithelial cells than for lymphoid cells, indicating that epithelial cells are more resistant to apoptosis than lymphoid cells. Also, there is some evidence for faster apoptosis in lymphocytes after high-LET irradiation (Hendry 1991).

GI injury biomarkers PCT and I-FABP were evaluated in mice irradiated with either mixed-field or pure-gamma exposure to evaluate the GI injury due to the presence of neutrons as reported in animal studies performed at the Nevada Test Site (Fehner and Gosling 2006). We demonstrated earlier that mice irradiated with 6 Gy with TRIGA reactor mixed-field showed a time-dependent increase in PCT beginning from d4 post-TBI and its level was significantly higher in mice irradiated with a higher percentage of neutrons (67% vs. 30%) reflecting the fact that the GI epithelium is more sensitive to neutron irradiation (Ossetrova et al. 2018). Our results from the pure-gamma study described herein demonstrated that PCT level significantly increased ($p < 0.008$) only in mice irradiated with 12 Gy on d7 without significant differences between groups irradiated at a dose rate of either 0.6 or 1.9 Gy/min ($p > 0.287$) and PCT level on d7 was about the same as in mice irradiated with 6 Gy with a mixed-field (67% n + 33% γ). Our PCT results in the pure-gamma study are in agreement with those reported by Biju and colleagues in mice total-body irradiated with lethal doses (9 or 10 Gy) using a photon radiation source (^{137}Cs) and a dose rate of 1.35 Gy/min (Biju et al. 2012). I-FABP has also been reported as a biomarker of radiation-induced GI injury in animal models (Niewold et al. 2004; Cronk et al. 2006; Li et al. 2010, Castillo et al.

2017). Li and colleagues demonstrated that, in a single abdominal radiotherapy session in BALB/c mice performed using an x-rays source (8-MeV clinical linear accelerator), the I-FABP level increased significantly with increasing radiation dose, radiation dose, roughly 2.5 to 10 times in 6 and 12 Gy groups, respectively, when compared to non-irradiated control mice (Li et al. 2010). Castillo and colleagues investigated the graft copolymer-formulated fibroblast growth factors in order to mitigate the lethality of partial body irradiation injury in C57BL/6J male mice after a partial body irradiation exposure to 15.7 Gy with 6-MeV linear accelerator photon source which targeted the GI system. They reported that the normal blood levels of I-FABP were 11 ± 3 ng mL-1 and these were not statistically different from those in irradiated groups; although, a 3- to 4-fold difference was seen between the non-irradiated and irradiated groups reflecting a large inter-individual variability in mice (Castillo et al. 2017). The use of plasma I-FABP as an early radiation injury biomarker in contrast to citrulline (Lutgens et al. 2007; Jones et al. 2015) is likely limited due to its association with intestinal necrosis (Lieberman et al. 1997). In addition to that, it was reported that the release of I-FABP possesses a fairly short half-life time (~20 min) (Pelsers et al. 2003). In addition to individual variability among mouse strains and a lack of consistency between survival data and changes in plasma I-FABP levels, another cause of differences in data reported could be due to different ELISA kits used (Li et al. 2010; Castillo et al. 2017).

The primary purpose of these studies was to demonstrate that mixed-field radiations were more damaging than photon radiations of comparable physical doses for a number of life-threatening situations. Fission neutrons produce greater biological damage than photons (γ- or x-rays) (Lawrence and Tennant 1937; Alpen 1991; MacVittie et al. 1991; Ledney and Elliott 2010; Cary et al. 2012). However, the extent of biological damage after different Dn/Dts, the biological endpoint, and the resulting tissue injury, as assessed by death from hematopoietic cell failure or death from GI cell failure is still not known. It was shown in animal radiation countermeasure survival studies that while the RBE for death from GI cell system failure and bone marrow syndrome failure increased as the Dn increased, cells of the GI system were more sensitive to increasing Dn in the Dt than cells of the hematopoietic system. This finding supports the idea that the increase in opportunity for bacterial translocation through the damaged gut as well as the lungs could contribute to sepsis leading to death (Strike 1970; Griffin and Hornsey 1986; Ledney and Elliott 2010).

The comparison of biomarker results from both studies (mixed-field and pure gamma) showed significant differences in ARS injury severity following exposure to the same radiation dose due to different mechanisms of injury resulting from either low-LET radiations or high-LET radiation, such as neutrons. While the project goal was not to test multiple Dn/Dts and LD50/30s, it was shown that the expression of some important hematopoietic cytokines and PCT were significantly higher in animals irradiated with a higher percentage of neutrons (67% vs. 30%). The data presented may be useful in evaluating the radiation-quality specific proteomic biodosimetry similar to the lymphocyte dicentric assay calibration curves created using AFRRI's different radiation sources (TRIGA nuclear reactor, ^{60}Co γ-rays, and 250-keV x-rays) (Prasanna et al. 2002) as well as testing effective medical countermeasures in situations associated with nuclear radiation disasters. For example, as demonstrated in mouse survival assays, G-CSF (filgrastim) was effective as a (post-irradiation) mitigator against both gamma and mixed-field radiation, while a TPO mimetic (ALXN4100TPO) was effective only against gamma-irradiation. These results indicate that radiation countermeasures should be tested against radiation qualities appropriate for specific scenarios before inclusion in response plans (Cary et al. 2012).

Results presented cover entirely new ground and supplement ongoing efforts to deliver an FDA approved MSD's proteomic POC biodosimetry device, which includes mixed-field radiation exposure analysis, and further bridges the gap between current capabilities and the anticipated demand to rapidly and effectively identify and assess radiation exposure after a radiation event, especially after a mass-casualty radiological incident.

11. BIODOSIMETRY ADVANCED STATISTICAL DATA ANALYSES

At AFRRI, we have established animal (*Mus musculus, Macaca mulatta*) total-body irradiation (TBI) models and have succeeded in evaluating a panel of radiation-responsive proteins that have been applied along with other biomarkers, for the development of a multi-parametric biodosimetry dose-predictive algorithm with a threshold for γ-exposure detection of ~1 Gy from 1 to 7 d after exposure (Ossetrova et. al, 2007-2017). We continue to demonstrate in animal radiation models that a panel of protein biomarkers selected from distinctly different pathways, each with different radiation responses, provides a more accurate assessment of exposure, an improvement in threshold for radiation dose received and enhanced dose-dependent separation of irradiated animal groups than any one biomarker alone.

The use of multiple radiation-responsive targets/biomarkers was evaluated using multiple linear regression analysis to provide dose-response calibration curves for radiation dose assessment/prediction using several selected biomarkers: absolute lymphocyte counts (ALC), absolute neutrophil counts (ANC), ratio of ANC to ALC (ANC/ALC), CD27 (ALC surface plasma protein marker), CD45 (ANC surface plasma protein marker), CD45 to CD27 ratio (CD45/CD27), FLT3 Ligand – protein biomarker of bone marrow aplasia, acute phase protein serum amyloid A or SAA, interleukins IL-5, IL-10, IL-12, IL-18 and G-CSF. Hematological and plasma protein profiles were evaluated using multivariate linear regression analysis to provide dose-response calibration curves for pure gamma and mixed-field (gammas + neutrons) irradiation dose assessment in 32 mice per each study time-point of sample collections. Due to a high-sensitivity of multiplex MSD's assay platform that allows to measure simultaneously multiple biomarkers using only up to ~25 μl of plasma per plate well, all biomarker measurements were performed in the each individual mouse.

Prior to performing the advanced SAS-based statistical data analyses, the analysis of variance (ANOVA) and discriminant analysis was performed first for every single biomarker for meaningful time expression to demonstrate any significant differences in separation of control/sham from irradiated animal groups as well as separation between irradiated groups (Tables 9.2.1.1 – 9.2.1.3 and 9.2.2.1 – 9.2.2.3). For each single biomarker, statistical data analysis results revealed limited discrimination power (65 – 80 %) to separate control/sham from irradiated animal groups. Multivariate analysis of variance (MANOVA) was performed next for different biomarker combinations in order to illustrate the enhanced discrimination of animal groups as the number of biomarkers increased. The discrimination power was improved by using combinations of two biomarkers (80 – 95 %). The complete separation of animal groups (100%) was observed using combinations of three or more biomarkers as reported earlier (Ossetrova et al. 2007-2016).

In order to illustrate the enhanced discrimination of animal groups, the best combinations of three biomarkers were selected based on their time-window of expression after irradiation for sham/control and male mice exposed to different TBI doses (3 and 6 Gy) with either mixed-field (67% n + 33% γ) or ^{60}Co γ-rays radiation at a dose rate of 0.6 Gy/min at various time points after exposure. As shown in Fig. 11.1, the MANOVA p values showed highly significant differences

($p < 0.005$) at all time-points between TRIGA reactor mixed-field irradiated groups and those irradiated with ^{60}Co γ-rays to the same doses and at the same dose-rate (Ossetrova et al. 2018).

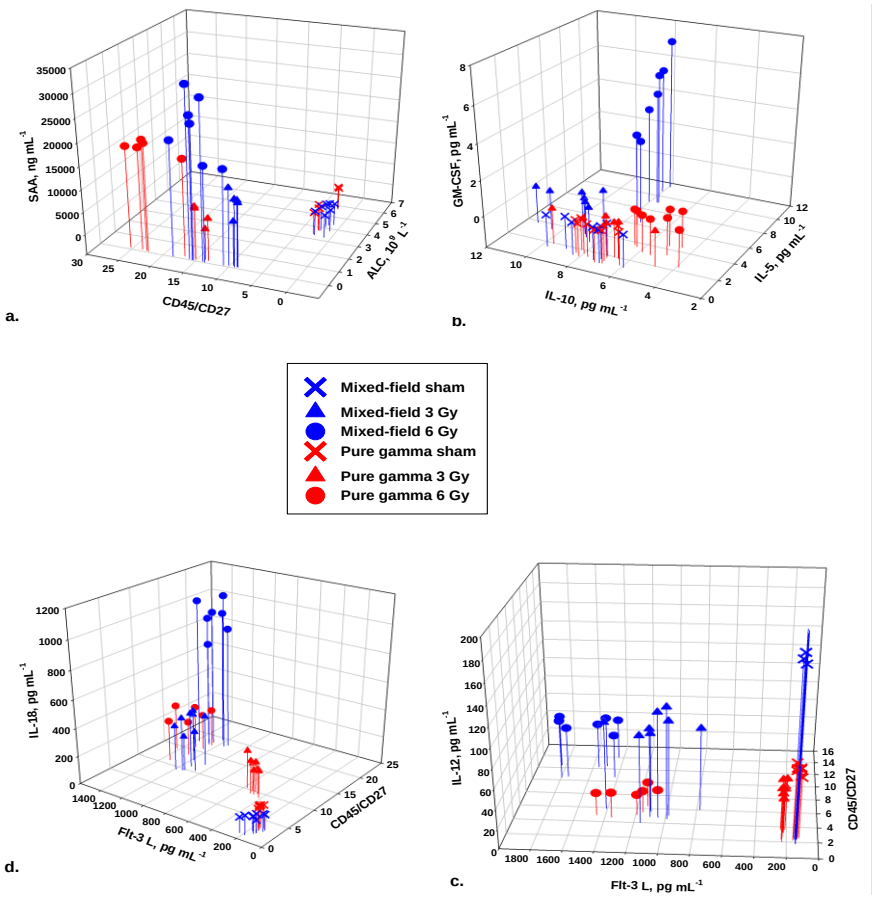

Fig. 11.1. Discrimination of male mouse groups exposed to different TBI doses (3 and 6 Gy) with either mixed-field (67% n + 33% γ) or ^{60}Co γ-rays radiation at dose rate of 0.6 Gy/min at various time points after exposure based on combinations of three biomarkers: (a) SAA, CD45 to CD27 ratio, and ALC on d1, (b) GM-CSF, IL-10, and IL-5 on d2, (c) IL-18, FLT3L, and CD45 to CD27 ratio on d4, and (d) IL-12, FLT3L, and CD45 to CD27 ratio on d7. Blue and red symbols represent individual animals (n=8 mice per group) in mixed-field and ^{60}Co γ-rays studies, respectively.

Multiple linear regression analysis was used to develop dose-response relationships for multiple biomarkers for radiation dose prediction. To study the dependence of each biomarker on dose assessment the analysis was performed according to following model: $Y=a+b_1*X_1+b_2*X_2+...+b_p*X_p$, where Y variable (dose assessment in Gy) can be expressed in terms of a constant (a) and a slope (b) times the X variables (biomarker data in pg/ml, or ng/ml, or number of cells per μl), p is a number of biomarkers in the model. The standardized raw regression coefficients (b) represent the independent contributions of each independent variable (biomarker) to the prediction of the dependent variable (dose). The magnitude of b coefficients allows one to compare the relative contribution of each independent variable in the prediction of radiation dose absorbed. After fitting a regression equation, the residual analysis was performed to examine the

predicted values and residual scores because, for example, extreme outliers may seriously bias results and lead to erroneous conclusions. This multivariate technique relies upon determining the linear relationship with the lowest sum of squared variances; therefore, assumptions of normality, linearity, and equal variance have been carefully tested before regression analysis as previously described (Ossetrova et al. 2007 – 2016).

The PC SAS stepwise multivariate discriminant function analysis was performed to separate irradiated animal groups from non-irradiated ones and also to demonstrate accurate radiological detection into tertiles of doses 0-1.5 Gy, 1.5-3 Gy, and 3-6 Gy and ARS RCs based on selected biomarker or combination of biomarkers detected from biological samples. The experimental data have met the assumptions for discriminant analysis (i.e., specific tests for normality, homogeneity of variances/covariances, correlations between means and variances, etc.). Effects of violations of these assumptions may seriously bias results and lead to erroneous conclusions. The discriminant function can use several quantitative variables (biomarkers); each of them makes an independent contribution to the overall discrimination. Taking into consideration the effect of all quantitative variables, this discriminant function produces the statistical decision for predicting to which subgroup of classification variable each subject (animal) belongs. The procedure calculates the posterior probability of each individual animal belonging to each of three subgroups and assigns the subject to a corresponding subgroup according to the higher probability; it then summarizes the squared distance between subgroups in multidimensional (dimension is a number of independent variables) space taking into account correlations between variables. The discriminant procedure produces quantitative variables: Wilks' Lambda that assume values in the range of 0 (perfect discrimination) to 1 (no discrimination) and provides information about upper limit for number of biomarkers and Partial Lambda associated with the unique contribution of the respective variable (biomarker) to the discriminatory power of the model. The procedure derives a list of misclassified observations, classification error-rate, the result of classification for each subject, and canonical scores that represent the observation in the multidimensional space. Canonical scores have been used for 2D-plots to aid the visual interpretation of subgroup differences. The purpose of the canonical score is to separate the classes as much as possible. Thus, when observations are plotted with canonical scores coordinated, observations belonging to the same class are grouped together. As a result of classification and discrimination analysis, we also have a list with detailed information for each animal: predicted and observed classification.

Receiver Operating Characteristic (ROC) analysis was performed using ROCCET on-line tool (Xia et al. 2013). Individual markers were analyzed using classical ROC and multiple markers with partial least squares – discriminant analysis approach. The area under the curve (AUC) with 95% confidence intervals was used to demonstrate the sensitivity and specificity of the proposed protein biomarkers to reflect subgroup (dose and sampling time-point) differences as well as to analyze the results from survival study to predict the ARS outcome. Results are shown as a ROC plot of the true positive rate against the false positive rate for the different possible cut-points of a diagnostic test.

11.1. TRIGA MIXED-FIELD STUDY BIODOSIMETRY DATA ANALYSES

Table 11.1.1 shows biodosimetry performance selected results for radiation dose prediction accuracy in mixed-field (67% n + 33% γ) gender-comparison studies. For biomarker combinations, multiple linear regression analysis was used to develop biodosimetry dose-response relationships in male mice (T6 experiment) and applied in female mice irradiated either at the same dose rate (0.6 Gy/min) (T1 + T3 experiments) or at dose rate of 1.9 Gy/min (T4 experiment) for comparison.

Results were also compared with ones collected in mice irradiated with different percentage of neutrons (30% vs. 67%) (T2 experiment). Summary results demonstrate that (1) no significant differences in dose prediction were observed in gender-comparison study (i.e., males vs. females), (2) no significant differences in radiation dose prediction were observed in dose-rate studies (i.e., 0.6 vs. 1.9 Gy/min), (3) evaluated subset of biomarkers that predicts the radiation dose and injury assessment regardless of percentage of neutrons and another subset of biomarkers that reflects the ~2-fold difference in percentage of neutrons (30% vs. 67%) and (4) accuracy in radiation dose prediction progressively increases with the increasing of number of biomarkers as reported in other animal studies (Ossetrova et al. 2007 – 2016). Selected multi-parameter algorithm equations for predicted vs. given radiation doses in samples collected 1d -7d post TBI in male B6D2F1 mice irradiated with 67% n + 33% γ at 0.6 Gy/min are shown in Table 11.1.2.

Table 11.1.1. Bidosimetry performance for selected biomarker combinations for radiation dose prediction accuracy in TRIGA reactor mixed-field (67% n + 33% γ) gender-comparison studies. Algorithm and equations were created in male mice (T6 experiment) and applied in female mice (T1 + T3 experiments).

Bidosimetry Performance for Selected Biomarker Combinations
Radiation Dose Assessment Accuracy in TRIGA Gender-comparison Studies Using Algorithm Equations Created in Male Mice

#	Biomarker Combination	TRIGA 67% n + 33% γ Males	^{60}Co 100% γ Females
1	ALC	95.6 ± 3.2	97.5 ± 2.6
2	CD27	97.1 ± 2.4	97.6 ± 2.2
3	Flt3L	98.1 ± 2.2	98.7± 1.9
4	CD45/CD27	98.6 ± 2.4	98.1 ± 2.1
5	Flt3L + CD27	99.1 ± 2.2	98.9 ± 2.4
6	Flt3L + CD45/CD27	99.3 ± 2.4	99.5 ± 1.9
7	Flt3L + CD45/CD27 + SAA	99.2 ± 2.7	99.3 ± 1.8
8	Flt3L + CD45/CD27 + IL-18	99.4 ± 2.2	99.5 ± 1.3
9	Flt3L + CD45/CD27 + IL-12	98.9 ± 2.3	99.5 ± 1.6
10	Flt3L + CD45/CD27 + IL-5	99.4 ± 2.2	99.3 ± 1.2
11	Flt3L + CD45/CD27 +G-CSF	99.1 ± 1.8	99.3 ± 1.7
12	Flt3L + CD45/CD27 + IL-18 + IL-5 + IL-12 + G-CSF	99.8 ± 0.3	99.9 ± 0.1

Table 11.1.2. Selected multiparameter algorithm equations for predicted vs. given radiation doses in samples collected 1d -7d post TBI in male B6D2F1 mice irradiated with 67%n + 33%γ at 0.6 Gy/min.

Multiparameter algorithm equations for TBI predicted vs. given radiation doses in samples collected 1d-7d post TBI in B6D2F1 male mice irradiated with 67% neutrons + 33% γ-rays at 0.6 Gy/min

Biomarker combination / Collection time (days)	TBI predicted dose for given dose, Mean+STD, Gy Actual dose, Gy 0	1.5	3	6
Day 1				
Dose (Gy) = 4.633 × $e^{(-1.624 \times ALC)}$	0.01 ± 0.01	1.67 ± 0.45	3.89 ± 0.19	4.33 ± 0.12
Dose (Gy) = -3.794 (± 0.859) - 0.0002 (± 0.0002) × CD27 + 0.018 (± 0.002) × FLT3L	-0.20 ± 0.60	2.25 ± 0.56	3.06 ± 0.33	5.39 ± 0.89
Dose (Gy) = -4.509 (±0.509) + 0.020 (± 0.001) × FLT3L	-0.08 ± 0.74	2.16 ± 0.58	2.98 ± 0.36	5.44 ± 0.95
Dose (Gy) = -0.708 (±0.183) + 0.427 ± (0.019) × CD45/CD27	0.01 ± 0.26	1.75 ± 0.22	3.00 ± 0.51	5.74 ± 0.91
Dose (Gy) = -2.732 (± 0.884) + 0.007 (± 0.002) × FLT3L + 0.476 (± 0.326) × IL-5 - 0.003 (± 0.001) × IL-12 + 0.026 (± 0.008) × G-CSF + 0.252 (± 0.047) × CD45/CD27 - 0.001 (± 0.002) × IL-18	0.02 ± 0.18	1.64 ± 0.35	2.97 ± 0.27	5.88 ± 0.67
Day 2				
Dose (Gy) = 5.184 × $e^{(-2.713 \times ALC)}$	0.00 ± 0.00	1.60 ± 0.45	3.81 ± 0.40	4.60 ± 0.31
Dose (Gy) = -2.345 (± 0.411) + 0.0001 (± 0.0001) × CD27 + 0.008 (± 0.0005) × FLT3L	-0.15 ± 0.40	1.74 ± 0.17	3.33 ± 0.41	5.58 ± 0.73
Dose (Gy) = -1.969 (± 0.235) + 0.007 (± 0.0004) × FLT3L	-0.25 ± 0.29	1.85 ± 0.16	3.37 ± 0.39	5.53 ± 0.70
Dose (Gy) = -0.349 (± 0.146) + 0.233 (± 0.009) × CD45/CD27	0.04 ± 0.14	1.74 ± 0.13	2.85 ± 0.30	5.86 ± 0.89
Dose (Gy) = -1.133 (± 0.246) + 0.003 (± 0.001) × FLT3L + 0.117 (± 0.029) × CD45/CD27 + 0.0004 (± 0.0001) × SAA	-0.07 ± 0.10	1.72 ± 0.33	2.99 ± 0.13	5.87 ± 0.61
Dose (Gy) = -0.577 (± 0.728) + 0.003 (± 0.001) × FLT3L + 0.152 (± 0.068) × IL-5 - 0.0002 (± 0.002) × IL-12 - 0.002 (± 0.007) × G-CSF + 0.115 (± 0.041) × CD45/CD27 - 0.002 (± 0.002) × IL-18	0.00 ± 0.11	1.58 ± 0.15	3.07 ± 0.20	5.85 ± 0.74
Day 4				
Dose (Gy) = 4.678 × $e^{(-2.381 \times ALC)}$	0.00 ± 0.00	1.60 ± 0.42	3.92 ± 0.30	4.44 ± 0.17
Dose (Gy) = -0.627 (± 0.6076) - 0.0001 (± 0.0002) × CD27 + 0.004 (± 0.001) × FLT3L	0.02 ± 0.14	1.34 ± 0.15	4.32 ± 0.25	4.83 ± 0.34
Dose (Gy) = -0.902 (± 0.336) + 0.004 (± 0.0004) × FLT3L	0.10 ± 0.17	1.23 ± 0.15	4.32 ± 0.26	4.85 ± 0.36
Dose (Gy) = -0.603 (± 0.159) + 0.355 (± 0.014) × CD45/CD27	-0.01 ± 0.22	1.43 ± 0.23	3.44 ± 0.49	5.64 ± 0.61
Dose (Gy) = -1.058 (± 0.137) + 0.001 (± 0.0004) × FLT3L + 0.240 (± 0.032) × CD45/CD27 + 0.001 (± 0.0001) × SAA	0.06 ± 0.26	1.43 ± 0.20	3.12 ± 0.38	5.90 ± 0.36
Dose (Gy) = 0.777 (± 0.316) + 0.001 (± 0.0003) × FLT3L + 0.038 (± 0.014) × IL-5 - 0.005 (± 0.001) × IL-12 + 0.001 (± 0.0004) × G-CSF + 0.076 (± 0.032) × CD45/CD27 + 0.001 (± 0.001) × IL-18	0.09 ± 0.16	1.38 ± 0.15	3.05 ± 0.23	5.98 ± 0.21
Day 7				
Dose (Gy) = 4.842 × $e^{(-3.015 \times ALC)}$	0.01 ± 0.01	1.64 ± 0.52	3.65 ± 0.29	4.74 ± 0.11
Dose (Gy) = 0.416 (± 0.322) - 0.0003 (± 0.0001) × CD27 + 0.003 (± 0.0002) × FLT3L	0.12 ± 0.34	1.21 ± 0.08	3.65 ± 0.57	5.52 ± 0.53
Dose (Gy) = -0.325 (± 0.208) + 0.003 (± 0.0002) × FLT3L	0.47 ± 0.13	0.90 ± 0.08	3.55 ± 0.65	5.58 ± 0.61
Dose (Gy) = -0.290 (± 0.205) + 0.515 (± 0.029) × CD45/CD27	0.57 ± 0.31	1.57 ± 0.37	2.34 ± 0.36	6.02 ± 0.87
Dose (Gy) = -0.68 (± 0.17) + 0.36 (± 0.06) × CD45/CD27 + 0.002 (± 0.0003) × FLT3L – 0.001 (± 0.001) × G-CSF	0.31 ± 0.18	1.23 ± 0.26	3.01 ± 0.42	5.96 ± 0.50
Dose (Gy) = 1.559 (± 0.681) + 0.0004 (± 0.0004) × FLT3L + 0.062 (± 0.027) × IL-5 - 0.010 (± 0.002) × IL-12 - 0.0003 (± 0.001) × G-CSF + 0.132 (± 0.083) × CD45/CD27 + 0.003 (± 0.001) × IL-18	0.22 ± 0.28	1.23 ± 0.26	3.09 ± 0.19	5.97 ± 0.24

ALC and CD27 depletion kinetics analysis for the radiation dose prediction was performed using a mathematical algorithm (e.g., exponential fitting function) similar to that established and reported in Chernobyl accident victims (Fig. 11.1.1; Baranov et al. 1995; Guskova et al, 1988).

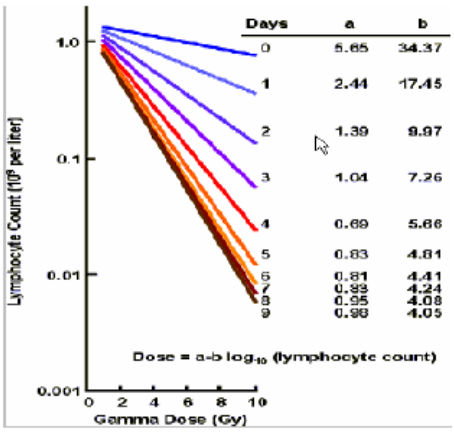

Fig. 11.1.1. Lymphocyte count depletion dose- and time-dependent equations created in Chernobyl accident victims (Baranov et al. 1995; Guskova et al. 1988).

Figs. 11.1.2 and 11.1.3 show ALC and CD27 dose- and time-dependency plots on d1 - d7 in TRIGA mixed-field study. Dose prediction equations are shown in Table 11.1.2.

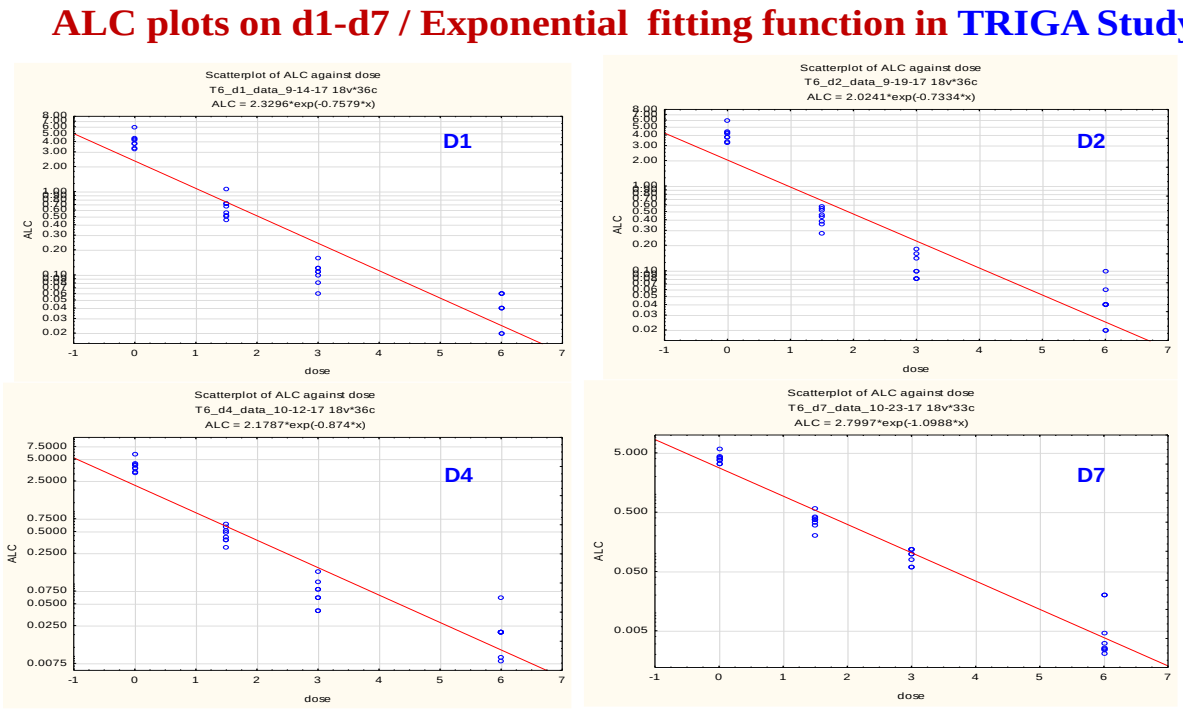

Fig. 11.1.2. ALC dose- and time-dependency plots on d1- d7 in TRIGA mixed-field study.

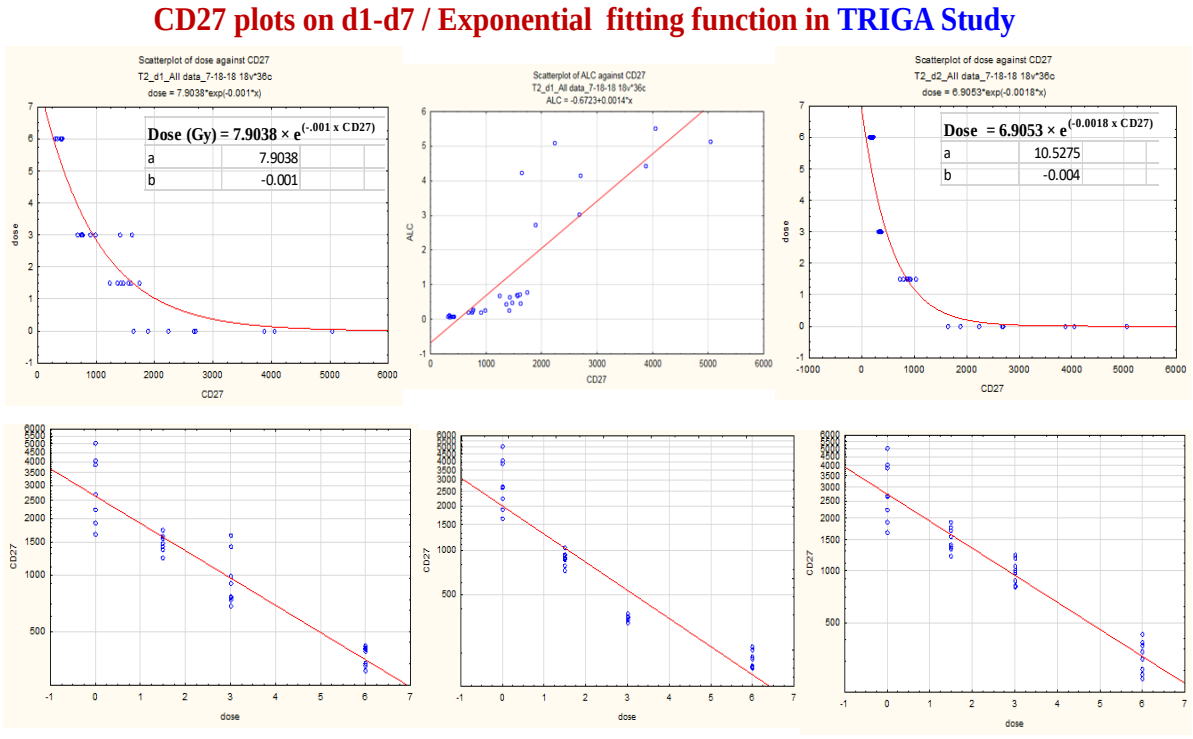

Fig. 11.1.3. CD27 dose- and time-dependency plots along with dose prediction equations and CD27 vs. ALC correlation on d1- d7 in TRIGA mixed-field study.

Linear Regression Analysis Results

Our results for dose prediction using ALC depletion calibration curves demonstrate that the given dose of 6 Gy was significantly underestimated as shown in Table 11.1.2 due to a high sensitivity of ALC that decrease and plateau at mixed-field doses >3 Gy. In the meantime, proteins show progressive dose-dependent changes, which indicates that these radiation responsive proteins have considerable potential as biodosimeters. Some examples for proteomic biodosimetry in mixed-field studies are shown in Figures and Tables below.

Observed or given dose is the nominal irradiation dose based on physical dosimetry in the experiments; predicted dose is a dose estimated in analysis; residual is difference between the predicted and given doses; standard error (SE) of predicted dose is accuracy for predicted dose at 95% confidence level (CL) and p values for the dose prediction. Outliers marked as (*) were defined by SAS software as values that fell out of 95% CL. Separate Tables also show the mean value and a range of predicted dose at 99.9% CL (i.e., 3 STDev or all animals). Tables show the residuals (the difference between given and predicted dose) and accuracy in dose prediction for the selected singe or a combination of biomarkers.

Tables and plots in Figs. 11.1.4 - 11.1.5 show results of linear regression analysis of dose assessment/prediction in each individual animal in this radiation model for total of 32 mice (n=8 per dose and time-point) using CD45/CD27 ratio alone.

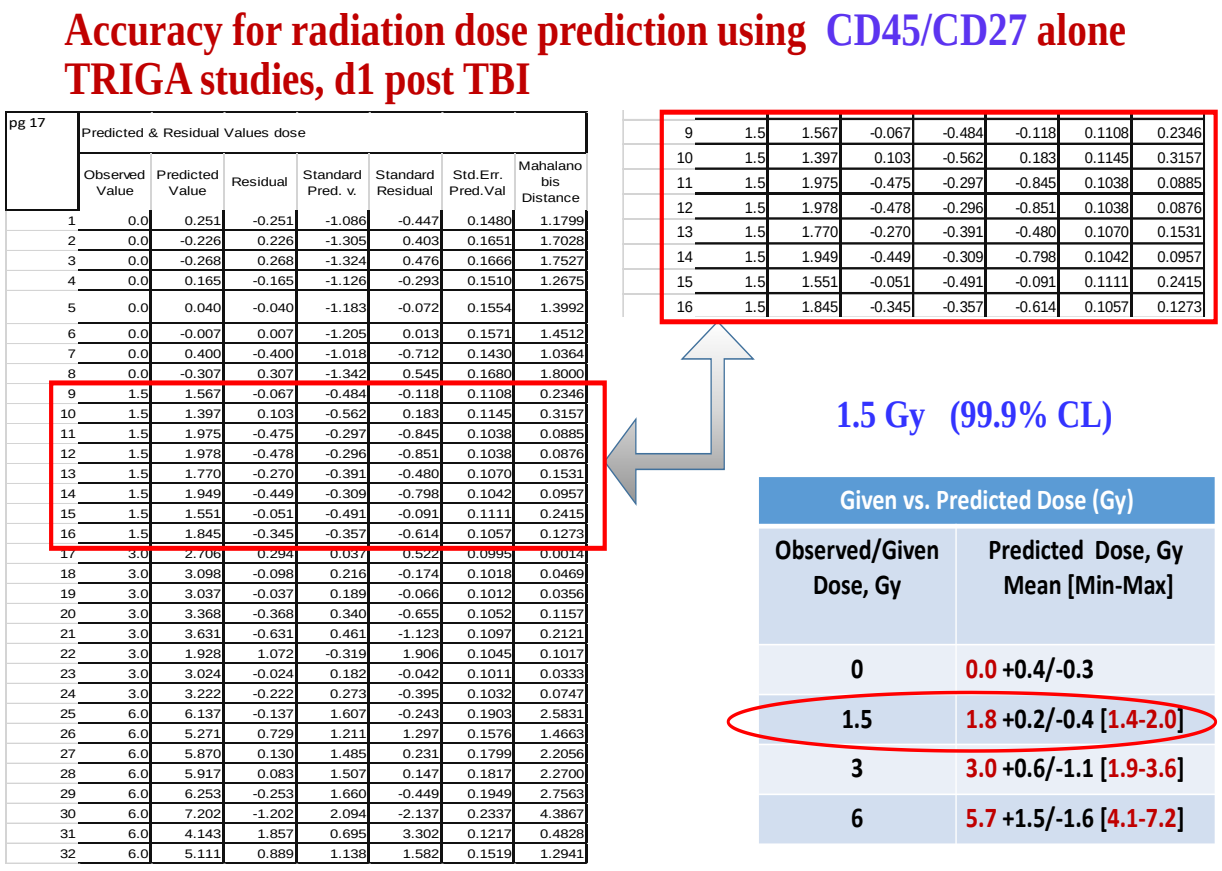

pg 17 — Predicted & Residual Values dose

	Observed Value	Predicted Value	Residual	Standard Pred. v.	Standard Residual	Std.Err. Pred.Val	Mahalanobis Distance
1	0.0	0.251	-0.251	-1.086	-0.447	0.1480	1.1799
2	0.0	-0.226	0.226	-1.305	0.403	0.1651	1.7028
3	0.0	-0.268	0.268	-1.324	0.476	0.1666	1.7527
4	0.0	0.165	-0.165	-1.126	-0.293	0.1510	1.2675
5	0.0	0.040	-0.040	-1.183	-0.072	0.1554	1.3992
6	0.0	-0.007	0.007	-1.205	0.013	0.1571	1.4512
7	0.0	0.400	-0.400	-1.018	-0.712	0.1430	1.0364
8	0.0	-0.307	0.307	-1.342	0.545	0.1680	1.8000
9	1.5	1.567	-0.067	-0.484	-0.118	0.1108	0.2346
10	1.5	1.397	0.103	-0.562	0.183	0.1145	0.3157
11	1.5	1.975	-0.475	-0.297	-0.845	0.1038	0.0885
12	1.5	1.978	-0.478	-0.296	-0.851	0.1038	0.0876
13	1.5	1.770	-0.270	-0.391	-0.480	0.1070	0.1531
14	1.5	1.949	-0.449	-0.309	-0.798	0.1042	0.0957
15	1.5	1.551	-0.051	-0.491	-0.091	0.1111	0.2415
16	1.5	1.845	-0.345	-0.357	-0.614	0.1057	0.1273
17	3.0	2.706	0.294	0.037	0.522	0.0995	0.0014
18	3.0	3.098	-0.098	0.216	-0.174	0.1018	0.0469
19	3.0	3.037	-0.037	0.189	-0.066	0.1012	0.0356
20	3.0	3.368	-0.368	0.340	-0.655	0.1052	0.1157
21	3.0	3.631	-0.631	0.461	-1.123	0.1097	0.2121
22	3.0	1.928	1.072	-0.319	1.906	0.1045	0.1017
23	3.0	3.024	-0.024	0.182	-0.042	0.1011	0.0333
24	3.0	3.222	-0.222	0.273	-0.395	0.1032	0.0747
25	6.0	6.137	-0.137	1.607	-0.243	0.1903	2.5831
26	6.0	5.271	0.729	1.211	1.297	0.1576	1.4663
27	6.0	5.870	0.130	1.485	0.231	0.1799	2.2056
28	6.0	5.917	0.083	1.507	0.147	0.1817	2.2700
29	6.0	6.253	-0.253	1.660	-0.449	0.1949	2.7563
30	6.0	7.202	-1.202	2.094	-2.137	0.2337	4.3867
31	6.0	4.143	1.857	0.695	3.302	0.1217	0.4828
32	6.0	5.111	0.889	1.138	1.582	0.1519	1.2941

Fig. 11.1.4. Accuracy for radiation dose prediction using CD45/CD27 ratio alone in TRIGA mixed-field studies on d1 post TBI.

Results for radiation dose prediction using CD45/CD27 alone TRIGA studies, 1 d post TBI

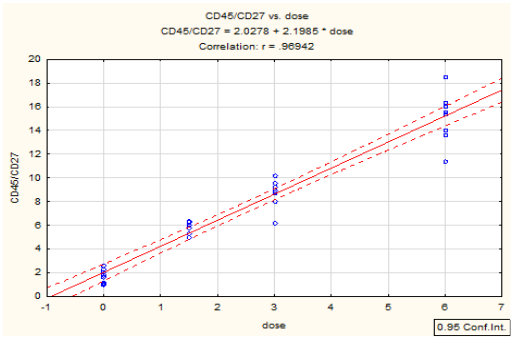

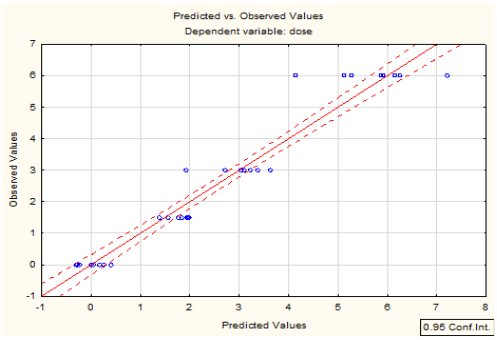

	Regression Summary for Dependent Variable: dose (T6_d1_data_9-14-17) R= .96942225 R²= .93977950 Adjusted R²= .93777215 F(1,30)=468.17 p					
N=32	b*	Std.Err. of b*	b	Std.Err. of b	t(30)	p-value
Intercept			-0.708709	0.183353	-3.86527	0.000552
CD45/CD27	0.969422	0.044803	0.427457	0.019756	21.63722	0.000000

	Variables currently in the Equation; DV: dose (T6_d1_data_9-14-17)						
Variable	b* in	Partial Cor.	Semipart Cor.	Tolerance	R-square	t(30)	p-value
CD45/CD27	0.969422	0.969422	0.969422	1.000000	-0.000000	21.63722	0.000000

Fig. 11.1.5. Linear regression analysis of dose prediction using CD45/CD27 ratio alone in TRIGA mixed-field studies. Left plot is CD45/CD27 vs. given dose; right plot is given vs. predicted dose.

Overall, the dose prediction accuracy is (98.6 ± 2.4) % and (98.1 ± 2.1) % in males and females, respectively (Table 11.1.1) using CD45/CD27 ratio alone. Dose prediction accuracy was significantly improved with increasing of number of biomarkers as shown in Figs. 11.1.6 - 11.1.9 and Tables 11.1.1 and 11.1.2 with no significant differences between male and female mice.

Accuracy for radiation dose prediction using CD45/CD27 + FLT3L + SAA

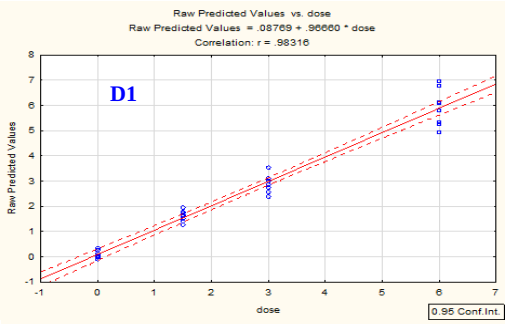

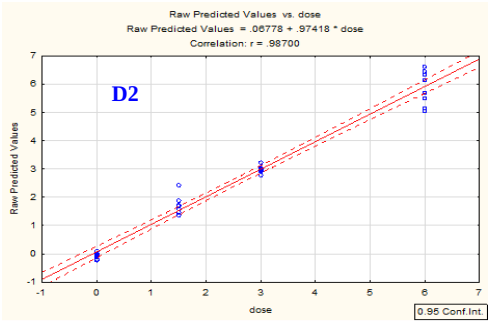

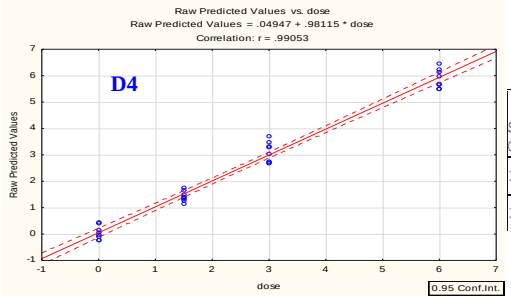

Outliers (D1)

	Standard Residual: dose (T6_d1_data_9-14-17) Outliers					
Standard Residuals Case -5. -4. -3. ±2. 3. 4. 5.	Observed Value	Predicted Value	Residual	Standard Pred. v.	Standard Residual	Std.Err. Pred.Val
30 . . . *| . . .	6.0	6.960	-0.960	1.956	-2.175	0.2658
31 . . . | * . . .	6.0	4.933	1.067	1.041	2.417	0.2519

Fig. 11.1.6. Linear regression analysis of dose prediction using a combination of three biomarkers: CD45/CD27 + FLT3L + SAA in TRIGA mixed-field studies. Plots represent predicted vs. given dose at 95% CL at different time-points. Table shows the calculated outliers on d1 post TBI.

CD45/CD27 + Flt3L + IL-18

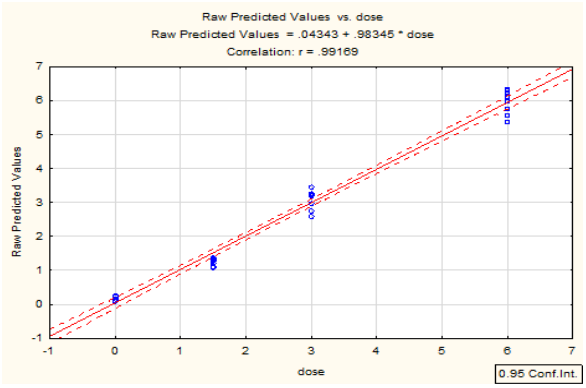

Regression Summary for Dependent Variable: dose (T6_d4_data_10-12-17) R= .99169269 R²= .98345440 Adjusted R²= .98168165 F(3,28)=554.76 p

N=32	b*	Std.Err. of b*	b	Std.Err. of b	t(28)	p-value
Intercept			-0.733914	0.112208	-6.54065	0.000000
CD45/CD27	0.443957	0.101004	0.161708	0.036790	4.39546	0.000144
FLT3L	0.183881	0.073567	0.000926	0.000370	2.49949	0.018572
IL-18	0.407103	0.055721	0.002801	0.000383	7.30617	0.000000

CD45/CD27 + Flt3L + IL-12

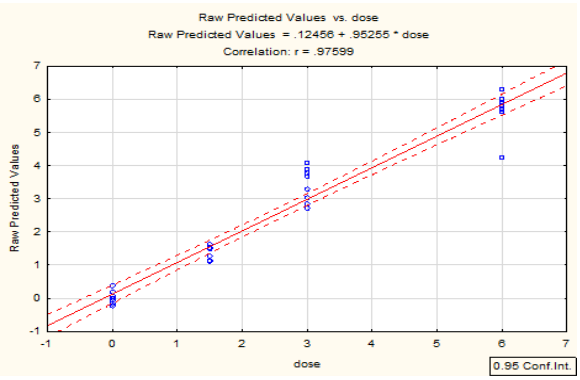

Regression Summary for Dependent Variable: dose (T6_d4_data_10-12-17) R= .97598599 R²= .95254865 Adjusted R²= .94746458 F(3,28)=187.36 p

N=32	b*	Std.Err. of b*	b	Std.Err. of b	t(28)	p-value
Intercept			-0.957590	0.620734	-1.54267	0.134138
CD45/CD27	0.997313	0.117632	0.363265	0.042847	8.47824	0.000000
FLT3L	0.015440	0.123781	0.000078	0.000623	0.12474	0.901621
IL-12	0.045025	0.073423	0.001662	0.002711	0.61323	0.544671

Fig. 11.1.7. Linear regression analysis of dose prediction using the combination of three biomarkers: CD45/CD27 + FLT3L + IL-18 and CD45/CD27+ FLT3L + IL-12 in TRIGA mixed-field studies. Plot represent predicted vs. given dose at 95% CL. Tables show multiple linear regression analysis summary results.

CD45/CD27 + Flt3L + IL-5

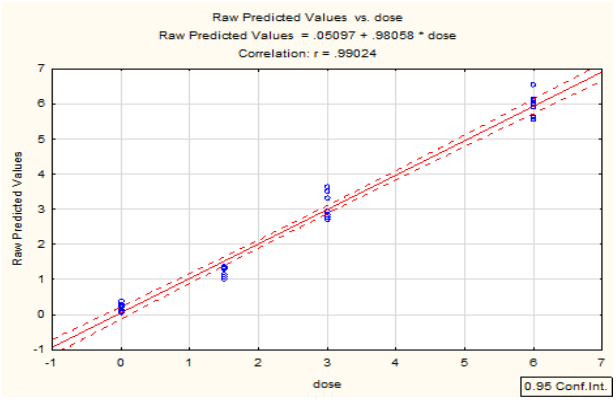

Regression Summary for Dependent Variable: dose (T6_d4_data_10-12-17) R= .99024444 R²= .98058406 Adjusted R²= .97850378 F(3,28)=471.37 p

N=32	b*	Std.Err. of b*	b	Std.Err. of b	t(28)	p-value
Intercept			-0.402053	0.123474	-3.25617	0.002953
CD45/CD27	0.552610	0.100277	0.201285	0.036525	5.51081	0.000007
FLT3L	0.133527	0.077599	0.000672	0.000391	1.72074	0.096333
IL-5	0.346710	0.053918	0.074009	0.011509	6.43034	0.000001

CD45/CD27 + Flt3L + G-CSF

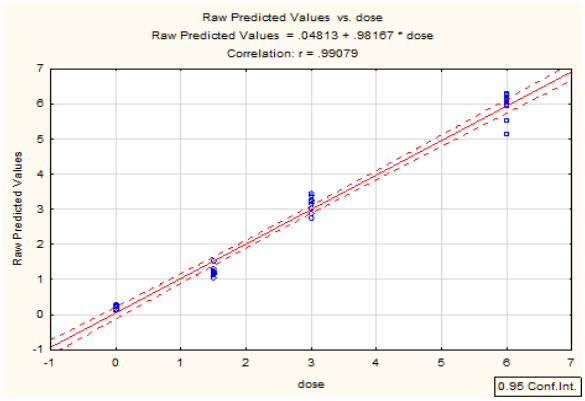

Regression Summary for Dependent Variable: dose (T6_d4_data_10-12-17) R= .99079054 R²= .98166590 Adjusted R²= .97970154 F(3,28)=499.74 p

N=32	b*	Std.Err. of b*	b	Std.Err. of b	t(28)	p-value
Intercept			-0.398294	0.119991	-3.31938	0.002513
CD45/CD27	0.380457	0.115212	0.138579	0.041965	3.30223	0.002625
FLT3L	0.278299	0.083964	0.001401	0.000423	3.31453	0.002544
G-CSF	0.390470	0.057924	0.002260	0.000335	6.74103	0.000000

Fig. 11.1.8. Linear regression analysis of dose prediction using the combination of three biomarkers: CD45/CD27 + FLT3L + IL-5 and CD45/CD27+ FLT3L + G-CSF in TRIGA mixed-field studies. Plot represent predicted vs. given dose at 95% CL. Tables show multiple linear regression analysis summary results.

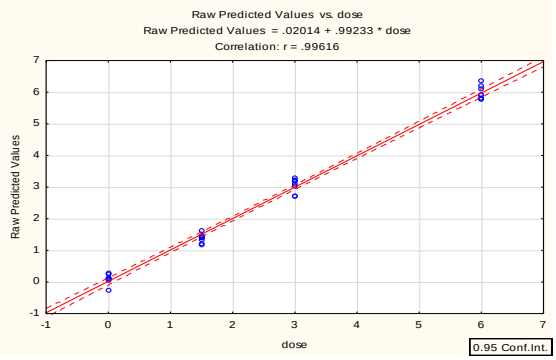

Dose Prediction at 99% CL	
Observed/Given Dose, Gy	**Predicted Dose, Gy Mean [Min-Max]**
0	**-0.1 +0.0/-0.1**
1.5	**1.5 +0.2/-0.3 [1.2-1.8]**
3	**3.0 +0.2/-0.4 [2.8-3.2]**
6	**5.9 +0.4/-0.2 [5.7-6.3]**

	Regression Summary for Dependent Variable: dose (T6_d4_data_10-12-17) R= .99615703 R²= .99232883 Adjusted R²= .99048775 F(6,25)=538.99 p					
N=32	b*	Std.Err. of b*	b	Std.Err. of b	t(25)	p-value
Intercept			0.777153	0.316158	2.45811	0.021244
CD45/CD27	0.210091	0.088437	0.076524	0.032213	2.37560	0.025500
FLT3L	0.179914	0.060099	0.000906	0.000303	2.99360	0.006132
G-CSF	0.136976	0.076668	0.000793	0.000444	1.78660	0.086137
IL-18	0.223665	0.079984	0.001539	0.000550	2.79638	0.009792
IL-12	-0.158723	0.036234	-0.005860	0.001338	-4.38045	0.000186
IL-5	0.180127	0.065822	0.038450	0.014050	2.73658	0.011260

Fig. 11.1.9. Linear regression analysis of dose prediction using the best combination of six biomarkers: CD45/CD27+ FLT3L + G-CSF + IL-18 + IL-12 +IL-5 in TRIGA mixed-field studies. Plot represent predicted vs. given dose at any time-point. Upper Table shows the given vs. predicted dose at 99.9% CL. Lower Table represent multiple linear regression analysis summary results.

The radiation dose predicted comparison analysis was performed for individual and combined biomarkers (Table 11.1.1) collected in groups after exposure with either (67% n + 33% γ) or (30% n + 70% γ). Selected results are shown in Figs. 11.1.10 – 11.1.12. For ALC-based biodosimetry, no significant difference at 95% CL was observed between T6 and T2 for all radiation doses. Mean coefficients ***a*** and ***b*** ratios of T6 to T2 are 0.871 and 1.095, respectively meaning that the same dose prediction equations might be used regardless of percentage of neutrons and gammas. However, on all days, 6-Gy doses were underestimated in T6 and T2 ranging from (4.33 ± 0.12) Gy to (4.74 ± 0.11) Gy on d1 and d7, respectively (Fig. 11.1.10, left panel). As described above, ALC results were also not significant different in gender (males vs. females) and dose-rate (0.6 vs. 1.9 Gy/min) comparison studies. Those findings indicate that lymphocyte depletion kinetics might be used in biodosimetry to estimate the radiation dose received regardless of mixed-field exposure conditions.

While ALC-based biodosimetry was not different on any day post exposure, FLT3L-based biosimetry showed no significant differences in dose prediction on days 1, 2 and 4; however, on day 7 in T6 and T2 experiments, the given doses 1.5 and 3 Gy were underestimated due to the fact of the bone marrow hematopoietic system faster recovery in mice irradiated to those sub-lethal doses. However, there is no significant difference in dose prediction was observed in groups irradiated to the lethal (6 Gy) dose (Figs. 11.1.10 - 11.1.11, middle panel).

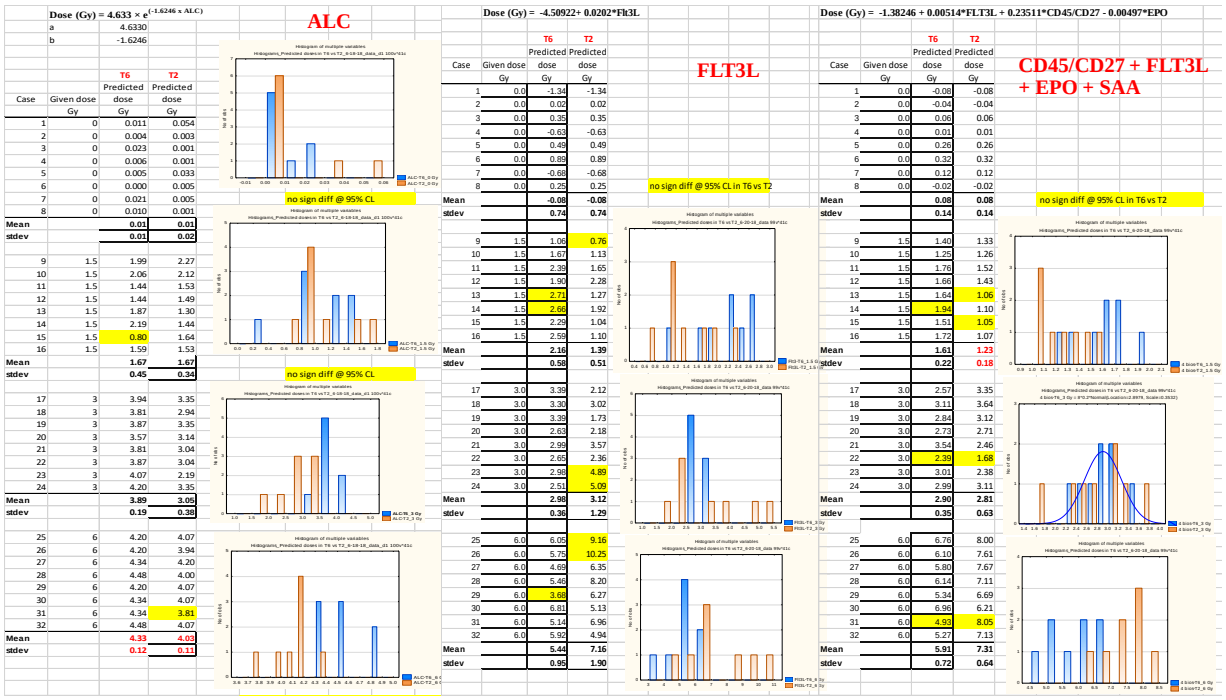

Fig. 11.1.10. The radiation dose predicted comparison analysis in groups after exposure with either (67% n + 33% γ) (T6 experiment) or (30% n + 70% γ) (T2 experiment) on day 1 using ALC (left panel), FLT3L (middle panel) and CD45/CD27 + FLT3L + EPO + SAA (right panel).

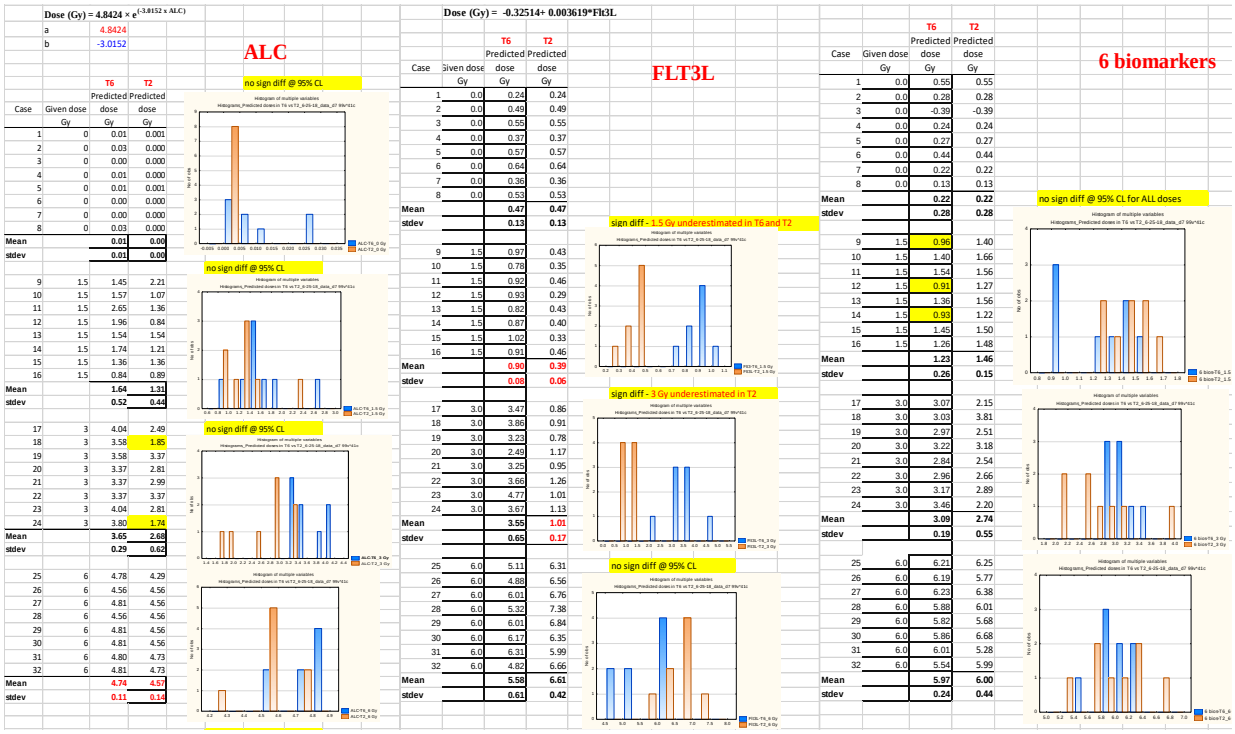

Fig. 11.1.11. The radiation dose predicted comparison analysis in groups after exposure with either (67% n + 33% γ) (T6 experiment) or (30% n + 70% γ) (T2 experiment) on day 7 using ALC (left panel), FLT3L (middle panel) and 6 biomarkers (right panel).

Histogram plots in Fig. 11.1.12 show the dose prediction accuracy/distribution and discrimination of study groups at 95% CL on day 1 after exposure with either (67% n + 33% γ) or (30% n + 70% γ) for six protein biomarkers analyzed together. Due to significant differences observed in levels of G-CSF, SAA and IL-18 in mice irradiated with 67% n vs. 30% n (Ossetrova et. al. 2018), all predicted doses in T2 (30% n, orange plots) using the equations shown in Table 11.1.2 are ~2-fold higher than in T6 (67% n, blue plots) reflecting the 2-fold difference in percentage of neutrons. However, in both experiments this combination of 6 biomarkers shows the perfect separation of all animal dose-groups and very good dose prediction accuracy (Table 11.1.1).

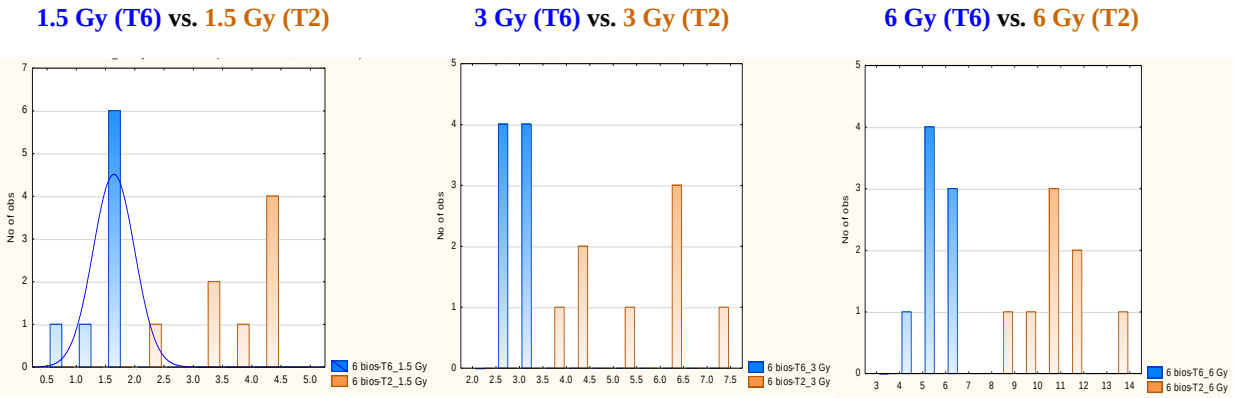

Fig. 11.1.12. Multi-parameter biodosimetry discriminant analysis summary results in mixed-field studies after exposure with either (67% n + 33% γ) or (30% n + 70% γ). Blue plots represent the distribution of predicted radiation doses on day 1 in T6 experiment (67% n + 33% γ); orange plots represent the distribution of predicted radiation doses in T2 experiment (30% n + 70% γ) that were estimated using biodosimetry equations shown in Table 11.1.1.

Receiver Operation Characteristic (ROC) and Discriminant Analyses Results

Receiver operating characteristic (or ROC) analysis of single biomarker and combination of biomarkers was performed using ROCCET on-line tool (Xia et al. 2013). Individual markers were analyzed using classical ROC and multiple markers with partial least squares – discriminant analysis approach. The area under the curve (AUC) with 95% confidence intervals was used to demonstrate the sensitivity and specificity of the proposed protein biomarkers to reflect subgroup (dose and sampling time-point) differences as well as to analyze the results from survival study to predict the ARS outcome. Results are shown as a ROC plot of the true positive rate against the false positive rate for the different possible cut-points of a diagnostic test. ROC and discriminant analyses (using a PC SAS software) were performed for the same biomarkers and time points as was done in multiple regression analysis described above.

Figures 11.1.13 - 11.1.15 show some ROC analysis results into tertiles of mixed-field doses 0-1.5 Gy, 1.5-3 Gy, and 3-6 Gy using selected hematological (ALC and ANC to ALC ratio) and protein FLT3L, SAA, and CD45 to CD27 ratio) biomarkers from biological samples. Red line on whisker plot indicates cutoff value, which corresponds to red dots on ROC plots. ROC table displayed in rank order by AUC, which indicates quality of discrimination by ROC (1= perfect). Multi-parameter (i.e., linear regression, discriminant and ROC) biodosimetry analyses summary results in mixed-field studies are shown in Fig. 11.1.16.

TRIGA Mixed-field

0-1.5 Gy

Biomarker	AUC	Cutoff Value
ALC (10^3/ul)	1	2.17
ANC/ALC	1	0.203
FLt3-L (pg/ml)	1	272
CD45/CD27	1	3.76
SAA (ng/ml)	0.890625	952 or 1180

Raw Data (for reference):

Case #	Dose	ALC (10^3/ul)	ANC/ALC	FLt3-L (pg/ml)	SAA (ng/ml)	CD45/CD27
1	0	3.7	0.13	156.9	1256.9	2.2
2	0	4.4	0.08	224.1	514.5	1.1
3	0	3.3	0.13	240.6	722.1	1.0
4	0	4.1	0.09	192.1	885.7	2.0
5	0	4.3	0.07	247.4	687.3	1.8
6	0	5.9	0.06	267.4	565.5	1.6
7	0	3.3	0.08	189.8	1130.1	2.6
8	0	3.8	0.12	235.5	573.4	0.9
9	1.5	0.5	0.54	275.9	4645.4	5.3
10	1.5	0.5	0.48	306.0	1674.0	4.9
11	1.5	0.7	0.36	341.7	1664.3	6.3
12	1.5	0.7	0.28	317.4	1017.5	6.3
13	1.5	0.6	0.43	357.6	691.5	5.8
14	1.5	0.5	0.83	355.2	3555.3	6.2
15	1.5	1.1	0.35	336.8	1577.7	5.3
16	1.5	0.7	0.42	351.6	1226.7	6.0

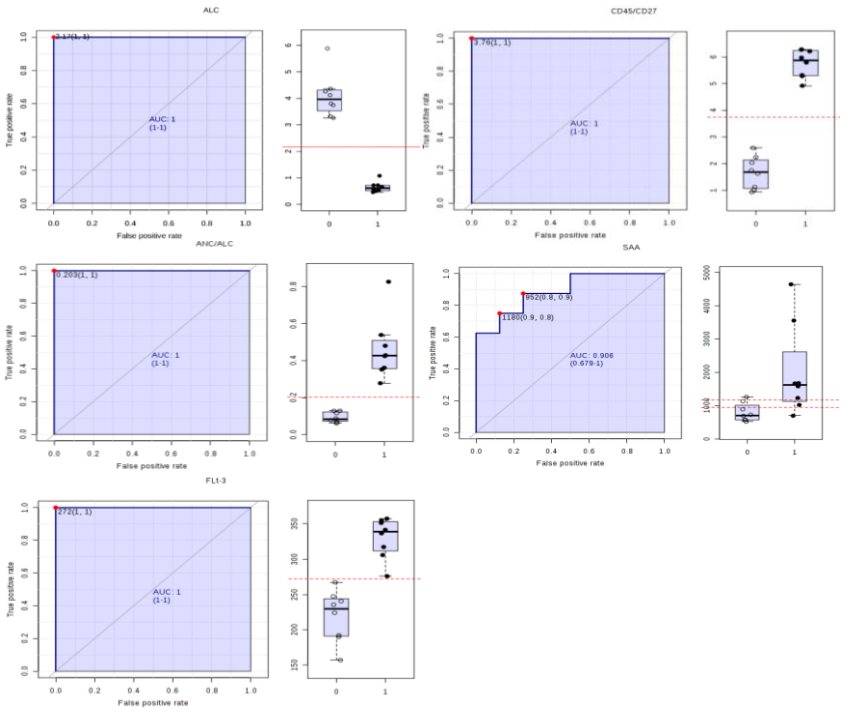

Fig. 11.1.13. ROC analysis results to separate sham (0 Gy) and 1.5-Gy groups in mixed-field studies. Four of five biomarkers surveyed had perfect separation, therefore, multi-parameter ROC analysis was considered unnecessary.

TRIGA Mixed-field

1.5 -3.0 Gy

Biomarker	AUC	Cutoff value
ALC (10^3/ul)	1.0	0.31
ANC/ALC	1.0	1.23
SAA (ng/ml)	1.0	5040
CD45/CD27	1.0	7.14
FLt3-L (pg/ml)	0.9	353

Raw Data (for reference):

Case #	Dose	ALC (10^3/ul)	ANC/ALC	FLt3-L (pg/ml)	SAA (ng/ml)	CD45/CD27
9	1.5	0.5	0.54	275.9	4645.4	5.3
10	1.5	0.5	0.48	306.0	1674.0	4.9
11	1.5	0.7	0.36	341.7	1664.3	6.3
12	1.5	0.7	0.28	317.4	1017.5	6.3
13	1.5	0.6	0.43	357.6	691.5	5.8
14	1.5	0.5	0.83	355.2	3555.3	6.2
15	1.5	1.1	0.35	336.8	1577.7	5.3
16	1.5	0.7	0.42	351.6	1226.7	6.0
17	3	0.1	3.20	391.3	7289.3	8.0
18	3	0.1	2.50	386.8	10256.7	8.9
19	3	0.1	2.46	391.2	5623.4	8.8
20	3	0.2	1.63	353.7	5430.1	9.5
21	3	0.1	1.67	371.2	12624.3	10.2
22	3	0.1	2.46	354.6	10001.4	6.2
23	3	0.1	2.75	370.9	9854.3	8.7
24	3	0.1	3.00	347.7	10570.7	9.2

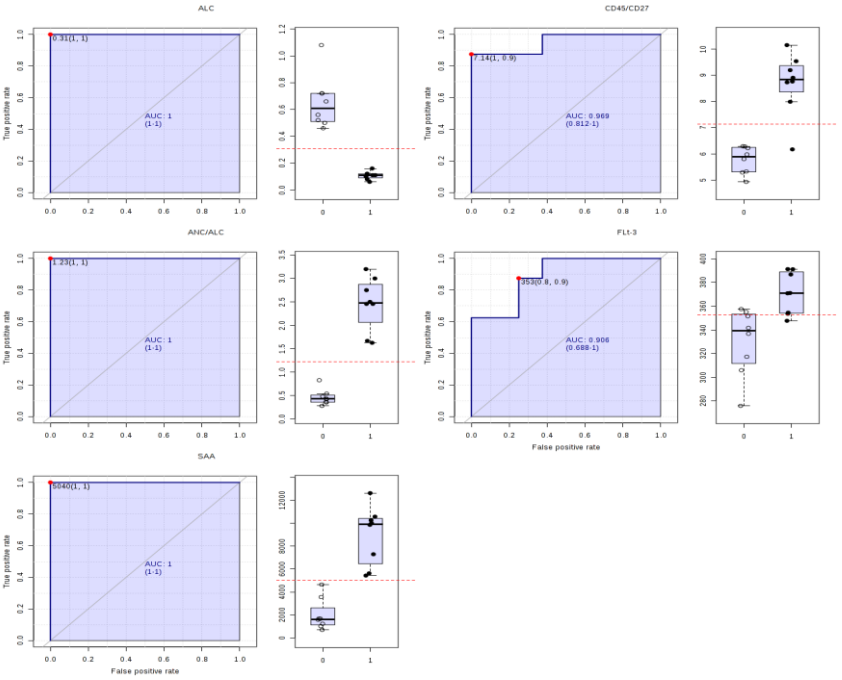

Fig. 11.1.14. ROC analysis results to separate 1.5- and 3-Gy groups in mixed-field studies. Full discrimination with 4 of 5 biomarkers.

TRIGA Mixed-field

3 - 6 Gy

Biomarker	AUC	Cutoff value
ANC/ALC	1.0	3.43
FLt3-L (pg/ml)	1.0	398
SAA (ng/ml)	1.0	14600
CD45/CD27	1.0	10.8
ALC (10^3/ul)	1.0	0.07

Raw Data (for reference):

Case #	Dose	ALC (10^3/ul)	ANC/ALC	FLt3-L (pg/ml)	SAA (ng/ml)	CD45/CD27
17	3	0.1	3.20	391.3	7289.3	8.0
18	3	0.1	2.50	386.8	10256.7	8.9
19	3	0.1	2.46	391.2	5623.4	8.8
20	3	0.2	1.63	353.7	5430.1	9.5
21	3	0.1	1.67	371.2	12624.3	10.2
22	3	0.1	2.46	354.6	10001.4	6.2
23	3	0.1	2.75	370.9	9854.3	8.7
24	3	0.1	3.00	347.7	10570.7	9.2
25	6	0.1	3.67	523.0	32582.7	16.0
26	6	0.1	4.00	508.0	30322.5	14.0
27	6	0.0	6.50	455.7	24900.9	15.4
28	6	0.0	13.00	493.4	26607.4	15.5
29	6	0.1	5.33	405.5	16534.7	16.3
30	6	0.0	6.50	560.6	20924.7	18.5
31	6	0.0	6.00	477.8	20782.2	11.4
32	6	0.0	7.00	516.5	16687.7	13.6

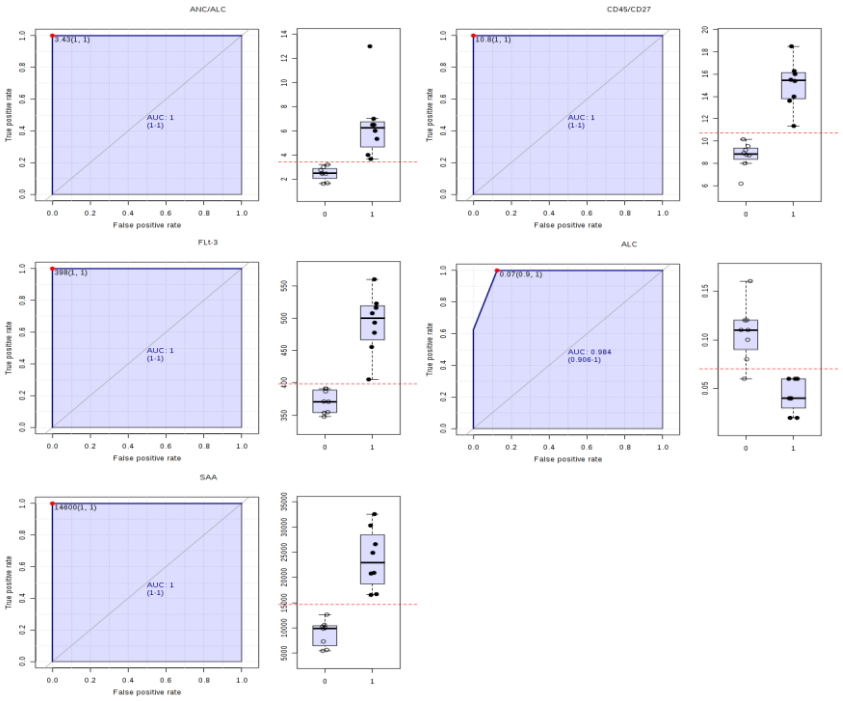

Fig. 11.1.15. ROC analysis results to separate 3- and 6-Gy groups in mixed-field studies. Full discrimination with 5 of 5 biomarkers.

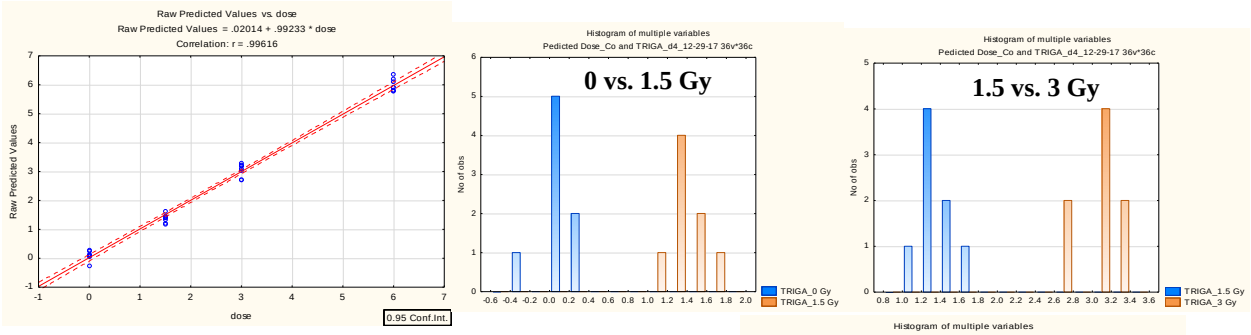

ROC Analysis Classification Performance in TRIGA Studies			
Classification Criteria	**0 vs. 1.5 Gy**	**1.5 vs. 3 Gy**	**3 vs. 6 Gy**
True Positive Fraction	**100%**	**100%**	**100%**
True Negative Fraction	**100%**	**100%**	**100%**
Prediction Accuracy (%)	**100%**	**100%**	**100%**
Area Under Curve (AUC)	**1.000**	**1.000**	**1.000**

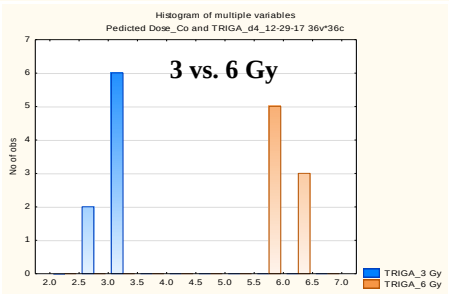

Fig. 11.1.16. Multi-parameter biodosimetry analyses summary results in mixed-field studies. Linear regression analysis (upper left plot), discriminant analysis (histograms of predicted vs. given radiation doses to separate study animal groups) and ROC analysis (Table) for the best combination of protein biomarkers: CD45/CD27+ FLT3L + G-CSF + IL-18 + IL-12 +IL-5.

Acute radiation sickness is characterized by time- and dose-dependent expression of various sub-syndromes of organ-specific systems (i.e., hematopoietic, gastrointestinal, and neurovascular). In the case of humans, Medical Treatment Protocols for Radiation Accident Victims (METREPOL) is the consensus system used to grade the severity of radiation injury (Fliedner et al. 2001). METREPOL incorporates clinical symptoms/signs and blood tests as prognostic indicators of ARS to assess post-exposure organ-specific systems damage. The initial response category (RC) concept was based on CBC, symptoms and signs (Fliedtner et al. 2001) and was extended later by including the multi-organ involvement/failure (MOI/MOF) concept and new biomarkers that can provide information about the severity of radiation-induced damage to specific physiological systems (Fliedner et al. 2005). However, a gap I still existed in evaluating the other bioindicators of radiation-induced tissue- and organ-damage.

A mouse mixed-field TBI model has been developed to create a METREPOL-like ARS severity score system that represents the likely scenario of exposure in the human population. In this study, we have expanded to the mixed-field exposure conditions the established earlier a murine multiple-parameter ARS severity score system after the gamma-exposure, modeled after the METREPOL, to permit quantification of radiation injury in hematopoietic and gastrointestinal syndromes of the ARS and also established some criteria for ARS prognosis and outcome (Ossetrova et al. 2016). This system was created under irradiation-dose controlled conditions and animal recovery prognosis includes: (1) clinical symptoms and signs; (2) peripheral blood cells (CBC/diff) and (3) a radiation-responsive proteomics profile.

Hematological biomarkers of radiation exposure are well characterized and used in medical management of radiological casualties for the radiation dose and ARS severity assessment (Guskova et al. 1988, Fliedner et al. 2001, 2005; Dainiak et al. 2003, Goans et al. 1997). However, since the accurate radiation exposure dose estimation by lymphocyte depletion kinetics or counting chromosome aberrations becomes problematic after high doses (LD50 or higher), there is a need for other biodosimetry methods as predictive biomarkers of ARS outcome.

In our gamma-ray studies performed earlier, it was demonstrated that selected hematological and protein biomarkers established very successful separation of mouse groups irradiated to different doses. Dynamic changes in the levels of SAA, IL-6, G-CSF, and Flt3L reflect the time course of ARS severity and may function as prognostic indicators of ARS outcome. It was also pointed out that the table with evaluated protein biomarkers might be extended as new biomarkers are discovered (Ossetrova et al. 2014; Ossetrova et al. 2016).

In our current study, a proof-of-concept has been demonstrated that the addition of several protein biomarkers might benefit in distinguishing the RCs (Fig. 11.1.16). According to discriminant analysis results, blood cell counts were able to distinguish between RCs 0, 1 and 2 at every time point studied in the week after exposure, but were not ideal for discrimination between RC2 and RC3 (Table in Fig. 11.1.16). This pattern is consistent with previous findings that the value of blood cell count in radiation victims decreases at LD50 doses (Dainiak et al. 2003, Goans et al. 1997; Baranov et al. 1995). Addition of circulating proteins to discriminant analysis on the basis of their specific time course of response allowed for complete (100%) discrimination between each RC at every time point studied (days 1, 2, 4 and 7 post irradiation) (Fig. 11.1.16).

ARS Severity Response Categories (RC) in TRIGA Mixed-field (67%n + 33%γ) Studies

Group	Sham	0-2 Gy	2-6 Gy	≥6 Gy
Parameter	Normal Degree 0 (RC0)	Mild Degree 1 (RC1)	Moderate Degree 2 (RC2)	Severe Degree 3 (RC3)

Discrimination power, %

Day Post-TBI	RCs compared	1	2	3	4	5	6
		Biomarker combinations					
		ALC	ANC	PLT	ALC+ ANC	ALC+ANC+PLT	CD45/CD27+ FLT3L + EPO + SAA
Day 1	RC0-RC1	100	75	75	100*	100*	100
	RC1-RC2	100	50	50	100*	100*	100
	RC2-RC3	88	50	50	88*	88*	100
							CD45/CD27 + FLT3L + SAA
Day 2	RC0-RC1	100	50	85	100*	100*	100
	RC1-RC2	100	50	50	100*	100*	100
	RC2-RC3	88	88	63	88	88	100
							CD45/CD27 + FLT3L + IL18 + IL12 + IL5 + GCSF
Day 4	RC0-RC1	100	100	50	100	100	100
	RC1-RC2	100	100	75	100	100*	100
	RC2-RC3	75	88	50	88	88	100
							CD45/CD27 + FLT3L + IL18 + IL12 + IL5 + GCSF
Day 7	RC0-RC1	100	75	100	100	100	100
	RC1-RC2	88	88	100	88*	100	100
	RC2-RC3	100	75	100	100	100	100

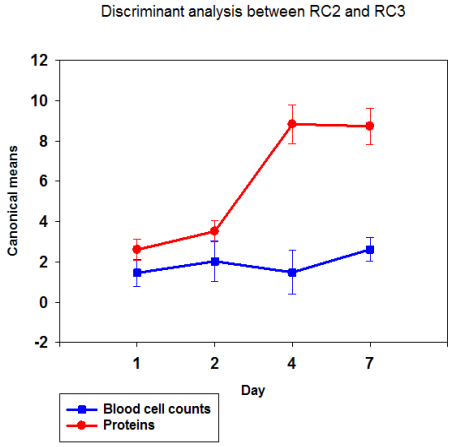

* **Separation due to ALC.**

Grey shading indicates marker not included in multivariate models which contained superior discriminators

Ossetrova et al. 2018

Fig. 11.1.16. Discriminant analysis results based on CBC/diff and proteomics profile to separate RCs at every time point studied in the week after exposure.

By using multiplexing technology, in combination with available, on-site knowledge of exposure incidents, emergency responders should be able to attain vital information to triage a mass casualty event. Results also demonstrate that proteomics shows promise as a complementary approach not only to conventional biodosimetry for early assessment of radiation exposure but also as an enhancement of accuracy and discrimination index in the ARS response categories and early prediction of ARS outcome. These research findings, along with their evaluation in a nonhuman primate radiation model (Ossetrova et al. 2016), will contribute to bridging gaps that exist in the current capabilities to rapidly and effectively identify and assess radiation exposure early after a radiation event, especially after a mass-casualty radiological incident, and the monitoring of patients with ARS.

11.2. ^{60}Co PURE GAMMA RAYS STUDY BIODOSIMETRY DATA ANALYSIS

In ^{60}Co γ-ray studies, the same biodosimetry performance matrix (Table 11.1.1) was used to create the radiation dose prediction algorithm. For biomarker combinations, multiple linear regression analysis was used to develop biodosimetry dose-response relationships in male mice (C6 experiment) and applied in female mice (C1 + C3 and C4 experiments) for comparison. Results demonstrate that (1) no significant differences in dose prediction in males vs. females, (2) so significant differences were observed in dose-rate studies (0.6 vs. 1.9 Gy/min) for radiation dose prediction and (3) accuracy in radiation dose prediction progressively increases with the increasing of number of biomarkers as reported in other animal studies (Ossetrova et al. 2007 – 2016). Selected multi-parameter algorithm equations for predicted vs. given radiation doses in samples collected 1d -7d post TBI in male B6D2F1 mice irradiated with ^{60}Co γ-rays at 0.6 Gy/min are shown in Table 11.2.1.

Table 11.2.1. Selected multi-parameter algorithm equations for predicted vs. given radiation doses in samples collected 1d -7d post TBI in male B6D2F1 mice irradiated with ^{60}Co γ-rays at 0.6 Gy/min.

Multiparameter algorithm equations for TBI predicted vs. given radiation doses in samples collected at 1d-7d post TBI in B6D2F1 male mice irradiated with ^{60}Co γ–rays at 0.6 Gy/min				
Biomarker combination / Collection time (days)	TBI predicted dose for given dose, Mean±STD, Gy			
	Given Dose, Gy			
	0	3	6	12
Day 1				
Dose (Gy) = 17.343 × $e^{(-9.033 \times ALC)}$	0.00 ± 0.00	3.87 ± 1.11	6.66 ± 1.83	9.29 ± 2.37
Dose (Gy) = -3.521 (±1.904) - 0.0002 (±0.001) × CD27 + 0.022 (±0.003) × FLT3L	-0.24 ± 0.28	4.50 ± 1.59	6.45 ± 2.03	10.29 ± 1.51
Dose (Gy) = -3.773 (±0.815) + 0.023 (±0.001) × FLT3L	-0.19 ± 0.29	4.45 ± 1.62	6.42 ± 2.07	10.32 ± 1.54
Dose (Gy) = -1.143 (±0.4070) + 0.3353 (±0.0178) × CD45/CD27	-0.24 ± 0.09	3.89 ± 0.63	6.17 ± 0.82	11.18 ± 2.04
Dose (Gy) = -1.922 (±2.050) + 0.001 (±0.003) × FLT3L - 0.665 (±0.511) × IL-5 + 0.008 (±0.006) × IL-12 + 0.012 (±0.020) × G-CSF + 0.315 (±0.056) x CD45/CD27 - 0.009 (±0.009) × IL-18	-0.55 ± 0.28	3.97 ± 0.48	6.45 ± 0.96	11.13 ± 1.34
Day 2				
Dose (Gy) = 10.495 × $e^{(-4.765 \times ALC)}$	0.00 ± 0.00	3.80 ± 1.43	6.80 ± 1.64	9.17 ± 0.43
Dose (Gy) = -7.009 (±1.369) + 0.003 (±0.001) × CD27 + 0.017 (±0.001) × FLT3L	-0.15 ± 0.69	3.20 ± 1.02	7.12 ± 1.51	10.82 ± 0.93
Dose (Gy) = -2.311 (±0.599) + 0.012 (±0.001) × FLT3L	-0.90 ± 0.15	4.38 ± 0.71	7.40 ± 1.04	10.13 ± 0.66
Dose (Gy) = -0.687 (±0.265) + 0.227 (±0.008) × CD45/CD27	-0.11 ± 0.07	3.3 1± 0.66	6.24 ± 0.51	11.56 ± 1.51
Dose (Gy) = -1.003 (±0.37) + 0.002 (±0.001)×FLT3L+ 0.199 (±0.025)×CD45/CD27 - 0.0001 (±0.0002)×SAA	-0.31 ± 0.07	3.45 ± 0.64	6.41 ± 0.47	11.45 ± 1.29
Dose (Gy) = -2.198 (±0.917) + 0.001 (±0.001) × FLT3L + 0.508 (±0.134) × IL-5 + 0.002 (±0.002) × IL-12 - 0.007 (±0.003) × G-CSF + 0.172 (±0.016) × CD45/CD27 + 0.004 (±0.003) × IL-18	0.01 ± 0.34	2.92 ± 0.41	6.25 ± 0.34	11.82 ± 0.71
Day 4				
Dose (Gy) = 9.284 × $e^{(-4.061 \times ALC)}$	0.00 ± 0.00	3.49 ± 1.22	7.90 ± 0.34	8.27 ± 0.33
Dose (Gy) = 0.319 (±1.516) - 0.001 (±0.001) × CD27 + 0.006 (±0.001) × FLT3L	-0.21 ± 0.14	3.23 ± 0.31	8.73 ± 0.42	9.24 ± 0.82
Dose (Gy) = -0.730 (±0.669) + 0.007 (±0.001) × FLT3L	0.11 ± 0.09	2.80 ± 0.33	8.81 ± 0.47	9.28 ± 0.91
Dose (Gy) = -1.002 (±0.376) + 0.471 (±0.023) × CD45/CD27	0.20 ± 0.14	3.43 ±0.35	5.86 ± 0.94	11.51 ± 2.15
Dose (Gy) = -1.396 (±0.167) + 0.116 (±0.032) × CD45/CD27 + 0.002 (±0.0003) × FLT3L + 0.008 (±0.001) × IL-18	0.18 ± 0.20	2.78 ± 0.42	6.12 ± 0.36	11.92 ± 0.77
Dose (Gy) = 1.456 (±0.456) + 0.001 (±0.0003) × FLT3L + 0.076 (±0.031) × IL-5 -0.007 (±0.001) × IL-12 + 0.001 (±0.001) × G-CSF + 0.040 (±0.026) × CD45/CD27 + 0.004 (±0.001) × IL-18	0.04 ± 0.22	3.03 ± 0.17	5.98 ± 0.23	11.97 ± 0.49
Day 7				
Dose (Gy) = 8.947 × $e^{(-2.65 \times ALC)}$	0.08 ± 0.13	3.24 ± 0.88	7.84 ± 0.39	8.81 ± 0.06
Dose (Gy) = 6.842 (±1.429) – 0.004 (±0.001) × CD27 + 0.002 (±0.001) × FLT3L	-0.32 ± 0.87	2.95 ± 0.30	7.84 ± 0.55	10.53 ± 0.30
Dose (Gy) = 0.311 (±0.494) + 0.005 (±0.001) × FLT3L	1.00 ± 0.08	1.64 ± 0.05	8.03 ± 1.36	10.33 ± 0.81
Dose (Gy) = -0.694 (±0.509) + 0.641 (±0.053) × CD45/CD27	2.34 ± 0.20	2.64 ± 0.44	4.15 ± 0.35	11.88 ± 2.23
Dose (Gy) = -1.79 (±0.39) + 0.099 (±0.06) × CD45/CD27+ 0.002 (±0.0004) × FLT3L + 0.019 (±0.004)× IL-18	0.88 ± 0.41	2.13 ± 0.30	5.93 ± 0.52	12.06 ± 0.57
Dose (Gy) = 0.027 (±0.228) + 0.001 (±0.0002) × FLT3L + 0.142 (±0.055) × IL-5 - 0.0066 (±0.0006) × IL-12 + 0.0001 (±0.0001) × G-CSF + 0.1697 (±0.030) × CD45/CD27 + 0.012 (±0.002) × IL-18	0.02 ± 0.20	2.94 ± 0.18	6.10 ± 0.40	11.94 ± 0.32

ALC and CD27 depletion kinetics analysis for the radiation dose prediction was performed using a mathematical algorithm (e.g., exponential fitting function) similar to that established and reported in Chernobyl accident victims (Fig. 11.1.1; Baranov et al. 1995; Guskova et al, 1988). Figs. 11.2.1 and 11.2.2 show ALC and CD27 dose- and time-dependency plots on d1-d7 in ^{60}Co γ-rays study, respectively. Dose prediction equations are shown in Table 11.2.1.

ALC plots on d1-d7 / Exponential fitting function in ^{60}Co Study

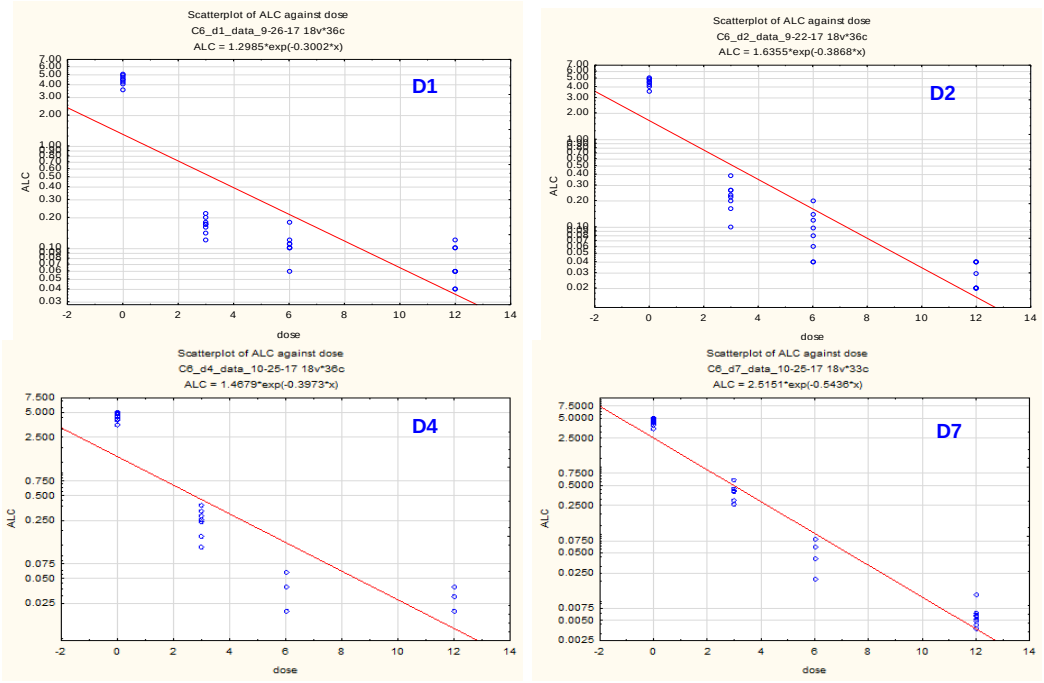

Fig. 11.2.1. ALC dose- and time-dependency plots on d1-d7 in ^{60}Co γ-ray study.

CD27 plots on d1-d7 / Exponential fitting function in Cobalt Study

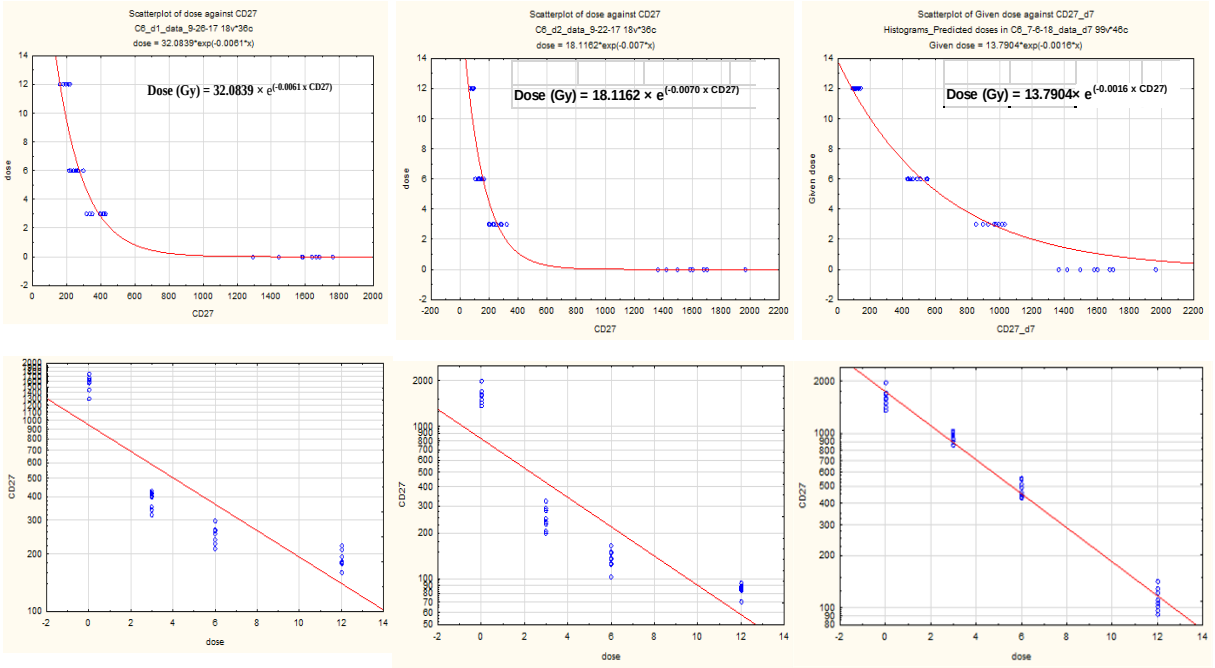

Fig. 11.2.2. CD27 dose- and time-dependency plots along with dose prediction equations on d1-d7 in ^{60}Co γ-ray study.

Linear Regression Analysis Results

Our results for dose prediction using ALC depletion calibration curves demonstrate that the given dose of 12 Gy was significantly underestimated as shown in Table 11.2.1 due to a high sensitivity of ALC that decrease and plateau at γ-rays doses >6 Gy. In the meantime, proteins show progressive dose-dependent changes, which indicates that these radiation responsive proteins have considerable potential as biodosimeters. Some examples for proteomic biodosimetry in ^{60}Co γ-rays studies are shown in Figs. 11.2.3 - 11.2.5.

CD45/CD27 + Flt3L + IL-18

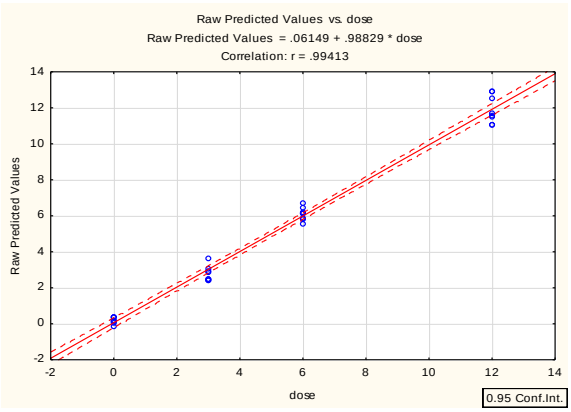

Regression Summary for Dependent Variable: dose (C6_d4_data_10-25-17) R= .99412672 R²= .98828794 Adjusted R²= .98703307 F(3,28)=787.57 p

N=32	b*	Std.Err. of b*	b	Std.Err. of b	t(28)	p-value
Intercept			-1.39611	0.167684	-8.32584	0.000000
FLT3L	0.309045	0.038351	0.00250	0.000310	8.05826	0.000000
CD45/CD27	0.238448	0.065565	0.11654	0.032046	3.63682	0.001102
IL-18	0.504585	0.053556	0.00881	0.000935	9.42166	0.000000

CD45/CD27 + Flt3L + IL-12

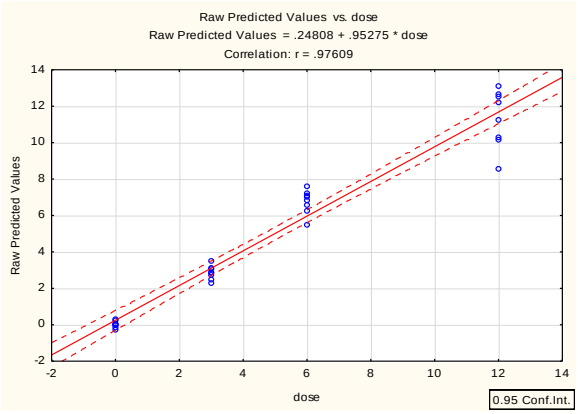

Regression Summary for Dependent Variable: dose (C6_d4_data_10-25-17) R= .97608737 R²= .95274655 Adjusted R²= .94768368 F(3,28)=188.18 p

N=32	b*	Std.Err. of b*	b	Std.Err. of b	t(28)	p-value
Intercept			-2.26613	1.017420	-2.22733	0.034140
FLT3L	0.334187	0.104616	0.00270	0.000846	3.19443	0.003453
CD45/CD27	0.752899	0.077366	0.36799	0.037814	9.73164	0.000000
IL-12	0.088677	0.091385	0.00315	0.003242	0.97037	0.340172

Fig. 11.2.3. Linear regression analysis of dose prediction using the combination of three biomarkers: CD45/CD27 + FLT3L + IL-18 and CD45/CD27+ FLT3L + IL-12 in ^{60}Co γ-ray studies. Plot represent predicted vs. given dose at 95% CL. Tables show multiple linear regression analysis summary results.

CD45/CD27 + Flt3L + IL-5

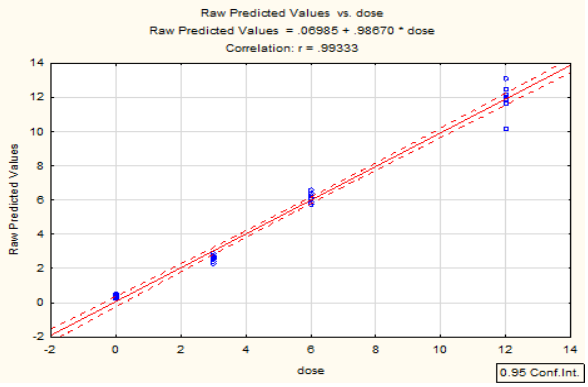

N=32	Regression Summary for Dependent Variable: dose (C6_d4_data_10-25-17) R= .99332549 R²= .98669552 Adjusted R²= .98527004 F(3,28)=692.18 p					
	b*	Std.Err. of b*	b	Std.Err. of b	t(28)	p-value
Intercept			-0.603568	0.197572	-3.05493	0.004901
FLT3L	0.327464	0.041209	0.002649	0.000333	7.94639	0.000000
CD45/CD27	0.334281	0.062146	0.163384	0.030375	5.37892	0.000010
IL-5	0.402800	0.046576	0.143060	0.016542	8.64823	0.000000

CD45/CD27 + Flt3L + G-CSF

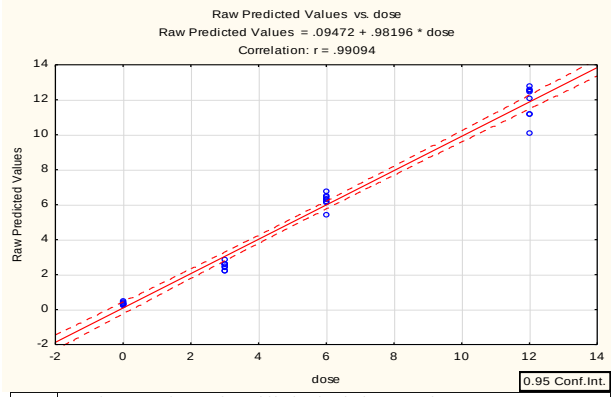

N=32	Regression Summary for Dependent Variable: dose (C6_d4_data_10-25-17) R= .99093772 R²= .98195757 Adjusted R²= .98002445 F(3,28)=507.97 p					
	b*	Std.Err. of b*	b	Std.Err. of b	t(28)	p-value
Intercept			-0.492905	0.240968	-2.04552	0.050302
FLT3L	0.379092	0.050048	0.003067	0.000405	7.57458	0.000000
CD45/CD27	0.272159	0.082698	0.133021	0.040420	3.29100	0.002702
G-CSF	0.416723	0.060275	0.004598	0.000665	6.91365	0.000000

Fig. 11.2.4. Linear regression analysis of dose prediction using the combination of three biomarkers: CD45/CD27 + FLT3L + IL-5 and CD45/CD27+ FLT3L + G-CSF in ^{60}Co γ-rays studies. Plot represent predicted vs. given dose at 95% CL. Tables show multiple linear regression analysis summary results.

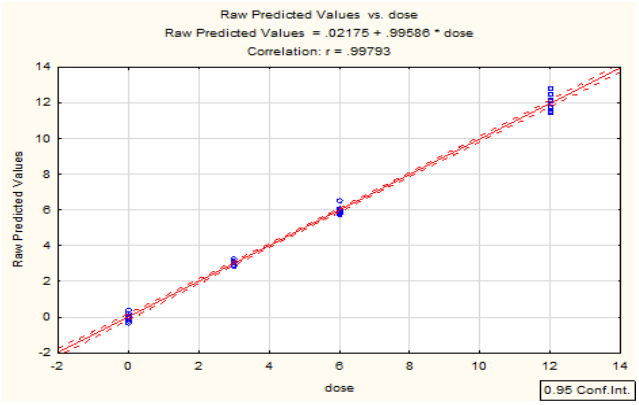

Dose Prediction at 99% CL	
Observed/Given Dose, Gy	**Predicted Dose, Gy Mean [Min-Max]**
0	**0.0+0.1/-0.1**
3	**3.0 +0.2/-0.2 [2.8-3.2]**
6	**6.0 +0.5/-0.2 [5.8-6.5]**
12	**12.0 +0.8/-0.5 [11.5-12.8]**

N=32	Regression Summary for Dependent Variable: dose (C6_d4_data_10-25-17) R= .99792689 R²= .99585807 Adjusted R²= .99486400 F(6,25)=1001.8 p					
	b*	Std.Err. of b*	b	Std.Err. of b	t(25)	p-value
Intercept			1.456703	0.456948	3.18790	0.003828
FLT3L	0.196365	0.034695	0.001589	0.000281	5.65976	0.000007
CD45/CD27	0.082451	0.054895	0.040299	0.026831	1.50197	0.145632
G-CSF	0.130829	0.084879	0.001443	0.000936	1.54135	0.135796
IL-12	-0.206425	0.035718	-0.007324	0.001267	-5.77926	0.000005
IL-5	0.215423	0.086571	0.076510	0.030747	2.48840	0.019853
IL-18	0.268038	0.065987	0.004680	0.001152	4.06196	0.000422

Fig. 11.2.5. Linear regression analysis of dose prediction using the best combination of six biomarkers: CD45/CD27+ FLT3L + G-CSF + IL-18 + IL-12 +IL-5 in ^{60}Co γ-ray studies. Plot represent predicted vs. given dose at any time-point. Upper Table shows the given vs. predicted dose at 99.9% CL. Lower Table represent multiple linear regression analysis summary results.

Receiver Operation Characteristic (ROC) and Discriminant Analyses Results

Receiver operating characteristic (or ROC) analysis of single biomarker and combination of biomarkers was performed using ROCCET on-line tool (Xia et al. 2013). Individual markers were analyzed using classical ROC and multiple markers with partial least squares – discriminant analysis approach. The area under the curve (AUC) with 95% confidence intervals was used to demonstrate the sensitivity and specificity of the proposed protein biomarkers to reflect subgroup (dose and sampling time-point) differences as well as to analyze the results from survival study to predict the ARS outcome. Results are shown as a ROC plot of the true positive rate against the false positive rate for the different possible cut-points of a diagnostic test. ROC and discriminant analyses (using a PC SAS software) were performed for the same biomarkers and time points as was done in multiple regression analysis described above.

Figs. 11.2.6 - 11.2.8 show some ROC analysis results into tertiles of ^{60}Co γ-ray doses 0-3 Gy, 3-6 Gy, and 6-12 Gy using selected hematological (ALC and ANC to ALC ratio) and protein FLT3L, SAA, and CD45 to CD27 ratio) biomarkers from biological samples; - the same ones that were used in mixed-field ROC data analysis (see in section 11.1). Red line on whisker plot indicates cutoff value, which corresponds to red dots on ROC plots. ROC table displayed in rank order by AUC, which indicates quality of discrimination by ROC (1= perfect).

^{60}Co γ-rays

0 - 3 Gy

Biomarker	AUC	Cutoff value
ALC (10^3/ul)	1.0	1.94
ANC/ALC	1.0	0.524
FLt3-L (pg/ml)	1.0	294
SAA (ng/ml)	1.0	990
CD45/CD27	1.0	8.09

Raw Data (for reference):

Case #	Dose	ALC (10^3/ul)	ANC/ALC	FLt3-L (pg/ml)	SAA (ng/ml)	CD45/CD27
1	0	3.5	0.11	130.8	874.1	2.3
2	0	4.5	0.11	109.8	632.7	2.8
3	0	4.9	0.15	114.8	685.9	2.7
4	0	5.0	0.15	93.2	927.8	2.5
5	0	4.7	0.12	124.6	773.1	2.4
6	0	4.2	0.09	132.9	568.6	3.0
7	0	4.0	0.08	111.6	752.3	2.5
8	0	4.4	0.12	116.8	273.0	2.0
9	3	0.2	1.40	528.0	1051.4	17.1
10	3	0.2	2.00	560.5	1613.5	20.1
11	3	0.4	0.90	552.1	3144.3	13.2
12	3	0.1	2.80	645.3	2414.1	21.8
13	3	0.3	3.08	617.6	2049.2	19.2
14	3	0.3	1.08	557.2	2660.7	15.5
15	3	0.2	1.39	456.1	1149.5	18.9
16	3	0.2	1.75	517.2	2311.0	15.2

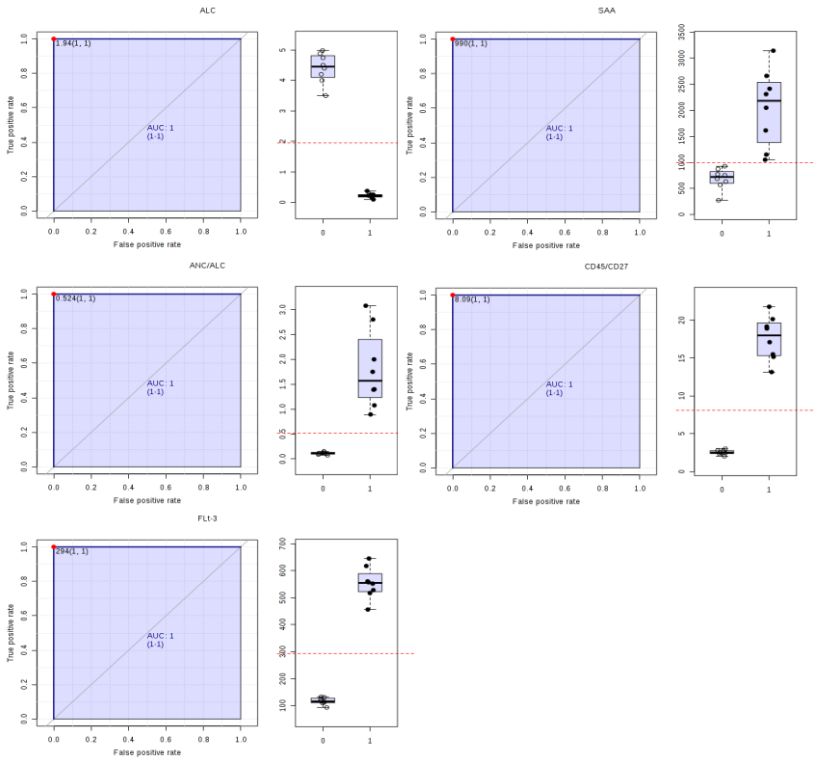

Fig. 11.2.6. ROC analysis results to separate sham (0 Gy) and 3-Gy groups in ^{60}Co γ-ray studies. Full discrimination with 5 of 5 biomarkers.

^{60}Co γ-rays

3 - 6 Gy

Biomarker	AUC	Cutoff value
FLt3-L (pg/ml)	1.0	679
CD45/CD27	1.0	24.2
SAA (ng/ml)	0.9	2790
ALC (10^3/ul)	0.9	0.15
ANC/ALC	0.9	2.82

Raw Data (for reference):

Case #	Dose	ALC (10^3/ul)	ANC/ALC	FLt3-L (pg/ml)	SAA (ng/ml)	CD45/CD27
9	3	0.2	1.40	528.0	1051.4	17.1
10	3	0.2	2.00	560.5	1613.5	20.1
11	3	0.4	0.90	552.1	3144.3	13.2
12	3	0.1	2.80	645.3	2414.1	21.8
13	3	0.3	3.08	617.6	2049.2	19.2
14	3	0.3	1.08	557.2	2660.7	15.5
15	3	0.2	1.39	456.1	1149.5	18.9
16	3	0.2	1.75	517.2	2311.0	15.2
17	6	0.1	2.83	811.6	5183.1	28.5
18	6	0.2	1.30	712.9	2618.1	32.4
19	6	0.1	4.33	822.3	3598.3	26.6
20	6	0.1	6.75	968.5	2922.9	31.4
21	6	0.1	5.00	774.0	3324.0	33.7
22	6	0.0	10.00	876.7	4101.8	30.5
23	6	0.0	14.00	714.5	4073.7	31.3
24	6	0.1	2.00	756.7	2964.6	29.7

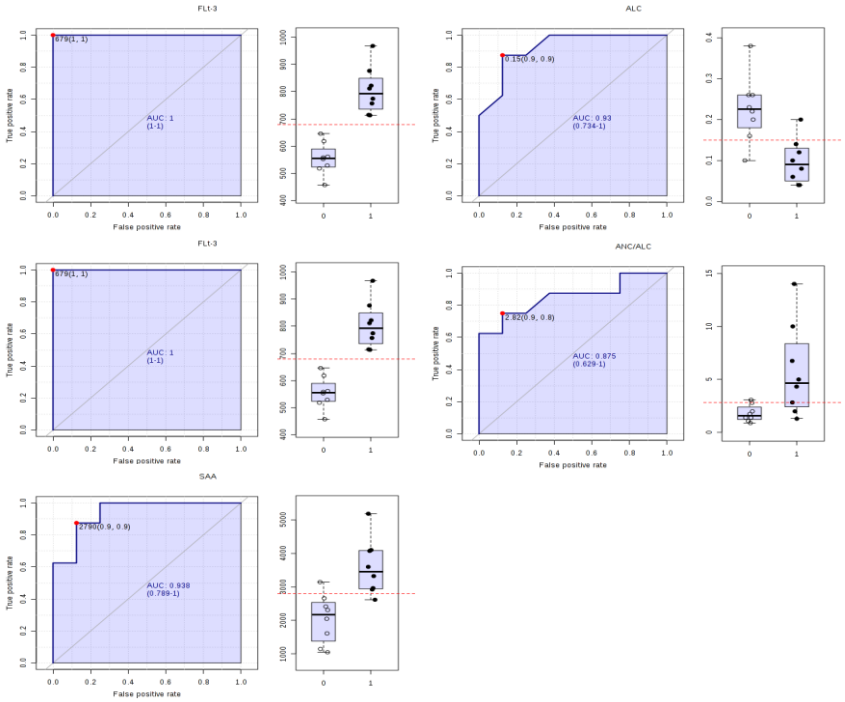

Fig. 11.2.7. ROC analysis results to separate 3- and 6-Gy groups in ^{60}Co γ-ray studies. Full discrimination with 2 of 5 biomarkers.

^{60}Co γ-rays

6 - 12 Gy

Biomarker	AUC	Cutoff value
ANC/ALC	1.0	15
FLt3-L (pg/ml)	1.0	970
CD45/CD27	1.0	40.2
ALC (10^3/ul)	1.0	0.05
SAA (ng/ml)	0.8	3670 and 4460

Raw Data (for reference):

Case #	Dose	ALC (10^3/ul)	ANC/ALC	FLt3-L (pg/ml)	SAA (ng/ml)	CD45/CD27
17	6	0.1	2.83	811.6	5183.1	28.5
18	6	0.2	1.30	712.9	2618.1	32.4
19	6	0.1	4.33	822.3	3598.3	26.6
20	6	0.1	6.75	968.5	2922.9	31.4
21	6	0.1	5.00	774.0	3324.0	33.7
22	6	0.0	10.00	876.7	4101.8	30.5
23	6	0.0	14.00	714.5	4073.7	31.3
24	6	0.1	2.00	756.7	2964.6	29.7
25	12	0.0	33.00	977.0	5062.8	54.9
26	12	0.0	27.00	1047.4	5248.9	67.1
27	12	0.0	18.00	1097.9	5880.4	57.3
28	12	0.0	21.97	1105.3	3746.5	47.5
29	12	0.0	21.00	976.2	4818.5	51.6
30	12	0.0	22.00	1013.6	2938.2	50.0
31	12	0.0	20.50	1056.6	4025.6	46.7
32	12	0.0	16.00	971.2	6225.6	56.2

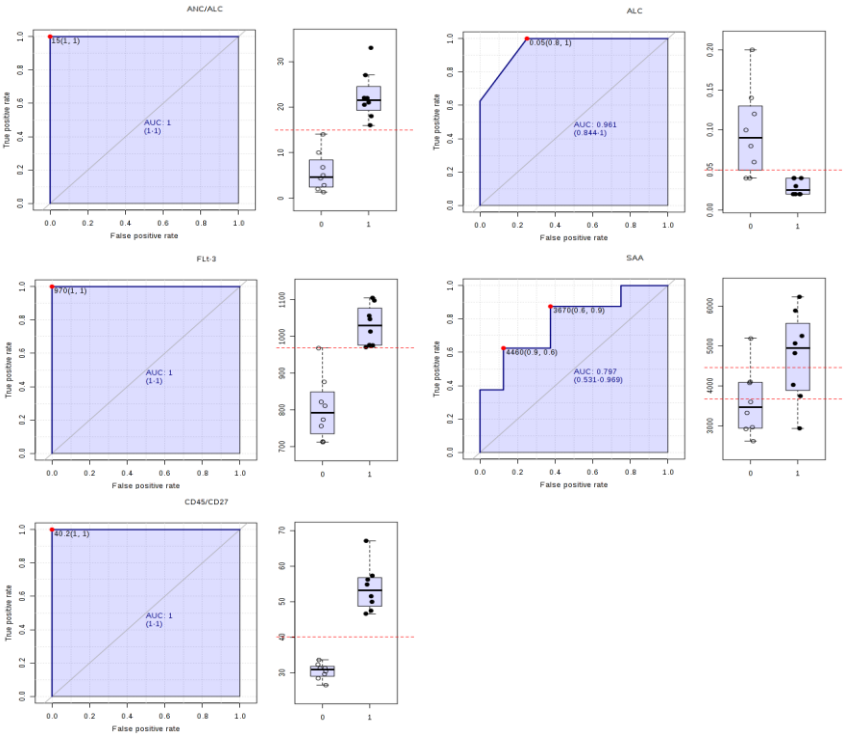

Fig. 11.2.8. ROC analysis results to separate 6- and 12-Gy groups in ^{60}Co γ-ray studies. Full discrimination with 4 of 5 biomarkers.

Multi-parameter (i.e., linear regression, discriminant and ROC) biodosimetry analyses summary results in ^{60}Co γ-ray studies are shown in Fig. 11.2.9.

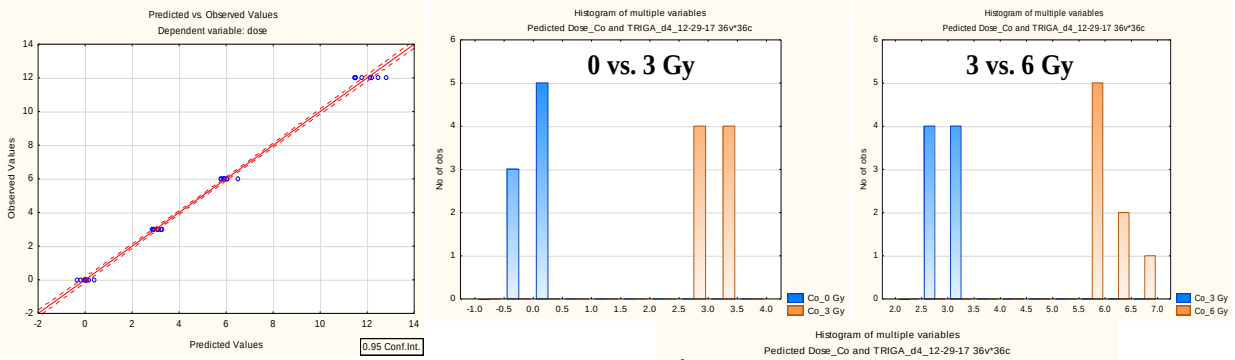

ROC Analysis Classification Performance in ^{60}Co Studies			
Classification Criteria	**0 vs. 3 Gy**	**3 vs. 6 Gy**	**6 vs. 12 Gy**
True Positive Fraction	**100%**	**100%**	**100%**
True Negative Fraction	**100%**	**100%**	**100%**
Prediction Accuracy (%)	**100%**	**100%**	**100%**
Area Under Curve (AUC)	**1.000**	**1.000**	**1.000**

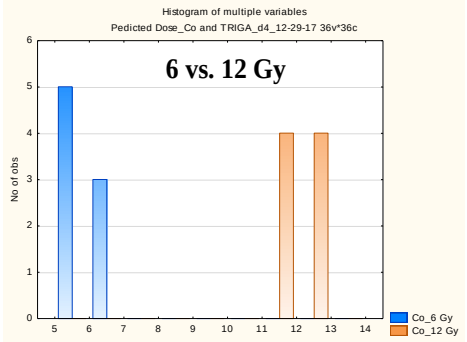

Fig. 11.2.9. Multi-parameter biodosimetry analyses summary results in ^{60}Co γ-ray studies. Linear regression analysis (upper left plot), discriminant analysis (histograms of predicted vs. given radiation doses to separate study animal groups) and ROC analysis (Table) for the best combination of protein biomarkers: CD45/CD27 + FLT3L + G-CSF + IL-18 + IL-12 + IL-5.

11.3. BIODOSIMETRY DATA ANALYSIS COMPARISON BETWEEN ^{60}Co PURE GAMMA RAYS AND TRIGA MIXED-FIELD STUDIES

Table 11.3.1 shows biodosimetry performance selected results for radiation dose prediction accuracy in TRIGA reactor mixed-field and ^{60}Co γ-ray studies at 0.6 Gy/min. For biomarker combinations, multiple linear regression analysis was used to develop biodosimetry dose-response relationships. Results from TRIGA and Cobalt studies demonstrate that accuracy in radiation dose prediction progressively increases with the increasing of number of biomarkers as reported in other animal radiation biodosimetry studies (Ossetrova et al. 2007 – 2016).

Selected multi-parameter algorithm equations for TBI predicted vs. given radiation doses in samples collected 1d -7d post TBI in male B6D2F1 mice irradiated either with 67% n + 33% γ or 100%γ at 0.6 Gy/min are shown in Tables 11.1.2 and 11.2.1, respectively.

Table 11.3.1. Bidosimetry performance for selected biomarker combinations for radiation dose prediction accuracy in TRIGA mixed-field and ^{60}Co (pure γ-rays) studies. Algorithm and equations were created in male mice (T6 and C6 experiments).

Bidosimetry Performance for Selected Biomarker Combinations
Radition Dose Assessment Acuracy in TRIGA and ^{60}Co Gender-comparison Studies Using Algorithm Equations
Created in Male Mice (T6 and C6 Experiments)

#	Biomarker Combination (number of biomarkers)	TRIGA 67% n + 33% γ	^{60}Co 100% γ
1	ALC	80.4 ± 8.2	78.5 ± 8.6
2	CD27	81.1 ± 9.4	77.6 ± 8.8
3	Flt3L	84.1 ± 7.6	82.3 ± 6.9
4	CD45/CD27	85.6 ± 5.4	86.7 ± 6.4
5	Flt3L + CD27	90.2 ± 3.6	89.7 ± 4.1
6	Flt3L + CD45/CD27	93.3 ± 2.1	92.5 ± 3.6
7	Flt3L + CD45/CD27 + SAA (3 bios)	94.5 ± 4.5	93.8 ± 3.3
8	Flt3L + CD45/CD27 + IL-18 (3 bios)	96.4 ± 3.8	95.1 ± 3.7
9	Flt3L + CD45/CD27 + IL-12 (3 bios)	96.1 ± 2.8	96.5 ± 3.2
10	Flt3L + CD45/CD27 +G-CSF (3 bios)	97.6 ± 2.5	98.1 ± 2.8
11	Flt3L + CD45/CD27 + EPO + SAA (4 bios)	99.1 ± 1.1	98.6 ± 1.4
12	Flt3L + CD45/CD27 + IL-18 + IL-5 + IL-12 + G-CSF (6 bios)	99.7 ± 0.3	99.8 ± 0.2

ALC depletion kinetics analysis for the radiation dose prediction was performed using a mathematical algorithm (e.g., exponential fitting function) similar to one that was established and reported in Chernobyl accident victims (Fig. 11.1.1; Baranov et al. 1995; Guskova et al, 1988). Table in Fig. 11.3.1 summarizes ALC results as a function of radiation dose received: ALC = A× exp (- B × Dose), where A and B are coefficients and dose is expressed in Gy. Results demonstrate that coefficients A and B in TRIGA study are about 2-fold higher than in Cobalt study that reflects the RBE = 1.95 seen in the same mouse strain in radiation countermeasure survival studies performed at AFRRI (Ledney and Elliott 2010).

ALC Data Comparison Summary in TRIGA (67%n + 33%γ) and ^{60}Co γ-rays

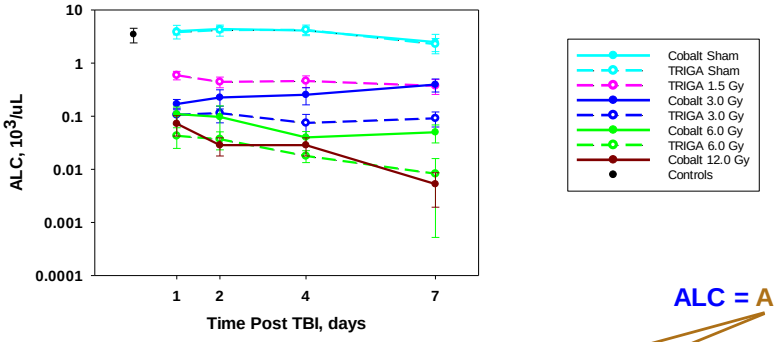

~ 2 fold

ALC = A × exp (-B × Dose)

TBI Study	ALC Dose- and Time-dependency Fitting Functions			
	D1	D2	D4	D7
TRIGA (67%n + 33%γ)	2.329 × exp(-0.758× Dose)	2.024 × exp(-0.733× Dose)	2.179 × exp(-0.874× Dose)	2.799 × exp(-1.099× Dose)
^{60}Co (100%γ)	1.299 × exp(-0.302× Dose)	1.634 × exp(-0.387× Dose)	1.468 × exp(-0.397× Dose)	2.515 × exp(-0.544× Dose)

Fig. 11.3.1. ALC data comparison summary in TRIGA (67% n + 33% γ) and ^{60}Co γ-rays studies.

Results for ALC-based radiation dose prediction after the mixed-field and pure γ-rays exposure shown in Tables 11.1.2 and 11.2.1, respectively, and Fig. 11.3.2 clearly reflect the radiation-quality specific biodosimetry. While A coefficients in TRIGA mixed-field studies are in the tight range of (4.832 ± 0.306), A coefficients in ^{60}Co γ-rays studies show the progressive time-dependent decrease from 17.343 (day 1) to 8.947 (day 7) resulted in their time-dependent decrease of Cobalt to TRIGA ratio. The similar pattern was observed for B coeffients and their ratio as well.

ALC-based biodosimetry after either mixed-field (67%n + 33%γ) or ^{60}Co (100%γ)

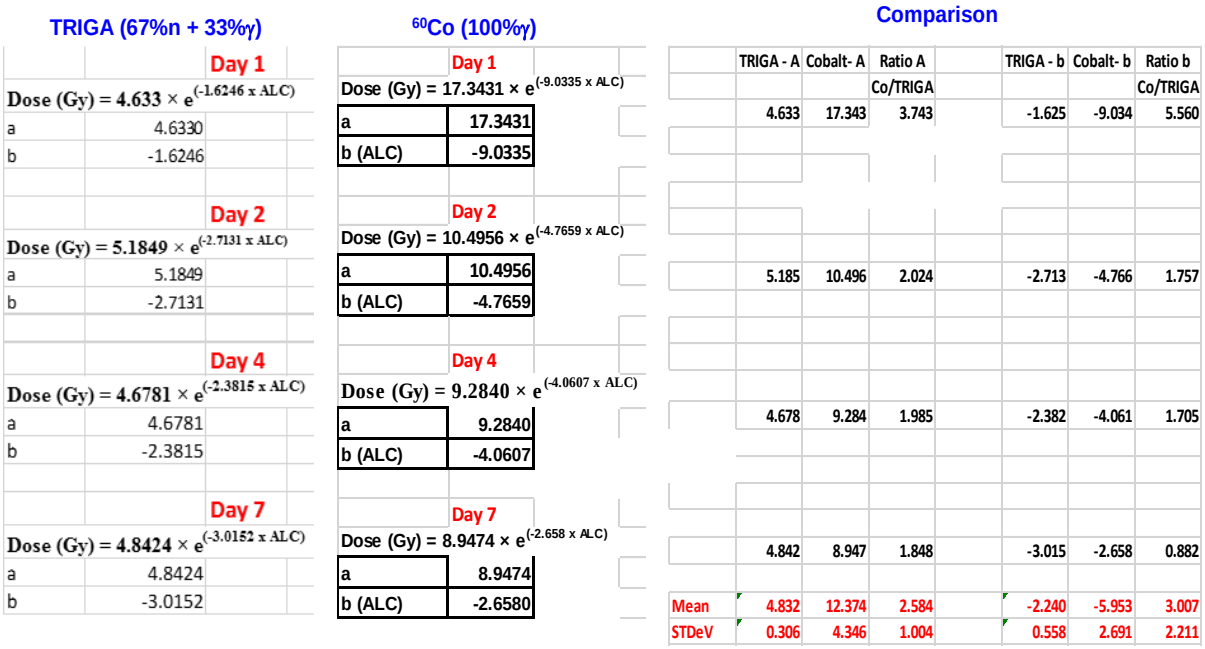

TRIGA (67%n + 33%γ)

	Day 1
Dose (Gy) = 4.633 × e^(-1.6246 x ALC)	
a	4.6330
b	-1.6246

	Day 2
Dose (Gy) = 5.1849 × e^(-2.7131 x ALC)	
a	5.1849
b	-2.7131

	Day 4
Dose (Gy) = 4.6781 × e^(-2.3815 x ALC)	
a	4.6781
b	-2.3815

	Day 7
Dose (Gy) = 4.8424 × e^(-3.0152 x ALC)	
a	4.8424
b	-3.0152

^{60}Co (100%γ)

	Day 1
Dose (Gy) = 17.3431 × e^(-9.0335 x ALC)	
a	17.3431
b (ALC)	-9.0335

	Day 2
Dose (Gy) = 10.4956 × e^(-4.7659 x ALC)	
a	10.4956
b (ALC)	-4.7659

	Day 4
Dose (Gy) = 9.2840 × e^(-4.0607 x ALC)	
a	9.2840
b (ALC)	-4.0607

	Day 7
Dose (Gy) = 8.9474 × e^(-2.658 x ALC)	
a	8.9474
b (ALC)	-2.6580

Comparison

	TRIGA - A	Cobalt- A	Ratio A Co/TRIGA	TRIGA - b	Cobalt- b	Ratio b Co/TRIGA
	4.633	17.343	3.743	-1.625	-9.034	5.560
	5.185	10.496	2.024	-2.713	-4.766	1.757
	4.678	9.284	1.985	-2.382	-4.061	1.705
	4.842	8.947	1.848	-3.015	-2.658	0.882
Mean	4.832	12.374	2.584	-2.240	-5.953	3.007
STDeV	0.306	4.346	1.004	0.558	2.691	2.211

Fig. 11.3.2. ALC-based radiation dose prediction after TBI either the mixed-field or pure γ-rays exposure.

Results for CD27-based radiation dose prediction after the mixed-field and pure γ-rays exposure shown in Tables on Fig. 11.3.3 also clearly reflect the radiation-quality specific biodosimetry. In both studies, A coefficients show the progressive time-dependent decrease resulted in their ratio distributed in range of (2.338 ± 0.722). The B coefficients are in range of (-0.003 ± 0.001) and (-0.005 ± 0.002) in mixed-field and γ-rays studies, respectively, and their ratio is in a range of (1.999 ± 0.908). CD27-based dosimetry results also are in agreement with RBE = 1.95 seen in the same mouse strain in radiation countermeasure survival studies performed at AFRRI (Ledney and Elliott 2010).

CD27-based biodosimetry after either mixed-field (67%n + 33%γ) or ^{60}Co (100%γ)

TRIGA (67%n + 33%γ)

Day 1

Dose (Gy) = 12.983 × $e^{(-.0021 \times CD27)}$

a	12.983
b	-0.0021

Day 2

Dose = 10.5275 × $e^{(-0.004 \times CD27)}$

a	10.5275
b	-0.004

Day 4

Dose (Gy) = 6.8436× $e^{(-0.0024 \times CD27)}$

a	6.8436
b	-0.0024

Day 7

Dose (Gy) = 7.4317 × $e^{(-0.0019 \times CD27)}$

a	7.4317
b	-0.0019

^{60}Co (100%γ)

Day 1

Dose (Gy) = 32.0839 × $e^{(-0.0061 \times CD27)}$

a	32.0839
b (CD27)	-0.0061

Day 2

Dose (Gy) = 18.1162 × $e^{(-0.0070 \times CD27)}$

a	18.1162
b (CD27)	-0.0070

Day 4

Dose (Gy) = 22.6066 × $e^{(-0.006 \times CD27)}$

a	**22.6066**
b (CD27)	**-0.0060**

Day 7

Dose (Gy) = 13.7904× $e^{(-0.0016 \times CD27)}$

a	**13.7904**
b (CD27)	**-0.0016**

Comparison

	TRIGA - A	Cobalt- A	Ratio A Co/TRIGA	TRIGA - b	Cobalt- b	Ratio b Co/TRIGA
	12.9830	32.0839	2.471	-0.0021	-0.0061	2.905
	10.5275	18.1162	1.721	-0.0040	-0.0070	1.750
	6.8436	22.6066	3.303	-0.0024	-0.0060	2.500
	7.4317	13.7904	1.856	-0.0019	-0.0016	0.842
Mean	9.446	21.649	2.338	-0.003	-0.005	1.999
STDeV	2.858	7.832	0.722	0.001	0.002	0.908

Fig. 11.3.3. CD27-based radiation dose prediction after TBI either the mixed-field or pure γ-rays exposure.

Hematological biomarkers of exposure to ionizing radiation are well characterized and used in medical management of radiological casualties (Dainiak et al. 2003). Measurements of lymphocyte depletion kinetics (Goans et. al. 1997) and time- and radiation severity changes in neutrophil cell counts observed after irradiation provide clinical information soon after exposure. However, the accurate radiation exposure dose estimation by lymphocyte depletion kinetics becomes problematic after doses close to the LD50, and certainly for higher doses due to significant declines (< 200 cells per uL) in peripheral lymphocyte counts by 24 h (Baranov et al. 1995; Goans et al. 1997). While absolute lymphocyte counts decrease and plateau at doses 3 Gy and higher 2 – 3 days after exposure, proteins show progressive dose-dependent changes.

Mean difference in regression slope coefficients in TRIGA (67% n + 33% γ) vs. ^{60}Co (100% γ) studies for a highly radiation-specific biomarker FLT3L is 1.65 as shown in Fig. 11.3.4. Those findings are in general agreement with AFRRI dicentric calibration curves created using different radiation sources (TRIGA nuclear reactor, ^{60}Co γ-rays, and 250-keV x-rays) (Prasanna et al. 2002) (Fig. 11.3.5) as well as results for relative biological effectiveness or RBE = 1.95 for the same percentage of neutrons and γ-rays seen in mice reported by AFRRI scientists in radiation countermeasure survival studies (Ledney and Elliott 2010) and our biodosimetry survival studies (Ossetrova et al. 2016; 2018).

Our biodosimetry results are consistent with a radiation dose detection threshold ~1 Gy and ~0.5 Gy for γ-rays and a mixed-field exposure, respectively, in mice of this strain (LD50/30 is ~ 9.65 Gy) based on the selected biomarker profile and sampling time-points after exposure.

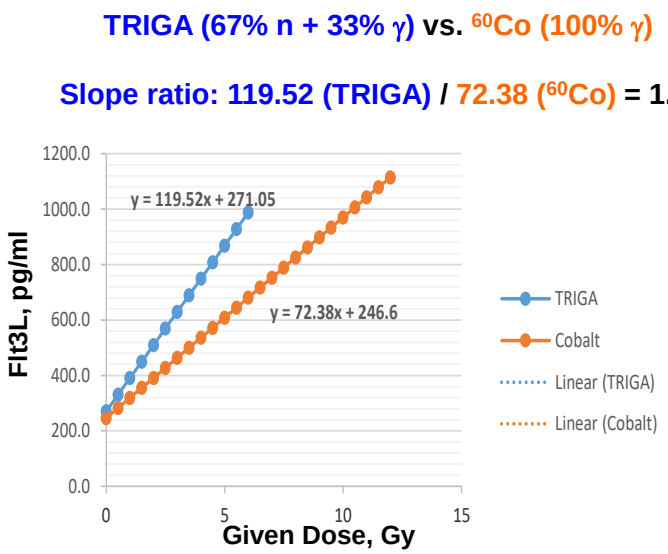

Fig. 11.3.4. FLT3L-based radiation dose prediction after either the mixed-field or pure γ-rays exposure. Mean difference in regression slope coefficients in TRIGA (67% n + 33% γ) vs. ^{60}Co (100% γ) studies.

In our past research in B6D2F1 female mouse TBI model, FLT3L was not found elevated in blood of mice challenged with stress, infection, or trauma (15% non-lethal total-body surface skin burns or wounds) performed within 1 hour after radiation injury. Those findings suggest that Flt3L is a highly radiation-specific biomarker. In addition, its persistent elevation up to three weeks makes it very useful to estimate the radiation dose received and the severity of radiation-induced bone-marrow aplasia (Ossetrova et al. 2014, 2016).

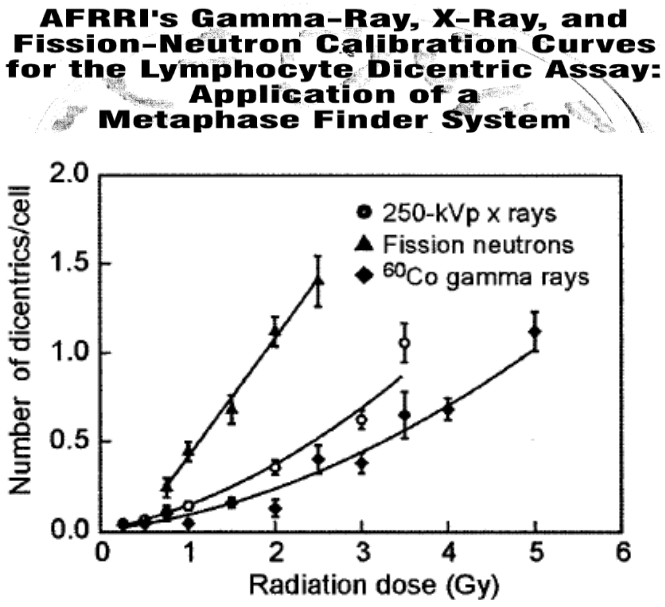

Fig. 11.3.5. AFRRI's gamma-ray, x-ray and fission neutron calibration curves created in-vitro in human lymphocyte dicentic assays (Prasanna et al. 2002).

The development of accurate methods for rapid individual dose assessment possesses some challenges. A major source of uncertainty is individual variability in radiation response. Animal species and strains show marked differences in radiation sensitivity. This inter-individual variation in response to radiation exposure is not unexpected, since it is well known from experimental studies, that populations of various mammalian species, including humans, contain a small proportion (from 5% to 12%) of individuals that show so-called hyper-radiosensitivity to both acute and chronic radiation, about 70% are normally sensitive and about 20% are radioresistant (Kovalev et al. 1996). The molecular reasons for species and individual radiosensitivity are not clarified in detail and explanation of these differences is beyond the scope of this project, however radiation-responsive protein profile may contribute to a molecular-based understanding of radiosensitivity. A proteomic approach may evaluate an individual's responses to radiation exposure, since the individual's characteristic and dynamic protein expression profile will reflect their unique biological system. An early and rapid dose assessment of a suspected exposed individual aides this effort.

11.4. BIOMARKER-BASED BIODOSIMETRY AT ANY TIME AFTER EXPOSURE

The Table Curve 2D and 3D statistical software were used to create the dose- and time-dependent fitting equations for biodosimetry-based biomarkers in order to estimate the radiation dose received based on biomarker level at any time-point after exposure other than at collection time in experiment (i.e., d1, d2, d4 and d7).

Fig. 11.4.1 shows 3D plots for ALC depletion as a function of radiation dose and time post TBI (upper plot) and radiation dose received as a function of ALC and time post TBI (lower plot). Radiation dose predicted is expressed as Dose (Gy) = $A \times e^{(B \times ALC)}$, where A and B are coefficients calculated by the SAS software. ALC data for all animals clearly fit function Z= F (X, Y), expressed as Z=a + LORX(b,c,d) + LORY(e,f,g) + LORX(h,c,d) × LORY(1,f,g), where Z is ALC (in number of cells per uL) for given radiation dose (X, in Gy) and time (Y, in hours/days). Model coefficients are a=0.2710, b=-13.1694, c=0.1608, d=0.4812, e=-0.2876, f=61.0703, g=312.0246, h=18.0027, R^2=0.9255 and a standard error of estimate FitStdErr=0.4903. This dose- and time-dependency might be used to estimate ALC value at any time-point other than at collection time in experiment. Radiation dose received for all animals clearly fit function Z= F (X, Y), expressed as Z=a + LOGNORMX(b,c,d) + GAUSSY(e,f,g) + LOGNORMX(h,c,d)×GAUSSY(1,f,g), where Z is radiation dose (in Gy)) for given time post TBI (X, in hour/days) and ALC (Y, in number of cells per uL). Model coefficients are a=-0.2220, b=6.4417, c=0.0046, d=2.6225, e=0.0104, f=34.9768, g=29.6304, h=1.5858, R^2=0.9323 and a standard error of estimate FitStdErr=0.6005. This equation might be used to estimate the radiation dose received based on ALC data at any time-point other than at collection time in experiment. Results of this analysis are shown in a Table on right. Numbers in red color represent the predicted doses evaluated by the SAS software based on biomarker levels at time-points of sample collections as described above (i.e. d1, d2, d4 and d7). Numbers in black color represent the predicted doses evaluated by Table Curve 3D fitting function with a good accuracy shown in the last column of this Table.

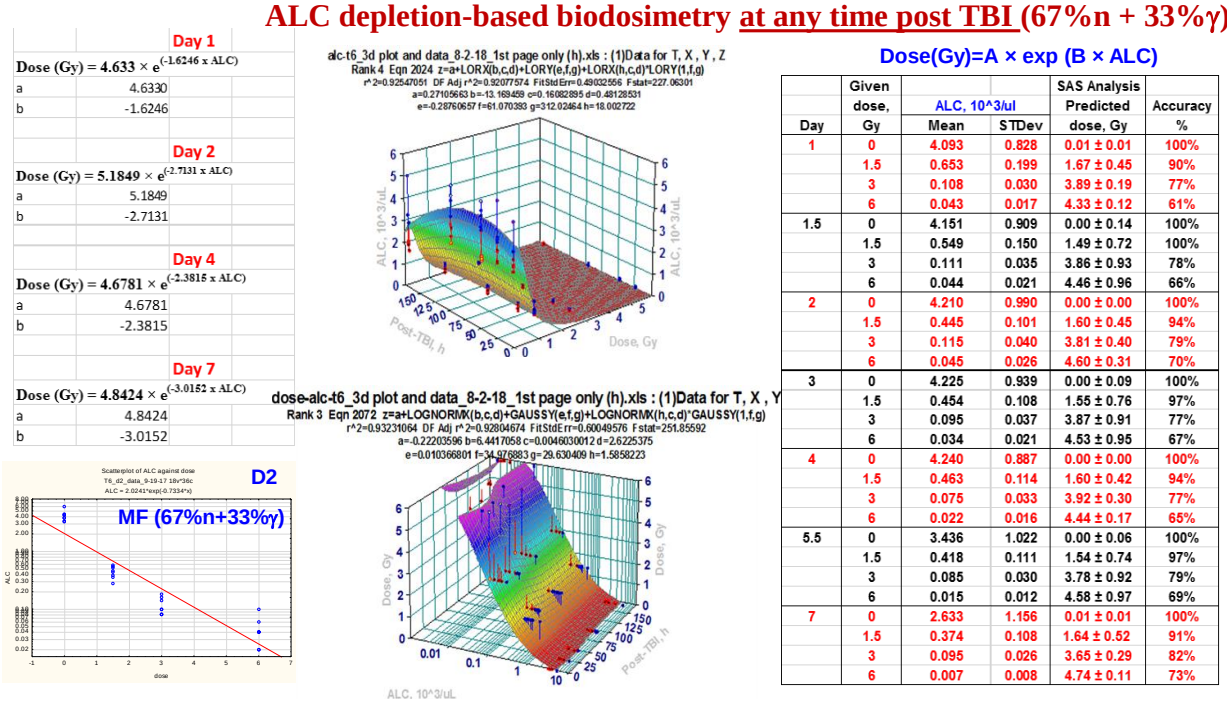

Day	Given dose, Gy	ALC, 10^3/ul Mean	ALC, 10^3/ul STDev	SAS Analysis Predicted dose, Gy	Accuracy %
1	0	4.093	0.828	0.01 ± 0.01	100%
	1.5	0.653	0.199	1.67 ± 0.45	90%
	3	0.108	0.030	3.89 ± 0.19	77%
	6	0.043	0.017	4.33 ± 0.12	61%
1.5	0	4.151	0.909	0.00 ± 0.14	100%
	1.5	0.549	0.150	1.49 ± 0.72	100%
	3	0.111	0.035	3.86 ± 0.93	78%
	6	0.044	0.021	4.46 ± 0.96	66%
2	0	4.210	0.990	0.00 ± 0.00	100%
	1.5	0.445	0.101	1.60 ± 0.45	94%
	3	0.115	0.040	3.81 ± 0.40	79%
	6	0.045	0.026	4.60 ± 0.31	70%
3	0	4.225	0.939	0.00 ± 0.09	100%
	1.5	0.454	0.108	1.55 ± 0.76	97%
	3	0.095	0.037	3.87 ± 0.91	77%
	6	0.034	0.021	4.53 ± 0.95	67%
4	0	4.240	0.887	0.00 ± 0.00	100%
	1.5	0.463	0.114	1.60 ± 0.42	94%
	3	0.075	0.033	3.92 ± 0.30	77%
	6	0.022	0.016	4.44 ± 0.17	65%
5.5	0	3.436	1.022	0.00 ± 0.06	100%
	1.5	0.418	0.111	1.54 ± 0.74	97%
	3	0.085	0.030	3.78 ± 0.92	79%
	6	0.015	0.012	4.58 ± 0.97	69%
7	0	2.633	1.156	0.01 ± 0.01	100%
	1.5	0.374	0.108	1.64 ± 0.52	91%
	3	0.095	0.026	3.65 ± 0.29	82%
	6	0.007	0.008	4.74 ± 0.11	73%

Fig. 11.4.1. ALC depletion-based biodosimetry at any time post TBI (67%n + 33%γ).

Fig. 11.4.2 shows statistical data analysis results for CD27-based biodosimetry at any time post TBI that includes the list of equations created at collection time in experiment (i.e., d1, d2, d4 and d7), 3D plots, etc. Radiation dose predicted is expressed as Dose (Gy) = A × e $^{(B \times CD27)}$, where A and B are coefficients calculated by the SAS software. Left Table in Fig. 11.4.2 shows a strong time-dependency for A coefficients while B coefficients are not significant different ($p>0.126$) within 95% CL over all time-points. This dose-dependency was applied using the Table Curve 2D software to create a fitting function in order to evaluate A coefficient values at any time after exposure from d1 to d7. The 3D plots were created for CD27 (as a function of time post TBI and radiation dose) and radiation dose (as a function of CD27 and time) along with fitting functions with ability to predict CD27 level and radiation dose received at any time post exposure. CD27 data for all animals clearly fit function $Z = a + blnX + clnY + d(lnX)^2 + e(lnY)^2 + flnXlnY + g(lnX)^3 + h(lnY)^3 + ilnX(lnY)^2 + j(lnX)^2lnY$, where Z is CD27 (in pg/ml) for given radiation dose (X, in Gy) and time (Y, in hours/days). Model coefficients are a=6315.702, b=-476.385, c=-2603.928, d=162.092, e=305.387, f=-55.019, g=0.235, h=0.740, i=-0.288, j=-0.084, R^2=0.8705 and a standard error of estimate FitStdErr=335.399. Radiation dose received for all animals clearly fit function Z = a + LORX(b,c,d) + LORY(e,f,g) + LORX(h,c,d)×LORY(1,f,g), where Z is radiation dose (in Gy)) for given time post TBI (X, in hour/days) and CD27 (Y, in pg/ml). Model coefficients are a=-0.0228, b=8.9998, c=-61.6445, d=285.04906, e=-0.0696, f=23.9985, g=0.3236, h=13.6282, R^2=0.9083 and a standard error of estimate FitStdErr=0.6988. Results of those analyses are shown in lower middle plot and a Table on right. Numbers in red color represent the predicted doses evaluated by the SAS software based on biomarker levels at time-points of sample collections as described above. Numbers in black color represent the predicted doses using Table Curve 2D and 3D software with a good accuracy shown in the last column of Table in right.

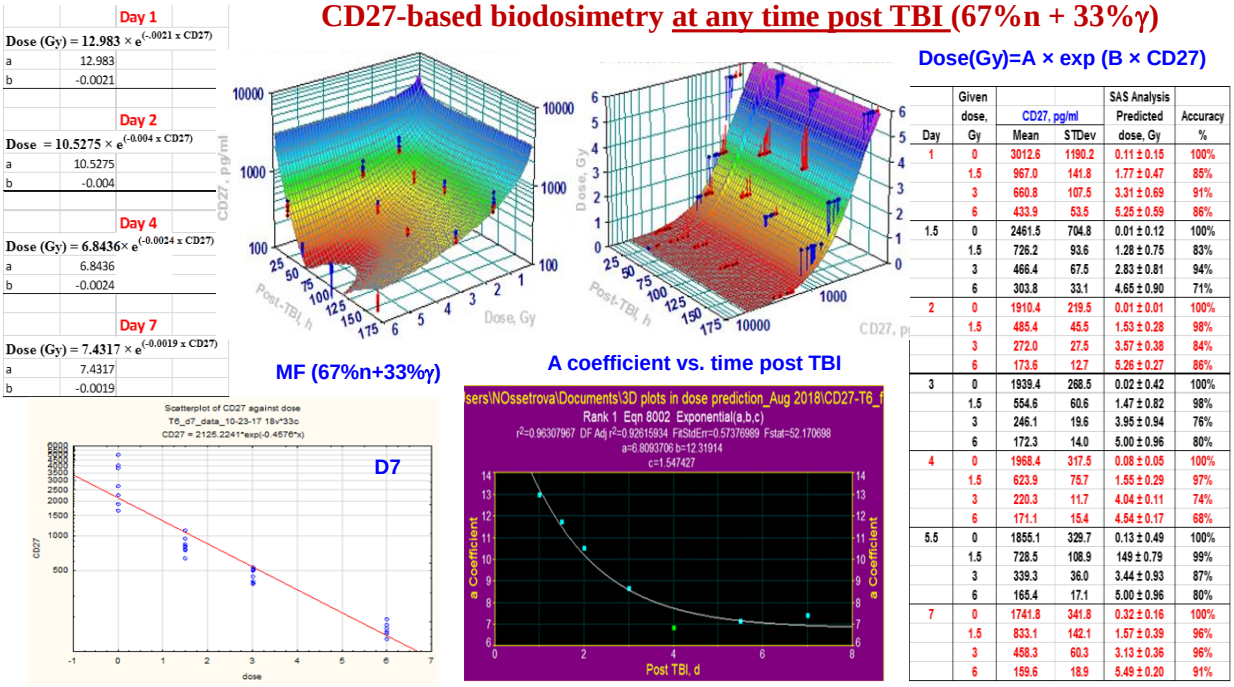

Day	Given dose, Gy	CD27, pg/ml Mean	CD27, pg/ml STDev	SAS Analysis Predicted dose, Gy	Accuracy %
1	0	3012.6	1190.2	0.11 ± 0.15	100%
	1.5	967.0	141.8	1.77 ± 0.47	85%
	3	660.8	107.5	3.31 ± 0.69	91%
	6	433.9	53.5	5.25 ± 0.59	86%
1.5	0	2461.5	704.8	0.01 ± 0.12	100%
	1.5	726.2	93.6	1.28 ± 0.75	83%
	3	466.4	67.5	2.83 ± 0.81	94%
	6	303.8	33.1	4.65 ± 0.90	71%
2	0	1910.4	219.5	0.01 ± 0.01	100%
	1.5	485.4	45.5	1.53 ± 0.28	98%
	3	272.0	27.5	3.57 ± 0.38	84%
	6	173.6	12.7	5.26 ± 0.27	86%
3	0	1939.4	268.5	0.02 ± 0.42	100%
	1.5	554.6	60.6	1.47 ± 0.82	98%
	3	246.1	19.6	3.95 ± 0.94	76%
	6	172.3	14.0	5.00 ± 0.96	80%
4	0	1968.4	317.5	0.08 ± 0.05	100%
	1.5	623.9	75.7	1.55 ± 0.29	97%
	3	220.3	11.7	4.04 ± 0.11	74%
	6	171.1	15.4	4.54 ± 0.17	68%
5.5	0	1855.1	329.7	0.13 ± 0.49	100%
	1.5	728.5	108.9	149 ± 0.79	99%
	3	339.3	36.0	3.44 ± 0.93	87%
	6	165.4	17.1	5.00 ± 0.96	80%
7	0	1741.8	341.8	0.32 ± 0.16	100%
	1.5	833.1	142.1	1.57 ± 0.39	96%
	3	458.3	60.3	3.13 ± 0.36	96%
	6	159.6	18.9	5.49 ± 0.20	91%

Fig. 11.4.2. CD27-based biodosimetry at any time post TBI (67%n + 33%γ).

Fig. 11.4.3 shows statistical data analysis results for FLT3L-based biodosimetry at any time post TBI using the same statistical methods as described above for ALC and CD27. Radiation dose predicted is expressed as Dose (Gy) = A + B×FLT3L, where A and B are coefficients calculated by the SAS software. Left Table in Fig. 11.4.3 shows a strong time-dependency for A coefficients while B coefficients are not significant different ($p>0.118$) within 95% CL over all time-points. This dose-dependency was applied using the Table Curve 2D software to create a fitting function in order to evaluate A coefficient values at any time after exposure from d1 to d7. The 3D plots were created for FLT3L (as a function of time post TBI and radiation dose) and radiation dose (as a function of FLT3L and time) along with fitting functions with ability to predict FLT3L level and radiation dose received at any time post exposure. FLT3L data for all animals clearly fit function $Z = a + blnX + clnY + d(lnX)^2 + e(lnY)^2 + flnXlnY + g(lnX)^3 + h(lnY)^3 + ilnX(lnY)^2 + j(lnX)^2lnY$, where Z is FLT3L (in pg/ml) for given radiation dose (X, in Gy) and time (Y, in hours/days). Model coefficients are a=-1419.8001, b=-885.3884, c=889.3757, d=-149.2315, e=-122.2391, f=406.721, g=-0.2141, h=0.0465, i=-0.2228, j=0.5862, R^2=0.9598 and a standard error of estimate FitStdErr=92.9116. Radiation dose received for all animals clearly fit function $Z = a + LORX(b,c,d) + LORY(e,f,g) + LORX(h,c,d)\times LORY(1,f,g)$, where Z is radiation dose (in Gy)) for given time post TBI (X, in hour/days) and FLT3L (Y, in pg/ml). Model coefficients are a=-1.7853, b=7.6378, c=1826.6737, d=1043.7041, e=-20.6186, f=0.8038, g=0.5080, h=67.6479, R^2=0.9018, and a standard error of estimate FitStdErr=0.7233. Results of those analyses are shown in lower middle plot and a Table on right. Numbers in red color represent the predicted doses evaluated by the SAS software based on biomarker levels at time-points of sample collections as described above. Numbers in black color represent the predicted doses using Table Curve 2D and 3D software with a good accuracy shown in the last column of Table in right.

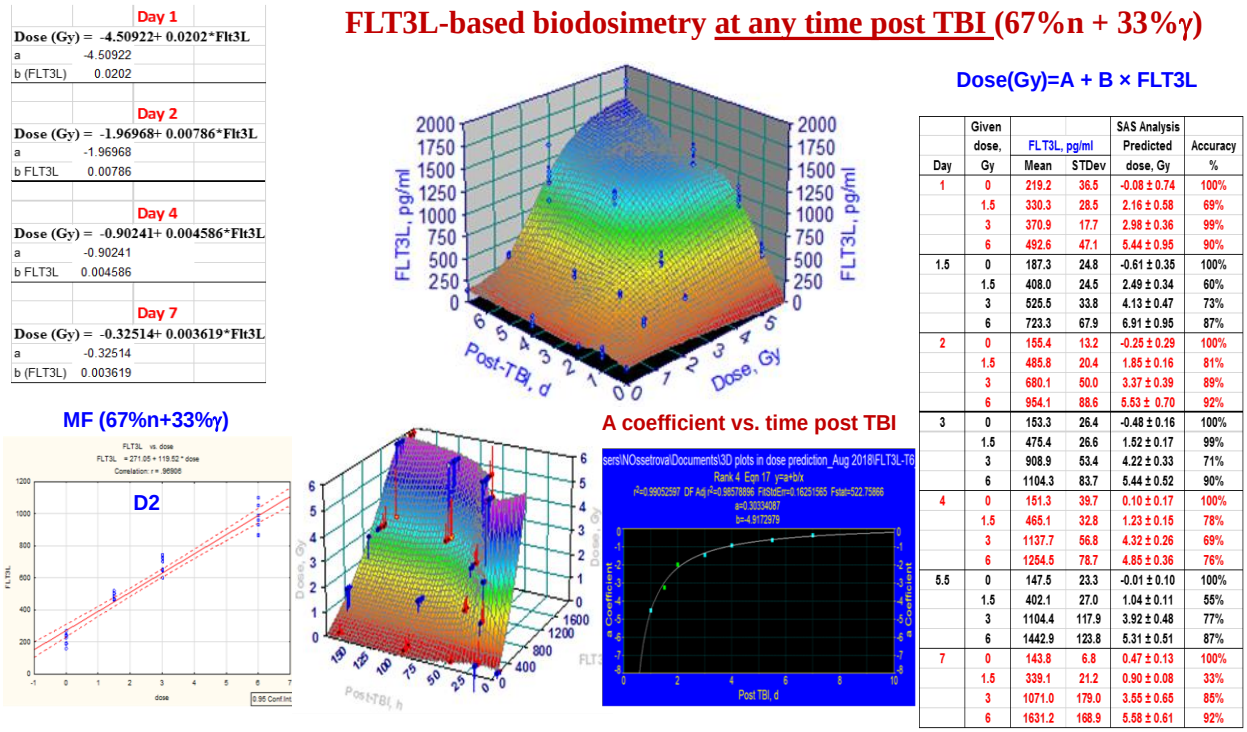

Day	Given dose, Gy	FLT3L, pg/ml Mean	FLT3L, pg/ml STDev	SAS Analysis Predicted dose, Gy	Accuracy %
1	0	219.2	36.5	-0.08 ± 0.74	100%
	1.5	330.3	28.5	2.16 ± 0.58	69%
	3	370.9	17.7	2.98 ± 0.36	99%
	6	492.6	47.1	5.44 ± 0.95	90%
1.5	0	187.3	24.8	-0.61 ± 0.35	100%
	1.5	408.0	24.5	2.49 ± 0.34	60%
	3	525.5	33.8	4.13 ± 0.47	73%
	6	723.3	67.9	6.91 ± 0.95	87%
2	0	155.4	13.2	-0.25 ± 0.29	100%
	1.5	485.8	20.4	1.85 ± 0.16	81%
	3	680.1	50.0	3.37 ± 0.39	89%
	6	954.1	88.6	5.53 ± 0.70	92%
3	0	153.3	26.4	-0.48 ± 0.16	100%
	1.5	475.4	26.6	1.52 ± 0.17	99%
	3	908.9	53.4	4.22 ± 0.33	71%
	6	1104.3	83.7	5.44 ± 0.52	90%
4	0	151.3	39.7	0.10 ± 0.17	100%
	1.5	465.1	32.8	1.23 ± 0.15	78%
	3	1137.7	56.8	4.32 ± 0.26	69%
	6	1254.5	78.7	4.85 ± 0.36	76%
5.5	0	147.5	23.3	-0.01 ± 0.10	100%
	1.5	402.1	27.0	1.04 ± 0.11	55%
	3	1104.4	117.9	3.92 ± 0.48	77%
	6	1442.9	123.8	5.31 ± 0.51	87%
7	0	143.8	6.8	0.47 ± 0.13	100%
	1.5	339.1	21.2	0.90 ± 0.08	33%
	3	1071.0	179.0	3.55 ± 0.65	85%
	6	1631.2	168.9	5.58 ± 0.61	92%

Fig. 11.4.3. FLT3L-based biodosimetry at any time post TBI (67%n + 33%γ).

12. LIST OF PROJECT MAJOR ACHIEVEMENTS AND RESULTS

1. Demonstrated that the equivalent doses of pure γ-rays (or photons) and mixed neutrons/γ-rays exposure do not produce equivalent biological effects due to the fact that neutrons, with a higher relative biological effectiveness (RBE), have different mechanisms of injury to cells and tissues compared to photons and are more biologically destructive than photons. Therefore, the ARS occurs at lower doses of mixed-field radiation and it's requiring the radiation-quality specific biodosimetry.
2. Mortality in mice was seen at lower doses and earlier time points after the exposure to mixed-field radiation compared to pure γ-rays reflecting the RBE≈2, which is in agreement with results from radiation countermeasure survival studies performed earlier at AFRRI.
3. Total of 24 biomarkers radiation-responsive blood-based hematological and proteomic biomarkers selected from different activation pathways were evaluated in mice after the total-body exposure with either mixed-field or pure γ-rays over a broad dose range (1.5 - 12 Gy), dose rates of 0.6 and 1.9 Gy/min, and different proportions of neutrons and γ-rays in mixed-field studies from 1 to 7 days after exposure.
4. Biomarker and survival results are in agreement with RBE = 1.95 for 67% n + 33% γ or Dn/Dt = 0.67 reported earlier by AFRRI scientists in mouse radiation countermeasure survival studies.
5. No dose-rate (0.6 vs. 1.9 Gy/min) and gender-effects were found in mixed-field and pure γ-rays biomarker studies.

6. In collaboration with other AFRRI PIs, it was demonstrated that no significant differences were observed in biomarker levels of interest after a pure γ-rays total-body exposure of mice to a broad radiation dose range (3, 6, 8, and 12 Gy) and multiple dose rates ranging from 0.04 to 1.9 Gy/min (i.e., ~50 fold). It means that the radiation dose absorbed (biodosimetry) strictly depends on biomarker levels regardless of exposure dose rate and this finding is advantageous for radiation dose assessment and triage-based treatment after nuclear weapon detonation or radiological accidents.
7. Ratios of biomarker means in mixed-field study to the pure gamma study at matched radiation doses were in ranges from 1.3 to 2.7.
8. Of total 24 biomarkers evaluated in project, a subset of 7 biomarkers (IL-18, G-CSF, GM-CSF, SAA, PCT, DAO and citrulline) was significantly different in animals irradiated with (67% n + 33% γ) compared to those irradiated with (30% n + 70% γ).
9. Gastrointestinal (GI) injury biomarker levels of PCT, DAO and citrulline were significantly different in mice irradiated with a higher percentage of neutrons (67% vs. 30%) reflecting the fact that the GI epithelium is more sensitive to neutron irradiation.
10. Multi-parametric acute radiation sickness (ARS) severity Response Category (RC) scoring system for radiation inquiry assessment and ARS prognosis outcome created earlier in pure γ-rays studies was expanded to mixed-field exposure conditions.
11. Performed the advanced statistical data analyses (i.e., SAS-based multivariate regression analysis to create the dose-response calibration curves for the radiation dose prediction accuracy and a threshold of exposure detection, multivariate discriminant function analysis to evaluate the separation animal groups and ARS RCs, multi-ROC analysis to evaluate the specificity and sensitivity, etc.) using evaluated biomarkers.
12. Multivariate analysis of variance (MANOVA) p values were highly significantly different at all time-points to separate animal groups irradiated with mixed-field from ones irradiated with pure gamma-rays to the same doses regardless of dose rate and gender.
13. It was demonstrated that lymphocyte depletion kinetics might be used in biodosimetry to estimate the radiation dose received regardless of gender, exposure dose rate (in both studies) and percentage of neutrons (in mixed-field study).
14. Evaluated subsets of proteomic biomarkers that accurately predict the radiation dose absorbed regardless of gender, exposure dose rate and percentage of neutrons (in both mixed-field and pure gamma studies).
15. Evaluated proteomic biomarker combinations that show difference in radiation dose prediction reflecting the percentage of neutrons (67% vs. 30%) in mixed-field studies.
16. It was shown that the combination of protein biomarkers provides greater accuracy for the radiation assessment/prediction as well as a perfect (100%) separations between irradiated animal groups than any biomarker alone. Note: Concept of use of multiple biomarkers for radiation injury and dose assessment - AFRRI U.S. Patent "Biomarker Panels for Assessing Radiation Injury and Exposure" Patent No. 8,871,455 (PCT No: PCT/US2007/013752), issued on October 28, 2014.
17. Mean differences in radiation dose prediction regression slope coefficients in mixed-field vs. pure gamma-ray studies for selected radiation-specific biomarkers were in range from 1.65 to 2.23. Those findings are in general agreement with AFRRI human lymphocyte dicentric calibration curves created using different radiation sources. Results are also in a good agreement with RBE=1.95 reported earlier by AFRRI scientists in mouse radiation countermeasure survival studies.

18. Suggested a computational-applied mathematical method for radiation dose prediction at any time-point after exposure other than at collection time in experiment (i.e., d1, d2, d4 and d7).
19. Our multi-parametric biodosimetry results are consistent with a radiation dose absorbed detection threshold of ~1 Gy and ~0.5 Gy for γ-rays and a mixed-field exposure, respectively, in mice of this strain, based on the selected biomarker profile.

13. LIST OF PUBLICATIONS, PRESENTATIONS AND REPORTS

1. Nine (9) Quarterly Technical Progress Reports have been sent to the Sponsor. Final Project Report was sent on 15 October 2018.
2. Dr. Ossetrova has provided a brief summaries of the project "Study of Biomarkers & Acute Radiation Sickness (ARS) Prognosis/Outcome Factors after Mixed-Field (Neutron and Gamma) Radiation in a Mouse Total-body Irradiation Model for Use in an FDA Approved Point-of-Care Biodosimetry System" per Ms. Fitch's email "Request for Seedling Information" on 28 April 2017.
3. Dr. Ossetrova's invited In-Progress Review (IPR) meeting presentation on project summaries to Mr. Dale Ormond, the Principal Director in the Office of the Assistant Secretary of Defense (Research and Engineering) and other EXCOM Deputies at the Pentagon on 24 May 2017.
4. Brief summaries of the project for Mr. Ormond's track metrics was provided by Dr. Natalia Ossetrova to Morgan, Khirah, Lt Col USAF OSD OUSD ATL (US) in October 2017.
5. Natalia I. Ossetrova, Paul Stanton, Katya Krasnopolsky, Mohammed Ismail, Arpitha Doreswamy, Kevin P. Hieber. "Biomarkers for radiation biodosimetry and injury assessment after the mixed-field (neutrons and gammas) radiation in mouse total-body irradiation model". Health Physics Journal 115(6): 727–742; 2018. DOI: 10.1097/HP.0000000000000938.
6. Natalia I. Ossetrova, Paul Stanton, Katya Krasnopolsky, Mohammed Ismail, Arpitha Doreswamy, Kevin P. Hieber. "Comparison of biodosimetry biomarkers for radiation dose and injury assessment after the mixed-field (neutrons and gammas) and pure gamma radiation in mouse total-body irradiation model". Health Physics Journal 115(6): 743–759; 2018. DOI: 10.1097/HP.0000000000000939.
7. Kiang JG, Smith JT, Hegge SR, Ossetrova NI. Circulating cytokine/chemokine concentrations respond to ionizing radiation doses but not radiation dose rates: granulocyte-colony stimulating factor and interleukin-18. Radiat Res 189: 634-643; 2018.
8. Dr. Ossetrova, "Study of Biomarkers and Acute Radiation Sickness Prognosis/Outcome after Mixed-Field (Neutron and Gamma) and ^{60}Co γ-ray Radiation in a Mouse Total-body Irradiation Model", invited presentation the Animal Model Development Workshop at the National Institutes of Health, Bethesda, MD, 22-23 September 2016.
9. Dr. Ossetrova "Biomarkers and Acute Radiation Sickness Prognosis/Outcome Factors after Mixed-Field (Neutron and Gamma) Radiation in a Mouse Total-body Irradiation Model", oral presentation at the AFRRI seminar, AFRRI/USUHS, 10 March 2017.
10. Natalia I. Ossetrova, Katya Krasnopolsky, Paul Stanton, Mohammed Ismail, Kevin P. Hieber. "Multi-parametric Biodosimetry and Acute Radiation Sickness Prognosis/Outcome after Mixed-Field (Neutron and Gamma) and ^{60}Co γ-ray Radiation in a Mouse Total-body Irradiation Model". Invited presentation at the ConRad 2017, Global Conference on Radiation Topics - Preparedness, Response, Protection and Research (22nd Nuclear Medical Defense Conference), Munich, Germany, 8-11 May, 2017.

11. Natalia I. Ossetrova, Katya Krasnopolsky, Paul Stanton, Mohammed Ismail, Arpitha Doreswamy, Kevin P. Hieber, "Biomarkers after TRIGA Reactor Mixed-field (Neutron and Gamma) and ^{60}Co (Pure Gamma) Radiation in a Mouse Total-body Irradiation Model". Poster presented at the USUHS Research Days, USUHS, Bethesda, MD, May, 2017.
12. Paul Stanton, Kevin P. Hieber, Katya Krasnopolsky, Mohammed Ismail, Natalia I. Ossetrova, "Survival Studies for Biodosimetry and Acute Radiation Sickness Prediction Outcome in Mouse Total-body Pure Gamma and Mixed-field (Neutron and Gamma) Irradiation Model". Poster presented at the USUHS Research Days, USUHS, Bethesda, MD, May, 2017.
13. Natalia I. Ossetrova, "Biomarkers and acute radiation sickness prognosis/outcome factors after mixed-field (neutron and gamma) radiation in a mouse total-body irradiation model for use in an FDA approved point-of-care biodosimetry system", Invited oral presentation at the Military Health System Research Symposium (MHSRS), Kissimmee, FL, 27-30 August 2017.
14. HM2 Mohammed Ismail, Paul Stanton, Katya Krasnopolsky, Arpitha Doreswamy, Kevin P. Hieber, and Natalia I. Ossetrova, "Biomarkers and acute radiation sickness prognosis/outcome factors after mixed-field (neutron and gamma) radiation in a mouse total-body irradiation model for use in an FDA approved point-of-care biodosimetry system" poster presented at the MHSRS, Kissimmee, FL, 27-30 August 2017.
15. Kevin P. Hieber, Katya Krasnopolsky, Paul Stanton, Arpitha Doreswamy, Mohammed Ismail, Natalia I. Ossetrova "Biomarkers of Gastrointestinal Damage after Mixed-Field (Neutron and Gamma) and Pure Gamma Radiation Exposure in Mouse Total-body Irradiation Model", Poster presented at the USU Research Days, USUHS, Bethesda, MD, May 2018.
16. Natalia I. Ossetrova, Paul Stanton, Katya Krasnopolsky, Mohammed Ismail, Arpitha Doreswamy, Kevin P. Hieber, "Biomarkers and Multi-parametric Biodosimetry after Exposure to Mixed-Field (Neutron and Gamma) vs Pure Gamma in Mouse Total-body Irradiation Model" presentation at the EPRBioDose International Conference, Munich, Germany, 11-15 June, 2018.
17. Mohammed Ismail, Kevin P. Hieber, Katya Krasnopolsky, Paul Stanton, Arpitha Doreswamy, Natalia I. Ossetrova "Biomarkers and Multi-parametric Biodosimetry after Mixed-Field (Neutron and Gamma) and Pure Gamma Radiation Exposure", Poster presented at the Military Health System Research Symposium (MHSRS), Kissimmee, FL, 20-23 August 2018.
18. Natalia I. Ossetrova, Invited Presentation "Biomarkers, Biodosimetry and Acute Radiation Sickness (ARS) Prognosis/Outcome Factors Comparison after Mixed-Field (Neutron + Gamma) vs. Pure-Gamma Radiation in Mouse Total-body Irradiation Model", DoD/DTRA/NASA/NIAID/ARA Webinar, 26 October 2018.

14. ACKNOWLEDGMENTS AND DISCLAIMER

The research was supported by Research and Engineering Science and Technology Priorities Program (Pentagon)/ JTCG-7 (Radiation Health Effects) under grant DWAM52221 awarded to Dr. Natalia I. Ossetrova. Principal Investigator (Dr. Ossetrova) and project personnel (Kevin Hieber, HM2 Mohammed Ismail, Katya Krasnopolsky, Paul Stanton and Arpitha Doreswamy) would like to thank the AFRRI Radiation Sciences (Dr. Vitaly Nagy, Mr. Stephen Miller, Mr. Mark Gee, Mr. Walter Tomlinson, MAJ McMahon, Mr. Sungyop Kim, Ms. Alia Weaver, and Ms. Alena Tsioplaya), Health Physics (RSO Mr. Daniel Shaw, LT Cole, SSG Manzanares, and HN

O'Neill), Veterinary Sciences Departments and Drs. Lynnette Cary and David Bolduc for their technical help.

The views expressed do not necessarily represent the opinions or policies of the Armed Forces Radiobiology Research Institute, the Uniformed Services University of the Health Sciences, the Department of Defense, or the United States Government.

15. REFERENCES

Ainsworth EJ, Leong GF, Kendall K, Alpen EL. The lethal effects of pulsed neutrons or gamma irradiation in mice. Rad Res 21:75-85; 1964a.

Ainsworth EJ, Leong GF, Kendall K, Alpen EL, Albright ML. Pulsed irradiation studies in mice, rats and dogs. In biological effects of neutron and proton irradiations. Vol II. Proceedings of the symposium on biological effects of neutrons irradiations. Vienna: International Atomic Energy Agency.15-27; 1964b.

Alpen E. The historical background for large animal studies with neutrons of varicose energies. Rad Res 128:S37-S41; 1991.

Armed Forces Radiobiology Research Institute (AFRRI). Medical management of radiological casualties. 3rd ed. Bethesda, MD; Armed Forces Radiobiology Research Institute; 2010.

Armed Forces Radiobiology Research Institute (AFRRI). Medical management of radiological casualties. 4th ed. Armed Forces Radiobiology Research Institute, Bethesda, MD; 2013.

Ainsworth EJ, Jordan DL, Miller M, Cooke EM, Hulesch JS, Dose rate studies with fission spectrum neutrons. Radiat Res 67:30-45; 1976.

Anno GH, Baum SJ, Withers HR, Young RW. Symptomatology of acute radiation effects in humans after exposure to doses of 0.5-30 Gy. Health Phys 56:821-838; 1989.

Awa AA, Honda T, Sofuni T, Neriishi S, Yoshida MC, Matsui T. Chromosome aberration frequency in cultured blood cells in relation to radiation dose of A- bomb survivors. Lancet 2:903-905; 1971.

Baranov AE, Guskova AK, Nadejina NM, Nugis VYu. Chernobyl experience: biological indicators of exposure to ionizing radiation. Stem Cells 13:69-77; 1995.

Balcer-Kubiczek E, Harrison GH, Hei TK. Neutron dose-rate experiments at the AFRRI nuclear reactor. Rad Res 128:S65-S70; 1991.

Bazan JG, Chang P, Balog R, D'Andrea A, Shaler T, Lin H, Lee S, Harrison T, Shura L, Schoen L, Knox SJ, Cooper DE.Novel human radiation exposure biomarker panel applicable for population triage. Int J Radiat Oncol Biol Phys 90:612-618; 2014.

Bertho JM, Demarquay C, Frick J, Joubert C, Arenales S, Jacquet N, Sorokine-Durm I, Chau Q, Lopez M, Aigueperse J, Gorin NC, Gourmelon P. Level of Flt3-ligand in plasma: a possible new bio-indicator for radiation-induced aplasia. Int J Radiat Biol 77:703-712; 2001.

Bertho JM, Roy L, Souidi M, Benderitter M, Gueguen Y, Lataillade JJ, Prat M, Fagot T, De Revel T, Gourmelon P. New biological indicators to evaluate and monitor radiation-induced damage: an accident case report. Rad Res 169:543-550; 2008.

Bertho JM, Roy L, Souidi M, Benderitter M, Bey E, Racine R, Fagot T, Gourmelon P. Initial evaluation and follow-up of acute radiation syndrome in two patients from the Dakar accident. Biomarkers 14:94-102; 2009.

Biju PG, Garg S, Wang W, Choudhry MA, Kovacs EJ, Fink LM, Hauer-Jensen M. Procalcitonin as a predictive biomarker for total body irradiation-induced bacterial load and lethality in mice. Shock. 38:170-176; 2012.

Brook I, Tom SP, Ledney GD. Quinolone and glycopeptide therapy for infection in mouse following exposure to mixed-field neutron-gamma-photon radiation. Int J Radiat Biol 46:771-777; 1993.

Bartley TD, Bogenberger J, Hunt P, Li YS, Lu HS, Martin F, Chang MS, Samal B, Nichol JL, Swift S. Identification and cloning of a megakaryocyte growth and development factor that is a ligand for the cytokine receptor mpl. Cell 77:1117-1124; 1994.

Basile LA, Ellefson D, Gluzman-Poltorak Z, Junes-Gill K, Mar V, Mendonca S, Miller JD, Tom J, Trinh A, Gallaher TK. HemaMaxTM, a Recombinant Human Interleukin-12, is a potent Mitigator of Acute Radiation Injury in Mice and Non-Human Primates. Plos One2012 DOI:10.1371/journal.pone.0030434.

Blakely WF, Ossetrova NI, Manglapus GL, Levine IH, Jackson WE, Grace MB, Prasanna PGS, Sandgren DJ, Ledney GD. Amylase and blood cell-count hematological radiation-injury biomarkers in a rhesus monkey radiation model – use of multiparameter and integrated biological dosimetry. Radiat Meas 42: 1164-1170; 2007.

Broerse JJ. RBE values of fast neutrons for damage to organized tissues in experimental animals. In Radiation Research; Biomedical, Chemical and Physical Perspectives, edited by O. F. Nygaard, H. I. Adler and W. K. Sinclair, Proceedings of the 5th International Congress on Radiation Research, Seattle, WA, July 14–20, 1974 (New York: Academic Press), 1073–1082; 1975.

Brook I, MacVittie TJ, Walker RI. Recovery of aerobic and anaerobic bacteria from irradiated mice. Infect Immun. 46:270–271; 1984.

Cary LH, Ngudiankama BF, Salber RE, Ledney GD, Whitnall MH. Efficacy of radiation countermeasures depends on radiation quality. Rad Res 177:663-675; 2012.

Castillo GM, Nishimoto-Ashfield A, Jones CC, Kabirov KK, Zakharov A, Lyubimov AV. Protected graft copolymer-formulated fibroblast growth factors mitigate the lethality of partial body irradiation injury. Plos One 2017DOI:10.1371/journal.pone.0171703.

Chida K, Kaga Y, Haga Y, Kataoka N, Kumasaka E, Meguro T, Zuguchi M. Occupational dose in interventional radiology procedures. AJR AM J Roentgenol. 200:138-141; 2013.

Colombo MP, Trinchieri G. Interleukin-12 in anti-tumor immunity and immunotherapy. Cytokine Growth Factor Rev 13: 155–168; 2002.

Cronk DR, Houseworth TP, Cuadrado DG, Herbert GS, McNutt PM, Azarow KS. Intestinal fatty acid binding protein (I-FABP) for the detection of strangulated mechanical small bowel obstruction. Current surgery 63:322-325; 2006DOI:10.1016/j.cursur.2006.05.006.

Dainiak N, Waselenko JK, Armitage JO, MacVittie TJ, Farese AM. The hematologist and radiation casualties. Hemat J1:473-496; 2003.

Debad J, Glezer E, Wohlstadter J, Sigal G. Clinical and biological applications of ECL, in Electrogenerated Chemiluminescence, ed. Bard AJ, Dekker M, 43-78; 2004.

Debell RM, Ledney GD. and Snyder SL. Quantification of gut injury with diamine oxidase activity: development of a fission neutron RBE and measurements with combined injury in mouse models. Radiat Res 112:508–516; 1987.

Dinarello CA. Immunological and inflammatory functions of the interleukin-1 family. Annu Rev Immunol. 27: 519-550; 2009.

Dressman HK, Muramoto GG, Chao NJ, et al. Gene expression signatures that predict radiation exposure in mice and humans. PLoS Med. 2007; 4:e106.

Egbert SD, Kerr GD, Cullings HM. DS02 fluence spectra for neutrons and gamma rays at Hiroshima and Nagasaki with fluence-to-kerma coefficients and transmission factors for sample measurements. Radiat Environ Biophys 464: 311-25; 2007.

Elliott S, Pham E, Macdougall IC. Erythropoietins: a common mechanism of action. Exp Hematol 36:1573-1584; 2008.

Fehner TR, Gosling FG. Atmospheric nuclear weapons testing, 1951-1963. Battlefield of the cold war: The Nevada test site. Vol 1. DOE/MA-0003. US Department of Energy 2006.

Fliedner TM, Friesecke I, Beyer K.Medical management of radiation accidents: Manual on the acute radiation syndrome.Br J Radiol 2001.

Fliedner TM, Dorr HD, Meineke V. Multi-organ involvement as a pathogenetic principle of the radiation syndromes: a study involving 110 case histories documented in SEARCH and classified as the bases of hematopoietic indicators of effect. Br J Radiol 27:1–8; 2014DOI: 10.1259/bjr/77700378; 2005.

Fueger GF. Blood Cells in Nuclear Medicine, part II: Migratory Blood Cells. Volume 7 of Developments in Nuclear Medicine, Springer Netherlands; 1984.

Gabay C, Kushner I. Acute-phase proteins and other systemic responses to inflammation. N Engl J Med 340: 448-454; 1999.

Gerber SA, Cummings RJ, Judge JL, Barlow ML, Nanduri J, Johnson DE, Palis J, Pentland AP, Lord EM, Ryan JL. Interleukin-12 preserves the cutaneous physical and immunological barrier after radiation exposure. Radiat Res.183: 72–81; 2015.

Goans RE, Holloway EC, Berger ME, Ricks RC. Early dose assessment following severe radiation accidents. Health Phys 72:513-518; 1997.

Goans RE, Flynn DF. Acute radiation syndrome in humans. In: Lenhart MK, editor. Textbook of military medicine, Medical consequences of radiological and nuclear weapons edition. Fort Detrick, MD: Borden Institute. 17-38; 2013.

Goans, RE, Iddins, CJ, Christensen, DM, Wiley, AL, Dainiak, N. Appearance pf pseudo-Pelger Huet anomaly after accidental exposure to ionizing radiation in vivo. Health Phys 108(3):303-307; 2015.

Goans RE, Iddins CJ, Ossetrova NI, Ney PH, Dainiak N. "The Pseudo-Pelger Huët Cell - a New Permanent Radiation Biomarker". 2017. Health Physics: March 2017 - Volume 112 (3): 252–257. Doi: 10.1097/HP.0000000000000618.

Goodman LJ. A practical guide to ionization chamber dosimetry at the AFRRI reactor. AFRRI Contract Report CR85-1. AFRRI, Bethesda, Maryland.pp 41; 1985. DOI: ***http://oai.dtic.mil/oai/oai?verb=getRecord&metadataPrefix=html&identifier=ADA155185***

Griffin CS, Hornsey S. The effect of neutron dose rate on jejunal crypt survival. Int J Radiat Biol 49: 589-595; 1986.

Guilmeau S, Niot I, Laigneau JP, Devaud H, Petit V, Brousse N, Bouvier R, Ferkdadji L, Besmond C, Aggerbeck LP, Bado A, Samson-Bouma ME. Decreased expression of Intestinal I- and L-FABP levels in rare human genetic lipid malabsorption syndromes. Histochem Cell Biol 128:115–123; 2007.

Guipaud O, Benderitter M. Protein biomarkers for radiation exposure: towards a proteomic approach as a new investigation tool. Ann Ist Super Sanita 45:278–286; 2009.

Guskova AK, Nadezhina NM, Barabanova AV, Baranov AE, Gusev IA, Protasova TG, Boguslayskij VB, Pokrovskaya VN. Acute effects of radiation exposure following the Chernobyl accident. In: Browne D, Weiss JF, MacVittie TJ, Pillai MV, eds. Treatment of radiation injuries. Boston, MA: Springer; 1990.

Guven H, Altintop L, Baydin A, Esen S, Aygun D, Hokelek M, Doganay Z, Bek Y. Diagnostic value of procalcitonin levels as an early indicator of sepsis. Am J Emerg Med20:202-206; 2002.

Haase MG, Klawitter A, Geyer P, Baretton GB. Expression of the immunomodulator IL-10 in type I pneumocytes of the rat: alterations of IL-10 expression in radiation-induced lung damage. J Histochem Cytochem 55: 1167–1172; 2007.

Ha CT, Li XH, Fu D, Moroni M, Fisher C, Arnott R, Srinivasan V, Xiao M. Circulating interleukin-18 as a biomarker of total-body radiation exposure in mice, minipigs, and nonhuman primates (NHP). PLoS One 2014. DOI:10.1371/journal.pone.0109249.

Ha CT, Li X, Fu D, Xiao M. Circulating IL-18 binding protein (IL-18BP) and IL-18 as dual biomarkers of total-body irradiation in mice. Radiat Res 185: 375-383; 2016.

Hall E. Radiobiology for the radiologist. 5th ed. Philadelphia: Lippincott Williams and Wilkins; 2000.

Hall DE, 2009. Modeling and Validation of Dosimetry Measurement Assumptions Within The Armed Forces Radiobiology Research Institute TRIGA Mark-F Reactor and associated Exposure Facilities using Monte Carlo Techniques.

Han SK, Song JY, Yun YS, Yi SY. Effect of gamma radiation on cytokine expression and cytokine-receptor mediated STAT activation. Int J Radiat Biol. 82: 686-97; 2006.

Hendry JH. The slower cellular recovery after higher-LET irradiations, including neutrons, focuses on the quality of DNA breaks. Radiat Res 128: S111–S113; 1991.

Hendry JH, Potten CS, Merritt A. Apoptosis induced by high- and low-LET radiations. Radiation and Environmental Biophysics 34: 59–62; 1995.

Hendrzak JA, Brunda MJ. Interleukin-12. Biologic activity, therapeutic utility, and role in disease. Lab Invest. 72: 619–637; 1995.

Hirama T, Tanosaki S, Kandatsu S, Kuroiwa N, Kamada T, Tsuji H, Yamada S, Katoh H, Yamamoto N, Tsujii H, Suzuki G, Akashi M. Initial medical management of patients severely irradiated in the Tokai-mura criticality accident. Br J Radiol 76:246-253; 2003DOI: 10.1259/bjr/82373369.

Hornsey SD, Adresozzi A, Warren PR, Sublethal damage in cells of the mouse gut after mixed treatment with X-rays and fast neutrons. Brit J Radiol 50: 513-517; 1977.

Huchet A, Belkacemi Y, Frick J, Prat M, Murescan-Kloos M, Altan D, Chapel A, Gorin NC, Gourmelon P, and Bertho JM. Plasma flt-3 ligand concentration correlated with radiation-induced bone marrow damage during local fractionated radiotherapy. Int J Radiat Oncol 57: 508-515; 2003.

International commission on radiation units and measurements. Neutron dosimetry for biology and medicine. ICRU Report 26. ICRU, Bethesda, MD, ISBN 0-913394-20-3 pp128; 1977.

Jensen LE, Whitehead AS. Regulation of serum amyloid A protein expression during the acute-phase response. Biochem J. 334: 489-503; 1998.

Jones JW, Tudor G, Li F, Tong Y, Katz B, Farese AM, MacVittie TJ, Booth C, Kane MA. Citrulline as a biomarker in the murine total-body irradiation model: Correlation of circulating and tissue citrulline to small intestine epithelial histopathology. Health Phys 109:452-65; 2015. DOI:10.1097/HP.0000000000000346.

Katata G, Terada H, Nagai H, Chino M. Numerical reconstruction of high dose rate zones due to the Fukushima Dai-ichi nuclear power plant accident. J Environ Radioact 111:2-12; 2012.

Kaushansky K, Lok S, Holly RD, Broudy VC, Lin N, Bailey MC, Forstrom JW, Buddle MM, Oort PJ, Hagen FS, Roth GJ, Papayannopoulou T, Foster DC. Promotion of megakaryocyte progenitor expansion and differentiation by the c-Mpl ligand thrombopoietin. Nature 369:568-571; 1994.

Kiang JG, Jiao W, Cary LH, Mog SR, Elliott TB, Pellmar TC, Ledney GD. Wound trauma increases radiation-induced mortality by activation of iNOS pathway and elevation of cytokine concentrations and bacterial infection. Radiat Res 173:319–332; 2010.

Kiang JG, Smith JT, Hegge SR, Ossetrova NI. Circulating cytokine/chemokine concentrations respond to ionizing radiation doses but not radiation dose rates: granulocyte-colony stimulating factor and interleukin-18. Radiat Res 189: 634-643; 2018.

Koch AL, Hieber KP, Gulani J, Chappell MG, Ossetrova NI. Establishments of early endpoints in mouse total-body irradiation model. PLos One; 2016DOI:10.1371/journal.pone.0161079.

Landauer MR, McChesney DG, Ledney GD. Synthetic trehalose dicorynomycolate (S-TDCM): behavioral effects and radioprotection. J Radiat Res 38: 45-54; 1997.
Lawrence JH, and R. Tennant R. The comparative effects of neutrons and x-rays on the whole body. J. Exp. Med. 66, 667-688; 1937.
Ledney GD, Madonna GS, Elliott TB, Moore MM, Jackson III WE. Therapy of infections in mice irradiated in mixed neutron/photon fields and inflicted with wound trauma: a review of current work. Radiat Res128: S18-S28; 1991.
Ledney GD, Elliott TB. Combined injury: factors with potential to impact radiation dose assessments. Health Phys 98:145-152; 2010DOI: 10.1097/01.HP.0000348466.09978.77.
Ledney GD, Elliott TB, Harding RA, Jackson III WE, Inal CE, Landauer MR. WR-151327 increases resistance to Klebsiella pneumoniae infection in mixed-field- and gamma-photon-irradiated mice. Int J Radiat Biol 76: 261- 271; 2000.
Ledney GD, Elliott TB. The AFRRI TRIGA reactor: a summary of applications in mouse studies. Physor1-25; 2010.
Li GH, Zhang YP, Tang JL, Chen ZT, Hu YD, Wei H, Li DZ, Hao P, Wang DL. Effects of berberine against radiation-induced intestinal injury in mice. Int J Radiat Oncol Biol Phys 77:1536–1544; 2010.
Lieberman JM, Sacchettini J, Marks C, Marks WH. Human intestinal fatty acid binding protein: report of an assay with studies in normal volunteers and intestinal ischemia. Surgery 121:335-342; 1997.
Lok S, Kaushansky K, Holly RD, Kuijper JL, Lofton-Day CE, Oort PJ, Grant FJ, Heipel MD, Burkhead SK, Kramer JM, Bell LA, Sprecher CA, Blumberg H, Johnson R, Prunkard D, Ching AFT, Mathewes SL, Balley MC, Forstrom JW, Buddle MM, Osborn SG, Evans SJ, Sheppard PO, Presnell SR, O'Hara PJ, Hagen FS, Roth GJ, Foster DC. Cloning and expression of murine thrombopoietin cDNA and stimulation of platelet production in vivo. Nature 369:565-568; 1994.
Lutgens L, Lambin P. Biomarkers for radiation-induced small bowel epithelial damage: an emerging role for plasma Citrulline. World J Gastroenterol 13:3033-3042; 2007. DOI:10.3748/wjg.v13.i22.3033.
MacVittie TJ, Monroy RL, Patchen ML, Souza LM. Therapeutic use of recombinant human G-CSF in a canine model of sublethal and lethal whole-body irradiation. Int J Radiat Biol. 57:723-736; 1990.
MacVittie TJ, Monroy R, Vigneulle RM, Zeman GH, Jackson WE. The relative biological effectiveness of mixed fission-neutron-gamma radiation on the hematopoietic syndrome in the canine: effect of therapy on survival. Radiat Res 128: S29-36; 1991.
MacVittie TJ, Farese AM, Jackson 3rd W. Defining the full therapeutic potential of recombinant growth factors in the post radiation-accident environment: the effect of supportive care plus administration of G-CSF. Health Phys 89: 546-555; 2005.
McChesney DG, Ledney GD, Madonna GS. Trehalose dimycolate enhances survival of fission neutron-irradiated mice and Klebsiella pneumoniae-challenged irradiated mice. Radiat Res 121: 71-75; 1990.
Metcalf D. The granulocyte-macrophage colony-stimulating factors. Science 229:16-22; 1985.
Matthews W, Jordan CT, Wiegand GW, Pardoll D, Lemischka IR. A receptor tyrosine kinase specific to hematopoietic stem and progenitor cell-enriched populations. Cell 65: 1143–1152; 1991.
Mognato M, Grifalconi M, Canova S, Girardi C, Celotti L. The DNA-damage response to ionizing radiation in human lymphocytes, selected topics in DNA repair, book edited by Chen CC, ISBN 978-953-307-606-5; 2011.

Monroy RL, Skelly RR, MacVittie TJ, Davis TA, Sauber JJ, Clark SC, Donahue RE. The effect of recombinant GM-CSF on the recovery of monkeys transplanted with autologous bone marrow. Blood 70:1696-1699; 1987.

Moyer B, BARDA Team. "Advanced development of biodosimetry: Bridging animal data to the human experience. NIAID biodosimetry workshop. Silver Spring, MD; 2015.

Muramatsu et al., 2001. J. RADIAT. RES., 42: SUPPL., S117–S128.

National planning scenarios (final version 21.3). Washington, DC. Homeland Security Council; 2006. DOI:***http://1.usa.gov/1gGvsQ7***

Nakamura A, Wada H, Ikejiri M, Hatada T, Sakurai H, Matsushima Y, Nishioka J, Maruyama K, Isaji S, Takeda T, Nobori T. Efficacy of procalcitonin in the early diagnosis of bacterial infections in a critical care unit. Shock 31:586–591; 2009.

Niewold TA, Meinen M, van der Meulen J. Plasma intestinal fatty acid binding protein (I-FABP) concentrations increase following intestinal ischemia in pigs. Res Vet Sci 77:89-91; 2004. DOI:10.1016/j.rvsc.2004.02.006.

Nunamaker EA, Artwohl JE, Anderson RJ, Fortman JD. Endpoint refinement for total body irradiation of C57BL/6 mice. Comp Med 63:22–28; 2013.

Ogilvie M, Yu X, Nicolas-Metral V, Pulido SM, Liu C, Ruegg UT, Noguchi CT. Erythropoietin stimulates proliferation and interferes with differentiation of myoblasts. J Biol Chem. 275: 39754-39761; 2000.

Okunieff P, Chen Y, Maguire DJ, Huser AK. Molecular markers of radiation-related normal tissue toxicity. Cancer Metastasis Rev 27:363–374; 2008DOI: 10.1007/s10555-008-9138-7.

ORNL Report on determination of dose from criticality accidents (ORNL/TM – 12028). Jun 1993; 99 p; CONTRACT AC05-84OR21400; Also available from OSTI as DE93016886; NTIS; US Govt. Printing Office Dep.

Ossetrova NI, Farese AM, MacVittie TJ, Manglapus GL, Blakely WF. The use of discriminant analysis for evaluation of early-response multiple biomarkers of radiation exposure using non-human primate 6-Gy whole-body radiation model. Radiat Meas 42:1158-1163; 2007.

Ossetrova NI, Blakely WF. Multiple blood-proteins approach for early-response exposure assessment using an *in vivo* murine radiation model. Int J Radiat Biol 85: 837-850; 2009.

Ossetrova NI, Sandgren DJ, Gallego S, Blakely WF. Combined approach of hematological biomarkers and plasma protein SAA for improvement of radiation dose assessment in triage biodosimetry applications. Health Phys 98: 204-208; 2010.

Ossetrova NI, Sandgren DJ. Biomarkers for early-response assessment of radiation exposure. Proceedings Book, 105-115. The Third International Symposium on Radiation Emergency Medicine, Hirosaki University, Japan, September 17, 2011.

Ossetrova NI, Sandgren DJ, Blakely WF. C-reactive protein and serum amyloid A as early-phase and prognostic indicators of acute radiation exposure in nonhuman primate total-body irradiation model. Radiat Meas 46:1019–1024; 2011DOI: 10.1016/j. radmeas.2011.05.021.

Ossetrova NI, Condliffe DP, Ney PH, Krasnopolsky K, Hieber KP, Rahman A, Sandgren DJ. Early-response biomarkers for assessment of radiation exposure in a mouse total-body irradiation model. Health Phys 106:772-786; 2014a. DOI: 10.1097/HP.0000000000000094.

Ossetrova NI, Sandgren DJ, Blakely WF. Protein Biomarkers for Enhancement of Radiation Dose and Injury Assessment in Nonhuman Primate Total-body Irradiation Model. Radiat Prot Dosimetry 159(1-4):61-76; 2014b.

Ossetrova NI, Blakely WF, Nagy V, McGann C, Ney PH, Christensen CL, Koch AL, Gulani J, Sigal GB, Glezer EN, Hieber KP. Non-human Primate Total-body Irradiation Model with Limited and

Full Medical Supportive Care Including Filgrastim for Biodosimetry and Injury Assessment. Radiat Prot Dosim 172(1-3): 174-191; 2016a. DOI:10.1093/rpd/ncw176.

Ossetrova NI, Ney PH, Condliffe DP, Krasnopolsky K, Hieber KP. Acute radiation syndrome severity score system in mouse total-body irradiation model. Health Phys111: 134-144; 2016b.DOI: 10.1097/HP.0000000000000499.

Ossetrova NI, Stanton P, Krasnopolsky K, Ismail M, Doreswamy A, Hieber KP. Biomarkers for radiation biodosimetry and injury assessment after the mixed-field (neutrons and gammas) radiation in mouse total-body irradiation model. Health Phys (in press); 2018a.

Ossetrova NI, Stanton P, Krasnopolsky K, Ismail M, Doreswamy A, Hieber KP. Biodosimetry biomarkers comparison for radiation dose and injury assessment after the mixed-field (neutrons and gammas) and pure gamma radiation in mouse total-body irradiation model. Health Phys (in press); 2018b.

Paschos N, Lykissas MG, Beris AE. The role of erythropoietin as an inhibitor of tissue ischemia. Int J Biol Sci 4:161–168; 2008.

Paul S and Amundson SA, Development of gene expression signatures for practical radiation biodosimetry. Int J Radiat Oncol Biol Phys. 2008 Jul 15; 71(4): 1236–1244.

Pelsers MM, Namiot Z, Kisielewski W, Namiot A, Januszkiewicz M, Hermens WT, Glatz JF. Intestinal-type and liver-type fatty acid-binding protein in the intestine. Tissue distribution and clinical utility. Clin Biochem 36: 529-35; 2003.

Pepys MB, Baltz ML. Acute phase proteins with special reference to C-reactive protein and related proteins (pentaxins) and serum amyloid A protein. Adv Immunol 34: 141-212; 1983.

Plett PA, Sampson CH, Chua HL, Joshi M, Booth C, Gough A, Johnson CS, Katz BP, Farese AM, Parker J, MacVittie TJ, Orschell CM. Health Phys. Oct;103(4):343-55. 2012 DOI: 10.1097/HP.0b013e3182667309.

Prasanna PG, Loats H, Gerstenberg HM, Torres BN, Shehata CW, Duffy KL, Floura RS, Khusen AW, Jackson WE, Blakely WF. AFRRI's Gamma-ray, X-ray, and fission-neutron calibration curves for the lymphocyte dicentric assay: application of a metaphase finder system. Armed Forces Radiobiology Research Institute, Special Publication 02:1; 2002.

Prat M, Demarquay C, Frick J, Dudoignon N, Thierry D, Bertho JM. Use of Flt2 ligand to evaluate residual hematopoiesis after heterogeneous irradiation in mice. Radiat Res 166: 504-511; 2006.

Radiation Emergency Assistance Center/Training Site (REAC/TS). The medical aspects of radiation incidents. 4th ed. Radiation Emergency Assistance Center/Training Site, Oak Ridge, Tennessee; July 2017.

Roy L, Berthro JM, Squidi M, Vozenin MC, Voisin P, Benderitter M. Biochemical approach to prediction of multiple organ dysfunction syndrome. Br J Radiol 27:146–151; 2005 DOI: http://dx.doi.org/10.1259/bjr/21244438.

Safwat A, Bentzen SM, Nielsen OS, Overgaard J. Time Course of the hazard of murine nephropathy induced by total body irradiation. Int J Radiat Biol 76: 979–983; 2000.

Schaff UY, Koh C-Y, Ossetrova NI, Blakely WF, Sommer GJ. SpinDxTM: A rapid, point-of-care biodosimetry platform that uses peripheral whole blood protein and leukocyte biomarkers, In: Wiley A, Sugarman S, O'Hara F, Christensen D editors. The Medical Basis for Radiation-Accident Preparedness: Parthenon, New York 371-374; 2013.

Shan YX, Jin SZ, Liu XD, Liu Y, Liu SZ, Ionizing radiation stimulates secretion of pro-inflammatory cytokines: dose-response relationship, mechanisms and implications. Radiat Environ Biophys 46: 21-29; 2007.

Sigal G, Glezer E, Kenten J, Kumar S, Ossetrova NI, Blakely W. Biomarker-based radiation –dosimetry diagnostics. In: Wiley A, Sugarman S, O'Hara F, Christensen D editors. The Medical Basis for Radiation-Accident Preparedness: Parthenon, New York 375-378; 2013.

Stewart DA, Ledney GD, Baker WH, Daxon EG, Sheehy PA. Bone marrow transplantation of mice exposed to a modified fission neutron (N/G-30:1) field. Radiat Res 92: 268-279; 1982.

Stoffel R, Wiestner A, Skoda RC. Thrombopoietin in thrombocytopenic mice: evidence against regulation at the mRNA level and for a direct regulatory role of platelets. Blood 87:567-573; 1996.

Strike TA. Acute mortality of mice and rats exposed to 14 MeV neutrons. Radiat Res 43:679-690; 1970.

Thompson-Snipes L, Dhar V, Bond MW, Mosmann TR, Moore KW, Rennick DM. Interleukin 10: a novel stimulatory factor for mast cells and their progenitors. J Exp Med 173: 507-510; 1991.

Thomas J, Liu F, Link DC. Mechanisms of mobilization of hematopoietic progenitors with granulocyte colony-stimulating factor. Curr Opin Hematol 9: 183–189; 2002.

Tsapogas P, Mooney CJ, Brown G, Rolink A. The cytokine Flt3-ligand in normal and malignant hematopoiesis. Int J Mol Sci 2017.DOI: 10.3390/ijms18061115.

Tsoulou E, Kalfas CA, Sideris EG. Changes in DNA flexibility after irradiation with gamma rays and neutrons studied with the perturbed angular correlation method. Radiat Res 159(1): 33-39; 2003.

Tsoulou E, Kalfas CA, Sideris EG. Conformational properties of DNA after exposure to gamma rays and neutrons. Radiat Res 163(1): 90-97; 2005.

Uzzan B, Cohen R, Nicolas P, Cucherat M, Perret GY. Procalcitonin as a diagnostic test for sepsis in critically ill adults and after surgery or trauma: a systematic review and meta-analysis. Crit Care Med 34:1996–2003; 2006.

Van der Meeren A, Monti P, Lebaron-Jacobs L, Marquette C, Gourmelon P. Characterization of the acute inflammatory response after irradiation in mice and its regulation by Interleukin 4 (Il4). Radiation Res 155: 858–865; 2001.

Wootton P, Almond P, Attix FH, Awschalom M, Bloch P, Eenmaa J, Goodman L, Graves R, Horton J, Kuchnir F, McDonald J, Otte V, Shapiro P, Smathers J, Suntharalingam M, Waterman F. (AAPM Task Group 18). Protocol for neutron beam dosimetry (AAPM Report No. 7). AIP, New York, ISBN 0-88318-276-9, pp 51; 1980.

Welte K, Bonilla MA, Gillio AP, Boone TC, Potter GK, Gabrilove JL, Moore MA, OReilly RJ, Souza LM. Recombinant human granulocyte colony-stimulating factor. Effects on hemopoiesis in normal and cyclophosphamide-treated primates. J Exp Med 165:941-948; 1987.

Wolf SF, Sieburth D, Sypek J. Interleukin 12: a key modulator of immune function. Stem Cells 12:154–168; 1994.

Xia J, Wishart DS. Using metaboanalyst 3.0 for comprehensive metabolomics data analysis current protocols in bioinformatics, 55:14; 2016DOI: 10.1-14.10.91.

Xiao M. The role of proinflammatory cytokine interleukin-18 in radiation injury. Health Phys 111: 212-217; 2016.

Xiao M, Bolduc DL, Li X, Cui W, Hieber KP, Bunger R, Ossetrova NI. Urine interleukin 18 (IL-18) as a predictive biomarker of total-body radiation exposure in nonhuman primates. Radiat Res 188:325-334; 2017. DOI: 10.1667/RR14768.1.

Zhou P, Streutker C, Borojevic R, Wang Y, Croitoru K. IL-10 modulates intestinal damage and epithelial cell apoptosis in T cell-mediated enteropathy. Am J Physiol Gastrointest Liver Physiol. 287: G599-604; 2004.